Breaking of the macroscopic centric symmetry in $Ba_{1-x}Sr_xTiO_3$ ceramics and single crystals

THÈSE N^{O} 6366 (2014)

PRÉSENTÉE LE 24 OCTOBRE 2014

À LA FACULTÉ DES SCIENCES ET TECHNIQUES DE L'INGÉNIEUR

LABORATOIRE DE CÉRAMIQUE

PROGRAMME DOCTORAL EN SCIENCE ET GÉNIE DES MATÉRIAUX

ÉCOLE POLYTECHNIQUE FÉDÉRALE DE LAUSANNE

POUR L'OBTENTION DU GRADE DE DOCTEUR ÈS SCIENCES

PAR

Alberto BIANCOLI

acceptée sur proposition du jury:

Dr S. Mischler, président du jury
Prof. D. Damjanovic, directeur de thèse
Dr P.-E. Janolin, rapporteur
Prof. N. Marzari, rapporteur
Dr D. Rytz, rapporteur

ÉCOLE POLYTECHNIQUE
FÉDÉRALE DE LAUSANNE

Suisse
2014

“There are two possible outcomes: if the result confirms the hypothesis, then you've made a measurement. If the result is contrary to the hypothesis, then you've made a discovery”.

- **Enrico Fermi**

Abstract

In the last years, the needs to replace lead because of environmental and health concerns raised the technological and scientific challenge of the substitution of $PbZr_{1-x}Ti_xO_3$ (PZT) ceramics, the most widely used piezoelectric material which contains more than 60% of lead in weight. Beyond the possibility of finding a lead-free piezoceramics as replacement for PZT, the world-wide research has focused on other mechanisms of electromechanical coupling alternative to piezoelectricity, such as electrostriction and, more recently, flexoelectricity.

Flexoelectric polarization or strain is proportional to elastic strain (or polarization) gradient which scales with the inverse of the size of material, and thus was initially expected to play a major role only on nano-scale. In the past decade however, the experimental finding of large flexoelectric coefficients in ferroelectric ceramics has raised the hope to exploit flexoelectricity for practical applications in bulk materials.

The mechanism of the flexoelectric polarization in bulk ceramics is still far from being fully understood. Above all, the controversy concerns the fact that the values of the flexoelectric coefficients measured in the ferroelectric ceramics exceed by several order of magnitude the theoretical estimations.

During this thesis work, the measurement of the flexoelectric properties in the paraelectric phase of unpoled ceramics of the $Ba_{0.67}Sr_{0.33}TiO_3$ composition, which was reported previously to exhibit the largest flexoelectric polarization ever measured, lead to the uncovering of an electro-mechanical coupling which cannot be ascribed to the flexoelectric response. This electro-mechanical coupling, which was accompanied by pyroelectric response in as-prepared samples, suggests breaking of the macroscopic centric symmetry of the ceramics.

In the effort to understand the mechanism of the symmetry breaking, the solid solutions $Ba_{1-x}Sr_XTiO_3$ (x=0, 0.025, 0.33, 0.40, 0.45, 0.50, 0.67, 0.90, 0.975, 1) were investigated and compared with properties of corresponding single crystals and other ceramic compositions. The study was conducted mainly by means of piezoelectric, pyroelectric and thermally stimulated current (TSC) characterization.

The experiments established that the symmetry breaking is present not only in unpoled ceramics but also in unpoled single crystals and has significant contribution originating from the bulk of the samples. The symmetry breaking in the $Ba_{1-x}Sr_xTiO_3$ solid solution is induced by two mechanisms: the formation or presence of polar defects (ionic vacancies or polar entities) in the ceramics and the alignment of such defects during the densification process. The alignment of the polar defects is induced by an asymmetry in the sintering environment. Possible causes of such an asymmetry can be a tiny thermal gradient or the effect of gravity. The pyroelectric experiments show that the polarization

associated to the breaking of the symmetry settles in after the full densification of the ceramics (about 96%) and cannot be erased by heating even at temperatures higher than the sintering temperature. The amplitude of the pyroelectric current in the (Ba,Sr)TiO_3 ceramics decreases with the decreasing of the barium content and it is not observed for the composition containing 2.5% of barium and in pure $SrTiO_3$ ceramics, suggesting that the defects at the origin of the polarity in $SrTiO_3$ are less pronounced. This is in agreement with X-ray microstrain analysis of (Ba,Sr)TiO_3 and $SrTiO_3$ ceramics processed in the same environment.

The thermally stimulated current studies allowed us to identify two contributions to the macroscopic polarization: the current peaks sensitive to orientation of samples are due to the release of trapped space charges whose direction is determined by the direction of the built-in polarization. It is this trapped charge that is responsible for the time and frequency dependence of the electromechanical response in the phases with broken symmetry. Importantly, the TSC analysis also reveals that $SrTiO_3$ ceramics and single crystals, in which no pyroelectric response is observed at room temperature, are actually polar indicating that the absence of pyroelectric response cannot be taken as the only criterion to exclude the existence of polarity in ceramics and single crystals. The measurements on other crystals show that the breaking of the symmetry is a phenomenon which is not specific to the (Ba,Sr)TiO_3 system but occurs in many other systems (1-x$(Ba_{0.7}Ca_{0.3})TiO_3$-x$Ba(Zr_{0.20}Ti_{0.80}O_3)$, $PbZr_{1-x}Ti_xO_3$, $PbMg_{1/3}Nb_{2/3}O_3$, Ka(Ta,Nb)O_3) both in ceramics and single crystal form.

In this work, it is proposed that the appearance of the polar symmetry in ceramics and single crystals above the Curie temperature is due to asymmetries associated to the high temperature processing of crystals and ceramics. These asymmetries are, in general, difficult to avoid leading to an inhomogeneous distribution of strain and ensuing redistribution of charged defects.

The symmetry breaking in $Ba_{1-x}Sr_xTiO_3$ ceramics and associated electromechanical response that is of the same order of magnitude as the flexoelectric response in the same materials, can at least partly help resolving the controversy existing between the theoretical models of flexoelectricity and the experiments.

Keywords: pyroelectricity, flexoelectricity, ferroelectric, paraelectric, strain, polar defects

Résumé

Récemment, l'exigence de remplacer le plomb en raison des problèmes pour l'environnement et pour la santé a engendré le défi technologique et scientifique de la substitution des céramiques de $PbZr_{1-x}Ti_xO_3$ (PZT), les céramiques piézoélectriques les plus utilisées, contenant plus de 60% en poids de plomb. A part la possibilité de trouver une céramique piézoélectrique sans plomb pour remplacer le PZT, au niveau mondial la recherche est concentrée sur d'autres mécanismes de couplage électromécanique alternatifs à la piézoélectricité, tels que l'électrostriction et, plus récemment, la flexoélectricité.

La polarisation flexoélectrique est proportionnelle au gradient de déformation élastique (ou de polarisation), lequel est, à son tour, proportionnel aux dimensions géométriques de l'échantillon, et donc elle a été considérée initialement avoir un rôle important seulement à l'échelle nanométrique. Cependant, au cours de la dernière décennie, la découverte expérimentale de coefficients flexoélectriques très élevés dans les céramiques ferroélectriques a fait naitre l'espoir de pouvoir utiliser la flexoélectricité pour des applications dans les céramiques massives.

Le mécanisme de la polarisation flexoélectrique dans les céramiques massives est encore loin d'être complètement compris. La débat concerne surtout le fait que les valeurs des coefficients flexoélectriques mesurés dans les céramiques ferroélectriques dépassent les estimations théorétiques des plusieurs ordres de grandeur.

Pendant ce travail de thèse, la mesure des propriétés flexoélectriques dans la phase paraélectrique des céramiques de $Ba_{0.67}Sr_{0.33}TiO_3$ non polarisées, composition laquelle a précédemment été reportée avoir la polarisation flexoélectrique la plus élevée jamais mesurée, conduit à la découverte d'un mécanisme de couplage électromécanique qui ne peu pas être attribué à une réponse flexoélectrique. Ce mécanisme de couplage électromécanique, qui est accompagné aussi par une réponse pyroélectrique dans des échantillons *as-prepared*, suggère un mécanisme de rupture de la symétrie centrique des céramiques.

Dans l'effort de comprendre le mécanisme de rupture de la symétrie, des solutions solides de $Ba_{1-x}Sr_xTiO_3$ (x=0, 0.025, 0.33, 0.40, 0.45, 0.50, 0.67, 0.90, 0.975, 1), ont été caractérisées et comparées avec les monocristaux correspondantes et d'autres compositions céramiques. L'étude a été menée principalement par moyen des caractérisations piézoélectrique, pyroélectriques et des courants stimulés thermiquement (TSC). Les expériences ont établie que la rupture de la symétrie n'est pas seulement présente dans les céramiques non polarisée mais aussi dans des monocristaux non polarisés et elle possède une contribution importante provenant du volume des échantillons.

La rupture de la symétrie dans la solution solide de $Ba_{1-x}Sr_xTiO_3$ est causée par deux mécanismes différents: la formation ou la présence de défauts polaires (lacunes ioniques ou entités polaires) dans les céramiques et alignement de ces défauts pendant le processus de densification. L'alignement des défauts polaires est causé par une asymétrie dans le milieu de frittage. Les causes possibles de cette asymétrie peuvent être un subtil gradient thermique ou l'effet de la gravité. Les mesures pyroélectriques montrent que la polarisation associée à la rupture de la symétrie est établie après la densification complète des céramiques (environ 96%) et elle n'est peu pas être effacée même après chauffage aux températures supérieures à la temperature du frittage. L'amplitude du courant pyroélectrique dans les céramiques de $(Ba,Sr)TiO_3$ diminue avec la diminution de la concentration de barium et elle n'est pas observée dans la composition contenant 2.5% de strontium et dans les céramiques de $SrTiO_3$ pur, fait qui suggère que les défauts à l'origine de la polarité dans le $SrTiO_3$ sont moins concentrés. Cela est in accord avec l'analyse de la microdéformation faite avec les rayons X sur des céramiques de $(Ba,Sr)TiO_3$ et de $SrTiO_3$, produites dans le même milieu.

Les analyses des courants stimulées thermiquement nous ont permis d'identifier deux contributions à la polarisation macroscopique: les pics de courants sensibles à l'orientation des échantillons sont causés par la relaxation des charges spatiales piégées orientées dans la direction déterminée par la polarisation built-in dans les céramiques. Cette charge piégée est responsable de la dépendance temporelle et en fréquence de la réponse électromécanique dans les phases dans lesquelles la symétrie est absente.

Remarquablement, l'analyses de TSC montre aussi que les céramiques et les monocristaux de $SrTiO_3$, dans lesquelles aucune réponse pyroélectrique n'a été mesurée à temperature ambiante, sont en réalité polaires et indique que l'absence d'une réponse pyroélectrique n'est peut pas être considérée comme le seule critère d'exclusion de l'existence de polarité dans les céramiques et les monocristaux. Les mesures sur d'autres cristaux montrent que la rupture de la symétrie est un phénomène qui n'est pas seulement présent dans le système $(Ba,Sr)TiO_3$mais aussi dans plusieurs autres systèmes $(1-x)(Ba_{0.7}Ca_{0.3})TiO_3$-$xBa(Zr_{0.20}Ti_{0.80}O_3)$, $PbZr_{1-x}Ti_xO_3$, $Pb(Mg_{1/3}Nb_{2/3})O_3$, $Ka(Ta,Nb)O_3$) soit sous forme de céramiques ou de monocristaux.

Dans ce travail, il est proposé que l'apparition d'une symétrie polaire dans les céramiques et les monocristaux au-dessus de la temperature de Curie soit causée par des asymétries associées avec le procédé de fabrication des cristaux et des céramiques à haute temperature. De telles asymétries sont, en général, difficiles à éviter et conduisent à une distribution non homogène de déformation causant une redistribution des défauts.

La rupture de la symétrie dans les céramiques $Ba_{1-x}Sr_xTiO_3$, conduit à une réponse électromécanique associée ayant le même ordre de grandeur que la réponse flexoélectrique mesuré dans le même matériau et peuvent, au moins en partie, aider à

résoudre le débat existant entre le modèle théorétique de la flexoelectricité et les mesures expérimentales.

Mots-clef: pyroélectricité, flexoelectricité, ferroélectrique, paraélectrique, déformation, défauts polaires.

Riassunto

Negli ultimi anni, l'esigenza di sostituire il piombo a causa di problemi ambientali e sanitari ha sollevato la sfida tecnologica e scientifica di rimpiazzare i ceramici di $PbZr_{1-x}Ti_xO_3$ (PZT), i ceramici piezoelettrici maggiormente utilizzati, che contengono piu' del 60% in peso di piombo. A parte la possibilità di trovare dei ceramici piezoelettrici senza piombo in sostituzione del PZT, a livello mondiale la ricerca si è concentrata su altri meccanismi di accoppiamento elettromeccanico alternativi alla piezoelettricità come l'elettrostrizione e, piu' recentemente, la flessoelettricità.

La polarizzazione flessoelettrica è proporzionale al gradiente di deformazione elastica (o di polarizzazione), il quale è a sua volta proporzionale all'inverso delle dimensioni del materiale e, per questa ragione, è stata inizialmente ritenuta avere un effetto importante solamente su scala nanometrica. Nel corso dell'ultimo decennio tuttavia, la scoperta sperimentale di elevati coefficienti flessoelettrici in alcuni ceramici ferroelettrici ha suscitato la speranza di poter utilizzare la flessoelettricità per applicazioni pratiche anche nei materiali di bulk.

Il meccanismo della polarizzazione flessoelettrica nei ceramici di bulk è ancora lontano dall'essere pienamente compreso. La controversia riguarda soprattutto il fatto che i coefficienti misuarati nei ceramici ferroelettrici superano di diversi ordini di grandezza le stime teoriche.

La misurazione delle proprietà flessoelettriche, effettuata nel corso di questa tesi, su dei ceramici non polarizzati in fase paraelettrica di $Ba_{0.67}Sr_{0.33}TiO_3$, composizione per la quale, in precedenza, è stata riportata la polarizzazione flessoelettrica piu' elevata mai misurata, ha portato alla scoperta di un meccanismo di accoppiamento elettromeccanico che non puo' essere attribuito alla flessoelettricità. Tale accoppiamento elettromeccanico, associato anche ad una risposta piroelettrica in campioni *as-prepared*, suggerisce una rottura macroscopica della simmetria centrica dei ceramici.

Nel tentativo di comprendere il meccanismo di rottura della simmetria, le soluzioni solide di $Ba_{1-x}Sr_XTiO_3$ (x=0, 0.025, 0.33, 0.40, 0.45, 0.50, 0.67, 0.90, 0.975, 1) sono state studiate e confrontate con le proprietà dei rispettivi monocristalli e con altre composizioni ceramiche. Lo studio è stato condotto principalmente mediante caratterizzazione piezolettrica, piroelettrica e della corrente termo-stimolata (TSC).

Gli esperimenti hanno stabilito che la rottura della simmetria è presente non soltanto nei ceramici non polarizzati ma anche in monocristalli non polarizzati e ha un importante contributo che trae origine dal volume dei campioni. La rottura della simmetria nella soluzione solida di $Ba_{1-x}Sr_XTiO_3$ è causata da due meccanismi: la formazione o la presenza nei ceramici di diffetti polari (vacanze ioniche o entità polari) e l'allineamento di questi difetti nel corso del processo di densificazione. L'allineamento dei

difetti polari è indotto da un'assimmetria presente nell' ambiente di sinterizzazione. Le possibili cause di questa assimmetria sono un piccolo gradiente di temperatura o l'effetto della gravità.

Gli esperimenti pirolettrici indicano che la polarizzazione associata alla rottura della simmetria si consolida dopo la completa densificazione dei ceramici (circa il 96 %) e non puo' essere eliminata anche a temperature piu' elevate della teamperatura di sinterizzazione. L'ampiezza della corrente piroelettrica nel (Ba,Sr)TiO_3, diminuisce con la diminuzione del contenuto di bario e non è osservata nella composizione contenente il 2.5% di stronzio e nel $SrTiO_3$ puro, circostanza che suggerisce che i difetti all'origine della polarità sono meno pronunciati. Cio' è in accordo con l'analisi della microdeformazione mediante raggi X dei ceramici di (Ba,Sr)TiO_3 e $SrTiO_3$ prodotti nello stesso ambiente.

Le corrente termo-stimolata ha permesso di identificare due contributi alla polarizzaione macroscopica : i picchi nella corrente che dipendono dall'orientazione dei campioni sono dovuti alla rilascio di cariche spaziali intrappolate la cui direzione è determinata dalla direzione della polarizazione di built-in. Queste cariche intrappolate sono le responsabili della dipendenza temporale e in frequenza della risposta elettromeccanica nelle fasi in cui la simmetria é scomparsa. L'aspetto importante è che l'analisi della TSC dimostra anche che i ceramici e i monocristalli di $SrTiO_3$, nei quali nessuna risposta piroelettrica è rilevata a temperatura ambiente , sono , in realtà polari e indica che, l'assenza di una risposta piroelettrica non puo'essere presa come l'unico criterio per escludere la presenza di polarità nei ceramici e nei monocristalli. Le misurazioni in altri cristalli mostrano che la rottura della simmetria è un fenomeno che non è specifico del sistema (Ba,Sr)TiO_3 ma è presente in altri sistemi (1-x($Ba_{0.7}Ca_{0.3}$)TiO_3-x$Ba(Zr_{0.20}Ti_{0.80}O_3)$, $PbZr_{1-x}Ti_xO_3$, $Pb(Mg_{1/3}Nb_{2/3})O_3$, Ka(Ta,Nb)O_3), sia nella forma di ceramico che in quella di monocristallo.

In questa tesi si propone che la comparsa di una simmetria polare nei ceramici e nei monocristalli al di sopra della temperatura di Curie è causata da delle asimmetrie insite nell processo di produzione ad alta temperatura dei ceramici e dei monocristalli stessi. Queste asimmetrie , in generale, sono difficili da evitare e conducono ad una distribuzione della deformazione non omogenea che risulta in una redistribuzione dei difetti. La rottura della simmetria nei ceramici di $Ba_{1-x}Sr_xTiO_3$ è associata ad un a risposta elettromeccanica dello stesso ordine di grandezza della risposta flessoelettrica negli stessi materiali, puo' aiutare a risolvere, almeno in parte, la controversia esistente tra il modello teorico della flessoelettricità e gli esperimenti.

Parole chiave: piroelettricità, flessoelettricità, ferroelettrico, paraelettrico, deformazione, difetti polari

Acknowledgements

First of all, I would like to thank my thesis director Prof. DRAGAN DAMJANOVIC, who gave me the possibility to work in the Ceramic Laboratory and introduced me to the challenging but interesting world of ferroelectrics. I am deeply grateful to him for the small part of his huge knowledge of the field which he transferred to me. I am glad for all he taught to me, especially because from him I learnt that, the answer to the very basic questions often bring the most surprising results.

Above all, I am in debt with him because from him I learned how a scientist should think, a lesson which I will never forget.

I wish to express my gratefulness to the members of my committee, Dr. PIERRE-EYMERIC JANOLIN, Dr. DANIEL RYTZ and Prof. NICOLA MARZARI, for reading the manuscript with very careful eye and for their questions, which for me were the most genuine expression of the deep interest they had for my work.

I would like also to acknowledge Prof. NAVA SETTER who provided an enjoyable working ambience in the laboratory and during these four years organized very interesting seminars where I had occasion to meet some of the most prominent experts in the field of ferroelectrics scientific community. I am grateful also to Prof. PAUL MURALT for the discussions about politics and history during lunch time which helped my mind to evade a bit from my daily “fight” against barium strontium titanate and to Prof. ALEKSANDER TAGANTSEV for his advices on hiking during the LC trips. I would like to thank both for the useful comment they always had during seminars and group meeting which were very effective in clarifying even the most difficult topics and helped me to” get the point”.

I also grateful to Mr. JACQUES CASTANO, who was very helpful in the first phase of the thesis when I had to learn how to deal with the ceramics processing and who found always very practical solutions to the technical problems of the processing, and to Mr. LINO OLIVETTA for helping me to fix many small issues with the instruments which always are encountered during the experimental work.

A special thank goes to my friends in the LC, ANDREA for the long discussions in front of a beer and for the funny moments shared in those years, DAVIDE and RAMIN

I want also to thank my mates of the MXD 220 office “the coolest office in LC” ALEX and ANIRBAN with whom I moved the first steps in the “odyssey“of the PhD more than 4 years ago

I want also to acknowledge all the pervious and the current members of the LC who I meet during my work, especially NACHI, TOMAS, ARNAUD, BARBARA, LEO, LUDWIG, KAUSHIK, PETR Y and MONIKA.

A big hug goes to all my friends across Europe and around the rest of the world: you are too numerous to be listed here but you know who you are.

At last but not least, the deepest thanks go to my parents, LUISELLA and GIORDANO who believed in me constantly and sometime even more than what I did. Without you this thesis would have never been written. All what I am, I owe to you

Alberto Biancoli

Lausanne 2014

Contents

Chapter 1 : Background, statement of the problem and thesis outline

1.1 Introduction

This chapter has the purpose to present to the reader the statement of the problem which motivated the work of this thesis and to introduce the background in which this problem has been originated. Initially, the concepts of ferroelectric materials and their polar properties such as pyroelectricity and piezoelectricity are introduced and the restrictions imposed by the crystal symmetry on these properties in single crystals and polycrystalline materials are discussed. It is shown that in reality, cases of symmetry breaking in which the materials exhibit properties in principle not allowed by their nominal symmetry are not uncommon. In particular the attention will be focused on the breaking of the symmetry in the paraelectric phase of ferroelectrics. In this context, a brief review from the early observations of the non-centrosymmetric character of the paraelectric phase until recently revived mechanisms of symmetry breaking such has flexoelectricity is given. Finally, the outline of the thesis is presented.

1.2 Ferroelectricity in perosvkite oxides and ferroelectric domains

A ferroelectric is a material which, in the absence of any external electric field exhibits a *spontaneous polarization* which can be reversed by the application of an electric field [1]. The presence of two (or more) equilibrium orientations of the polarization is intimately related to the symmetry of the material and the phase transition between a high symmetry paraelectric and lower symmetry ferroelectric phase. Ferroelectricity was first identified in sodium potassium tartrate tetrahydrate ($NaKC_4H_4O_6$*$4H_2O$), better known as Rochelle salt by Valasek in 1921 [2]. Initially, the interest about ferroelectricity as phenomenon deserving a deeper investigation was low. The situation changed in the 1940's, when ferroelectricity was reported in $BaTiO_3$, which has a much simpler structure than Rochelle salt [3]. The $BaTiO_3$ has, in fact, the same structure as mineral perosvkite, $CaTiO_3$. The perovskite structure is common to a wide number of other oxides. The discovery of ferroelectricity in $BaTiO_3$ was a breakthrough and encouraged the idea that ferroelectricity was a phenomenon much more widely spread in nature then what was previously thought. In fact, shortly after $BaTiO_3$, ferroelectricity was reported in other perosvkite oxides such as $KNbO_3$, $KTaO_3$ (1949)[4] and $PbTiO_3$(1950)[5].

The perosvkite oxides have a general chemical formula ABO_3 were the A site is occupied by a metal cation with a larger ionic radius and the B position by a metallic cation with a smaller ionic radius and O is oxygen.

In most cases, the crystallographic structure of the perosvkite is idealized with a cubic unit cell with the larger cation (with valence from +1 to +3) in the A site at the corners of the cube and the smaller cation (with valence from +3 to +6) in the B site located in the cube's center. The B cation is in octahedral coordination with the oxygen atoms occupying the center of the faces of the unit cell (Figure 1.1)

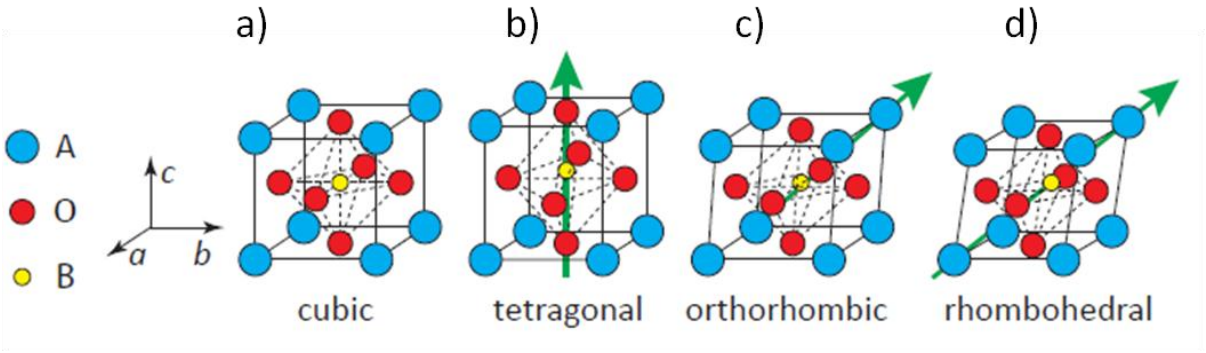

Figure 1.1-Structure of the perosvkite cubic unit cell (a) and tetragonal (b), orthorhombic (c) and rhombohedral (d) ferroelectric distortions. Adapted from [6]

In general most ferroelectrics undergo a structural phase transition from a high temperature non-ferroelectric (*paraelectric phase*) which has usually a cubic symmetry, to a low temperature ferroelectric phase. Tetragonal, orthorhombic and rhombohedral are the most common symmetries for the ferroelectric phases encountered in many oxides (Figure 1.1). The temperature at which the paraelectric to ferroelectric transition occurs is called the *Curie temperature* (T_C). The ferroelectric to paraelectric and the other ferroelectric to ferroelectric phase transitions can be described as distortions of the ideal perosvkite cubic cell where all the cations may move with respect the equilibrium positions of the cubic cell.

While most ferroelectrics exhibit a paraelectric to ferroelectric phase transition at T_c, not all experience ferroelectric to ferroelectric phase transitions below their Curie temperature. For example $BaTiO_3$ posses three different ferroelectric phases (tetragonal, orthorhombic and rhombohedral) while $PbTiO_3$ remains in a tetragonal ferroelectric phase below T_c [7].

In a material which undergoes phase transition from the cubic paraelectric phase to a tetragonal ferroelectric phase, for example, the *spontaneous polarization* may develop along one of the six directions corresponding to the three crystallographic axes of the cube (including the positive and negative orientations). The orientation along which the polarization arises depends on the electrical and mechanical boundaries conditions

imposed to the crystal. In general however, the ferroelectric polarization is not uniformly aligned in the same direction across the whole crystal. The regions, where the spontaneous polarization has a uniform orientation are called *ferroelectric domains.* The domains are separated by a region which is called *domain- wall* (Figure 1.2).

The domain-walls are identified by the orientation of the polarization in the two adjacent domains. For example, the domain-walls separating two domains with a polarization oriented in opposite directions are referred to as 180^o walls while those separating domains with mutually perpendicular polarization are 90^o walls.

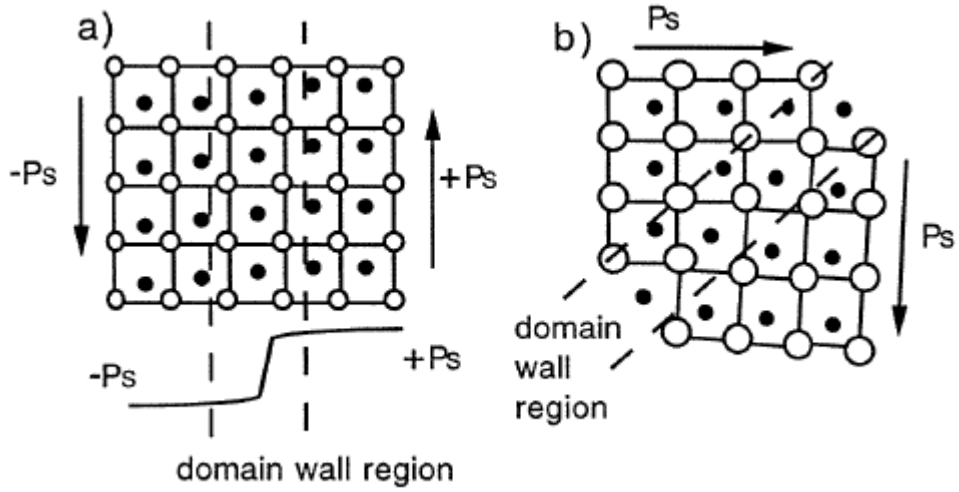

Figure 1.2-Illustration of 180^o (a) and 90^o (b) domains and domain-wall regions in a ferroelectric tetragonal crystal lattice. The arrows indicate the orientation of the spontaneous polarization. Taken from [8]

The ferroelectric domains form to minimize the electrostatic energy of the *depolarizing field* which develops opposite to the spontaneous polarization and the elastic energy coming from the constraints to which the ferroelectric crystal is subjected when cooled below T_c.

Having an intrinsic polar axis, the ferroelectric crystals exhibit also other polar and non-centrosymmetric properties such as pyroelectricity and piezoelectricity.

1.3 Pyroelectricity and piezoelectricity

Pyroelectricity is the relation between the change in the spontaneous polarization P and the change in the temperature ΔT. The coupling coefficient between the polarization (a vector) and the temperature (a scalar) is the pyroelectric coefficient p which is therefore expressed by a first rank tensor:

$$P_i = p_i \Delta T \quad (1.1)$$

where the P_i is the spontaneous polarization along a given direction i. The units of the pyroelectric coefficient are ($C\,K^{-1}\,m^{-2}$)
Piezoelectricity is the linear coupling between the polarization and the elastic stress or strain and electric field. The *direct piezoelectric* effect is written in tensor form as:

$$D_i = d_{ijk}\sigma_{jk} \quad (1.2)$$

where d_{ijk} is the piezoelectric coefficient, a third rank tensor coupling the charge density D_i (first rank tensor) to the elastic stress σ_{jk}, represented by a second rank tensor. The equation 1.2 describes the ability of a material to produce charge upon the application of a mechanical excitation. The direct piezoelectric coefficient is measured in $C\,N^{-1}$.
Piezoelectric materials can also change their dimensions when they are subjected to an external electric field, exhibiting the so called *converse piezoelectric effect*. The expression for converse piezoelectricity is:

$$x_{ij} = d_{kij}E_k \quad (1.3)$$

In the equation 1.3, x_{ij} is the elastic strain, E_k the electric field and d_{kij} is the converse piezoelectric coefficient. The units for the converse piezoelectric effect are $m\,V^{-1}$.
On the basis of thermodynamic arguments, it can be shown, that the coefficients for the direct and the converse piezoelectric effect are equal [9].
The fact that pyroelectricity and piezoelectricity are described by odd rank tensors, respectively of the first and of the third rank, imposes important restrictions on the symmetry of the crystals which can exhibit such properties. The relations and between the symmetry and the physical properties of the crystal are discussed in the next section.

1.4 Physical properties of the crystals and symmetry

The physical properties which a crystal can, in principle exhibit, are strictly dependent on the symmetry of its crystallographic structure. The important criterion, which must be always satisfied by all physical properties of a crystal, is contained in the Neumann's principle which states that *"the symmetry of any physical property of the crystal must include the symmetry elements of the point group of the crystal"* [9].

According to the symmetry operation with respect to a point, the crystals are classified in 32 *points group*. Among them, 10 have a unique polar axis and are therefore

referred as polar point groups. From Neumann's principle it follows that only crystals belonging to one of the polar groups can show pyroelectricity and ferroelectricity. To be observed pyroelectricity simply requires the presence of a unique polar axis in the crystal while to have ferroelectricity, the existence of at least two stable directions of spontaneous polarization is needed. As a consequence, all crystals which are ferroelectric are also pyroelectric but not all pyroelectric crystals exhibit ferroelectricity.

To exhibit piezoelectricity, a crystal should belong to a point group which does not have a center of symmetry in its point group. Out of 32 crystal point groups, 21 of them are non centro symmetric (including the 10 polar point groups). Piezoelectricity is possible in 20 of them being suppressed in the non centro-symmetric 432 cubic class where the charges which develop along the [111] direction cancel each others.

Most of the common ferroelectric crystal such as $BaTiO_3$ and $PbTiO_3$ crystal in the paraelectric phase have a symmetry belonging to a centro-symmetric point group and on the basis of what was discussed above, should not show any property which requires the absence of the center of inversion (e.g., second harmonic generation, pyroelectricity and piezoelectricity).

The restrictions discussed up to this points concern the relations between the properties and the symmetry of a single crystal. However, the crystal point groups with discrete symmetry elements are not enough to describe the properties of amorphous and polycrystalline materials. For example, in ceramics with crystallites (or grains) with a random orientation, the macroscopic properties are the same in all directions and therefore they exhibit higher symmetry than the symmetry of the point groups of each individual grain.

To describe the relation between the symmetry and the properties in amorphous and polycrystalline materials, 7 Curie groups or limit groups have been introduced. They are listed in Table 1.1.

Curie group	Symmetry operator
∞	$\infty \parallel Z_3$
∞m	$\infty \parallel Z_3, m \perp Z_1$
$\infty 2$	$\infty \parallel Z_3, 2 \parallel Z_1$
∞ / m	$\infty \parallel Z_3, m \perp Z_3$
∞ / mm	$\infty \parallel Z_3, m, \perp Z_3, m \perp Z_1$
$\infty\infty$	$\infty \parallel Z_3, \infty \parallel Z_1$
$\infty\infty m$	$\infty \parallel Z_3, \infty \parallel Z_1, m \perp Z_1$

Table 1.1-Symmetry operations of the 7 Curie or limit groups which describe the properties of polycrystalline and amorphous materials.

All the Curie groups have a common symmetry element, the rotation axis of infinite order, whose symbol is ∞, which implies that the material can be rotated by any angle without changing its properties.

The non poled ferroelectric ceramics, with randomly oriented grains and/or ferroelectric domains belong to the $\infty\infty m$ Curie group (described geometrically by a sphere) and therefore they are not expected to exhibit pyroelectricity and piezoelectricity on the macroscopic scale (Figure 1.3 a). Nevertheless the spontaneous polarization of each individual ferroelectric domain can be reoriented in a stable way upon the application of an electric field. This is so because polarization in a ferroelectric material has at least two equilibrium directions. This process is called *poling.* After poling, the ferroelectric ceramics acquire the symmetry of the polar Curie group ∞m (geometrically described by a cone) and shows macroscopic pyroelectricity and piezoelectricity (Figure 1.3 b).

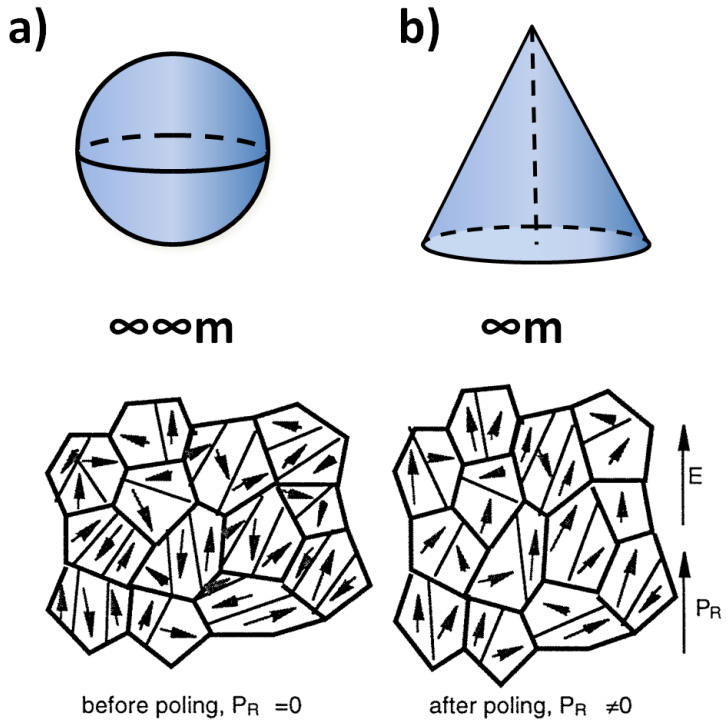

Figure 1.3-The macroscopic symmetry of a ferroelectric ceramics before poling is that of ∞∞m Curie group (a). The application of the electric field E orients the ferroelectrics domains along the same direction and breaks the spherical symmetry. In the conic ∞m Curie group (b) the ferroelectric ceramics acquire a spontaneous polarization P_R and can therefore exhibit pyroelectricity and piezoelectricity. Note that in the ∞m Curie group only d_{33} (longitudinal), d_{31} (transversal), and d_{15} (shear) piezoelectric coefficients are non-zero even in the case that the crystal point group of each individual grain would allow more than three non-zero piezoelectric coefficients.

In real single crystals and ceramics, the situation is rather far from the ideal model presented above and violations of the relation between the symmetry and the properties can be observed. The understanding of this symmetry breaking is very complex because, in different cases, it might be caused by different mechanisms acting on different scales.

1.5 Mechanisms of symmetry breaking in the ferroelectric and the paraelectric phases of ferroelectrics on microscopic and macroscopic scales

In this section, a brief overview on the breaking of the expected symmetry in ferroelectrics is outlined. Since the argument is very broad and complex, the discussion is focused mainly on the case of non centro-symmetric character of the paraelectric phase of ferroelectrics, which is relevant to the results of this work.

Before discussing symmetry breaking in the paraelectric phase, it should be mentioned that, even for the ferroelectric phase of unpoled ferroelectrics (such as ceramics and polycrystalline thin films), where cases of unexpected macroscopic polarity

are observed, the mechanism of symmetry breaking is not well understood and remains still an argument of great debate[10].

Self polarization, in other words, the presence of a non-zero remnant polarization without any poling treatment, is commonly reported in ferroelectrics thin films. Cases of self poling are observed in different systems like ferroelectric $Pb(Zr_{1-x}Ti_x)O_3$ [10], $BaTiO_3$ [11], $BiFeO_3$ [12, 13] and relaxor $Pb(Mg_{1/3}Nb_{2/3})O_3$.[14] In each specific example, the self polarization is attributed to very different origins, such as the degree of texture of the films, the inhomogeneous distribution and concentration of defects and impurities and the different properties of the top and bottom electrodes. Most of the earlier explanations of self-polarization in films were based on electrical properties of the film and the electrodes. More recently, however, the strain gradient induced by the substrate into the film itself has been identified as an important factor responsible for the self-polarization. The inhomogeneous strain gradient has been thus reported as the origin for upward self polarization in epitaxial $BaTiO_3$ films [11]. More recently, self poling has been observed also in the ferroelectric phase of bulk ceramics [15].

The mechanisms of symmetry breaking in the paraelectric phase of ferroelectrics are even more disputed.

On the microscopic scale, the local disappearance of the center of symmetry in the paraelectric phase of ferroelectrics is often associated with the presence of *polar regions* or *polar clusters* with local non-zero polarization within the main paraelectric matrix. The global symmetry of the material remains centrosymmetric. These regions or cluster are common to a wide number of ferroelectric perovskites like $BaTiO_3$, $KNbO_3$ [16], $PbTiO_3$ [17] and are thought to be responsible for the mixed displacive and order-disorder character of the ferroelectric to paraelectric phase transition [18]. In $BaTiO_3$ single crystals and ceramics, it has been proposed that the polar regions are related to the observation of second harmonic generation (SHG) [19-22]; SHG is possible only in the absence of the center of inversion. The existence of polar regions or clusters is consistent with the observations of non linear properties [23], birefringence [24], piezoelectricity [25] deviation of the dielectric permittivity from the expected Curie-Weiss law and acoustic anomalies [26] in paraelectric $BaTiO_3$.

Evidences of the existence of polar regions or clusters above T_c have been provided by a wide number of studies carried out with different techniques such as Raman [16, 27] and Brillouin scattering [28] and X rays absorption fine structure (EXAFS) [29].

However, the polar regions or cluster are local distortions of the symmetry of the cubic lattice, involving the presence of polarization only on the microscopic scale and are not expected, in the absence of field (electric or elastic) to align and lead to a macroscopic polarization.

On the other hand, examples of induced macroscopic polarization in the paraelectric phase of ferroelectrics upon the application of an external electric field are

well known. We except here cases of field induced ferroelectricity which may happen at sufficiently high fields a few degrees above the T_c.

In the paraelectric phase of $BaTiO_3$ and $PbTiO_3$ single crystals, converse piezoelectricity under the application of an electric field was associated to the dynamics of the polar regions [25]. Poled $BaTiO_3$ ceramics were reported to show a piezoelectric resonance upon heating from the ferroelectric phase well above the Curie temperature [30]. More recently, persistent piezoelectric activity, attributed to polar cluster induced by inhomogeneities or chemical defects has been observed in poled $50(Ba_{0.7}\text{-}Ca_{0.3})TiO_3\text{-}50Ba(Ti_{0.8}Zr_{0.2})O_3$ ceramics up to about 30°C above the paraelectric to ferroelectric phase transition [31]. Further examples have been reported in PZT and $Bi_{1/2}Na_{1/2}TiO_3$ based piezoceramics [32].

It is also possible, that the breaking of the symmetry in the centrosymmetric phase is induced by the application of an elastic field. Almost 50 years ago Scott [33] reported that centrosymmetric crystals of $CaWO_4$ and $CaMoO_4$ under strain show infrared and Raman vibration modes which are inactive in unstrained conditions.

In the recent year a new type of symmetry breaking based on the application of elastic strain gradients has been proposed theoretically [34] to be exploited in design of meta-materials which can exhibit piezoelectricity even if all their components are centro-symmetric. The effect involved in the symmetry breaking is *flexoelectricity.*

The flexoelectric effect can be defined as the linear coupling between the polarization and the gradient of the elastic strain (*direct flexoelectric effect*) (Equation 1.4) or the coupling between the elastic stress and the gradient of the electric field (*converse flexoelectric effect*) (Equation 1.5). In tensor notation, it can be written as:

$$P_i = \mu_{ijkl} \frac{dx_{jk}}{dz_l} \qquad 1.4$$

$$\sigma_{ij} = \mu_{ijkl} \frac{dE_k}{dz_l} \qquad 1.5$$

where the P_i is the polarization, x_{jk} and σ_{ij} are respectively the elastic strain and elastic stress, (d/dz_l) is the gradient along the direction z_l and μ_{ijkl} are the direct and converse flexoelectric coefficients. On the basis of thermodynamic arguments, it can be shown that the direct and converse flexoelectric coefficients are equal. The flexoelectric coupling coefficients are tensors of the fourth rank and therefore flexoelectricity, like electrostriction, is a property which can be present in all insulating materials, even in those with a crystal structure belonging to a centro symmetric point group.

The flexoelectric effect was identified in the 1950's by Mashkevic and Tolpygo [35]. In 1964 Kogan [36] gave the first phenomenological framework for the description of flexoelectricity. In the early studies of flexoelectricity, the attention was not immediately

focused on ferroelectrics. In the late 1960's, Bursian and coworkers, characterized the flexoelectric effect in the classical ferroelectric $BaTiO_3$ demonstrating the switching of the polarization promoted by the stain gradient [37].They were also the first to show that the flexoelectric effect is enhanced in materials with high dielectric permittivity [38]. This finding had an important role in the development of the whole field.

In 1981, Indebom developed the first Landau type theory of the flexoelectric effect in ferroelectrics [39]. In fact, Indenbom was the first to use the term flexoelectricity applied to solids, borrowing it from the physics of liquid crystals where it describes a similar phenomenon. Before him, the effect was sometimes referred as "non-local piezoelectricity". Such a terminology reflected the fact that the flexoelectric effect was approached as analog to the piezoelectric effect. The situation was changed by the work of Tagantsev in the late 1980's [40, 41], who demonstrated that there are no trivial dynamic and surface contributions to the flexoelectric effect. He also developed a simple theoretical framework, based on a rigid ionic model, for the calculation of the flexoelectric coefficients from the dynamical matrix of the crystals. No consensus has been reached on phenomenological description of even simplest materials as illustrated by a recent paper of Resta [42]. A comprehensive theory using *ab-initio* approach has been published while our work was ongoing [43].

The flexoelectric effect has attracted very small interest until recent times, because it was expected to be, in general, very small in bulk, solid materials. A new research interest in flexoelectricity has started to grow in last few years and it develops along two main directions.

On one side, the fact that the flexoelectric polarization is coupled with the strain gradient which is inversely proportional to the size of the material, together with the development of the techniques of micro and nano-fabrication, has generated interest in the research on flexoelectricity in thin films. In thin films, especially the epitaxial ones, the flexoelectric effect is not only large but it can be modulated through the control of the strain gradient (stain gradient engineering) and it can have significant influence on the ferroelectric polarization [44]. Catalan et al suggested significantly high flexoelectric polarization associated to strong lateral strain gradients in twinned a and c ferroelectric domains in epitaxial films of $PbTiO_3$ [45]. The presence of a lateral flexoelectric polarization causes the ferroelectric polarization in c domains to rotate away from the direction normal to the substrate. The authors suggest that such tilted polarization can lead to an enhanced piezoelectric effect, in analogy to what has been shown for morphotropic phase boundary systems. [46, 47]. The flexoelectric effect has also been used to mechanically switch by 180° the polarization in ferroelectric domains in $BaTiO_3$ ultrathin films without application of any electric field [48]. Recently Sharma et al [49] proposed a strategy to realize in thin films the concept of piezoelectric meta-materials made of non piezoelectric components discussed by Fousek et al [34]. The macroscopic

piezoelectricity is achieved with odd order layered structures (i.e. superposition of three different layers).

On the other side, the systematic studies of the flexoelectric effect in bulk ferroelectrics have shown unexpectedly high values for the flexoelectric coefficients opening new perspectives for the exploitation of the flexoelectric effect on the macroscopic scale [50-53]. It was believed that these results would open path for realization of large piezoelectric-like effect in non piezoelectric lead free materials.

Composites using the flexoelectric effect to produce effective piezoelectric charge large enough for practical applications were produced and tested at the Pennsylvania State University [54, 55] (Figure 1.4). These meta-materials are based on the $Ba_{0.67}Sr_{0.33}TiO_3$, the composition which exhibits the highest values of the flexoelectric coefficients measured until now [52]. In the composites produced up to now, an effective piezoelectric coefficient of 40 pC/N has been measured via the converse flexoelectric effect [54].

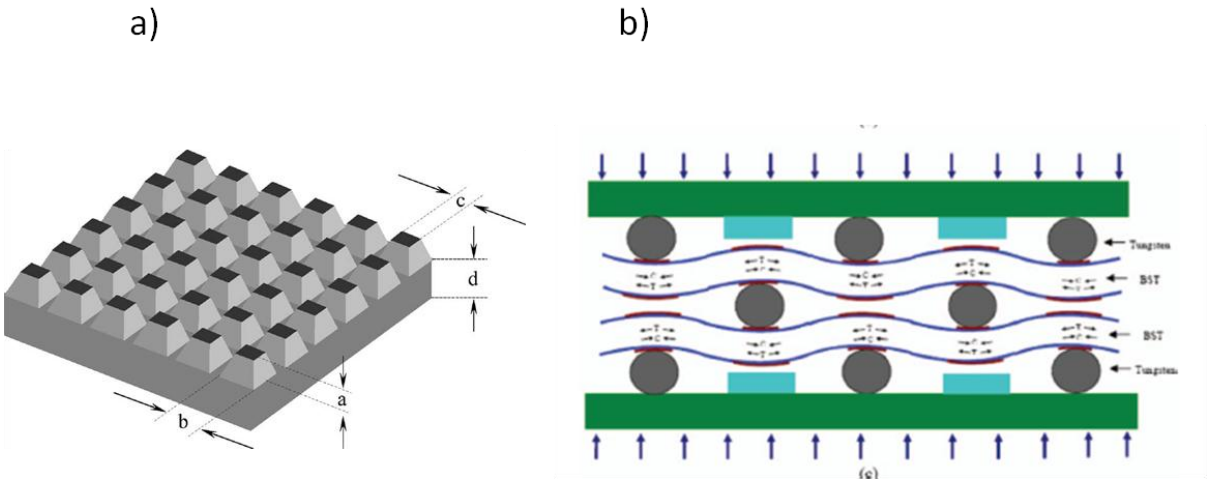

Figure 1.4-Schematic of two different types of piezoelectric composites based on the flexoelectric effect: a) a periodical array of truncated pyramids exploiting the longitudinal flexoelectric effect [54]. b) Cross section, under stress conditions of a flexure mode composite, producing piezoelectric charge through the transverse flexoelectric effect [55].

Despite the advances made in the research on flexoelectricity in recent years, the flexoelectric effect in solids is still far from being fully understood, especially in ceramics. While in $SrTiO_3$ single crystals, all the three non zero components of the flexoelectric tensor are in excellent agreement with the theoretical estimations [56], in ferroelectric ceramics of other classical ferroelectric systems such $BaTiO_3$ and $PbZr_{1-x}Ti_xO_3$, the flexoelectric coefficients exceed by two to three orders of magnitude the theoretical predictions [57]. This large discrepancy between the values of the components of the flexoelectric tensor predicted theoretically with those measured experimentally in bulk ferroelectrics is the main aspect that needs to be clarified. The experimental values reported are in fact so large that they raise the question about their compatibility with the

criteria for the stability of the perosvkite structure [58]. It is therefore possible that other mechanisms interfere with the flexoelectric polarization in ferroelectrics. In this direction, it was recently shown that during homogeneous bending of a non polar dielectric, a piezoelectric surface contribution proportional to the bulk dielectric constant of the material, is present [59]. In high dielectric constant materials, such as ferroelectrics, the surface piezoelectric contribution might screen the weaker flexoelectric contribution of the bulk and be misidentified as flexoelectricity. A part of the discrepancy between theoretical and experimental results has been accounted for by different boundary conditions normally used in experiments and assumed in theoretical derivations [43]. However, the origin of the extremely large experimental values of flexoelectric coefficients in paraelectric phase of some ferroelectric materials remains unexplained.

1.6 Thesis context and outline

From what it is discussed in the previous sections, it appears clear that, in the investigation of ferroelectrics oxides, the general assumption that the paraelectric phase is centrosymmetric should be evaluated very carefully. Clearly, the ideal cubic, paraelectric structure is crystallographically centrosymmetric. However, the real materials are not ideal. This aspect becomes particularly important in the study of the flexoelectric effect. The unexpectedly high flexoelectric polarization reported recently in the paraelectric phase of ferroelectrics ceramics differs significantly from the theoretical predictions and suggests that probably other mechanisms, not necessarily flexoelectric in origin, might contribute to the measured charge. Ferroelectric ceramics are systems that are very sensitive to the parameters related to different preparation steps and the concentration and the type of defects, among others. Even in ferroelectric single crystals, the growth process may introduce defects and inhomogeneities that are not expected or obvious. It is therefore not unusual that properties of ferroelectric materials are affected significantly by these extrinsic contributions. The identification and separation of these contributions is needed in the final goal of understanding the mechanism of flexoelectric polarization and to quantify correctly its magnitude in ferroelectric materials, in particular ceramics.

We started our work in 2010 with experiments to confirm the large direct flexoelectric effect in paraelectric $Ba_{0.67}Sr_{0.33}TiO_3$ ceramics. Up to that date, to our knowledge, this large response has not been independently examined since the original measurements made at the Pennsylvania State University. Our plan was to investigate the whole $Ba_{1-x}Sr_xTiO_3$ solid solution and look for crystal chemistry parameters that may give clues on the origins of the unexpected flexoelectric behavior. The preliminary experiments indicated an order of magnitude of the electromechanical response in the paraelectric phase of $Ba_{0.67}Sr_{0.33}TiO_3$ that was in agreement with the reports by the Penn State group.

However, observations made on samples in shape of trapezoids and disks of the same composition suggested that the origin of the electromechanical coupling could not be ascribed purely to the flexoelectric effect. This conclusion leads us to investigate closely the nature of the large response observed and to reveal the existence of polarization in the paraelectric phase of unpoled ceramics. The detection of the macroscopic polar symmetry in the paraelectric ceramics changed, quite significantly, the direction of our initial plan to study flexoelectric effect in ceramics and raised the fundamental questions about the causes of the unexpected symmetry breaking. We thus focused our study on origins of the symmetry breaking. To answer these questions ceramics and single crystals of different ferroelectrics and non ferroelectric materials were investigated with different techniques.

The thesis is organized according to the following outline:

In **Chapter 2**, the processing method of the ceramic materials used in the study and the techniques employed to characterize their structure and their dielectric properties are described.

In **Chapter 3** a short overview of the measurements methods used for investigation of ceramics and single crystals are given and the principles and limits of the measurement techniques are briefly discussed.

In **Chapter 4**, the results of the investigation of the direct flexoelectric response of the paraelectric phase of $Ba_{0.67}Sr_{0.33}TiO_3$ ceramics are reported. These measurements reveal the existence of a mechanism of electromechanical coupling beyond the flexoelectric effect that could be induced by the geometry of the samples. The presence of non flexoelectric electromechanical coupling suggests a breaking of the expected centric symmetry in the paraelectric phase; this symmetry breaking is intrinsic to the material and not induced by the application of external electric or elastic field. This is confirmed by the detection of non-zero piezoelectric and pyroelectric current in as prepared paraelectric ceramics.

In **Chapter 5**, the pyroelectric technique is used as technique to study systematically the symmetry breaking in the paraelectric phase and identify the mechanism at the origin of the polar response. The experiments are directed to understand if the breaking of the symmetry is associated to the granular nature of the ceramics and if the main contributions are due to surface effects or they come from the bulk of the samples. The influence of the preparation of the samples on the symmetry breaking was systematically investigated. The study allowed us to identify the step of the processing at which the polarization is imprinted in the ceramics. The investigations was extended to several compositions of the $Ba_{1-x}Sr_xTiO_3$ (x=0, 0.025 0.33, 0.40, 0.45, 0.50, 0.67, 0.90, 0.975, 1) solid solution. Based on the experimental results, a qualitative model is proposed to explain the observed symmetry breaking.

In **Chapter 6**, the $Ba_{1-x}Sr_xTiO_3$ ceramics are analyzed with the Thermally Stimulated Current (TSC) technique to study the stability of the polarity in the paraelectric phase as

function of temperature. The TSC measurements indicate that the polar response, at the origin of the pyroelectric current, consists of two different contributions: a volatile one due to the presence of mobile charges which is erased during heating and a second one strongly imprinted in the ceramics, which persists in the samples even after the annealing at elevated temperatures. For comparison, the study is extended to other ceramics and single crystals. The TSC technique is also a complementary tool with respect to the pyroelectric measurement because it can reveal the presence of a polarity even in materials which do not show any pyroelectric current at temperatures close to ambient. On cooling the TSC do not show any peak, this may signify that the built-in polarization in the samples does not disappear below 550^{o}C (the upper limit of our measurement) and the peaks observed upon heating are associated whit the volatile component of the polarization and only the direction of the peak is determined by the built-in polarization.

The **Chapter 7** presents conclusions about origins of the symmetry breaking and suggests possible directions for future studies.

1.7 Bibliography

[1] M. E. Lines and A. M. Glass, *Principles and applications of ferroelectrics and related materials*: Clarendon Press, 1977.

[2] J. Fousek, *Joseph Valasek and the discovery of ferroelectricity*, 1994.

[3] L. E. Cross and R. E. Newnham, ""History of ferroelectrics"," *Ceramics and Civilization High-Technology Ceramics-Past,Present, and Future,* vol. III, p. 287, 1987.

[4] B. T. Matthias, "New ferroelectric crystals," *Physical Review,* vol. 75, pp. 1771-1771, 1949.

[5] G. Shirane, S. Hoshino, and K. Suzuki, "Crystal structures of lead titanate and of lead-barium titanate," *Journal of the Physical Society of Japan,* vol. 5, pp. 453-455, 1950.

[6] L. Jin, "Broadband Dielectric Response in Hard and Soft PZT - Understanding Softening and Hardening Mechanisms," EPFL, 2011.

[7] B. Jaffe, W. R. Cook, and H. L. Jaffe, *Piezoelectric ceramics*: Academic Press, 1971.

[8] D. Damjanovic, "Ferroelectric, dielectric and piezoelectric properties of ferroelectric thin films and ceramics," *Reports on Progress in Physics,* vol. 61, pp. 1267-1324, Sep 1998.

[9] R. E. Newnham, *Properties of Materials: Anisotropy, Symmetry, Structure*: OUP Oxford, 2005.

[10] V. P. Afanas'ev, I. P. Pronin, and A. L. Kholkin, "Formation and relaxation mechanisms of the self-polarization in thin ferroelectric films," *Physics of the Solid State,* vol. 48, pp. 1214-1218, Jun 2006.

[11] J. P. Chen, Y. Luo, X. Ou, G. L. Yuan, Y. P. Wang, Y. Yang, *et al.*, "Upward ferroelectric self-polarization induced by compressive epitaxial strain in (001) $BaTiO_3$ films," *Journal of Applied Physics,* vol. 113, May 2013.

[12] I. Coondoo, N. Panwar, I. Bdikin, V. S. Puli, R. S. Katiyar, and A. L. Kholkin, "Structural, morphological and piezoresponse studies of Pr and Sc co-substituted $BiFeO_3$ ceramics," *Journal of Physics D-Applied Physics,* vol. 45, Feb 2012.

[13] Y. H. Chu, M. P. Cruz, C. H. Yang, L. W. Martin, P. L. Yang, J. X. Zhang, *et al.*, "Domain control in mulfiferroic $BiFeO_3$ through substrate vicinality," *Advanced Materials,* vol. 19, pp. 2662-2666, Sep 2007.

[14] Z. Kighelman, D. Damjanovic, and N. Setter, "Electromechanical properties and self-polarization in relaxor $Pb(Mg_{1/3}Nb_{2/3})O_3$ thin films," *Journal of Applied Physics,* vol. 89, pp. 1393-1401, Jan 2001.

[15] X. Chen, Y. Zou, G. Yuan, M. Zeng, J. M. Liu, J. Yin, *et al.*, "Temperature Gradient Introduced Ferroelectric Self-Poling in $BiFeO_3$ Ceramics," *Journal of the American Ceramic Society,* vol. 96, pp. 3788-3792, Dec 2013.

[16] J. P. Sokoloff, L. L. Chase, and D. Rytz, "Direct observatiion of the relaxation modes in $KNbO_3$ AND $BaTiO_3$ using inelastic light-scattering," *Physical Review B,* vol. 38, pp. 597-605, Jul 1988.

[17] J. Kwapulinski, M. Pawelczyk, and J. Dec, "Thermal vibrations in $PbTiO_3$ crystals," *Ferroelectrics,* vol. 192, pp. 307-311, 1997.

[18] A. Bussmann-Holder, H. Beige, and G. Volkel, "Precursor effects, broken local symmetry, and coexistence of order-disorder and displacive dynamics in perovskite ferroelectrics," *Physical Review B,* vol. 79, May 2009.

[19] J. P. Dougherty and S. K. Kurtz, "2nd harmonic analyzer for detection of non-centrosymmetry," *Journal of Applied Crystallography,* vol. 9, pp. 145-158, 1976.

[20] G. V. Liberts and V. Y. Fritsberg, "SHG investigations in the paraelectric phase of perovskite type ferroelectrics," *Physica Status Solidi a-Applied Research,* vol. 67, pp. K81-K84, 1981.

[21] G. R. Fox, J. K. Yamamoto, D. V. Miller, L. E. Cross, and S. K. Kurtz, "Thermal hysteresis of optical second harmonic in paraelectric $BaTiO_3$," *Materials Letters,* vol. 9, pp. 284-288, 4// 1990.

[22] A. M. Pugachev, V. I. Kovalevskii, N. V. Surovtsev, S. Kojima, S. A. Prosandeev, I. P. Raevski, *et al.*, "Broken Local Symmetry in Paraelectric $BaTiO_3$ Proved by Second Harmonic Generation," *Physical Review Letters,* vol. 108, Jun 2012.

[23] K. Rusek, J. Kruczek, K. Szot, D. Rytz, M. Gorny, and K. Roleder, "Non-Linear Properties of $BaTiO_3$ above T-C," *Ferroelectrics,* vol. 375, pp. 165-169, 2008.

[24] A. Ziebinska, D. Rytz, K. Szot, M. Gorny, and K. Roleder, "Birefringence above T_c in single crystals of barium titanate," *Journal of Physics-Condensed Matter,* vol. 20, Apr 2008.

[25] K. Wieczorek, A. Ziebinska, Z. Ujma, K. Szot, M. Gorny, I. Franke, *et al.*, "Electrostrictive and piezoelectric effect in BaTiO3 and $PbZrO_3$," *Ferroelectrics,* vol. 336, pp. 61-67, 2006.

[26] J. H. Ko, T. H. Kim, K. Roleder, D. Rytz, and S. Kojima, "Precursor dynamics in the ferroelectric phase transition of barium titanate single crystals studied by Brillouin light scattering," *Physical Review B,* vol. 84, Sep 2011.

[27] K. Inoue and S. Akimoto, "Hyper-Raman scattering spectra in the low-frequency range in cubic $BaTiO_3$ and the mechanism of the phase transition," *Solid State Communications,* vol. 46, pp. 441-445, 1983.

[28] J. H. Ko, S. Kojima, T. Y. Koo, J. H. Jung, C. J. Won, and N. J. Hur, "Elastic softening and central peaks in $BaTiO_3$ single crystals above the cubic-tetragonal phase-transition temperature," *Applied Physics Letters,* vol. 93, Sep 2008.

[29] B. Ravel, E. A. Stern, R. I. Vedrinskii, and V. Kraizman, "Local structure and the phase transitions of $BaTiO_3$," *Ferroelectrics,* vol. 206, pp. 407-430, 1998.

[30] H. Beige and G. Schmidt, "Electro-mechanical resonances for investigating linear and non-linear properties of dielectrics," *Ferroelectrics,* vol. 41, pp. 173-183, 1982.

[31] D. Damjanovic, A. Biancoli, L. Batooli, A. Vahabzadeh, and J. Trodahl, "Elastic, dielectric, and piezoelectric anomalies and Raman spectroscopy of $0.5Ba(Ti_{0.8}Zr_{0.2})O_3$-$0.5(Ba_{0.7}Ca_{0.3})TiO_3$," *Applied Physics Letters,* vol. 100, May 2012.

[32] E. M. Anton, W. Jo, D. Damjanovic, and J. Rodel, "Determination of depolarization temperature of $(Bi_{1/2}Na_{1/2})TiO_3$-based lead-free piezoceramics," *Journal of Applied Physics,* vol. 110, Nov 2011.

[33] J. F. Scott, "Lattice perturbations in $CaWO_4$ and$CaMoO_4$," *Journal of Chemical Physics,* vol. 48, pp. 874-&, 1968.

[34] J. Fousek, L. E. Cross, and D. B. Litvin, "Possible piezoelectric composites based on the flexoelectric effect," *Materials Letters,* vol. 39, pp. 287-291, Jun 1999.

[35] V. S. Mashkevich and K. B. Tolpygo, "Electrical, optical and elastic properties of diamond type crystals.1," *Soviet Physics* JETP-USSR, vol. 5, pp. 435-439, 1957.

[36] S. M. Kogan, "Piezolectric effect during inhomogeneous deformation and acoustic scattering of carriers in crystals," *Soviet Physics-Solid State,* vol. 5, pp. 2069-2070, 1964.

[37] E. V. Bursian and Zaikovsk.Oi, "Changes in Curvature of a Ferroelectric Film Due to Polarization," *Soviet Physics Solid State,Ussr,* vol. 10, pp. 1121-&, 1968.

[38] E. V. Bursian, Zaikovsk.Oi, and K. V. Makarov, "Ferroelectric plate polarization by bending," *Izvestiya Akademii Nauk Sssr Seriya Fizicheskaya,* vol. 33, pp. 1098-&, 1969.

[39] V. L. Indenbom, E. B. Loginov, and M. A. Osipov, "Flexoelectric effect and crystal-structure," *Kristallografiya,* vol. 26, pp. 1157-1162, 1981.

[40] A. K. Tagantsev, "Piezoelectricity and Flexoelectricity in Crystalline Dielectrics," *Physical Review B,* vol. 34, pp. 5883-5889, Oct 15 1986.

[41] A. K. Tagantsev, "Electric Polarization in Crystals and Its Response to Thermal and Elastic Perturbations," *Phase Transitions,* vol. 35, pp. 119-203, 1991.

[42] R. Resta, "Towards a Bulk Theory of Flexoelectricity," *Physical Review Letters,* vol. 105, Sep 2010.

[43] J. W. Hong and D. Vanderbilt, "First-principles theory and calculation of flexoelectricity," *Physical Review B,* vol. 88, Nov 2013.

[44] D. Lee, A. Yoon, S. Y. Jang, J. G. Yoon, J. S. Chung, M. Kim*, et al.*, "Giant Flexoelectric Effect in Ferroelectric Epitaxial Thin Films," *Physical Review Letters,* vol. 107, Jul 2011.

[45] G. Catalan, A. Lubk, A. H. G. Vlooswijk, E. Snoeck, C. Magen, A. Janssens*, et al.*, "Flexoelectric rotation of polarization in ferroelectric thin films," *Nature Materials,* vol. 10, pp. 963-967, Dec 2011.

[46] L. Bellaiche, A. Garcia, and D. Vanderbilt, "Finite-temperature properties of $Pb(Zr_{1-x}Ti_x)O_3$ alloys from first principles," *Physical Review Letters,* vol. 84, pp. 5427-5430, Jun 2000.

[47] D. Damjanovic, "A morphotropic phase boundary system based on polarization rotation and polarization extension," *Applied Physics Letters,* vol. 97, Aug 2010.

[48] H. Lu, C. W. Bark, D. E. de los Ojos, J. Alcala, C. B. Eom, G. Catalan*, et al.*, "Mechanical Writing of Ferroelectric Polarization," *Science,* vol. 336, pp. 59-61, Apr 2012.

[49] N. D. Sharma, C. M. Landis, and P. Sharma, "Piezoelectric thin-film superlattices without using piezoelectric materials," *Journal of Applied Physics,* vol. 108, Jul 2010.

[50] W. Ma and L. E. Cross, "Large flexoelectric polarization in ceramic lead magnesium niobate," *Applied Physics Letters,* vol. 79, pp. 4420-4422, Dec 24 2001.

[51] W. H. Ma and L. E. Cross, "Flexoelectric effect in ceramic lead zirconate titanate," *Applied Physics Letters,* vol. 86, Feb 14 2005.

[52] W. H. Ma and L. E. Cross, "Flexoelectric polarization of barium strontium titanate in the paraelectric state," *Applied Physics Letters,* vol. 81, pp. 3440-3442, Oct 28 2002.

[53] W. H. Ma and L. E. Cross, "Flexoelectricity of barium titanate," *Applied Physics Letters,* vol. 88, Jun 5 2006.

[54] J. Y. Fu, W. Y. Zhu, N. Li, N. B. Smith, and L. E. Cross, "Gradient scaling phenomenon in microsize flexoelectric piezoelectric composites," *Applied Physics Letters,* vol. 91, Oct 29 2007.

[55] B. J. Chu, W. Y. Zhu, N. Li, and L. E. Cross, "Flexure mode flexoelectric piezoelectric composites," *Journal of Applied Physics,* vol. 106, Nov 15 2009.

[56] P. Zubko, G. Catalan, A. Buckley, P. R. L. Welche, and J. F. Scott, "Strain-gradient-induced polarization in $SrTiO_3$ single crystals," *Physical Review Letters,* vol. 99, Oct 19 2007.

[57] P. V. Yudin and A. K. Tagantsev, "Fundamentals of flexoelectricity in solids," *Nanotechnology,* vol. 24, Nov 1 2013.

[58] P. Zubko, G. Catalan, and A. K. Tagantsev, "Flexoelectric Effect in Solids," *Annual Review of Materials Research, Vol 43,* vol. 43, pp. 387-421, 2013.
[59] A. K. Tagantsev and A. S. Yurkov, "Flexoelectric effect in finite samples," *Journal of Applied Physics,* vol. 112, Aug 15 2012.

Chapter 2: Processing and characterization

2.1 Introduction

In this chapter, the synthesis by the solid state route of the $Ba_{1-x}Sr_xTiO_3$ ceramics investigated in this work is described. This system has been studied now for more than 60 years, yet its properties are not completely understood. Different processing routes reported in the literature lead to a large variation of density and dielectric properties of the final ceramics. This is not surprising considering that the processing routes of the ceramics depend on many parameters such as particle size of the starting powders and the type and concentration of the impurities among others. The goal here was therefore not to establish a novel way for the preparation of the ceramics but to optimize the processing steps of the solid state route to obtain homogeneous ceramics samples with high densities and reproducible properties. In the beginning of the chapter, a short overview of $BaTiO_3$ and of its modification with other cations, in particular strontium is given. Then, the processing method used is described. The structural and compositional properties of the ceramics were characterized with techniques such as XRPD (X-Rays powder diffraction), Scanning Electron Microscopy (SEM) and Energy dispersive spectroscopy (EDS) and the dielectric properties were measured in order to verify the results of the processing and the final quality of the ceramics.

2.2 Barium Titanate

Barium titanate ($BaTiO_3$) was the first piezoelectric ceramics to be discovered [1]. At high temperature, $BaTiO_3$ exists in two basic forms, a cubic form, which becomes ferroelectric upon cooling below certain temperature (the Curie point) and a hexagonal form which is not ferroelectric (see Figure 2.1). The hexagonal form is stable above 1460^{o}C [2] and below that temperature the conversion to the cubic form takes usually place. However, it is possible for the hexagonal phase to be stabilized by the impurities (i.e. Mn [3]), or in general by a sufficiently high concentration of oxygen vacancies [4] and be metastably present a room temperature. On cooling, between 130^{o}C-120^{o}C (the Curie point), the cubic perosvkite structure elongates along the edge of the unit cell and becomes tetragonal and ferroelectric.

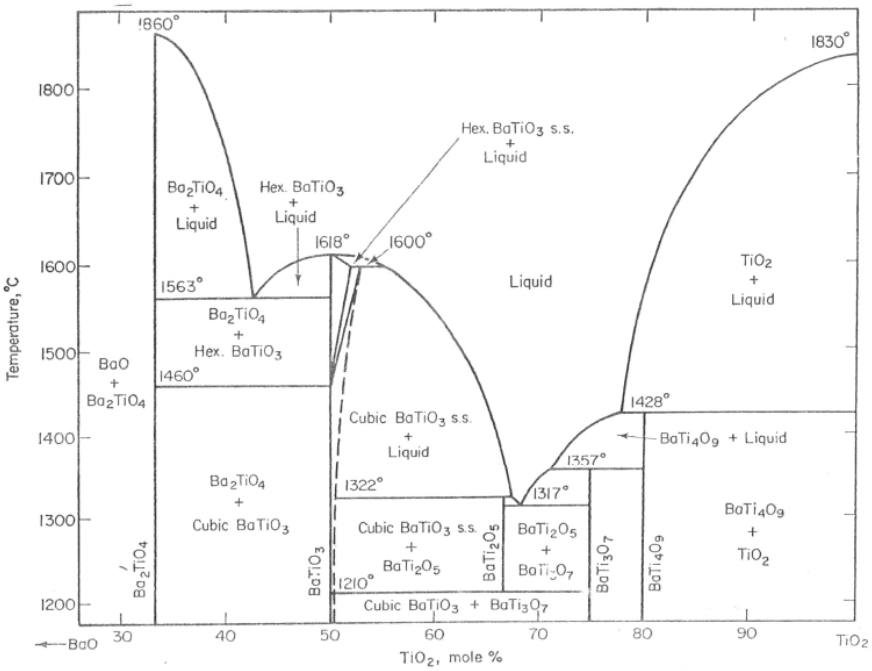

Figure 2.1-Phase diagram of the BaO-TiO_2 system [5]

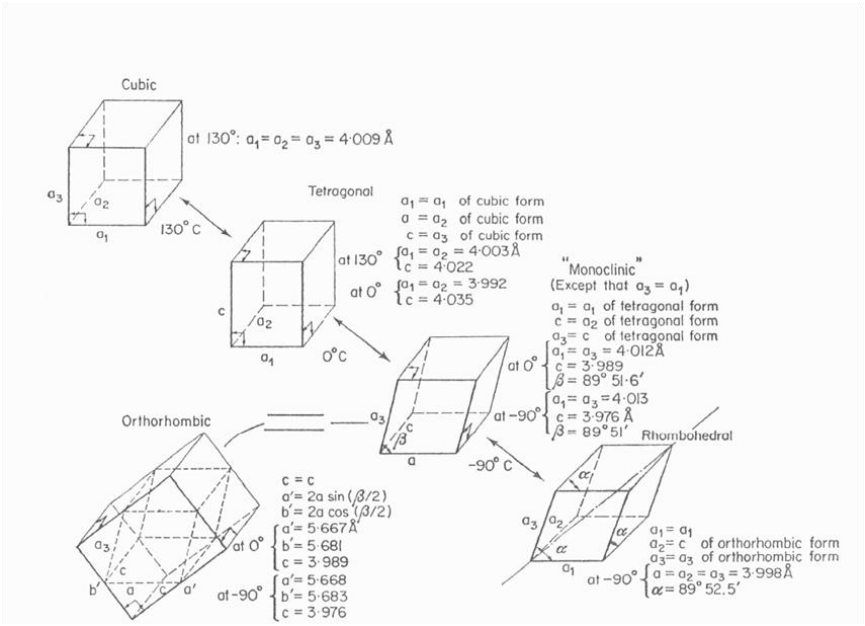

Figure 2.2- Sequence of polymorphic phase transitions in $BaTiO_3$. Taken from [5]

Upon further cooling, other polymorphic transitions occur; one, from the tetragonal to the orthorhombic structure at around 0°C, and a second one, from the orthorhombic to the rhombohedral structure at -90°C (Figure 2.2). Both these low temperature polymorphs are ferroelectrics.

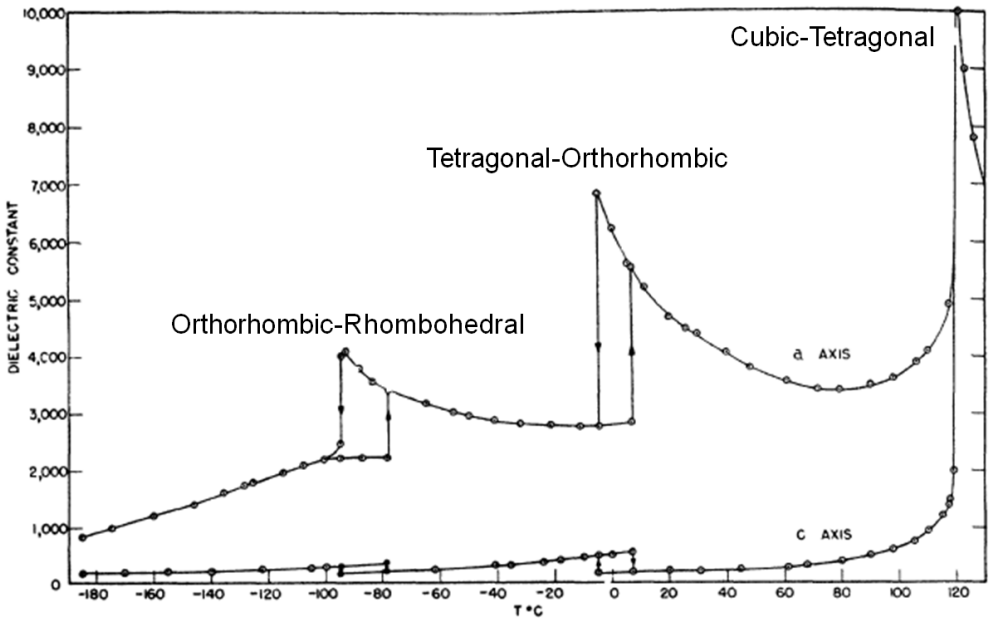

Figure 2.3-Dielectric constant in single crystals of $BaTiO_3$ along the a axis and c axis of the perosvkite unit cell as a function of temperature. Adapted from [6]

Large anomalies in the dielectric permittivity [6] are observed at the onset of ferroelectricity at the cubic to tetragonal phase transition temperature and at phase transition temperatures of the other two ferroelectric to ferroelectric phase transitions (Figure 2.3). The exact temperature of the phase transition depends on the crystallite size [7, 8], the rate of the temperature variation, the stress conditions and the purity of the material [9]. As it was shown a long time ago, by measurements of the discontinuities in the thermal expansion of $BaTiO_3$ ceramics [10], the three ferroelectrics phase transitions are of the first order, therefore a thermal hysteresis in properties is observed for all phase transitions.

As the $BaTiO_3$ is cooled below the Curie point into the tetragonal ferroelectric phase, the ferroelectrics domains start to nucleate. In the tetragonal symmetry the polarization can rise along each one of the six equivalent crystallographic directions (100) of the original cubic phase, giving rise to rather complicated twinned configurations called domain patterns (see Figure 2.4). The exact structure of the domain patterns depends on a wide range of parameters such as the stress present at the Curie point, uncompensated surface charges and imperfections of the crystal. When the crystallographic symmetry of the ferroelectric phase changes from tetragonal to orthorhombic or from orthorhombic to rhombohedral, new ferroelectrics domains arise, following the directions.

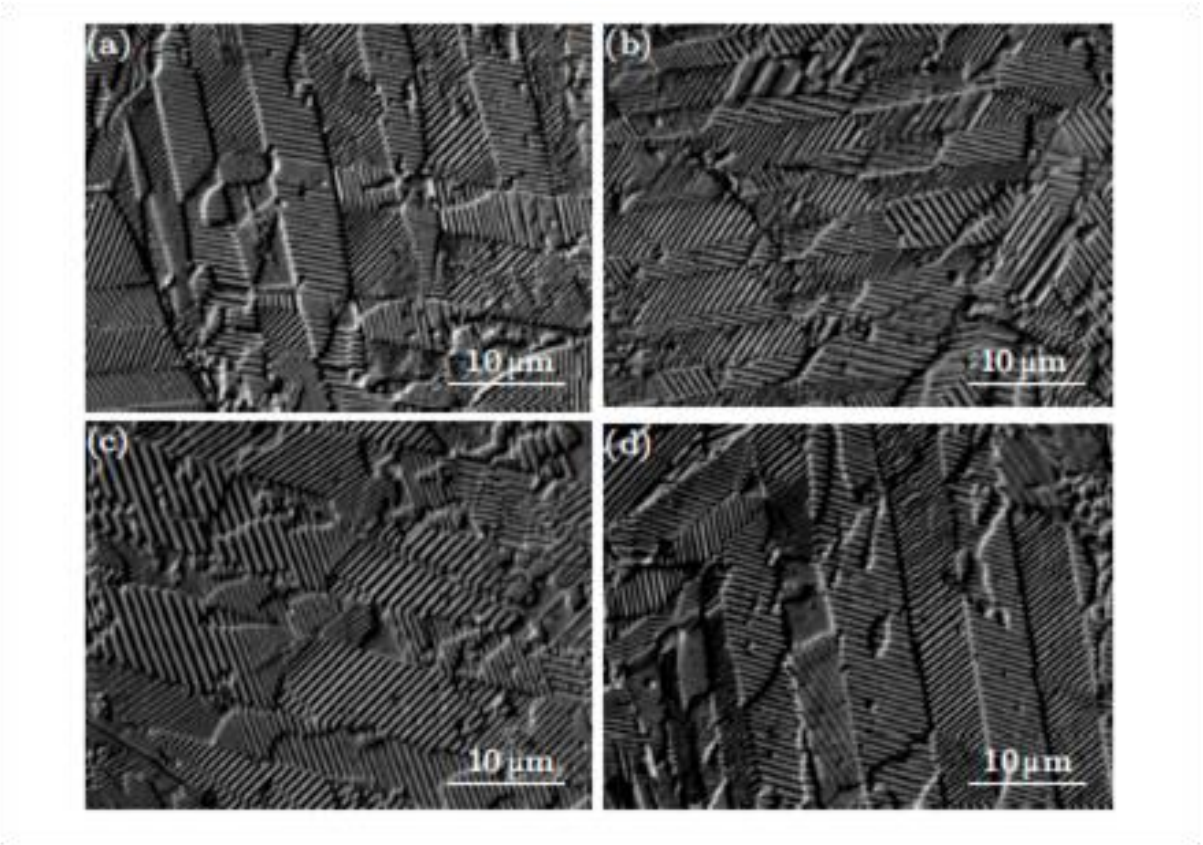

Figure 2.4-Typical tetragonal domain pattern observed by optical microscopy in $BaTiO_3$ ceramics near the grain boundaries a) and b) and in the inner part of the grains c) and d) [11].

2.3 Compositional modification of $BaTiO_3$

Pure $BaTiO_3$ can be modified by substitution of both Ba^{2+} and $Ti^{4+}$with cations of other elements. The replacing cations can be either of the same valence as barium or titanium (isovalent substitution) or of a different valance (aliovalent substitution).

Since the discovery of $BaTiO_3$ an important effort was directed to the studies of the properties of its modifications [5]. The effect of the typical isovalent substitution for Ba^{2+} and Ti^{4+}cations is shown in Figure 2.5. The purpose of the modification of pure $BaTiO_3$ is usually to increase or decrease the temperature of the Curie point or modify the stability region of the different polymorphs. For example, the isovalent substitution of Ba^{2+} with Pb^{2+} has the effect to increase the Curie point. The substitution of Ba^{2+} with Ca^{2+}, leaves the Curie point almost unaffected, but lowers significantly the tetragonal to orthorhombic phase transition temperature [12]. This modification has an important role in stabilizing the dielectric, piezoelectric and elastic properties in a wide range of engineering applications. In the case of substitution of Ba^{2+} with Sr^{2+}, the Curie temperature of pure $BaTiO_3$ is decreased as the strontium content increases. The research on the $Ba_{1-x}Sr_xTiO_3$ has started more the 50 years ago [13]. Since that time, a wide number of studies on the

processing of powders [14], single crystal [15], thin films [16] and properties [17, 18] have been reported. This broad research interest is justified by the fact that the $Ba_{1-x}Sr_xTiO_3$ solid solution finds application in many devices such as radio frequency (RF) and microwave capacitors [19, 20], infrared pyroelectric sensors [21] and dynamic random access memories (DRAMs) [22]. The recent discovery of large flexoelectric properties in the $Ba_{0.67}Sr_{0.33}TiO_3$ composition [23] has renewed the interest in the study of the $Ba_{1-x}Sr_xTiO_3$ system and opened a completely new research direction.

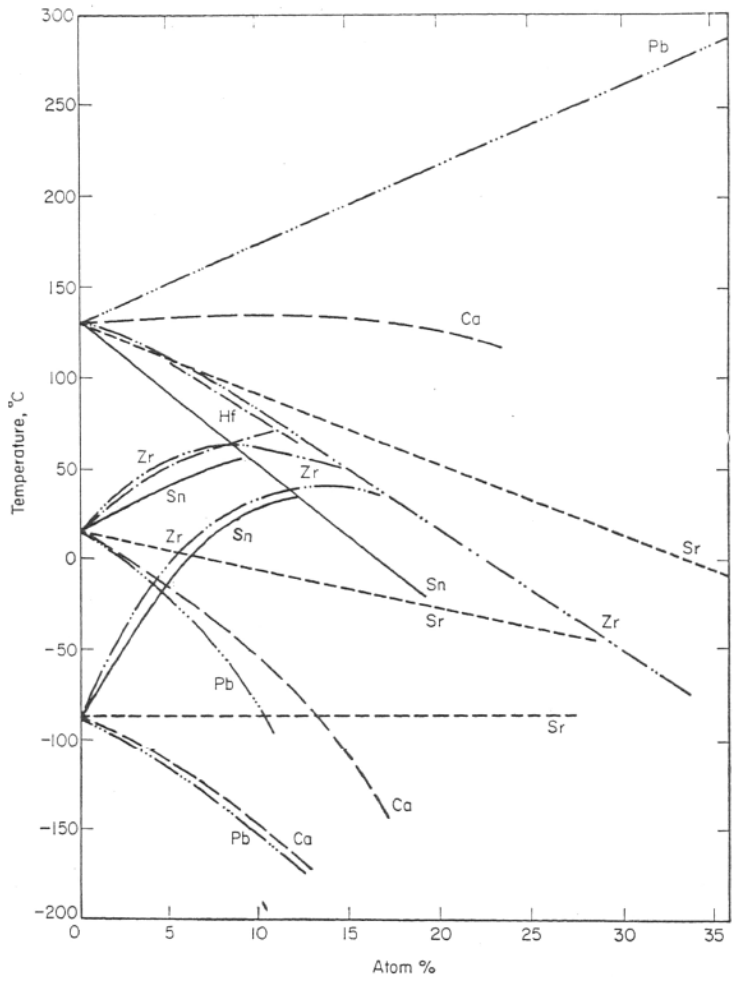

Figure 2.5-Diagram of the typical isovalent substitutions for Ba and Ti cations in $BaTiO_3$ [5].

2.4 Materials selection

In the present work the $Ba_{1-x}Sr_xTiO_3$ solid solution was systematically investigated. In the beginning, this solid solution was selected as a model system in the attempt to investigate and understand the mechanism at the origin of the reported large flexoelectric polarization. After the uncovering of the polar character of the paraelectric phase in unpoled barium strontium titanate ceramics, the solid solution represented an ideal system for the studies of the origin of the symmetry breaking. One reason is that the

complete solubility of barium and strontium gives the advantage to change the temperature stability of the ferroelectric and paraelectric phases only by varying the relative amount of the two elements, keeping constant all the processing parameters.

Another reason is that for Sr content larger than 80%, the system changes the behavior from normal ferroelectric to relaxor [24]. This feature offers the possibility to compare the polar response in the paraelectric phase of ferroelectrics and in the ergodic phase of relaxors without being affected by the variation of the chemical background. In addition, the two end members provide convenient systems to study flexoelectricity in chemically simpler systems. Finally, the room temperature relative permittivity of the ceramics changes by about two orders of magnitude as x changes from 0 to 1, allowing us to verify influence of the permittivity on apparent electromechanical response.

Several compositions, covering the entire range of the solid solution were produced and investigated in our study. Ceramics of pure $BaTiO_3$ and pure $SrTiO_3$ were also prepared to be used as references. All the ceramics were synthesized from the same starting powders with constant processing parameters. For simplicity, the $Ba_{1-x}Sr_xTiO_3$ solid solution will be labeled as follow: for example $Ba_{0.67}Sr_{0.33}TiO_3$ will be referred as BST6733. In Table 2.1 a list of all compositions investigated is presented.

Table 2.1-Compositions of the $Ba_{1-x}Sr_xTiO_3$ solid solution investigated in this study. The value of T_c refers to the maximum of the dielectric constant ε_r. The Curie temperature of BST025975 and $SrTiO_3$ were not determined and lie below -210°C.

Composition	Short label	T_C or T_{max} on heating	T_C or T_{max} on cooling	Permittivity at room temperature (21°C)	T_c or T_{max} extracted from Lemanov et al [25]
$BaTiO_3$	BTO	128°C	120°C	1960	127°C
$Ba_{0.975}Sr_{0.025}TiO_3$	BST975025	119°C	113°C	1870	122°C
$Ba_{0.67}Sr_{0.33}TiO_3$	BST6733	33°C	20°C	20000	14°C
$Ba_{0.60}Sr_{0.40}TiO_3$	BST6040	8°C	-1°C	6500	-14°C
$Ba_{0.55}Sr_{0.45}TiO_3$	BST5545	-9°C	-19.5°C	3000	-31°C
$Ba_{0.50}Sr_{0.50}TiO_3$	BST5050	-25°C	-36°C	1800	-39°C
Ba0.33Sr0.67TiO3	BST3367	-92°C	-103°C	600	-98°C
$Ba_{0.10}Sr_{0.90}TiO_3$	BST1090	/	-208°C	300	-189°C
$Ba_{0.025}Sr_{0.975}TiO_3$	BST025975	/	/	260	-248°C
$SrTiO_3$	STO	/	/	260	-267°C

2.5 Processing of the ceramics

The method used to process the ceramics is the *solid state route*, a well established technique for the synthesis of polycrystalline ferroelectric ceramics [5]. The process flow is shown in the chart in Figure 2.6.

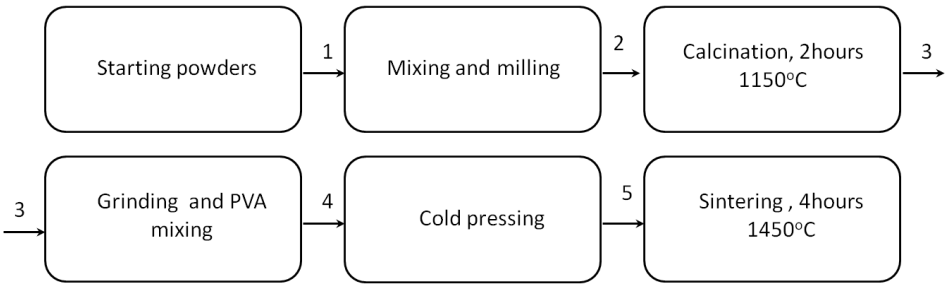

Figure 2.6-Process flow chart of the processing of the $Ba_{1-x}Sr_xTiO_3$ ceramics.

Already formed titanates of barium and strontium, with very high purity and very fine particle size were chosen as starting powders. The characteristics of the raw powders are resumed in Table 2.2.

Table 2.2- Characteristics of the raw titanates powder used as for ceramics processing.

Powder	Manufacturer	Particle size	Purity	Impurities
$BaTiO_3$	Inframat Advanced Materials	0.2 μm	99.95%	Ca(<0.001%) Fe(<0.001%) K(<0.001%) Mg(<0.001%) Na(<0.001%) Sr(<0.0015%)
$SrTiO_3$	Inframat Advanced materials	0.1 μm	99.95%	Ca(<0.008%) Fe(<0.006%) K(<0.002%) Mg(<0.005%) Na(<0.006%)

The raw powders were weighed according to stoichiometric amount required for each composition and dispersed in isopropanol. The obtained slurry was milled in a jar filled with ZrO_2 balls (diameter 5mm) as grinding media and milled by mean of a planetary milling machine. The typical composition of the mill in one jar is 70 g of powders, 80ml of isopropanol and 550 g of ZrO_2 balls.

The milling time was set to 24 hours in order to reach a good homogeneity of the mixture and avoid the formation of a secondary phase during calcination. It is also reported [24] that in $Ba_{1-x}Sr_xTiO_3$ system a too short mixing time can lead to a non homogenous distribution of Ba^{2+} and Sr^{2+} cations. This inhomogeneous distribution usually results in a broad peak in the dielectric constant at the ferroelectric to paraelectric phase transition (diffuse phase transition). As it will be shown later, this was not observed in our samples.

After milling the slurry was put in a glass beaker and dried on a hot plate at 85^{o}C, under an IR lamp, to increase the evaporation rate of the isopropanol, for about 3 hours.

The dried powders were transferred in a covered high density alumina crucible and calcined at 1150^{o}C with a heating rate of 5^{o}C/minute for 2 hours and cooled down with the rate of 5^{o}C/minute to room temperature. After calcination the powders were ground in a porcelain mortar with a pestle and a 4% solution of polyvinyl alcohol (PVA) and deionized water was added as binder. The ratio between the binder and the powder was 1:25 in weight. The addition of PVA increases the plasticity of the powder and prevents the formation of cracks during pressing. The calcined powders with the binder were introduced in a stainless steel cylindrical die with a tungsten inner core and pressed into pellets with the application of a uniaxial load.

For the standard dielectric characterization the powders were pressed with a load of 150 MPa into disks with a diameter of 9 mm and a thickness between 1 and 2 mm. For the pyroelectric measurements, where very thin samples were required, the pellets were 0.5 mm in thickness and 5 mm in diameter. In this latter case a uniaxial load 100 of MPa was applied. After pressing, the pellets were fired in air in a high temperature furnace at 1450^{o}C for 4 hours with a heating and cooling rate of 5^{o}C /minute.

2.6 Density measurements

The theoretical densities of the ceramics were calculated according to the relation:

$$\rho_{theoretical} = \frac{\text{Molar Mass} \times Z}{N_A \times V_{cell}} \qquad 2.1$$

where N_A is the Avogadro number, V_{cell} the volume of the unit cell and Z is the number of formula unit contained in one unit cell (for perosvkites like $Ba_{1-x}Sr_xTiO_3$ Z= 1). The volume of the unit cell was calculated from the lattice parameter extracted from the X-rays diffraction pattern collected on the sintered ceramics.

The geometrical densities of the ceramics after sintering were calculated from the ratio between their weight and the geometrical volume. The weight determination was done on pellets of around 0.6 grams. The pellets were cleaned in acetone for 5 minutes before weighing. The relative densities of the ceramics were calculated as:

$$\rho_{relative} = \frac{\rho_{geometrical}}{\rho_{theoretical}} \qquad 2.2$$

The relative densities were found to be around 95% -96% of the theoretical for of all compositions. The theoretical density calculated from the X-ray data has a linear decrease with the increase of the strontium content. This suggests absence of significant amounts of secondary phases.

2.7 Scanning Electron Microscopy (SEM)

The raw powders (as received by the supplier) of $BaTiO_3$ and $SrTiO_3$ were investigated with the scanning electron microscopy technique (SEM) to verify their morphology. The scans were conducted with a FEI XL30-SFEG electron microscope. The micrographs of the raw powders used for ceramics processing are shown in Figure 2.7.

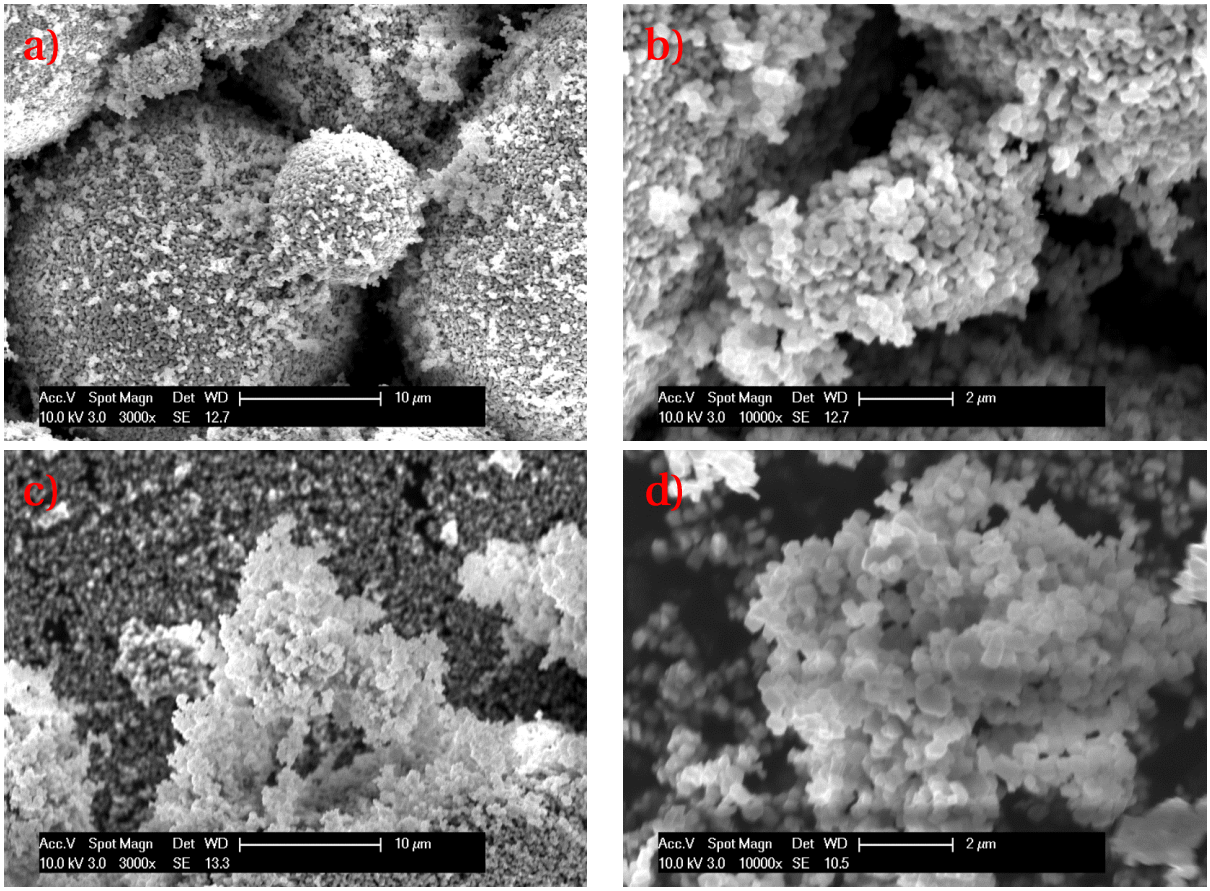

Figure 2.7-Images of the raw powders of $BaTiO_3$ a)-b) and $SrTiO_3$ c)-d)

The micrographs reveal large agglomerates of the size >10 µm, in both powders (Figure 2.7 a and c). These large agglomerates consist of fine particles (nominally 0.2µm for $BaTiO_3$ and 0.1 µm for $SrTiO_3$) with a quite spherical shape (Figure 2.7 b and d). The presence of the agglomerates is undesired because it can lead to inhomogeneous reaction of $BaTiO_3$ and $SrTiO_3$ and induce compositional variations or even the formation of a secondary phase during the calcination. It was therefore necessary to break these large particle agglomerates in order to improve the homogeneity of the powders and to have an effective mixing of the powders.

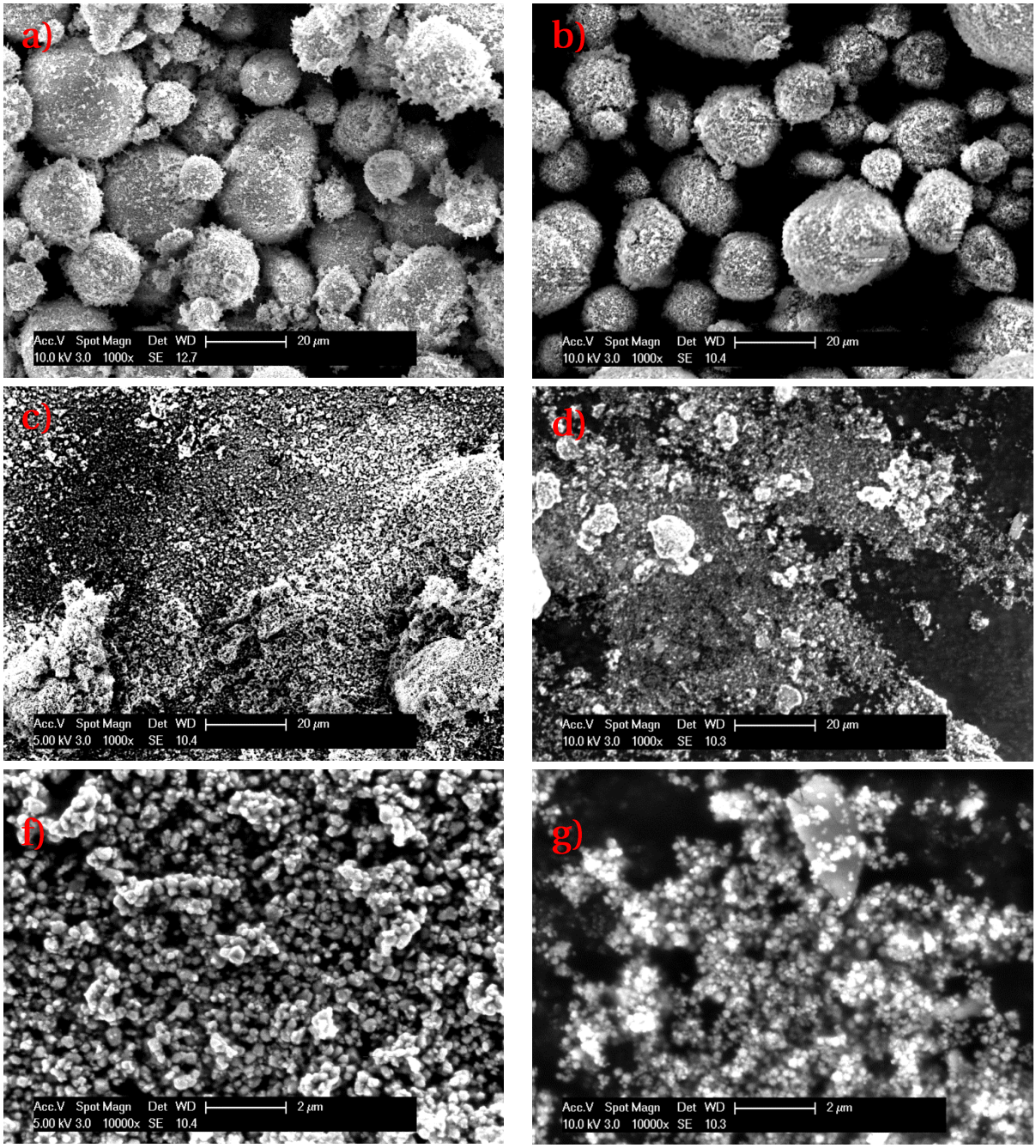

Figure 2.8-Starting powders of $BaTiO_3$ and $SrTiO_3$ before (a and b) and after milling in isopropanol with zirconia balls (c and d). Comparison of the morphology of $BaTiO_3$ (f) and $SrTiO_3$ (g) particles after the agglomerates are broken by milling.

The images of the powders taken after the 24 hours milling in isopropanol with zirconia balls, show that most of the agglomerates are broken (Figure 2.8 c and d) and that the milling step was effective in improving the homogeneity of the raw powders before calcination. The morphology of the powders of $BaTiO_3$ and $SrTiO_3$ after the agglomerates are broken does not appear to be significantly different (Figure 2.8 g and f). This is an important aspect for an ideal mixing. In order to have a homogeneous mixing of the

components, the powders should have a narrow particle size distribution (PSD) and a shape as close as possible to the spherical. These two properties should not differ too much between the different powders.

After sintering, the surfaces of pellets of all prepared compositions were analyzed with SEM in order to collect informations on the grain size, grain boundaries and surface porosity of the ceramics. Representative images of the microstructures for barium rich and strontium rich compositions are shown in Figure 2.9 and Figure 2.10 respectively.

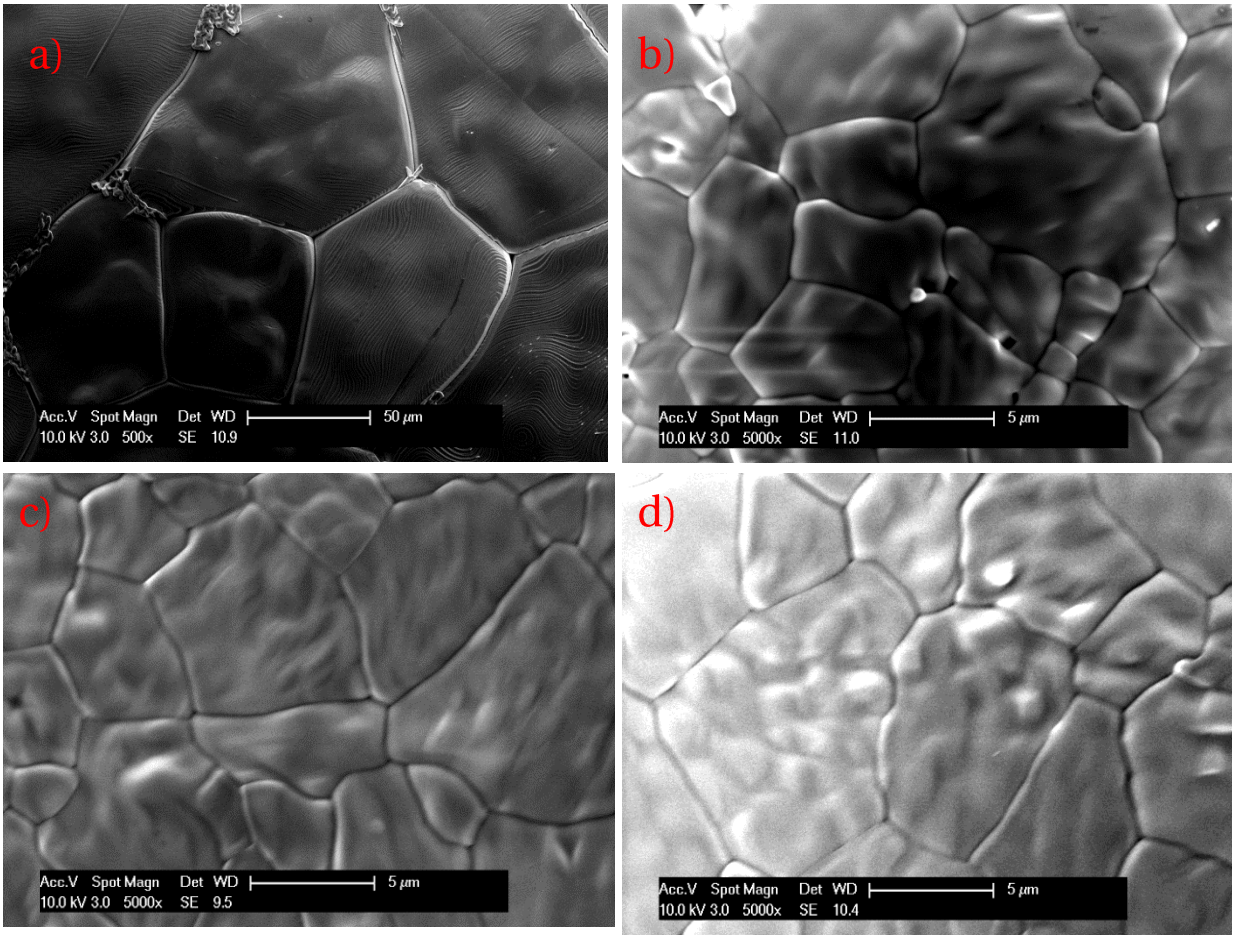

Figure 2.9-Images of the surfaces of as sintered ceramics samples for barium rich compositions: a) $BaTiO_3$, b) BST6733, c) BST6040, d) BST 5050.

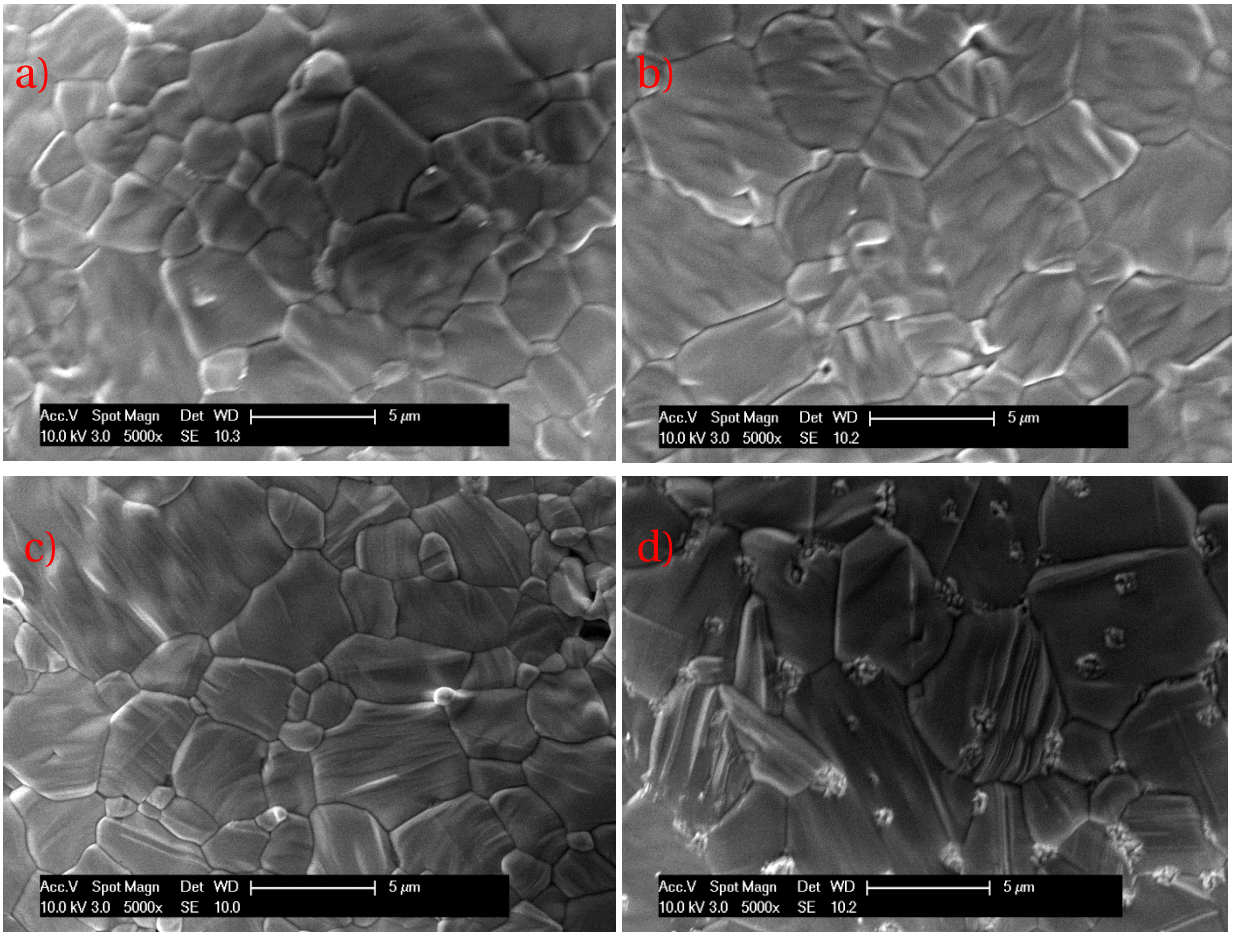

Figure 2.10-Images of the surfaces of as sintered ceramics samples for strontium rich compositions: a) BST3367, b) BST1090 c) BST025975, d) $SrTiO_3$.

The SEM images reveal well packed and compact microstructures with very small amount of pores. Large grains of around 50 μm are observed in pure $BaTiO_3$ (Figure 2.9 image a) and in the 2.5% strontium doped composition (not shown in the images). As the strontium content increases the average grain size decreases significantly with respect to the pure $BaTiO_3$. All the $Ba_{1-x}Sr_xTiO_3$ compositions with barium content of 67% or less have a very similar microstructure with grains ranging between 5 μm and 10 μm in average. The increase of porosity in the ceramics with the progressive addition of strontium due to the smaller ionic radius of Sr^{2+} cation with respect to the Ba^{2+} cation reported in the literature [26], is not observed in this work.

2.8 X Ray powder diffraction

The crystalline quality and the phase formation were analyzed by means of X ray powder diffraction technique (XRPD) performed on the powders after calcination. The scans were conducted at room temperature with a Bruker D8 Discovery diffractometer. The reflections were recorded in the region 20^o-90^o in a θ-2θ geometry with a scanning

speed of 2 degrees per minute. Powder Diffraction Files (PDF) were used to index the diffracted peaks. $BaTiO_3$ and the $Ba_{1-x}Sr_xTiO_3$ compositions in tetragonal symmetry at room temperature were indexed according to the tetragonal symmetry ($BaTiO_3$ 00-005-0626). The $Ba_{1-x}Sr_xTiO_3$ compositions in cubic symmetry at room temperature and $SrTiO_3$ were indexed according to the cubic structure ($BaTiO_3$ (01-089-247) and $SrTiO_3$ (00-00-1018)). The diffraction patterns in the region 20^o-60^o for $BaTiO_3$ and $SrTiO_3$ raw powders and for $Ba_{1-x}Sr_xTiO_3$ calcined powders are shown in Figure 2.11.

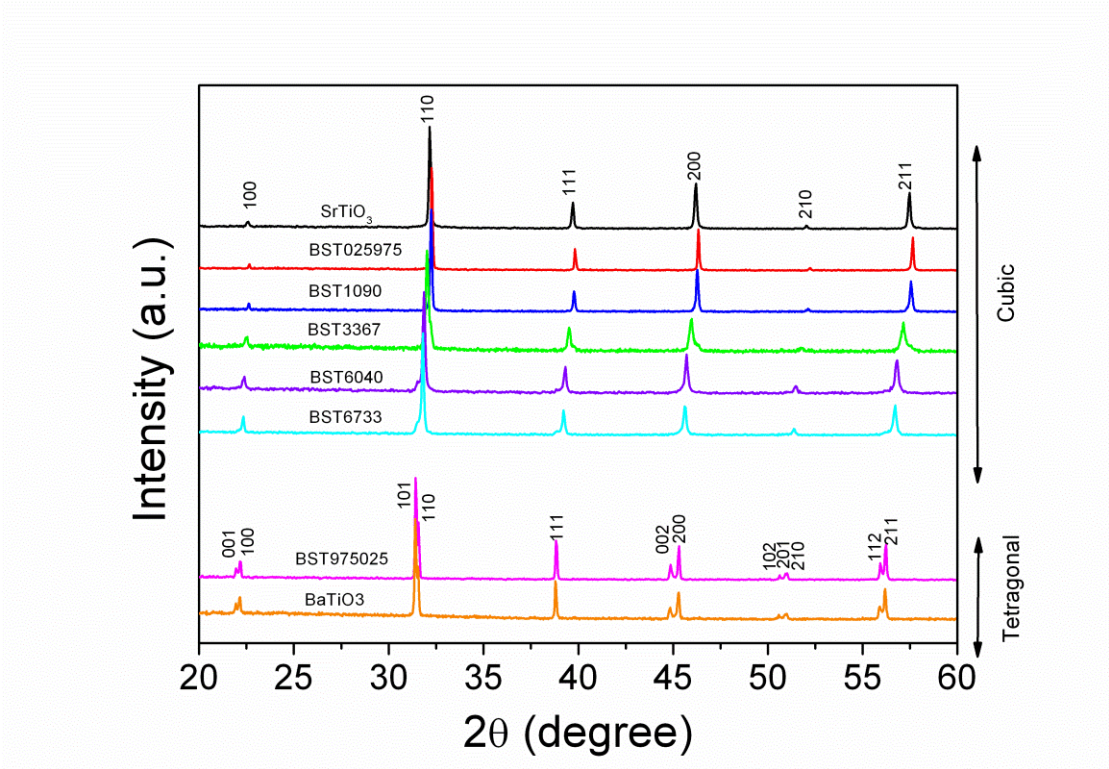

Figure 2.11-Representative XRD spectra on the calcined powders for BST barium and strontium rich compositions. The spectra for pure $BaTiO_3$ and pure $SrTiO_3$ were taken on the raw powders.

Sharp crystalline peaks, characteristics of the tetragonal or cubic symmetry are observed in $BaTiO_3$ and $SrTiO_3$ raw powders as well as in all $Ba_{1-x}Sr_xTiO_3$ compositions, indicating that the calcination process was homogeneous. The splitting of the {100},{110}, {101} and {200}, {002} peaks of the tetragonal *P*4*mm* space group can be clearly observed for pure $BaTiO_3$ and BST975025 compositions which are in the tetragonal (ferroelectric) phase at room temperature. For a barium content of 67% or less, the ceramics are in the cubic paraelectric phase at room temperature and the tetragonal peaks merge into single peaks ({100},{ 110},{200} reflections of the *Pm*(-3)*m* cubic space group). It can be seen that as the strontium content increases, the peaks are progressively shifted to higher 2θ angles. This indicates clearly that the lattice parameter of the unit cell decreases as the smaller Sr^{2+}

(ionic radius 1.40 Å) cation replaces the larger Ba^{2+} cation (ionic radius 1.60 Å) in the lattice.

After sintering, XRD scans were performed on the surfaces of the pellets to check for the formation of a secondary phase or contamination originated from the sintering process (Figure 2.12). The spectra do not show any extra peaks related to presence of a secondary phase. However, as the detection limit for the X-rays diffraction is high (above 2-3%) a small quantity of secondary phase cannot, in principle, be excluded only on the base of this analysis.

It can be also noted that higher sintering temperature (1450°C) with respect to the calcination temperature (1150°C) results in sharper peaks, indication that the size of the crystallites has increased during sintering.

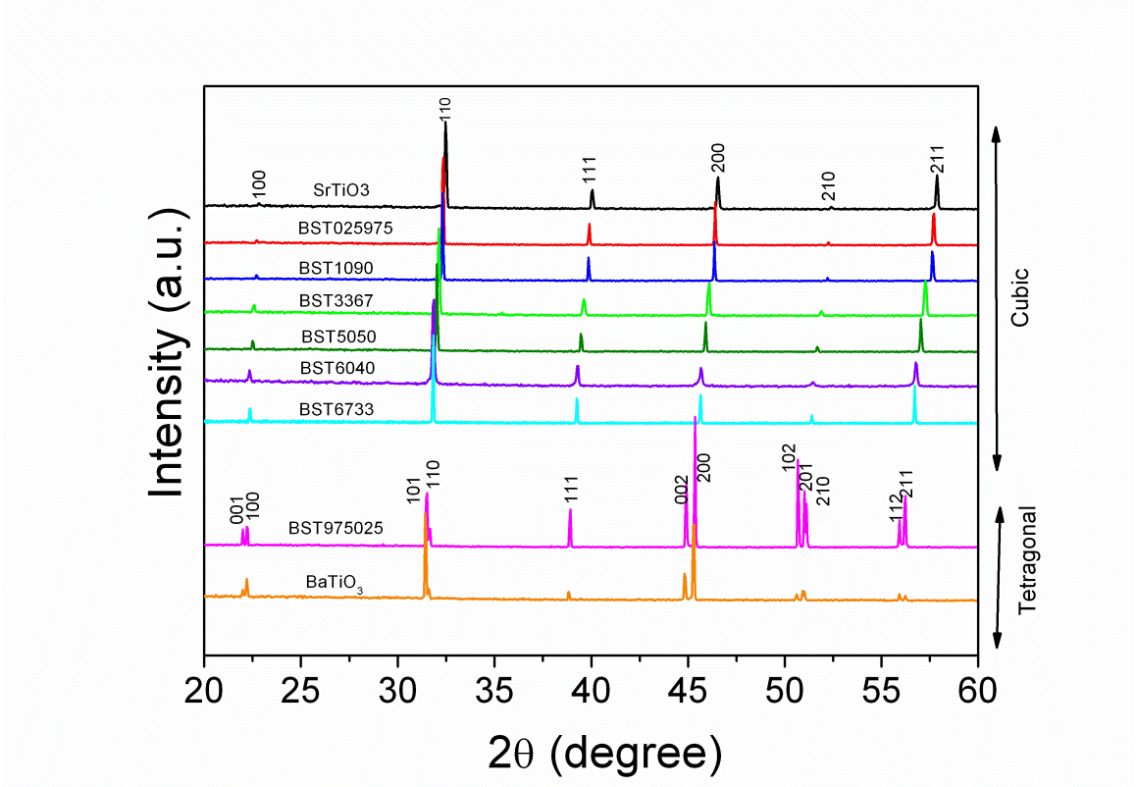

Figure 2.12-Representative XRD spectra on the sintered ceramics for pure $BaTiO_3$, $SrTiO_3$ and BST compositions.

2.9 Energy dispersive X ray Spectrometry (EDS)

The compositional homogeneity of the sintered ceramics was investigated by means of Energy Dispersive X-rays Spectroscopy (EDS). A cross section of a thin (about 320 μm) BST6040 disk was analyzed. In order to have an ideal surface for the compositional characterization a sector of about 250 μm in diameter of the cross section of the pellet was

polished with the ion beam milling technique. After milling the region of the cross section bombarded with ions, shows a very flat and homogeneous surface (Figure 2.13).

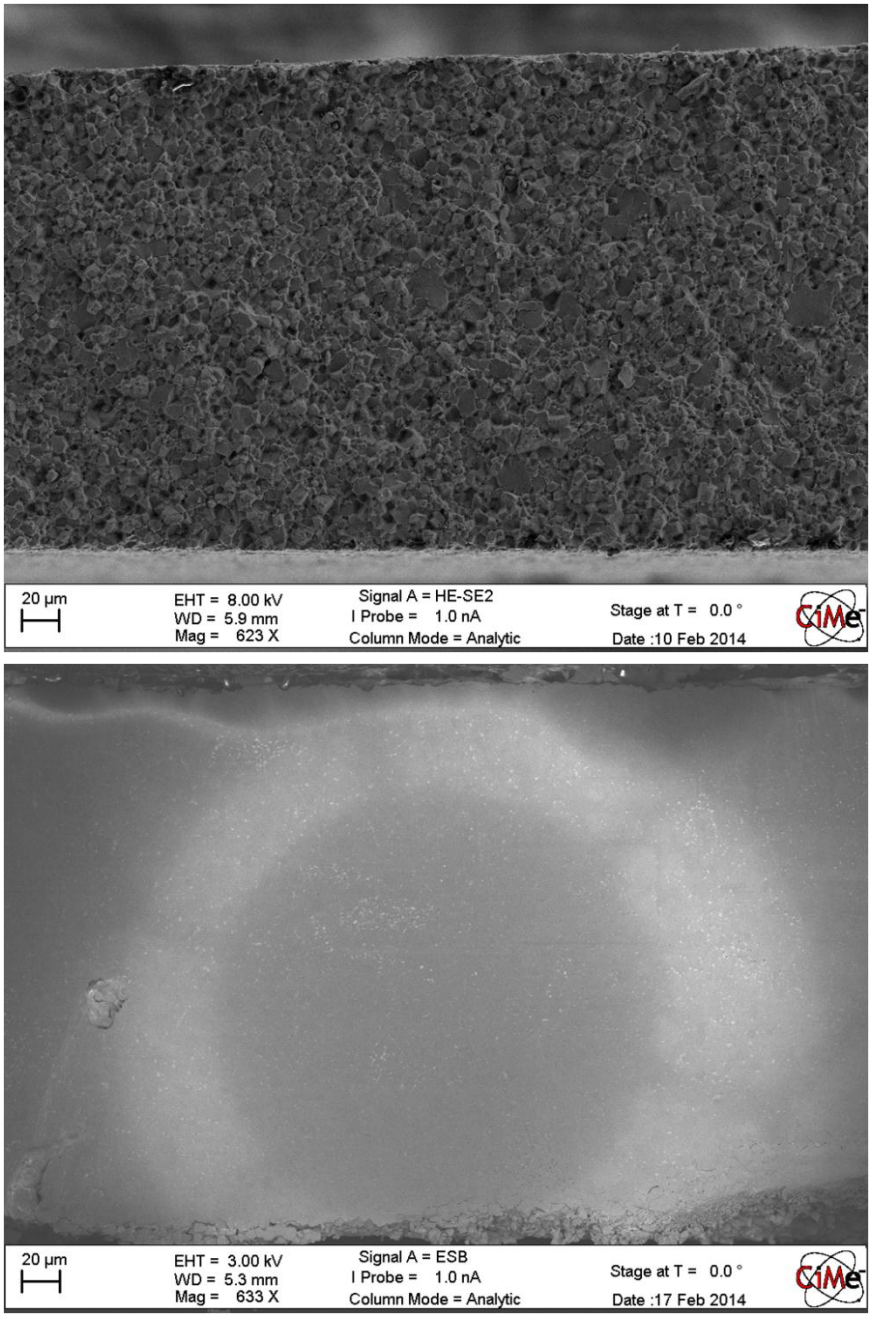

Figure 2.13-Cross section of a BST6040 pellet before (top) and after (bottom) ion milling. The ion milling was done by Mrs. Danièle Laub of CIME.

The scan of the polished surface reveals the presence of pores of the diameter of around 2 µm and the existence of small regions, about 1 µm in size, with a different contrast with respect to matrix (Figure 2.14).

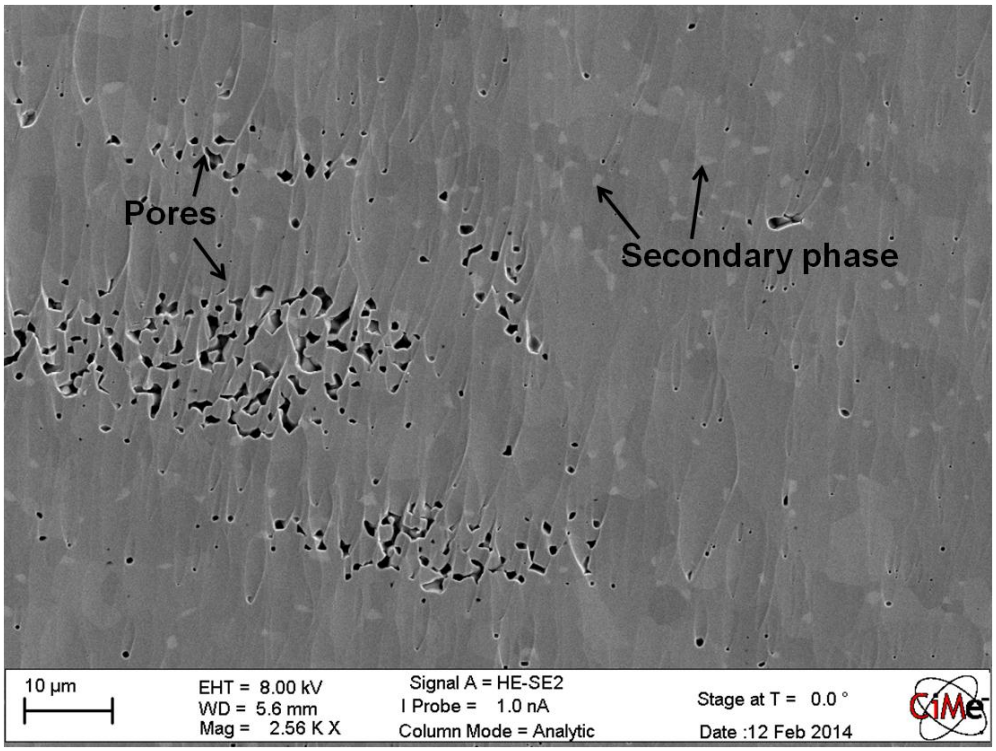

Figure 2.14-Image of the ion milled cross section of the BST6040 pellet showing pores and traces of the secondary phase.

These regions with different contrast are, most likely, a secondary phase, within the main barium strontium titanate phase. This was eventually confirmed by EDS compositional analysis. The EDS spectra collected scanning some grains of the secondary phase, show that such a phase consists almost entirely of barium-based compound with very small traces of strontium. This is well illustrated by the comparison of the elemental mapping of barium and strontium (Figure 2.15).

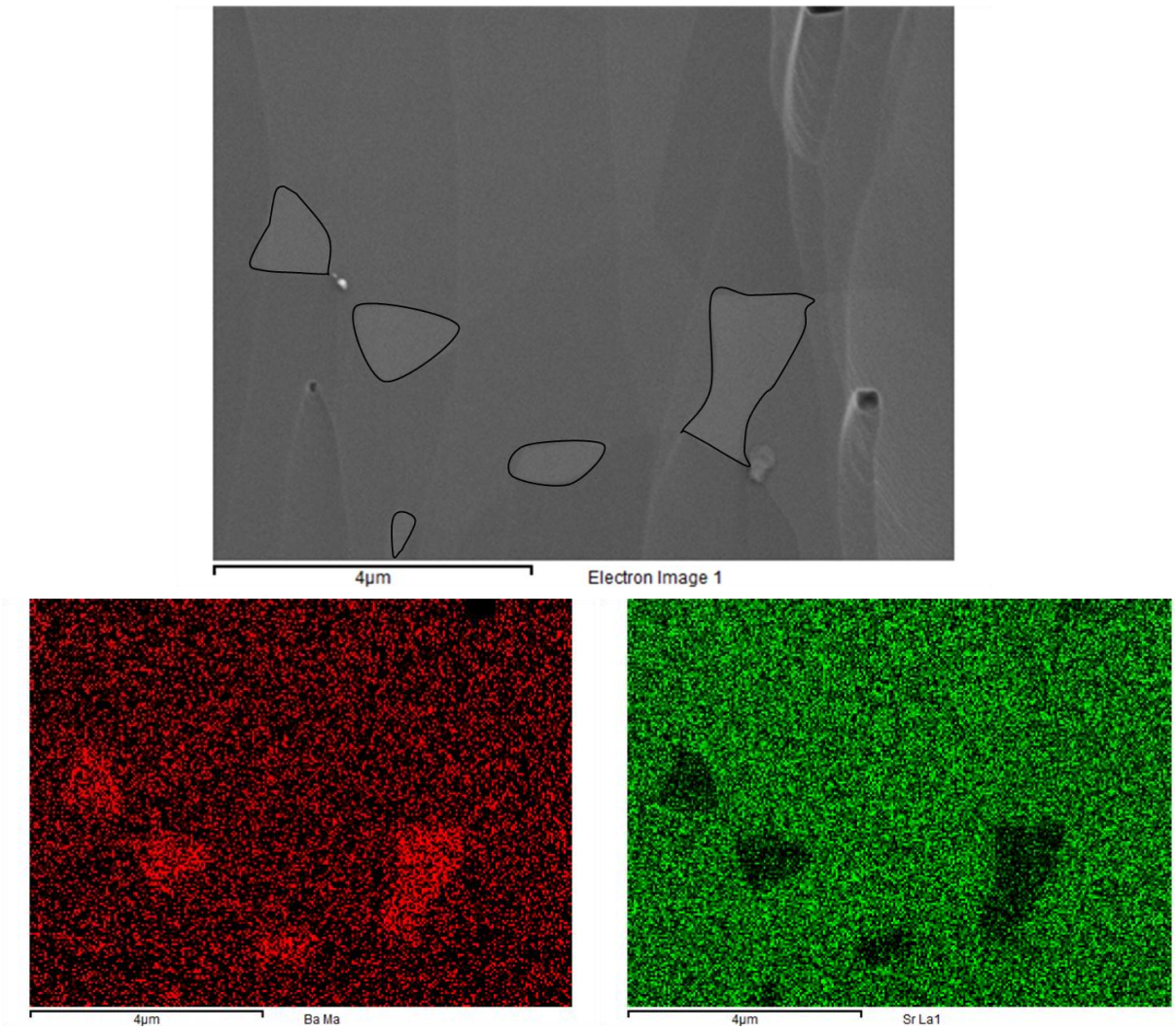

Figure 2.15-EDS elemental mapping for barium (red) and strontium (green) of the main BST6040 ceramic matrix and of the secondary phase. As indicated from the difference in the brightness, in the secondary phase the barium concentration is much higher and strontium much lower than in the matrix. The EDS analysis was performed by Dr Cosmin Sandu.

The compositional analysis on the main phase indicates a concentration of barium and strontium corresponding to the expected composition 60/40 (within the EDS analytical limit). In the secondary phase, the ratio between barium and titanium obtained by the elemental quantification is about to 2 to 1 with very small traces of strontium, suggesting that the secondary phase is likely to be the Ba_2TiO_4 orthotitanate [2, 27].

Since the secondary phase occupies a very small fraction of the volume of the ceramics (no more than 1%) it could not be detected with the XRD analysis (see section 2.8).The origin of the secondary phase cannot be explained with the high sintering temperature (1450^{o}C) since EDS analysis on BST6040 ceramics sintered at a lower temperature (1300^{o}C) also show the presence of a barium rich phase. This, together with the fact that the ceramics are processed by mixing directly $BaTiO_3$ and $SrTiO_3$ and not

formed from the decomposition of $BaCO_3$ and $SrCO_3$ suggests that the secondary phase could likely be present already in the starting $BaTiO_3$ powder. If this is the case, this phase should be detected in $BaTiO_3$

2.10 Determination of the dielectric properties

The measurement of the dielectric constant as a function of temperature was the method used to determine the paraelectric to ferroelectric phase transition in the different compositions of $(Ba,Sr)TiO_3$ ceramics and estimate the Curie point, taken as the maxima of the real part of the relative permittivity ε_r (see Table 2.1). Dielectric losses were also measured to obtain informations about the conductivity of the samples. For this analysis disks of 7.5 mm in diameter and 1.5 to 2 mm in thickness were used. The two faces of the disks were polished in order to have flat and parallel surfaces and were electroded with gold deposited by sputtering.

The relative permittivity ε_r was determined from the measurement of the capacitance of the ceramics according to the relation:

$$\varepsilon_r = \frac{C \times t}{\varepsilon_0 \times A} \qquad 2.3$$

where ε_0 is the permittivity of the vacuum, C is the capacitance of the ceramics samples, A the area of the electrode and t the sample thickness.

The capacitance and the losses were measured with a high precision HP 4284A LCR meter. The temperature of the samples was controlled with a 9023 Delta Design chamber. Measurements were performed upon heating and cooling with a rate of 2^0C minute. The capacitance was measured at several discrete frequencies in the range between 0.1 kHz and 100 kHz. The temperature of the Curie point decreases with the decreasing of the barium concentration (Figure 2.16). In the barium rich region of the solid solution, the decreasing of the Curie point follows an almost linear dependency with Sr concentration which becomes progressively non linear as the strontium content increases. This behavior is consistent with previous study on the $Ba_{1-x}Sr_xTiO_3$ solid solution [25]. The variation of Curie point follows closely the Vegard's law and indicates that the Ba and Sr cations are well mixed and homogeneously distributed over the sites of the perovskite structure.

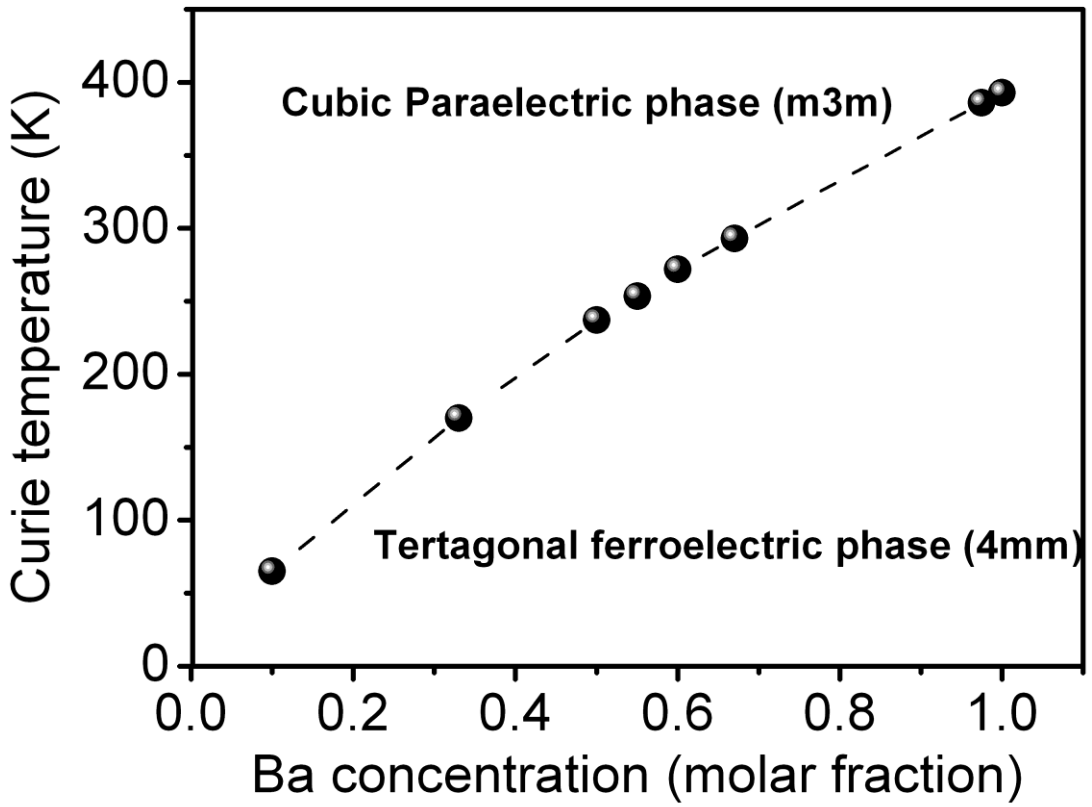

Figure 2.16-Variation of the Curie temperature as a function of barium content for $Ba_{1-x}Sr_xTiO_3$ ceramics down to 0.1 molar fraction of barium.

The relative permittivity measured as of function of temperature for $Ba_{1-x}Sr_xTiO_3$ compositions between down to 10% of barium are shown in Figure 2.17.

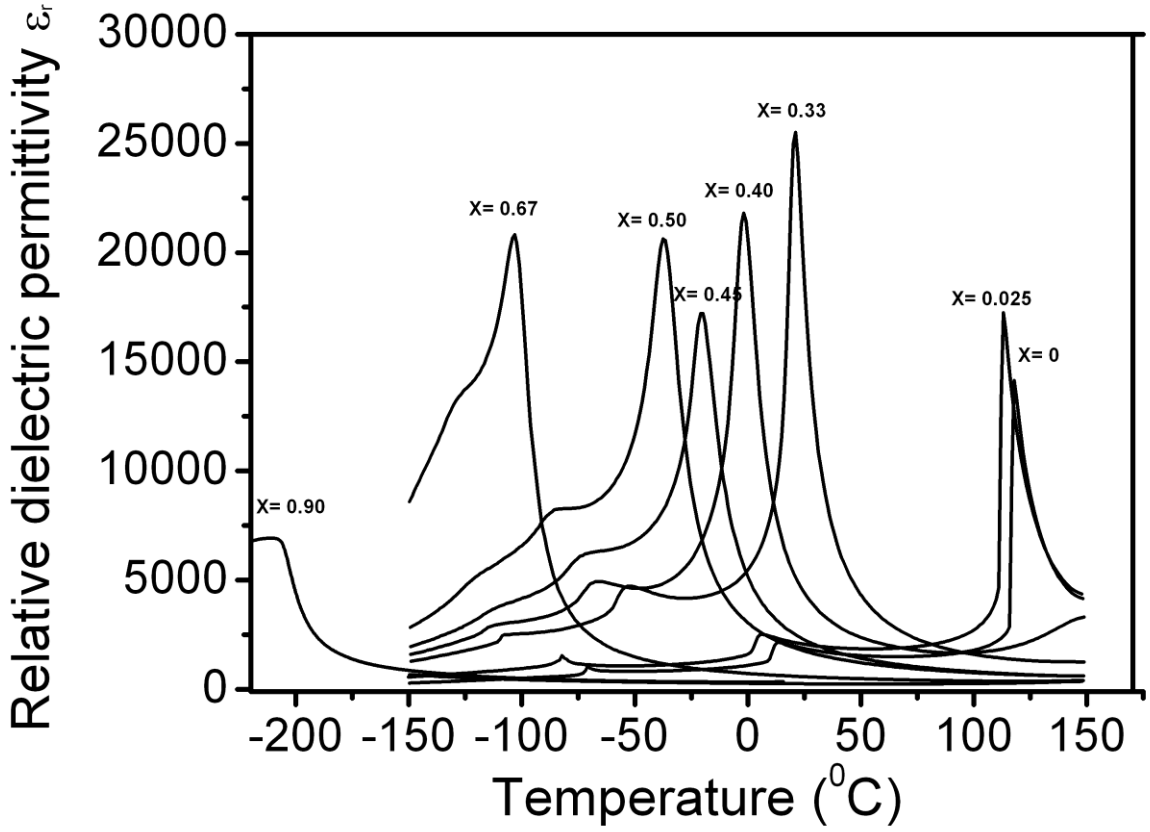

Figure 2.17-Realtive permittivity as a function of temperature for pure $BaTiO_3$ and $Ba_{1-x}Sr_xTiO_3$ compositions down to 10% of barium measured on cooling at the frequency of 100Hz. The x refers to the strontium amount.

The measurements show a thermal hysteresis in the Curie temperature and in the temperatures of the two polymorphic phase transitions (Figure 2.18).

The presence of a thermal hysteresis indicates that all phase transitions are of the first order. The first order character of the phase transitions also suggests that the sintered ceramics have a high compositional order and that the distribution of Ba^{2+} and Sr^{2+} cations on the A sites of the perosvkite is quite homogeneous. The compositional homogeneity is also indicated by the absence of diffuse phase transition (DFT) at the paraelectric to the ferroelectric phase, which in highly inhomogeneous $(Ba,Sr)TiO_3$ ceramics is observed even for a low amount of strontium [28]. A broad peak in the permittivity is observed only for BST1090 which is already in the region where the solid solution changes its behavior from ferroelectric to relaxor.

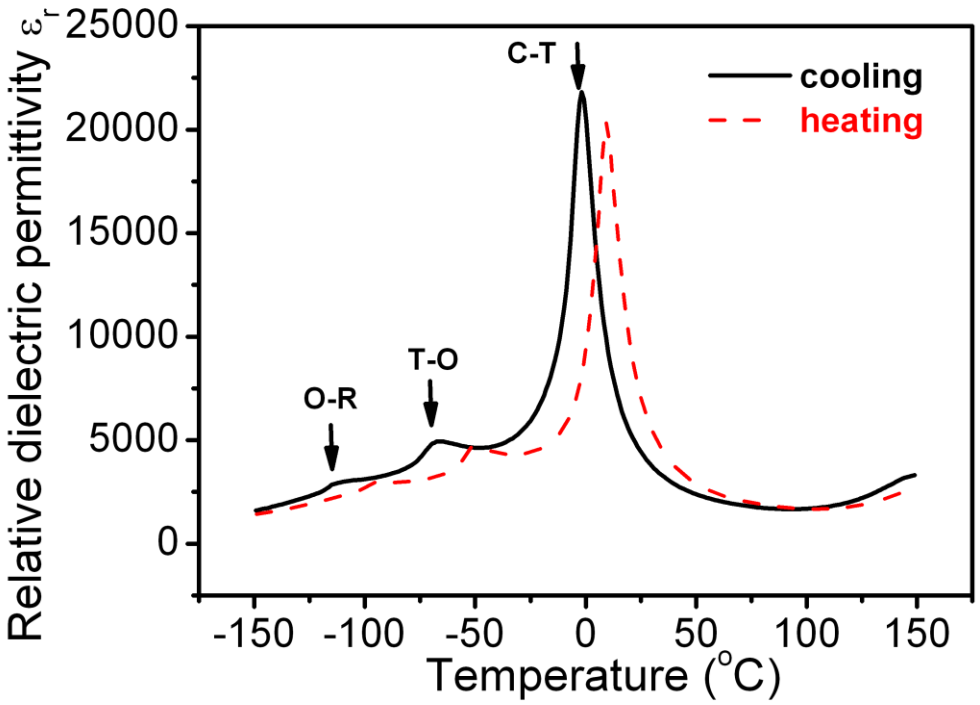

Figure 2.18-Relative dielectric permittivity for BST6040 ceramics measured as a function of temperature during cooling (solid line) and then upon heating (dashed line) at 100 Hz showing the polymorphic phase transitions: from cubic (C) to tetragonal (T) to orthorhombic (O) to rhombohedral (R) The Curie temperature (C-T phase transition) on heating is about 9°C higher than on cooling. This difference is nearly constant for all measured compositions.

In Figure 2.19 the dielectric constant and the loss tangent for pure $BaTiO_3$, BST6040 and BST3367 are shown. As the concentration of strontium increases the peaks in the permittivity at the three phase transition temperatures become more diffuse. Similarly to what is observed in previous studies of the $Ba_{1-x}Sr_xTiO_3$ solid solution [24, 25], with the increase of the strontium content the dielectric anomalies corresponding to the tetragonal to orthorhombic and to the orthorhombic to rhombohedral phase transition become less pronounced until they are suppressed for high strontium concentrations. The reported critical concentration for the disappearance of the low temperature polymorphic transitions is around 80% [25] and in fact a weak signature of the ferroelectric to ferroelectric phase transitions is still present in BST3367(67% of strontium content) indicated by the shoulder near the Curie peak. The critical temperature for pure $SrTiO_3$ can be estimated extrapolating the line for Sr reported in Figure 2.5. In the barium rich region of $(Ba,Sr)TiO_3$ solid solution, very low frequency dispersion in the dielectric constants are observed at the paraelectric to ferroelectric phase transition. The frequency dispersion increases with the strontium content indicating that with the addition of strontium the order of the system decreases.

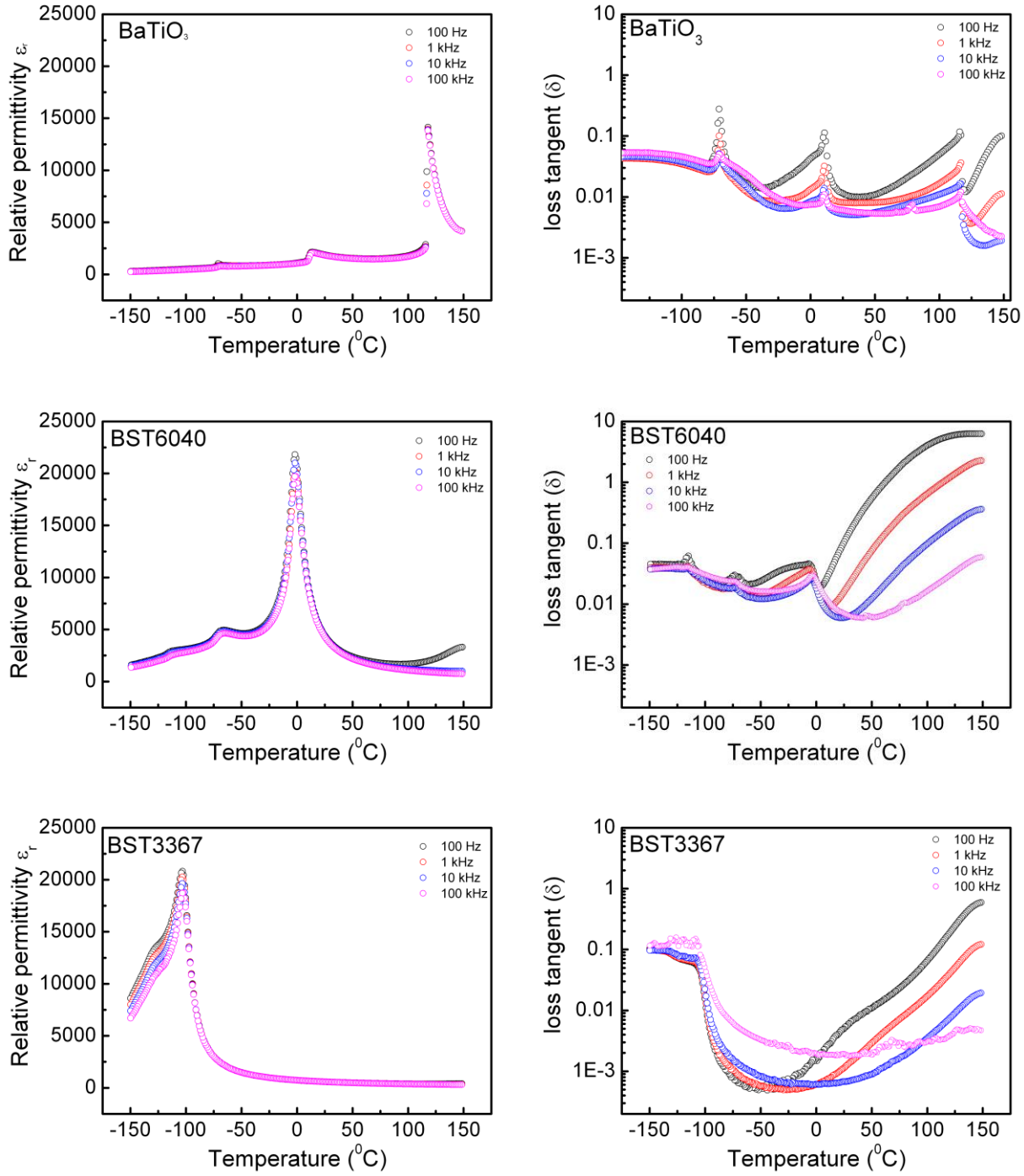

Figure 2.19-Temperature dependence of the real part of the dielectric constant and of the loss tangent in pure $BaTiO_3$ and in $(Ba,Sr)TiO_3$ solid solution for barium rich (BST6040) and strontium rich compositions (BST 3367).

At room temperature, the dielectric losses are between 1and 10% in all compositions for all the measured frequencies. However they show a huge increase as the temperature is raised above 100^{0}C especially at low frequency (100Hz). These high losses in the

paraelectric phase are most likely associated to the increase of the conductivity due to the detrapping of the inhomogeneous space charges present in the ceramics and which will be discussed in Chapter 5 and Chapter 6.

2.11 Conclusions

In this chapter, the optimization of the solid state route method to the synthesis of high quality $Ba_{1-x}Sr_xTiO_3$ ceramics has been reported. The characterization with SEM and X-ray diffraction indicates high density ceramics with compact microstructures and in the single perosvkite phase. Small traces (below 1%) of a secondary phase are detected with EDS analysis. The measurement of the dielectric properties confirms the high compositional order of the ceramics, good chemical homogeneity of the samples and show values and variation of the dielectric constant in good agreement with what has been reported in the literature for the $Ba_{1-x}Sr_xTiO_3$ solid solution.

2.12 Bibliography

[1] R. E. Newnham and L. E. Cross, "Ferroelectricity: The foundation of a field from form to function," *Mrs Bulletin,* vol. 30, pp. 845-848, Nov 2005.

[2] D. E. Rase and R. Roy, "Phase Equilibria in the System BaO-TiO_2," *Journal of the American Ceramic Society,* vol. 38, pp. 102-113, 1955.

[3] R. M. Glaister and H. F. Kay, "An investigation of the cubic-hexagonal transition in baium titanate," *Proceedings of the Physical Society of London,* vol. 76, pp. 763-771, 1960.

[4] D. C. Sinclair, J. M. S. Skakle, F. D. Morrison, R. I. Smith, and T. P. Beales, "Structure and electrical properties of oxygen-deficient hexagonal $BaTiO_3$," *Journal of Materials Chemistry,* vol. 9, pp. 1327-1331, Jun 1999.

[5] B. Jaffe, W. R. Cook, and H. L. Jaffe, *Piezoelectric ceramics*: Academic Press, 1971.

[6] W. J. Merz, "The electric and optical behaviour of $BaTiO_3$ single-domain crystals " *Physical Review,* vol. 76, pp. 1221-1225, 1949.

[7] K. Uchino, E. Sadanaga, and T. Hirose, "Dependence of the crystal structure on particle size in barium titanate," *Journal of the American Ceramic Society,* vol. 72, pp. 1555-1558, Aug 1989.

[8] K. Kinoshita and A. Yamaji, "Grain-size effects on dielectric properties in barium-titanate ceramics," *Journal of Applied Physics,* vol. 47, pp. 371-373, 1976.

[9] H. F. Kay, H. J. Wellard, and P. Vousden, "Atomic positions and optical properties of barium titanate," *Nature,* vol. 163, pp. 636-637, 1949.

[10] G. Shirane and A. Takeda, "Volume change at 3 transitions in $BaTiO_3$ ceramics," *Journal of the Physical Society of Japan,* vol. 6, pp. 128-129, 1951.

[11] W. T. Hao, J. L. Zhang, P. Zheng, Y. Q. Wu, Y. Q. Tan, and X. Zhao, "Influence of Orthorhombic-Tetragonal Phase Transition on Microwave Dielectric Dispersion of $BaTiO_3$ Ceramic," *Chinese Physics Letters,* vol. 30, Dec 2013.

[12] D. A. Berlincourt and F. Kulcsar, "Eelectromechanical properties of $BaTiO_3$ compositions showing substantial shifts in pahse transitions points," *Journal of the Acoustical Society of America,* vol. 24, pp. 709-713, 1952.

[13] S. Nomura, "Solid state reaction between barium titanate and strontium titanate," *Journal of the Physical Society of Japan,* vol. 11, pp. 924-929, 1956.

[14] F. Schrey, "Effect of pH on chemical preparation of barium-stromtium titanate," *Journal of the American Ceramic Society,* vol. 48, pp. 401-&, 1965.

[15] S. Ueda, "Crystal-growth and dielectric properties of barium strontium-titanate Ba0.97SrO.03TiO3," *Materials Research Bulletin,* vol. 9, pp. 469-476, 1974.

[16] P. Padmini, T. R. Taylor, M. J. Lefevre, A. S. Nagra, R. A. York, and J. S. Speck, "Realization of high tunability barium strontium titanate thin films by rf magnetron sputtering," *Applied Physics Letters,* vol. 75, pp. 3186-3188, Nov 1999.

[17] G. Shirane and K. Sato, "Effects of mecahnical pressures on the dielectric properties of polycrystalline barium-strontium titanate," *Journal of the Physical Society of Japan,* vol. 6, pp. 20-26, 1951.

[18] A. K. Tagantsev, V. O. Sherman, K. F. Astafiev, J. Venkatesh, and N. Setter, "Ferroelectric materials for microwave tunable applications," *Journal of Electroceramics,* vol. 11, pp. 5-66, Sep-Nov 2003.

[19] F. A. Miranda, C. H. Mueller, C. D. Cubbage, K. B. Bhasin, R. K. Singh, and S. D. Harkness, "HTS Ferroelectric Thin-films for tunable microwave components," *Ieee Transactions on Applied Superconductivity,* vol. 5, pp. 3191-3194, Jun 1995.

[20] A. Tombak, F. T. Ayguavives, J. P. Maria, G. T. Stauf, A. I. Kingon, and A. Mortazawi, "Low voltage tunable barium strontium titanate thin film capacitors for RF and microwave applications," in *2000 Ieee Mtt-S International Microwave Symposium Digest, Vols 1-3*, T. Perkins, Ed., ed New York: Ieee, 2000, pp. 1345-1348.

[21] J. S. Lee, J. S. Park, J. S. Kim, J. H. Lee, Y. H. Lee, and S. R. Hahn, "Preparation of (Ba, Sr)TiO3 thin films with high pyroelectric coefficients at ambient temperatures," *Japanese Journal of Applied Physics Part 2-Letters,* vol. 38, pp. L574-L576, May 1999.

[22] W. Y. Hsu, J. D. Luttmer, R. Tsu, S. Summerfelt, M. Bedekar, T. Tokumoto*, et al.*, "Direct-current conduction properties of sputtered Pt/$(Ba_{0.7}Sr_{0.3})TiO_3$/Pt thin-films capacitors," *Applied Physics Letters,* vol. 66, pp. 2975-2977, May 1995.

[23] W. H. Ma and L. E. Cross, "Flexoelectric polarization of barium strontium titanate in the paraelectric state," *Applied Physics Letters,* vol. 81, pp. 3440-3442, Oct 28 2002.

[24] L. Q. Zhou, P. M. Vilarinho, and J. L. Baptista, "Dependence of the structural and dielectric properties of $Ba_{1-x}Sr_xTiO_3$ ceramic solid solutions on raw material processing," *Journal of the European Ceramic Society,* vol. 19, pp. 2015-2020, 1999.

[25] V. V. Lemanov, E. P. Smirnova, P. P. Syrnikov, and E. A. Tarakanov, "Phase transitions and glasslike behavior in $Sr_{1-x}Ba_xTiO_3$," *Physical Review B,* vol. 54, pp. 3151-3157, Aug 1996.

[26] L. Nedelcu, M. I. Toacsan, M. G. Banciu, and A. Ioachim, "Dielectric Properties of Paraelectric $Ba_{1-x}Sr_xTiO_3$ Ceramics," *Ferroelectrics,* vol. 391, pp. 33-41, 2009.

[27] J. A. Bland, "Crystal Structure of Barium Orthotitanate, Ba_2TiO_4," *Acta Crystallographica,* vol. 14, pp. 875-&, 1961.

[28] V. S. Tiwari, N. Singh, and D. Pandey, "Diffuse ferroelectric transition and relaxational dipolar freezing in (Ba,Sr)TiO_3," *Journal of Physics-Condensed Matter,* vol. 7, pp. 1441-1460, Feb 1995.

Chapter 3 : Experimental techniques

3.1 Introduction

The scope of this chapter is to give to the reader a short overview of the main experimental methods used to characterize the materials investigated in this study. The designs of the instruments are briefly presented and possible issues encountered in each technique are discussed.

3.2 Pyroelectric measurement

A pyroelectric material exhibits spontaneous polarization which changes when its temperature is varied. The pyroelectric effect at constant stress can be written in the form [1]:

$$dD_i = p_i^{\sigma} dT \qquad 3.1$$

where D_i is the dielectric displacement, p_i^{σ} the pyroelectric coefficient at constant stress and T is the temperature. At constant (or zero) electric field (short circuit conditions), the equation 3.1 can be written as:

$$dP_i = p_i^{\sigma} dT \text{ or } p_i^{\sigma} = \left(\frac{\partial P_i}{\partial T}\right)_{\sigma} \qquad 3.2$$

where P_i is the polarization present in material. The change in polarization is related to the surface charge Q distributed over the sample area A. The pyroelectric coefficient can be therefore expressed as:

$$p = \frac{1}{A}\left(\frac{\partial Q}{\partial T}\right)_{\sigma} \qquad 3.3$$

The flow of the charge into an external circuit is known as the pyroelectric current i_p. The pyroelectric coefficient can be written in terms of the rate of change of temperature as:

$$p = \frac{i_p}{A\left(\frac{dT}{dt}\right)} \qquad 3.4$$

where the index i has been omitted for simplicity. The units for the pyroelectric coefficient p are $Cm^{-2}K^{-1}$ [2]. The equation 3.4 has been widely adopted as definition of the measured

pyroelectric coefficient. The coefficient p is the total pyroelectric coefficient which comprises a primary component (at constant strain x) and a secondary component (at constant stress σ) [3]:

$$p_{total} = \left(\frac{\partial D}{\partial T}\right)_{x,E} + \left(\frac{\partial D}{\partial x}\right)_{E,T}\left(\frac{\partial x}{\partial T}\right)_{\sigma,E} \qquad 3.5$$

Experimentally it is difficult to measure the different components separately and the coefficient considered is usually the total one. The measurement technique to determine the pyroelectric properties are divided in 3 categories according to the classification proposed by Lang [4]: static, indirect and dynamic. The static methods are those methods in which the samples are subjected to an incremental change of temperature whilst measuring the charge displacement. The measurements are taken only at discrete temperatures. Because these methods are time consuming, they are rarely used. In the indirect methods, the pyroelectric coefficient is derived from the measurement of a related parameter such as polarization.

The most widely used techniques are, however, the dynamic ones, which imply measurement of the pyroelectric current while the temperature of the specimen is varied in a continuous way.

One of the traditional dynamic methods to measure the pyroelectric charge is the linear temperature-ramp (Byer-Roundy) [5, 6] technique. According to this method, the temperature of the sample is ramped at a constant rate (dT/dt) and the thermally stimulated current flowing between the electrodes is measured.

It is possible to calculate the pyroelectric coefficient using equation 3.4. The disadvantages of this method are: i) the difficulty of generating an accurate linear temperature rate ii) the inability of the technique to distinguish between the reversible pyroelectric current and the irreversible thermally stimulated current, which is not necessarily pyroelectric in origin.

To avoid this inconvenience, the temperature-oscillation (or a.c. or Chynoweth [7]) method is preferred, as it offers the advantage to distinguish between reversible and irreversible currents.

This was the technique used for all pyroelectric characterization discussed in this study. The set-up used for the measurements is similar to that described by Daglish [1]. A scheme of the setup is given in Figure 3.1.

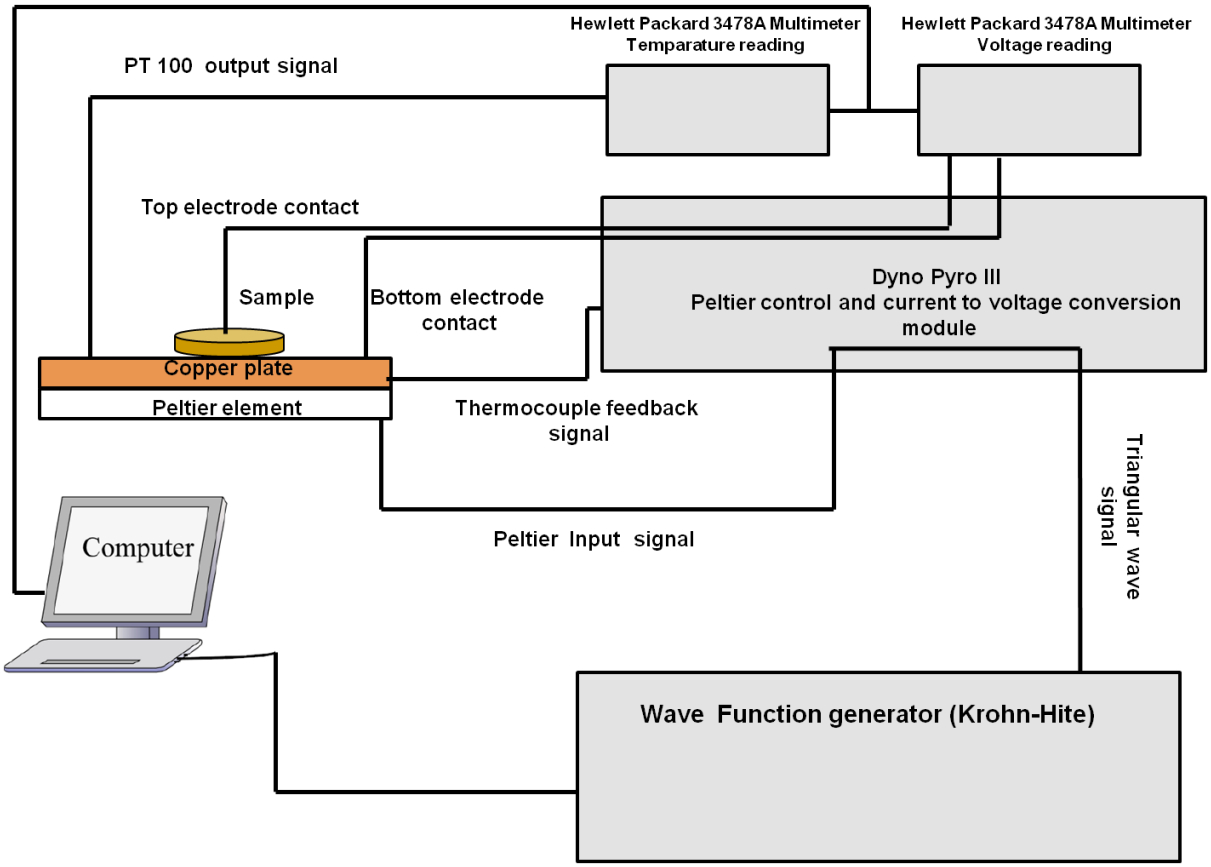

Figure 3.1-Scheme of the experimental setup used for the pyroelectric measurements.

During the measurement, the temperature of the sample is modulated by a Peltier element in a regular periodic fashion (a triangular wave), whilst the current wave form is recorded. The temperature is regulated by a resistance temperature detector (RTD) PT 100 based on the temperature variation of the resistance of platinum (resistance 100 ohms at $0^{o}C$) positioned close to the sample, and a thermocouple providing a feed-back mechanism. The temperature of the PT 100 is read with a Multimeter. The modulation of the temperature is cycled at low frequency (between 10 and 100 mHz). The amplitude of the variation of the temperature was usually 1K peak-to-peak. The sample was placed on a copper plate placed on the top of the Peltier element. The current signal flowing through the sample during the temperature variation is sent to a home-made control module (Dyno Pyro III), where it is electronically converted into voltage and amplified. The voltage output is measured with a Multimeter. The setup is controlled automatically by a computer running a Labview program, which also records all the data.

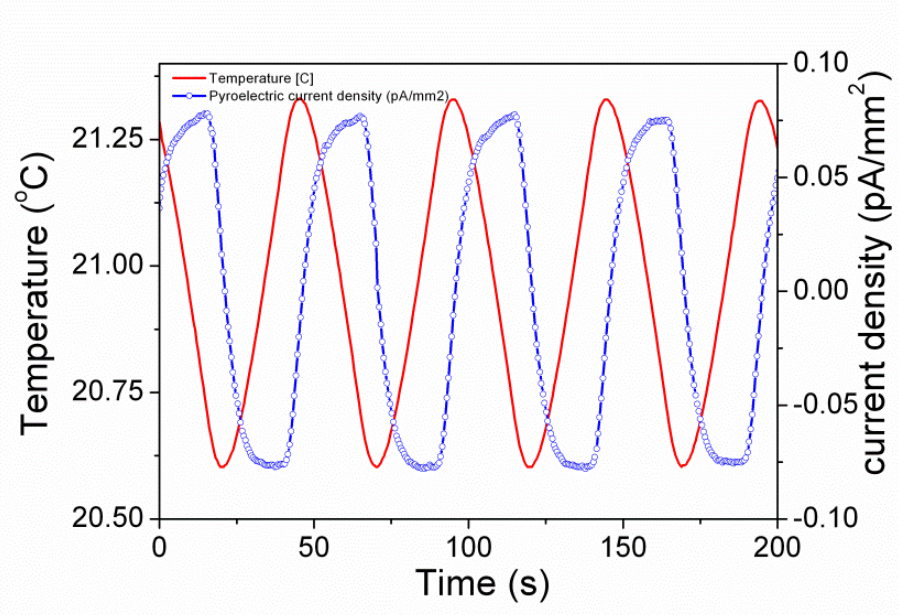

Figure 3.2-Typical pyroelectric response to an applied triangular wave of a BST6040 as-sintered and electroded ceramics. The current is normalized to the area of the sample.

The typical current signal for the (Ba,Sr)TiO_3 ceramics is a slightly distorted square wave as it is shown in Figure 3.2. The pyroelectric response has a direction. This implies that the current signal reverses its phase by 180^o with respect to the temperature change when the sample is inverted.

When the pyroelectric measurement is performed, it is very important to have homogenous change of temperature across the sample. If the temperature does not change uniformly, an additional pyroelectric contribution can be induced through piezoelectric effect present in all pyroelectric materials. This referred to as “false” or “tertiary pyroelectric effect”, to distinguish it from the first two contributions to the pyroelectric effect (Equation 3.5). This effect is observable in all piezoelectrics even if there is not true pyroelectric effect (one example is quartz). To avoid the problem of non homogeneous heating, the samples used for pyroelectric characterization were not thicker than 0.5-0.6 mm and diameter was about 5.70 mm. The pyroelectric temperature oscillation method is precise (better than 1%) and reliable. Although in our case we are not dealing with the exact quantification of the pyroelectric coefficient of the paraelectric apparently polar ceramics it is important to have a precise and reliable method since the magnitude of the pyroelectric effect in such ceramics is quite small. For example, the value of the pyroelectric coefficient reported for poled ceramics of $BaTiO_3$ is about 200 $\mu Cm^{-2}K^{-1}$ (considering the combination of the primary and secondary pyroelectric effect) [2] while in the case of the BST6040 paraelectric polar ceramics the magnitude of the pyroelectric coefficient is in the range of 0.5 -5 $\mu Cm^{-2}K^{-1}$.

The temperature oscillation method has the advantage that the reference temperature is fixed during the measurement and it is therefore straightforward to study

the time evolution of the pyroelectric response and to monitor its stabilization. If distortions are present in the current traces, they are immediately apparent and they can provide useful informations about the samples state. For example, a saw-tooth profile of the current often indicates the presence of space charges [1].

3.3 Direct piezoelectric effect measurement

One way to measure the piezoelectric properties of crystal and ceramics is via the direct piezoelectric effect. The method consists in measuring charge upon the application of a mechanical stress. The piezoelectric longitudinal coefficient d_{33} refers to the component of the piezoelectric tensor parallel to the direction where the load is applied. In Voigt notation [3], the longitudinal piezoelectric coefficient is expressed as:

$$D_3 = d_{33}\sigma_3 \qquad 3.6$$

where D_3 is the charge density resulting from the applied stress σ_{33}.

The piezoelectric longitudinal coefficient can be measured with the Berlincourt method [8], named after the physicist Don Berlincourt. The charge Q_s ($D_3=Q_s/A$) released by the sample is measured with a parallel sensing capacitance C_s large enough to collect all the piezoelectric charge generated by the sample but not so large that the measured voltage is too small. The force applied on the sample is probed with a sensor of a known piezoelectric coefficient d_r placed mechanically in series with the sample, in such a way that the sample and the quartz sensor feel the same force F. The charges produced on the samples and the reference, Q_s and Q_r are measured as voltage across the parallel capacitance C_s and C_r. Since the sample and the reference feel the same force it can be written that $Q_s=d_sF$ and $Q_r= d_rF$.
The piezoelectric coefficient of the sample is then:

$$d_s = d_r\left(\frac{Q_s}{Q_r}\right) \qquad 3.7$$

This can be equated to the measured voltages since $Q_s = C_s V_s$ and $Q_r = C_r V_r$. The expression for the piezoelectric coefficient d_s becomes then:

$$d_s = d_r\left(\frac{C_s}{C_r}\right) \times \left(\frac{V_S}{V_r}\right) \qquad 3.8$$

d_r is a known quantity and the ratio C_r/C_s can be set to unity. From the equation 3.8, it follows that it is possible to determine the piezoelectric coefficient of the sample

measuring the two voltages V_s and V_r. A schematic of the set-up for the direct piezoelectric measurement is shown in Figure 3.3.

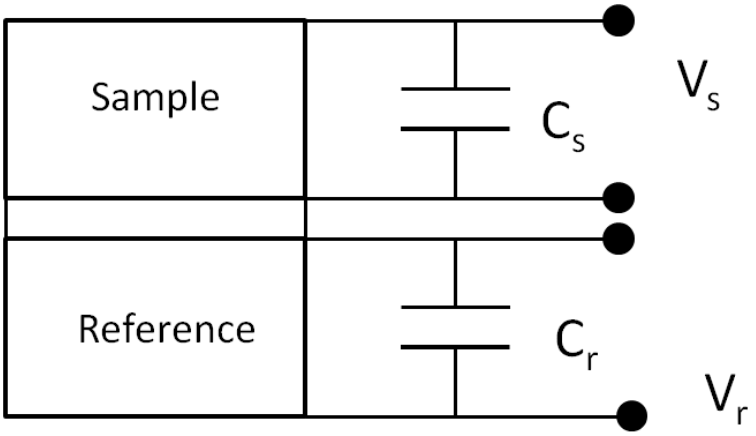

Figure 3.3-Schematic of a Berlincourt-type set up for the determination of the piezoelectric coefficient of a ceramic.

The piezoelectric characterizations reported in this study where performed with a sophisticated Berlincourt-type press, assembled in our laboratory. The schematic of the instrument is shown in Figure 3.4.

The press consists of a quartz reference sensor, a PZT actuator and a sample holder mounted in series between two zirconia columns, which are held together within a rigid steel frame .The quartz sensor, a Kistler 9061A is used to sense the force on the sample. The charge is measured with a Kistler type 5011 charge amplifier whose output is sent to a Tektronix 430A digital oscilloscope. A PZT actuator from PI systems, driven by a signal generator via a high voltage amplifier, provides both the static and the dynamic components of the force. The static component of the force is defined as the offset bias, while the dynamic one is defined as the amplitude of the sinusoidal voltage.

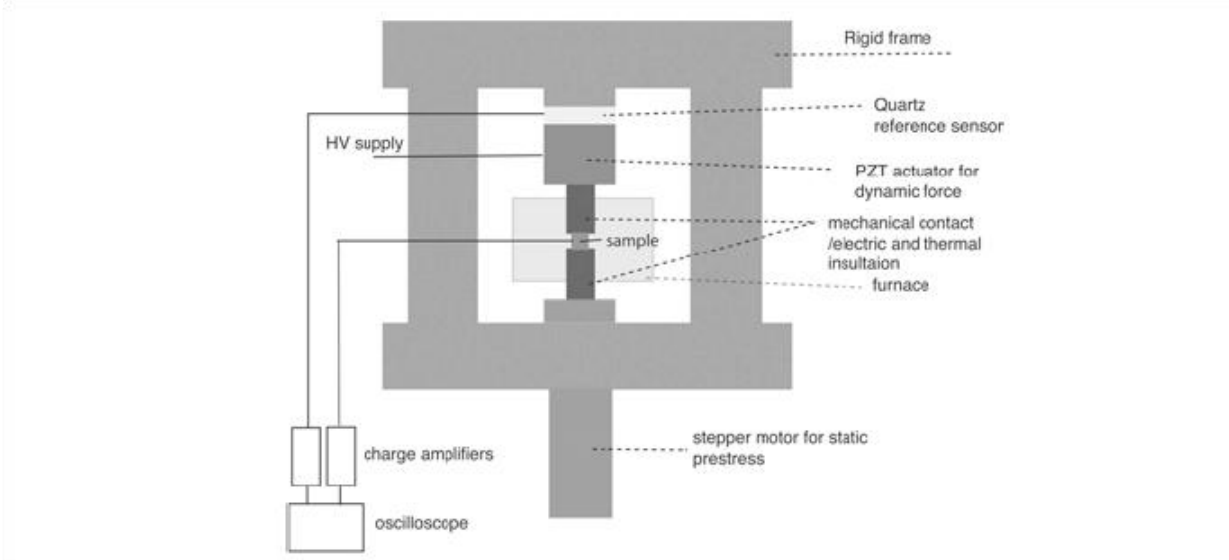

Figure 3.4-Schematic of the Berlincourt-type press used for the piezoelectric properties determination [9].

The sample is inserted in between two flat stainless steel plates fixed at the ends of the zirconia columns. A steel hemisphere is placed on the top of the sample to compensate for imperfect alignment of the zirconia columns and imperfect parallelism of the sample surfaces. The metal plates act both as mechanical contacts to the sample and electrical contacts for charge collection. The piezoelectric charge produced by the sample is measured by a second charge amplifier Kistler 9061A connected to the second channel of the oscilloscope. All measurement are automatically controlled by a computer. A Labview program is used to record the data from the oscilloscope.

The piezoelectric properties can be measured as function of temperature (up to 300^{o}C) placing the zirconia columns and the sample inside a furnace. During the measurement, a prestress σ is applied by raising the bottom column with a stepper motor to put the entire system under compression. For dynamical measurements, after the application of a fixed amount of prestress, a dynamical load ($\sigma_d=\sigma_0 \sin(\omega t)$) and a static pressure (σ_s) are applied on the prestress σ with the actuator. The dynamic stress applied never exceeds the total prestress ($\sigma+\sigma_s$), in such a way that the system is always in compression. The maximum static force which can be applied is >4000N while the maximum dynamical force is around 1000N.

The frequency range of the measurements is limited at high frequencies (600 Hz) by the piezoelectric resonance of the press, which is around 1.2 KHz. At very low frequencies, the problem is “charge drift” which can lead to unclosed charge-stress loops. The charge drift is particularly detrimental in materials with low piezoelectric response such as the $Ba_{1-x}Sr_xTiO_3$ ceramics. The most common origin of the charge drift is conductivity of the sample, reduced insulation of connection lines, and, in polar samples, pyroelectric effect due to thermal oscillations.

In the setup described here, in contrast to many other commercial setups developed on the Berlincourt method, the pressure is applied across the entire surface of the sample. The metal plates are designed to have flat and parallel surfaces in order to give a more homogeneous distribution of the forces. However, due to the friction between the sample and the metal, the expansion of the sample is impeded and lateral forces are produced. This leads to a reduction of the effective piezoelectric coefficient which depends on the aspect ratio of the sample. Furthermore, even for well polished plates small roughness cannot be completely avoided. Any deviation from the ideal flatness of the metal will introduce an error in the measurement of the piezoelectric coefficient [10]. The points discussed above are particularly crucial when the piezoelectric response of the sample is very small, as in the case of the unpoled $Ba_{1-x}Sr_xTiO_3$ ceramics.

3.4 Thermally stimulated current.

In this section we present a short discussion on the thermally stimulated current technique used in the Chapter 6 to investigate the polar character of the polar paraelectric phase of (Ba,Sr)TiO_3 ceramics.

The *Thermally Depolarization Current* (TDC), technique, which in our work will be referred simply as *Thermally Stimulated Current* (TSC) technique is a part of a wider group of thermally stimulated processes which include *thermoluminescence*, *thermally stimulated conductivity*, *thermally stimulated electrons emission* and *differential scanning calorimetry,* only to cite some. All these processes are caused by different mechanism but often give very similar thermograms.

For the analysis of some of the thermally stimulated process, theories have been developed describing the current originating from a known or an assumed process. These theories are not directly applicable here because we do not know the exact origin of the charge. In addition, we are not using measured currents to exactly identify the charged species contributing to the thermally stimulated signal of our samples but rather to correlate the change in the sign of the thermally stimulated peaks with the presence of the built-in polarization in the ceramics. In addition, we use TSC to identify presence of unstable component of polarization, as will be discussed later in Chapter 6.

It should be stressed that, while the measurement of the thermally stimulated current is rather simple to perform, its analysis is quite complicated and the interpretation of the results in terms of microscopic models is often not straightforward, due to the complexity of the processes involved. The application of oversimplified models can lead to apparently successful but completely misleading results [11]. For these reasons, the mathematical descriptions developed for the analysis of simple thermally stimulated phenomena are not discussed in details in this section

It is nevertheless useful to give a short overview of the TSC process and to describe which mechanisms may be involved in it. This helps us in identifying presence of built-in polarization in our samples and separating it from the variable (volatile) component.

The TSC technique is a powerful method to study the relaxation of oriented dipoles in polymers or non uniform distribution of electronic or ionic charge carriers in inorganic materials. The technique usually requires that the samples are polarized under a constant electric field E_p, at a given temperature T_p and then cooled while the field is still applied, to a lower temperature T_o. Such poled sample is called an electret. The defects present in the material will respond to the applied field reorienting a dipole or a charge distribution [12] which freezes-in at T_o, and remains frozen even if the electric field is removed. When the temperature is increased again, providing that sufficient thermal energy is supplied, the oriented dipoles are free to rotate while the trapped charges, activated by the thermal energy, become mobile. The rotation of the dipoles toward the equilibrium position or the detrapping of the charges gives rise to a small current which can be recorded in an external circuit as thermally stimulated current.

Historically, Frei and Groetzinger [13] reported the first TSC as a function of temperature caused by the discharge of an electret.

The first theoretical background of the TSC technique was developed by Bucci and Fieschi [14]. Their model was developed for the study of the relaxation of point defects dipoles in ionic crystals and material response was referred to as *ionic thermocurrent* (ITC)

Besides the orientation of the dipoles, the polarization of a dielectric can be due to the polarization by the space charges. Space charge polarization can results from carrier drift or injection process such as i) the drift of electrons and holes toward the electrodes and their trapping; ii) the migration under the field of ions and ionic vacancies over macroscopic distances and their accumulation at the electrodes or at the grain boundaries (the Maxwell Wagner effect); and iii) the injection of electrons and holes from the electrodes into the dielectric [11].

The charge trapping around the imperfections present in the material (impurities, dislocations…) is not only caused by the application of an electric field but also by the excitation of the sample with electromagnetic radiation as in the case of *thermoluminescence* (TL). A first model for the study of the single trap thermoluminescence was proposed 1945 by Randal and Wilkins [15]. In this model the authors supposed that the intensity of the thermoluminescence signal is proportional to the rate at which the trapped charges are thermally released and that rate it is proportional to the population of trapped charges.

Ionic solids contain mobile electrons or ions which can migrate toward the electrodes during the application of the electric field. The field will drive the positive carriers toward the negative electrode and the negative carriers toward the positive electrode. The migration of the charge carriers induced by the electric field is weakened by diffusion, as

part of the electrons is lost in the recombination process with charges of opposite sign. However, the net effect of the electric field will dominate causing an accumulation of the excess charges at the interface with the electrodes. The charges are frozen in a metastable state during the cooling process under field. When the temperature is raised again the frozen charge carriers are thermally activated and start to move under their own field and by diffusion [12]. Another source of thermally stimulated current is temperature dependence of the spontaneous polarization in ferroelectric and polar materials, as explained in section 3.2. The sign of the current will depend on orientation of the sample. In the same way, the current from an electret formed by an electric field, discussed above, will depend on the orientation of the sample.

Besides the mechanisms mentioned above and associated to the charged defects specific to each material, the thermal current can also be produced by a thermal gradient across the sample (Seeback effect) [16] or by a small voltage on the operational amplifier of the picoammaeter [17]. The sign of these currents does not depend on the orientation of the sample.

The thermally stimulated current measurements were made with the setup show in Figure 3.5.

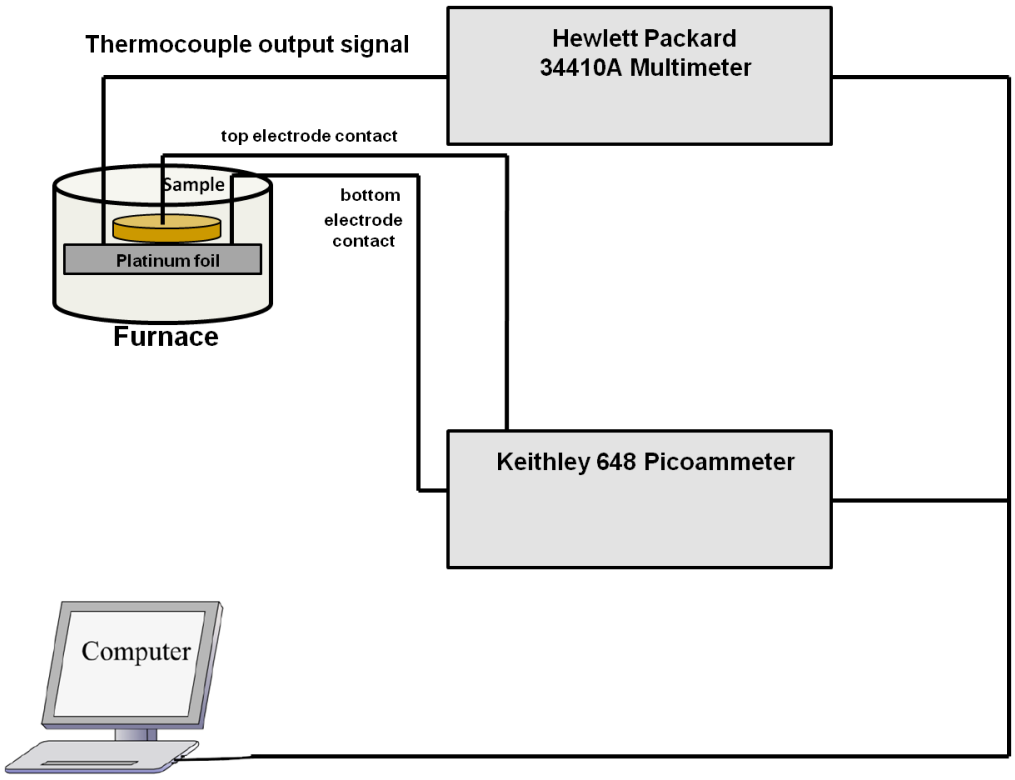

Figure 3.5-Schematic of the setup for thermally stimulated current measurement

In the setup, the current released by the samples is measured with a Keithley 648 picoammeter. The samples are heated at constant temperature rate in a furnace controlled by a Eurotherm temperature controller. To ensure a uniform heating and a good thermal

conductivity, the samples are placed on a small platinum foil put on the top of a sapphire disk. The temperature is measured with a thermocouple connected to the sapphire. The thermocouple is fixed to the sapphire support with temperature cement from OMEGA which ensures the thermal contact. The signal of the thermocouple is read by a Hewlett Packard 34401A multimeter. Both the picommater and the multimeter are connected to a computer, where a Labwiew program records automatically the data.

For each measurement, the current was recorded upon heating and cooling with a rate of 2.5^{o}C/minutes.

3.5 Bibliography

[1] M. Daglish, "A dynamic method for determining the pyroelectric response of thin films," *Integrated Ferroelectrics,* vol. 22, pp. 993-1008, 1998.

[2] R. E. Newnham, *Properties of Materials: Anisotropy, Symmetry, Structure*: OUP Oxford, 2005.

[3] J. F. Nye, *Physical properties of crystals: their representation by tensors and matrices*: Clarendon Press, 1972.

[4] S. B. Lang, *Sourcebook of Pyroelectricity*: Gordon and Breach Science Publishers, 1974.

[5] M. Adachi, T. Matsuzaki, T. Yamada, T. Shiosaki, and A. Kawabata, "Sputter-deposition of 111-axis oriented Rhombohedral PZT films and their dielectric, ferroelectric and pyroelectric properties," *Japanese Journal of Applied Physics Part 1-Regular Papers Short Notes & Review Papers,* vol. 26, pp. 550-553, Apr 1987.

[6] D. L. Polla, C. P. Ye, and T. Tamagawa, "Surface-micromachined PbTiO3 Pyroelectric detector," *Applied Physics Letters,* vol. 59, pp. 3539-3541, Dec 1991.

[7] A. G. Chynoweth, "Dynamic method for measuring the pyroelectric effect with special reference to barium titanate," *Journal of Applied Physics,* vol. 27, pp. 78-84, 1956.

[8] J. Erhart and L. Burianova, "What is really measured on a d(33)-meter?," *Journal of the European Ceramic Society,* vol. 21, pp. 1413-1415, 2001.

[9] M. Davis, "Phase transitions, anisotropy and domain engineering - the piezoelectric properties of relaxor-ferroelectric single crystals," EPFL, 2006.

[10] A. Barzegar, D. Damjanovic, and N. Setter, "Analytical modeling of the apparent d(33) piezoelectric coefficient determined by the direct quasistatic method for different boundary conditions," *Ieee Transactions on Ultrasonics Ferroelectrics and Frequency Control,* vol. 52, pp. 1897-1903, Nov 2005.

[11] R. Chen and Y. Kirsh, *Analysis of thermally stimulated processes*: Pergamon Press, 1981.

[12] W.-E. Liu, "Impedance/thermally stimulated depolarization current and microstructural relations at interfaces in degraded perovskite dielectrics," 3374511 Ph.D., The Pennsylvania State University, Ann Arbor, 2009.

[13] H. Frei and G. Groetzinger, *Phys. Z.,* vol. 37, p. 720, // 1936.

[14] C. Bucci, R. Fieschi, and G. Guidi, "Ionic thermocurrents in dielectrics," *Physical Review,* vol. 148, pp. 816-&, 1966.

[15] J. T. Randall and M. H. F. Wilkins, "The phosphorescence of various solids," *Proceedings of the Royal Society of London Series a-Mathematical and Physical Sciences,* vol. 184, pp. 347-&, 1945.

[16] W. S. Lau, K. F. Wong, T. Han, and N. P. Sandler, "Application of zero-temperature-gradient zero-bias thermally stimulated current spectroscopy to ultrathin high-dielectric-constant insulator film characterization," *Applied Physics Letters,* vol. 88, Apr 2006.

[17] W. S. Lau, T. C. Chong, L. S. Tan, C. H. Goo, and K. S. Goh, "The characterization of traps in seimiinsulating gallium-arsenide buffer layers grown at low-temperature by molecular-beam epitaxy with an improved zero-bias theramlly stimulated current technique," *Japanese Journal of Applied Physics Part 2-Letters,* vol. 30, pp. L1843-L1846, Nov 1991.

Chapter 4: Uncovering of the polar character in unpoled ceramics

4.1 Introduction

The possibility to produce an effective piezoelectric charge in ceramics composite whose components are not by themselves piezoelectric was first discussed by Fousek et al [1]. In this type of meta-materials the mechanism of charge generation is the flexoelectric effect both in the direct and in converse form (see Chapter 1).

The design proposed for the composites is based on the connectivity between two different phases Figure 4.1. At least one of these phases is required to have high flexoelectric properties in order to produce large effective charge. As suggested by Bursian [2] and confirmed theoretically by Tagantsev [3], the flexoelectric response is enhanced in materials with high dielectric constant (such as ferroelectrics). For this reason ferroelectrics were good candidate to be employed as "flexoelectric phase" in composites.

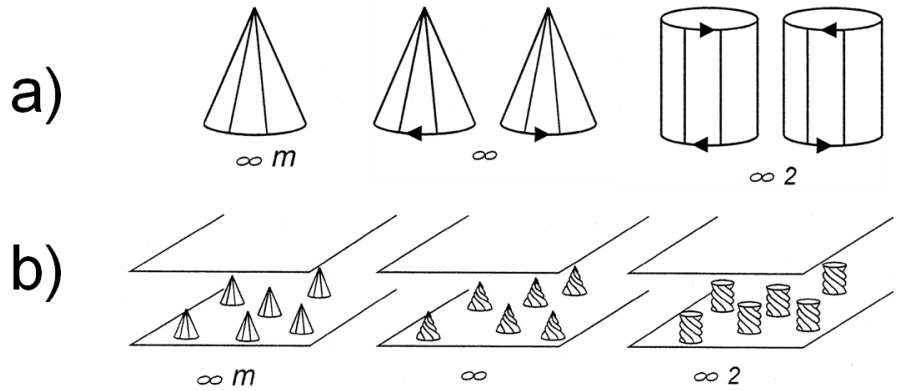

Figure 4.1-Representation of the Curie groups which allow for piezoelectricity (a) and illustration of the connectivity in composites (b). In the case of "flexoelectric composites" the phase described by the three piezoelectric Curie groups, is the active flexoelectric phase. Adapted from [1].

However, when the concept of this new type of composites was first introduced, no data on the flexoelectric properties of ferroelectrics were available. For this reason, systematic studies were conducted by Cross and coworkers in order to collect information about the flexoelectric properties of bulk ferroelectrics. Lead-based and lead-free ferroelectric compositions and relaxor materials, which exhibit very large permittivity, were investigated [4-7]. The predicted proportionality between the dielectric permittivity (susceptibility) and the flexoelectric coefficient was confirmed experimentally. However, the experimental flexoelectric coefficients were found to vary between about 1 μC/m (for

lead titanate zirconate) to 100 μC/m (for $Ba_{0.67}Sr_{0.33}TiO_3$). These values were three to four orders of magnitude larger than theoretical predictions (2-20 nC/m) [8].

Because of their very high flexoelectric properties, the $Ba_{0.67}Sr_{0.33}TiO_3$ (BST6733) ceramics were selected as flexoelectric phase in different type of composites developed and tested by the Cross's group at the Pennsylvania State University. The effective piezoelectric properties in the composites were found to be promising for practical applications [9, 10]. Furthermore, since lead-free ferroelectrics showed larger flexoelectric properties than lead-based compositions, flexoelectric composites were also seen as possible replacement for lead-based piezoelectric devices.

The huge discrepancy between theoretical and experimental values of the flexoelectric coefficients however, was an indication of the lack in understanding of electromechanical coupling in these materials and that either the existing theory is not complete or important contributions to the total electromechanical response are neglected in interpretation of experimental results.

4.2 Investigation of the direct flexoelectric effect in ferroelectric ceramics

In the early stage of this work, we focused on the $Ba_{1-x}Sr_xTiO_3$ solid solution as model system to study the origins of the large flexoelectric properties measured in this system. The idea was to systematically investigate the response of several compositions across the solid solution and see if the unusually high flexoelectric behavior is sensitive to crystal-chemistry parameters such as ionic size, element distribution, concentration and nature of atomic defects, and nature of the phase transitions.

To quantify the direct flexoelectric effect in solids, two methods can be used [11]. One consists in bending the material in cantilever beam geometry to generate a transverse strain gradient. In such a case, what is measured is the effective transverse component of the flexoelectric tensor μ^{eff}_{12}. A second approach consists in the compression of a sample with non-symmetrical geometry (for example, a truncated pyramid). In this case the measurement determines the effective longitudinal component of flexoelectric coefficient μ^{eff}_{11}. The coefficients measured with both methods are effective coefficients since they always involve a combination of different components of the general flexoelectric tensor [12, 13].

In our investigation, we started with a version of the pyramid compression experiment to test the direct flexoelectric response in the BST6733 ceramics, the same material that has been investigated by Cross et al. and to have an experimental confirmation of the high flexoelectric properties of this composition since, at the time of our experiments those first results have not been independently confirmed.

When a truncated pyramid is loaded with a uniaxial pressure, the pair of equal forces F generate a different stresses σ_1 and σ_2 ($\sigma_{1/2} = F/S_{1/2}$) on the top and on the bottom base because of the difference in the areas S_1 and S_2 (Figure 4.2).

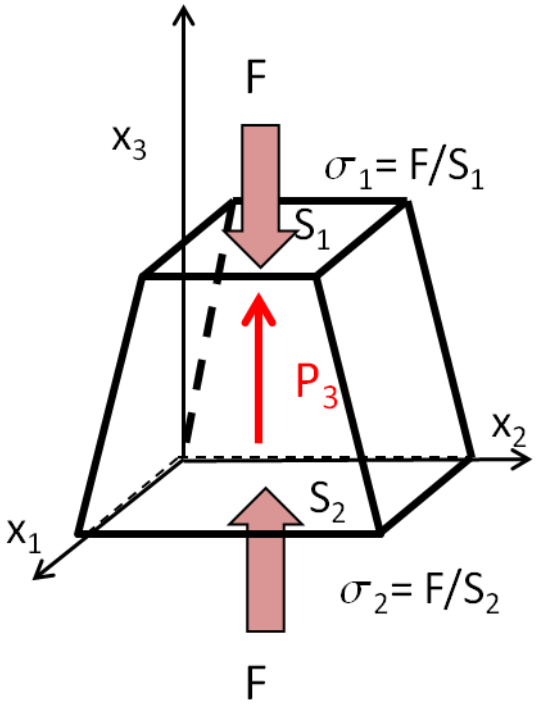

Figure 4.2-Flexolectric polarization generated in a truncated pyramid in a uniaxial compression experiment. The direction of the polarization (red arrow) is chosen arbitrarily.

The resulting strain gradient across the pyramid will induce a macroscopic polarization trough the flexoelectric effect according to the relation:

$$P_3 = \mu_{11}^{eff} \frac{\partial u_3}{\partial x_3} \qquad 4.1$$

where P_3 is the polarization along the vertical axis of the trapezoid, μ_{11}^{eff} the effective longitudinal flexoelectric coefficient, x_3 is the direction along which the load is applied and u_{33} is the strain. Note that the equation is not written in the tensor form. The effective flexoelectric coefficient μ_{11}^{eff} is related to an effective piezoelectric longitudinal coefficient d_{33} [14] via the equation:

$$d_{33} = \mu_{11}^{eff} \frac{\frac{(S_2 - S_1)}{S_1}}{h\, c_{11}} \qquad 4.2$$

where S_1 and S_2 are the upper and the bottom areas of the pyramid, h is the height and c_{11} is the elastic modulus of the material. It should be specified that the equation 4.2 is strictly valid only in the case that the side walls of the pyramid are configured in such a way that the area of the trapezoid varies linearly with the height.

The precise quantitative estimation of the longitudinal effective flexoelectric coefficient is also complicated by the fact that the strain gradient inside the samples can be highly inhomogeneous. For example, as shown by finite elements simulation (Figure 4.3), the stress can concentrate mainly at the edges of the pyramids and trapezoids.

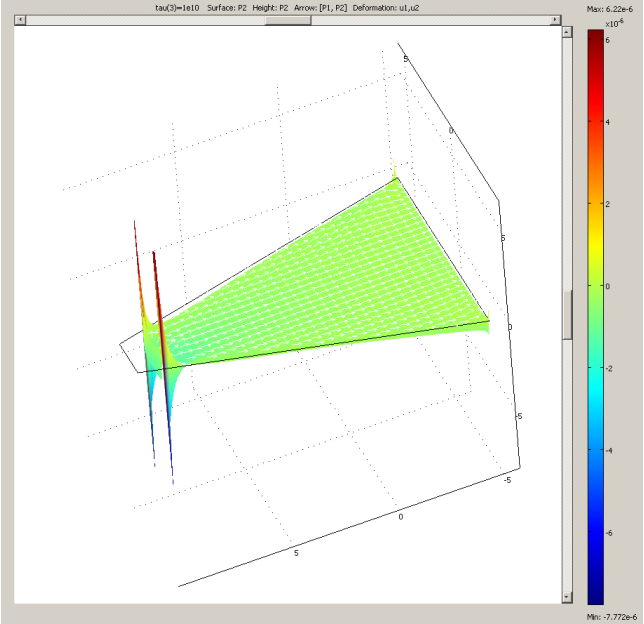

Figure 4.3-Two dimensional finite elements simulation of a pyramid clamped on the large base and loaded with the uniaxial pressure on the small base. The strain gradient is significantly higher at the corners. The simulations were performed with Comsol Multiphysics by Dr. Tomas Sluka.

However, this technique can give a first qualitative experimental estimation of the order of magnitude of the flexoelectric polarization.

In our experiments, samples of unpoled BST6733 ceramics were cut from disks with a diameter of 9 mm and a thickness of 2 mm in a shape of isosceles trapezoidal prisms (two bases and two sides were parallel (height 5.30 mm, bases 7.96 mm^2 and 5.20 mm^2, lateral thickness between 1.92 and 2.09 mm).

The electromechanical response was measured with the press setup described in Chapter 3. The trapezoids were loaded with a total static force of 130 N (100 N of prestress +30 N of static DC offset). On the top of the static force, a dynamic load of the amplitude of 40 N was applied, with frequency of 1 Hz. A piezoelectric-like charge was observed when the trapezoid was loaded along the symmetry axis (Figure 4.4-a).

The effective piezoelectric coefficient associated with the charge was in the range of 0.1-1 pC/N. The fluctuation between these values is related to the small amplitude of the signal measured. The accuracy of the measurement is affected by the position of the sample in the sample holder. The precision is affected by electrical noise, charge drift and temperature variations during the measurement.

According to equation 4.2, the estimate of the effective flexoelectric coefficient μ^{eff}_{11},even considering the lowest value of the piezoelectric charge, ,was of the order of 10^{-4} C/m and therefore consistent with the values previously reported for BST6733 [5].

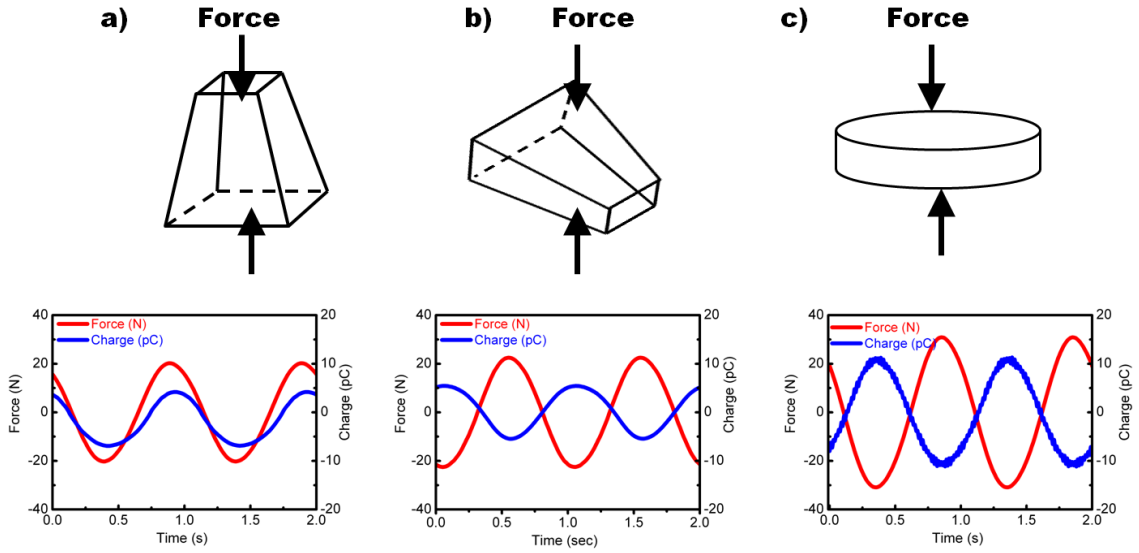

Figure 4.4-Effective piezoelectric charge in BST6733 ceramics in a trapezoid (height 5.30 mm, bases 7.96 mm^2 and 5.20 mm^2, thickness between 1.92 and 2.09 mm) measured(a) along the symmetry axis (b) along the direction perpendicular to it and(c) for a disk (diameter 7.66 and thickness 0.44mm).

To check if the signal was indeed flexoelectric in origin, the trapezoid was flipped by 90^o and the load was applied along the direction of the flat sides, where no significant shape asymmetry was present (Figure 4.4-b). In this case, surprisingly, a charge of comparable order of magnitude was also observed.

A possible explanation for the signal in the direction perpendicular to the symmetry axis of the trapezoid was that small geometrical imperfections (certainly present in the samples) were inducing flexoelectric polarization. In the case of the trapezoid reported in Figure 4.4, for example, the thickness near the small base was 0.17 mm wider than near the large base (a difference of less than 10%). This difference was many times smaller than the difference in area between the two bases, so that possibility was discarded. Furthermore, to compensate for such imperfections and to have more homogeneous distribution of the pressure, the force was applied via a steel hemisphere placed on one side of the sample (Figure 4.5).

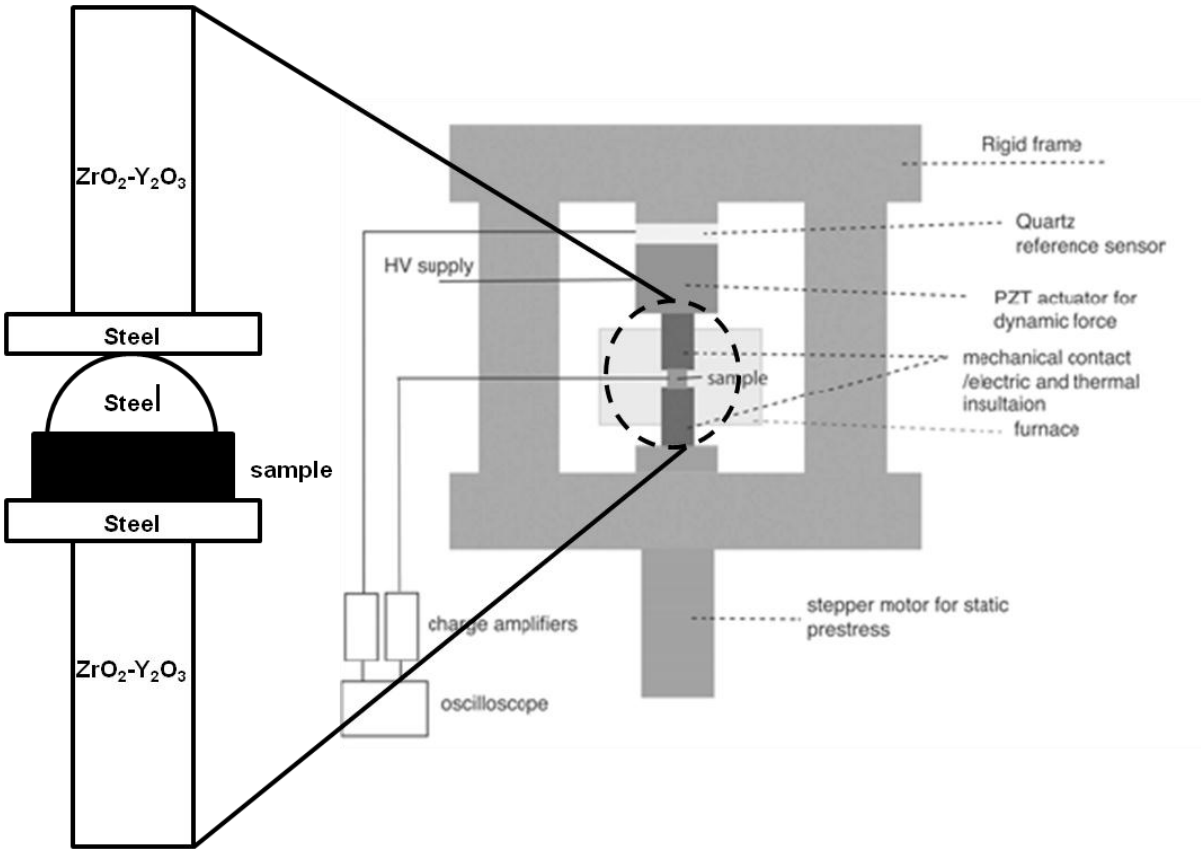

Figure 4.5-Detail of the geometry used for piezoelectric measurement on trapezoid and disk. The flat surface of the steel hemisphere was polished to the optical grade to reduce as much as possible the roughness and avoid surface friction.

In addition, a comparable amount of charge is measured when the pressure is applied on the parallel surfaces of disks of the same BST6733 ceramics (Figure 4.4-c). If geometrical strain gradient would be responsible for polarization in the disks the corresponding flexoelectric polarization would have to be significantly larger than in trapezoids when pressed along the symmetry axis, because the disk was geometrically more symmetrical. This result indicates clearly that another type of electromechanical coupling is present beyond the flexoelectric effect induced by the geometrical shape.

Different hypothesis about the origin of such mechanism were considered. A first one is the presence of an internal built-in strain gradient created during the ceramics preparation. The hypothetical strain gradient needed to generate the polarization measured in the samples can be easily estimated. If we assume a flexoelectric coefficient of 10 nC/m (in agreement with the theoretical estimations) for an experimental polarization of about $1x10^{-6}$ C/m^2 (Figure 4.2), using equation 4.1, we obtain a strain gradient of the order of 100m^{-1} corresponding to a stress gradient of 10^{12} Pa. This value is clearly nonphysical for ceramics. On the other hand, assuming an intrinsic flexoelectric coefficient of BST6733 of the order of the large experimental values would imply that the

flexoelectric polarization induced by the built-in strain gradient is at least as large as the one induced by the geometrical gradient. Both of these possibilities are unlikely.

A second possibility is that the ferroelectric state was induced by the static pre-stress, since the measurements were conducted at room temperature (21°C-25°C), very close to the paraelectric to ferroelectric phase transition of BST6733 (T_c=21°C) [15]. Nevertheless, even in the presence of ferroelectric domains, no piezoelectric response is in principle expected in a polycrystalline sample, since the random orientation of domains and grains should ideally lead to a complete cancellation of the macroscopic polarization. It is shown below that even if the local pressure was sufficiently high to induce transformation into ferroelectric phase in BST6733 and if averaging of the domain orientations did not lead to zero macroscopic polarization, this is not the main reason for the observed electromechanical response above T_C in these materials.

To avoid the interference with the proximity of the ferroelectric phase transition, the compression experiment was repeated on disks of $Ba_{0.60}Sr_{0.40}TiO_3$ (BST6040) composition (T_c =-1°C). A charge of the magnitude similar to the one measured in BST6733 was detected in this material, too. The presence of piezoelectric response in the paraelectric phase of BST6040 more than 20°C above T_c and the fact that the samples were never cooled into the ferroelectric phase is an indication that the origin of the charge is not related to either induced or residual ferroelectricity.

The conclusion that an incomplete averaging of ferroelectric domains is probably not at the origin of the electromechanical response is suggested also by the piezoelectric measurements performed on unpoled $BaTiO_3$, $0.5(Ba_{0.7}Ca_{0.30})$-$0.5Ba(Zr_{0.10}Ti_{0.90})$(BCZT50) and soft $PZr_{0.52}Ti_{0.48}O_3$ -1%Nb ceramics, all of them ferroelectric at room temperature. All compositions show an electromechanical response in the ferroelectric phase, similar to the one of the paraelectric BST6040. This is well illustrated in the case of $BaTiO_3$, where the piezoelectric signal was measured through the Curie temperature (T_c about 127°C) and the amplitude of the electromechanical response was comparable in the ferroelectric and in the paraelectric phase (Figure 4.6).

A fact that should not be neglected is that piezoelectric coupling can be induced in all materials by a small bending induced by the application of the pressure. As recently demonstrated theoretically by Tagantsev and Yurkov [16], during the homogeneous bending of a plate of a non-piezoelectric material, a piezoelectric contribution from the surface is present even under short circuit conditions. This contribution is predicted to scale with the bulk dielectric constant of the material. For this reason in high permittivity dielectrics, such as BST6733 (ε_r about 20000 at 22°C), BST6040 (ε_r about 5000 at 22°C), $BaTiO_3$ (ε_r about 4000 at 22°C) the surface piezoelectricity can have the same magnitude as the bulk flexoelectric effect.

Even with the precautions adopted in the measurement (application of the pressure with the steel hemisphere) and using thick samples (2-3 mm) that cannot bend easily, we

were concerned that a small bending of the ceramics under pressure cannot be entirely excluded. It is shown in the next section that the symmetry-breaking is not due to the bending of the samples.

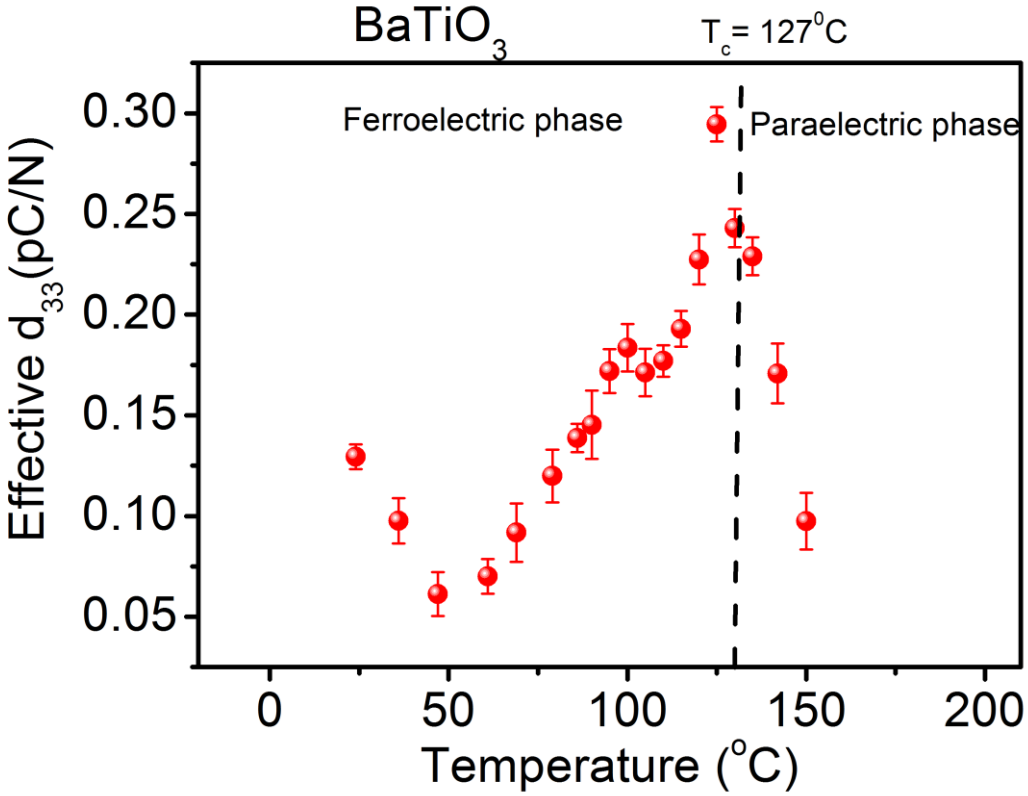

Figure 4.6-Dependence of the effective piezoelectric coefficient as a function of temperature in $BaTiO_3$ unpoled ceramics. The vertical lines represent the error bars on the estimation of the value of the piezoelectric coefficient defined as $d_{33}= Q_{max} / F_{max}$.

4.3 Pyroelectric character in the paraelectric phase of unpoled ceramics

To test if the polarity originates from the application of the mechanical load and to compensate for other possible artifacts related to the piezoelectric technique (i.e. charge generation due to the friction at the interface between the sample and the steel), the ceramics were investigated with the pyroelectric technique.

The advantage of the pyroelectric measurement is that it is less destructive for the initial state of the samples in comparison to the piezoelectric characterization, since no external mechanical or electrical fields are applied and only small temperature changes are used (within one degree or less).

Very thin disks (about 0.5mm) of as-sintered BST6040 ceramics (removed from the furnace after sintering and covered with electrodes) were measured with the pyroelectric set-up described in Chapter 3.

In a material were no polar axis is present, no modulation in the current proportional to the rate of temperature change (dT/dt) is observed when the material is heated or cooled in a periodic way. In the case of as prepared BST6040 ceramics however, a clear square modulation of the current is observed when the temperature is changed with triangular wave, indicating that the current is proportional to the temperature rate (Figure 4.7). The current reverses its sign when the samples are turned upside down. This is direct experimental evidence that the ceramics have a unique polar axis.

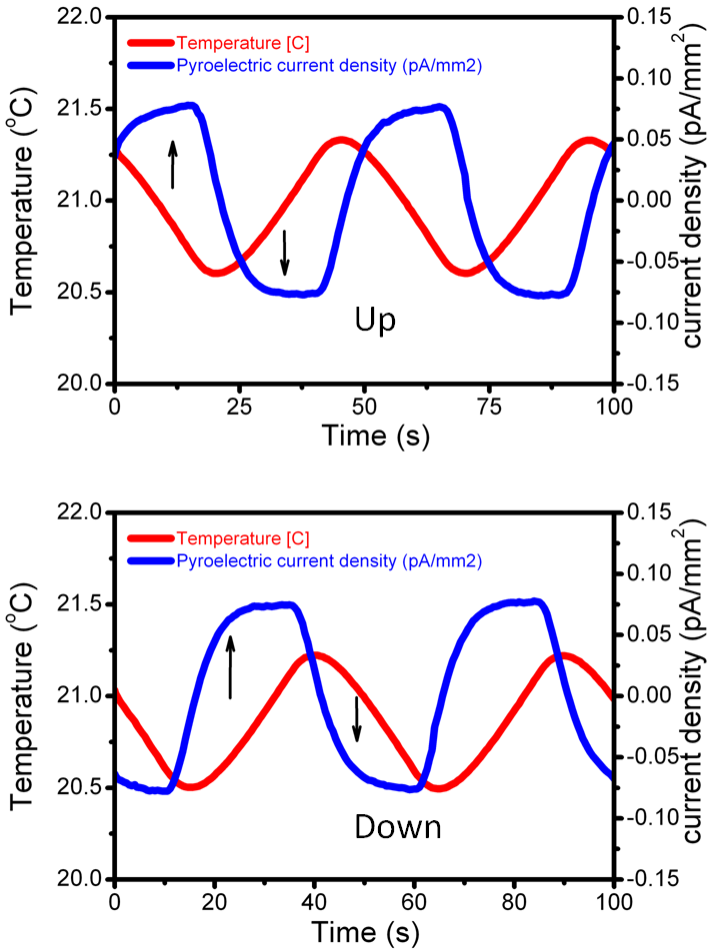

Figure 4.7-Pyroelectric current in BST6040 as prepared samples. The current reverses the sign (see arrows) when the sample is inverted ("up" versus "down" state). The temperature variation was ± 0.5°C and the frequency 20 mHz. Measurements were done at 21°C. Note that in this particular example the temperature waveform is not perfectly triangular, which contributes to deformation of the current waveform from ideal square form.

Furthermore, the detection of a pyroelectric current in as prepared and unpoled samples indicates that the polarity is not induced by the application of an external field (elastic or electric) or stresses at the surface induced by polishing but is built in the ceramics.

The reliability of our equipment was verified comparing the response of other nominally non-polar materials. Low dielectric constant (ε_r about 10) ceramics of Al_2O_3 (alumina), slightly doped with magnesium oxide, and as-prepared ceramics of paraelectric $SrTiO_3$ oxide were used as control materials. In both cases no pyroelectric current was detected (Figure 4.8).

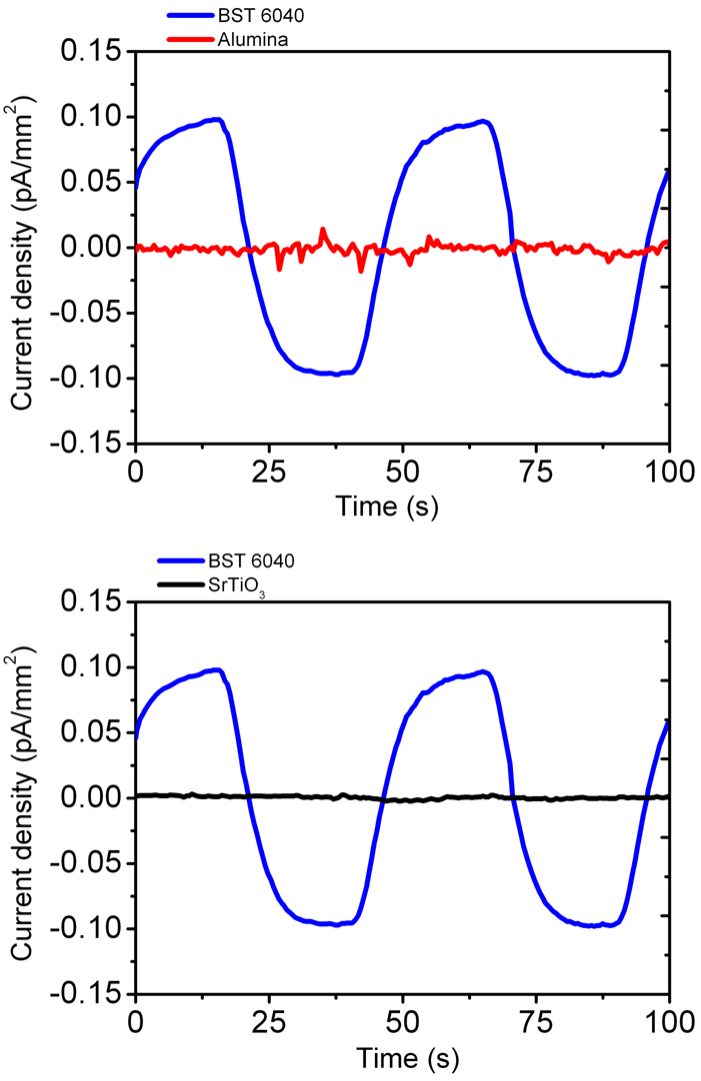

Figure 4.8-Comparison of the pyroelectric current in BST6040 unpoled ceramics and Alumina (top panel) and $SrTiO_3$ as prepared ceramics (bottom panel) at room temperature 21°C. The level of the noise in Alumina and $SrTiO_3$ ceramics is on the order of 10^{-3}pA/mm^2, 100 times smaller than the current amplitude in BST6040 ceramics.

The discovery of a built-in polarization in the paraelectric phase of ceramics samples changes the approach to the study of the flexoelectric effect. The electro-

mechanical coupling associated with the built-in polarization is of the same order of magnitude as the electromechanical effect identified previously as flexoelectricity. This suggests that the large flexoelectric response might have been misidentified and that the symmetry breaking-mechanism is responsible for a part of the apparent flexoelectric response. The fundamental question about the mechanism of the symmetry breaking needs to be answered since its understanding may provide a rationalization for the high flexoelectric coefficients reported previously and, above all, it is essential to make correct interpretations of the results of future studies. For these reasons our following investigations are focused on the effort to identify the origin of such mechanism.

4.4 Extrinsic contribution to the mechanism of symmetry breaking revealed in the piezoelectric response

As discussed in section 4.2, the mechanism of symmetry breaking cannot be explained with a flexoelectric polarization originated from a macroscopic strain gradient across the whole volume of the ceramics.

It still remains possible that strain gradients concentrated at the grains boundaries or within the grains induce a local flexoelectric polarization that does not average to zero on the macroscopic scale. Recently the large piezoelectric response observed in unpoled ceramic composites of $Na_{0.5}Bi_{0.5}TiO_3$-$Bi_{12}TiO_{20}$ was associated to the flexoelectric effect generated by strain induced at interfaces [17].

In the case of a pure, intrinsic flexoelectric origin of the polarization, the electromechanical response is expected to be frequency independent. The reason for this is that in the frame of the existing flexoelectric theory, the flexoelectric coefficient μ is proportional to the lattice parameters and the lattice permittivity, which is not dispersive in the low frequency range.

However, in the case of the paraelectric BST6040 ceramics, the electromechanical response reveals clear frequency dispersion. The data in Figure 4.9 show that both the effective piezoelectric coefficient and relative permittivity increase at low frequency.

The electromechanical response in BST6040 reaches 2 pC/N at 0.01 Hz. This value is close to the piezoelectric response of quartz (2.3 pC/N). This increase of the electromechanical response in the low frequency range indicates that the mechanism at the origin of the polarity carries a strong extrinsic contribution and it is not only related to the lattice response. The increase of permittivity at low frequency in oxide perovskites is generally explained with a contribution from the conductivity due to hopping [18] or to a Maxwell-Wagner mechanism.

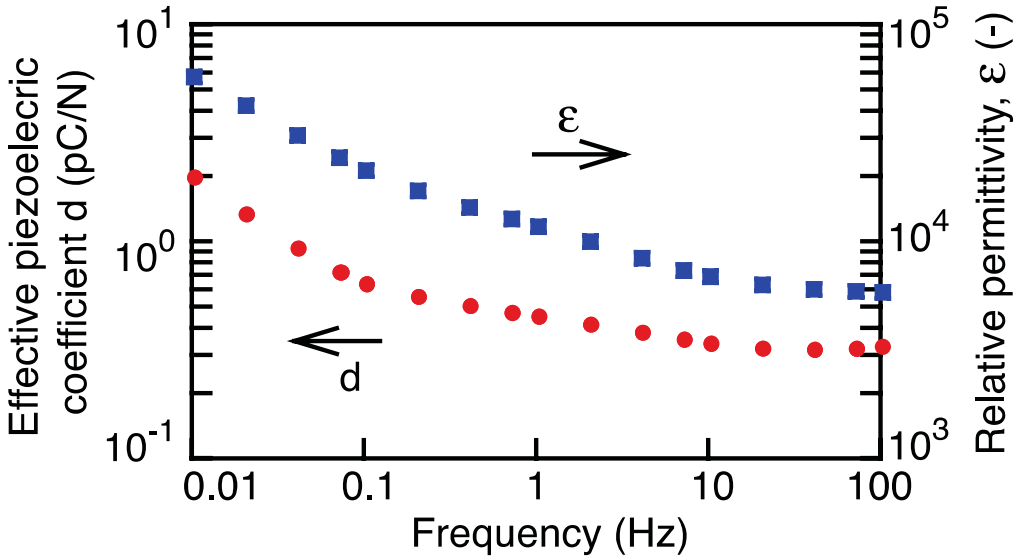

Figure 4.9-The dependency of the dielectric constant ε and the effective piezoelectric coefficient in BST6040 ceramics. The piezoelectric coefficient is defined as $d = Q_{max}/F_{max}$ where Q_{max} is the amplitude of the charge and F_{max} is the amplitude of the force.

4.5 Polarization switching under elastic field

The electromechanical response in unpoled ceramics shows a very surprising feature: the possibility to switch the direction of the macroscopic polarization during the application of the uniaxial compression. This unusual behavior was observed in the paraelectric phase of unpoled BST6040 ceramics and in the ferroelectric phase of unpoled $PbZr_{0.35}Ti_{0.65}O_3$ (PZT3565). The experiment, whose main result is reported in Figure 4.10, shows the partial switching of the polarization in a BST6040 disk loaded with a static force (~130N) and dynamic force applied for a very long time (48 hours). The charge inverts its sign with respect to the force when the force reaches a certain threshold (about 20N).

The initial direction of the polarization is restored when the dynamic force decreases to 10 N. The back switching attests the presence of a restoring mechanism which pulls back the polarization to an initial built-in direction.

In the case of unpoled $PbZr_{0.35}Ti_{0.65}O_3$ (PZT 3565) the direction of polarization was completely switched upon the application of a moderate static load above 350N or 6MPa (Figure 4.11). In this case also the polarization comes back to its initial direction when the static load is decreased. The fact that the polarization switches easier in the ferroelectric phase of PTZ3565 ceramics than in the paraelectric phase of BST6040, is probably related to the presence of the ferroelectric domains in the former. This switching in polarization in PZT can be explained by the tetragonal crystal structure of the material. Ferroelastic domains may switch under uniaxial pressure by 90°. The accompanying change in charge distribution around the domain may then produce electric fields which will switch this

domain by additional 90°, resulting in apparent switching of polarization by 180° by uniaxial pressure. This is not the case in paraelectric BST6040 were ferroelectric-ferroelastic domains are absent. The switching is probably related to two components of polarization, as will be discussed later: one built in the sample and the other composed of trapped space charges. The built-in component is stable and gives a small piezoelectric-like response under pressure, while, the space charges may be released by the pressure from trapping sites and move in–phase and out–of–phase with the pressure and compete with the charges from built-in polarization. The macroscopic effect of this space charge motion is an apparent partial switching of polarization.

The tendency of the polarization to switch back to an initial preferential orientation is consistent with the existences of a built in-polar axis in the unpoled ceramics which causes the pyroelectric and the piezoelectric effect.

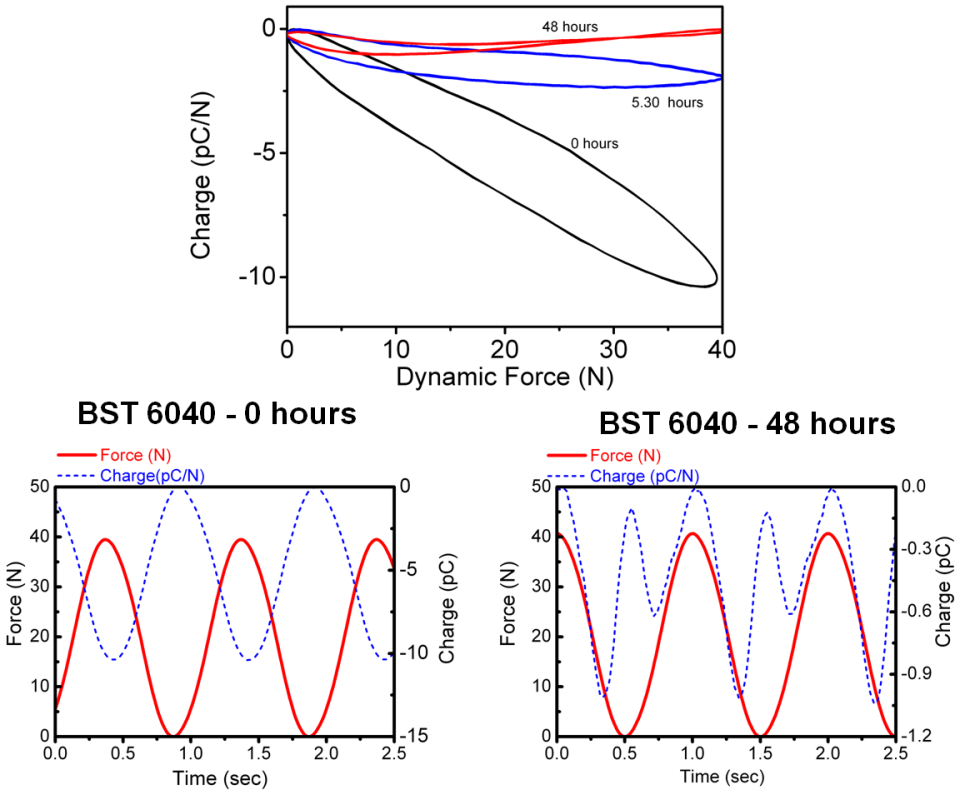

Figure 4.10-Switching of the polarization direction during a compression experiment of a BST6040 disk (thickness = 2.6 mm and diameter= 7.6 mm). The upper panel shows the evolution of the charges amplitude under a dynamical load run for several hours. Immediately after application of the dynamic force the charge and the force are almost 180^0C out of phase (left panel on the bottom). After 48 hours the force and charge are in phase when the force reaches 20N. The charge and the force are again 180^o C out of phase when the force decreases to 10 N (bottom panel on the right)

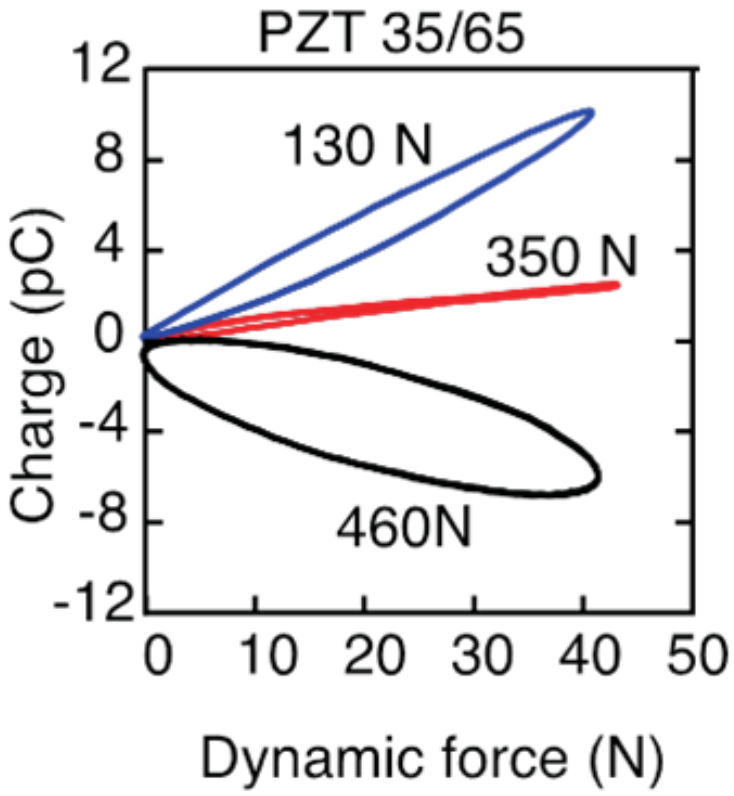

Figure 4.11- Switching of the polarization in PZT3565 under static load(diameter ≈ 8.5 mm thickness 2.2 mm).The sign of the charge inverts completely when the static load is increased above 350N(6MPa).

The possibility to affect the polarization by the application of an elastic field (static or dynamic) makes the study of the origin of the symmetry breaking by the mean of the piezoelectric technique more difficult since the switching process may change the direction and the amplitude of the piezoelectric charge during the measurement. For example in BST6040, the initial value of the effective piezoelectric coefficient dropped by about 20 times (from 0.27 pC/N to 0.015pC/N) during the switching experiment (Figure 4.10).

It was decided, for this reason to use the pyroelectric technique as the main characterization technique to investigate the origin of the polar character as this technique is certainly less destructive for the initial state of the samples. In addition, TSC is used to study thermal effects on macroscopic polarization.

4.6 Summary

In the chapter, are reported the results of the investigation of the direct flexoelectric response of the paraelectric phase of $Ba_{0.67}Sr_{0.33}TiO_3$ ceramics. The measurements reveal the existence of a mechanism of electromechanical coupling beyond the flexoelectric

effect that could be induced by the geometry of the samples. The presence of non flexoelectric electromechanical coupling suggests a breaking of the expected centric symmetry in the paraelectric phase; this symmetry breaking is intrinsic to the material and not induced by the application of external electric or elastic field. This is confirmed by the detection of non-zero piezoelectric and pyroelectric current in as prepared paraelectric ceramics of $Ba_{0.60}Sr_{0.40}TiO_3$ ceramics which were never exposed to any electric field (excluding the possibility of electret effect induced by the field) and never cooled in to the ferroelectric phase from the paraelectric phase (ruling out the presence of residual domains above T_c as possible origin of the polarization). The measurements indicates that the electromechanical response is dispersive in the low frequency limit (100 Hz-10 mHz) aspect which further point against the origin of the electromechanical coupling from the pure flexoelectric response of the lattice. The BST6040 polar ceramics shows an apparent switching of the polarization upon the application of a dynamic elastic field. The apparent switching is probably related to the release of trapped charges which move in-phase or out-of-phase with the applied pressure.

4.7 Bibliography

[1] J. Fousek, L. E. Cross, and D. B. Litvin, "Possible piezoelectric composites based on the flexoelectric effect," *Materials Letters,* vol. 39, pp. 287-291, Jun 1999.

[2] E. V. Bursian and Zaikovsk.Oi, "Changes in Curvature of a Ferroelectric Film Due to Polarization," *Soviet Physics Solid State,Ussr,* vol. 10, pp. 1121-&, 1968.

[3] A. K. Tagantsev, "Electric Polarization in Crystals and Its Response to Thermal and Elastic Perturbations," *Phase Transitions,* vol. 35, pp. 119-203, 1991.

[4] W. Ma and L. E. Cross, "Large flexoelectric polarization in ceramic lead magnesium niobate," *Applied Physics Letters,* vol. 79, pp. 4420-4422, Dec 24 2001.

[5] W. H. Ma and L. E. Cross, "Flexoelectric polarization of barium strontium titanate in the paraelectric state," *Applied Physics Letters,* vol. 81, pp. 3440-3442, Oct 28 2002.

[6] W. H. Ma and L. E. Cross, "Flexoelectric effect in ceramic lead zirconate titanate," *Applied Physics Letters,* vol. 86, Feb 14 2005.

[7] W. H. Ma and L. E. Cross, "Flexoelectricity of barium titanate," *Applied Physics Letters,* vol. 88, Jun 5 2006.

[8] I. Ponomareva, A. K. Tagantsev, and L. Bellaiche, "Finite-temperature flexoelectricity in ferroelectric thin films from first principles," *Physical Review B,* vol. 85, Mar 2012.

[9] J. Y. Fu, W. Y. Zhu, N. Li, N. B. Smith, and L. E. Cross, "Gradient scaling phenomenon in microsize flexoelectric piezoelectric composites," *Applied Physics Letters,* vol. 91, Oct 29 2007.

[10] B. J. Chu, W. Y. Zhu, N. Li, and L. E. Cross, "Flexure mode flexoelectric piezoelectric composites," *Journal of Applied Physics,* vol. 106, Nov 15 2009.

[11] P. Zubko, G. Catalan, and A. K. Tagantsev, "Flexoelectric Effect in Solids," *Annual Review of Materials Research, Vol 43,* vol. 43, pp. 387-421, 2013.

[12] P. V. Yudin and A. K. Tagantsev, "Fundamentals of flexoelectricity in solids," *Nanotechnology,* vol. 24, Nov 1 2013.

[13] P. Zubko, G. Catalan, A. Buckley, P. R. L. Welche, and J. F. Scott, "Strain-gradient-induced polarization in $SrTiO_3$ single crystals," *Physical Review Letters,* vol. 99, Oct 19 2007.

[14] L. E. Cross, "Flexoelectric effects: Charge separation in insulating solids subjected to elastic strain gradients," *Journal of Materials Science,* vol. 41, pp. 53-63, 2006/01/01 2006.

[15] G. Picht, K. G. Webber, Y. N. Zhang, H. Kungl, D. Damjanovic, and M. J. Hoffmann, "Critical mechanical and electrical transition behavior of $BaTiO_3$: The observation of mechanical double loop behavior," *Journal of Applied Physics,* vol. 112, Dec 2012.

[16] A. K. Tagantsev and A. S. Yurkov, "Flexoelectric effect in finite samples," *Journal of Applied Physics,* vol. 112, Aug 15 2012.

[17] M. L. Zhao, L. H. Wang, C. L. Wang, J. L. Zhang, Z. G. Gai, C. M. Wang*, et al.*, "Interface-induced piezoelectricity in an unpoled $Na_{0.5}Bi_{0.5}TiO_3$-based composite ceramic," *Applied Physics Letters,* vol. 95, Jul 2009.

[18] M. I. Morozov and D. Damjanovic, "Charge migration in $Pb(Zr,Ti)O_3$ ceramics and its relation to ageing, hardening, and softening," *Journal of Applied Physics,* vol. 107, Feb 2010.

Chapter 5 : Identification of the mechanism leading to the symmetry breaking

5.1 Introduction

The experiments discussed in Chapter 4 show that paraelectric polycrystalline samples (BST6040), never exposed to any external electric or elastic field, have an intrinsic polar axis which causes a pyroelectric and piezoelectric response. In this chapter, the pyroelectric technique, because of the less destructive nature for the initial state of the samples, is used as the main characterization tool to answer the following questions:

i) is the polarity observed in paraelectric ceramics associated to the presence of grain boundaries?

ii) is the symmetry breaking a bulk effect or does it have significant surface contributions?

iii) at which stage of the sample preparation does the symmetry breaking occur?

iv) what is the possible mechanism at the origin of the polarity in the paraelectric phase?

5.2 Pyroelectric response in the paraelectric phase of unpoled single crystals

In order to proceed with our study, an important point, which should be clarified at the beginning, is if the polar character observed in the paraelectric phase of the ceramics can simply be explained with the presence of the grain boundaries.

In ceramics grain boundaries represent extrinsic defects with respect to ideal lattice structure and they are a preferential location for the concentration of oxygen vacancies and other space charges [1]. In ferroelectric ceramics, polarization within domains and grains may affect the state of defects at the grain boundaries [2].

A first indication that the simple granular nature of the ceramics by itself is not enough to explain the pyroelectric response in unpoled paraelectric ceramics is the absence of a pyroelectric signal in as prepared $SrTiO_3$ ceramics (see Chapter 4), where the grain boundaries are not only present but can have a polar nature, as shown by IR and Raman studies [3].

To further clarify if the pyroelectric response observed in the paraelectric phase of the BST 6040 ceramics is related to their granular nature, pyroelectric measurements were

performed on single crystals of different chemical compositions and compared with their ceramics forms. Unpoled single crystals of $BaTiO_3$, $SrTiO_3$ and a (Ba, Sr)TiO_3 composition containing 2.5% of strontium (BST975025) were investigated.

As shown in Figure 5.1, while no pyroelectric current is observed in the paraelectric phase of $SrTiO_3$, in both single crystal and ceramics form, a pyroelectric response is present in the paraelectric phase of single crystals and ceramics of $BaTiO_3$ and BST975025 (2.5% strontium).

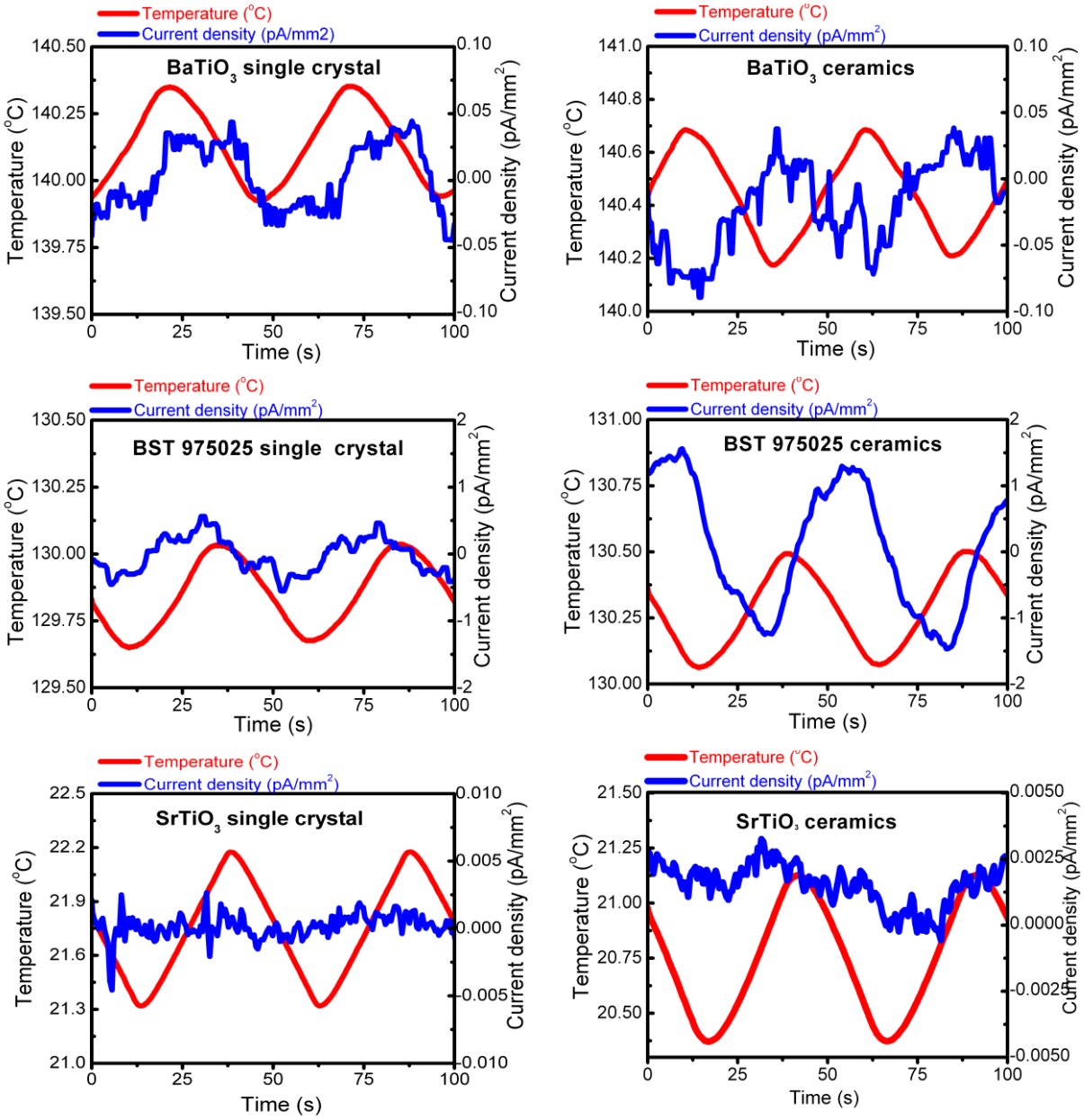

Figure 5.1-Comparison between the pyroelectric current of single crystal and ceramics in pure $BaTiO_3$, $(Ba,Sr)TiO_3$ system and pure $SrTiO_3$ The $BaTiO_3$ (T_c=128°C) and BST975205 (T_c=119°C) ceramics samples were prepared in our laboratory by the solid state method described in Chapter 2. The $BaTiO_3$ single crystal (T_c =135°C) was oriented in the [001] direction (dimensions 2.66 x 4.60 mm^2). The $SrTiO_3$ single crystal was a [100] oriented substrate for thin films supplied by MaTeck (dimension 5.02x4.98 mm^2). The BST975025 single crystal (dimensions 2.5 x 3.6mm^2) was grown in FEE GmbH, Germany.

These measurements demonstrate that the paraelectric phase can exhibit polarity even when the grain boundaries are not present. The absence of pyroelectricity in both single crystal and ceramics of $SrTiO_3$ suggests that the polar character in the paraelectric phase is more dependent on the specific chemical composition of the material rather than on the presence of grain boundaries.

A polar paraelectric phase is a feature which is not limited to $BaTiO_3$ and related solid solution. This is confirmed by pyroelectric measurements performed in the paraelectric phase of a single crystal of $Ka(Ta,Nb)O_3$ containing 41% of niobium (T_c about 33°C). In KTN single crystal, the pyroelectric response is observed up to 40°C above T_c (Figure 5.2).

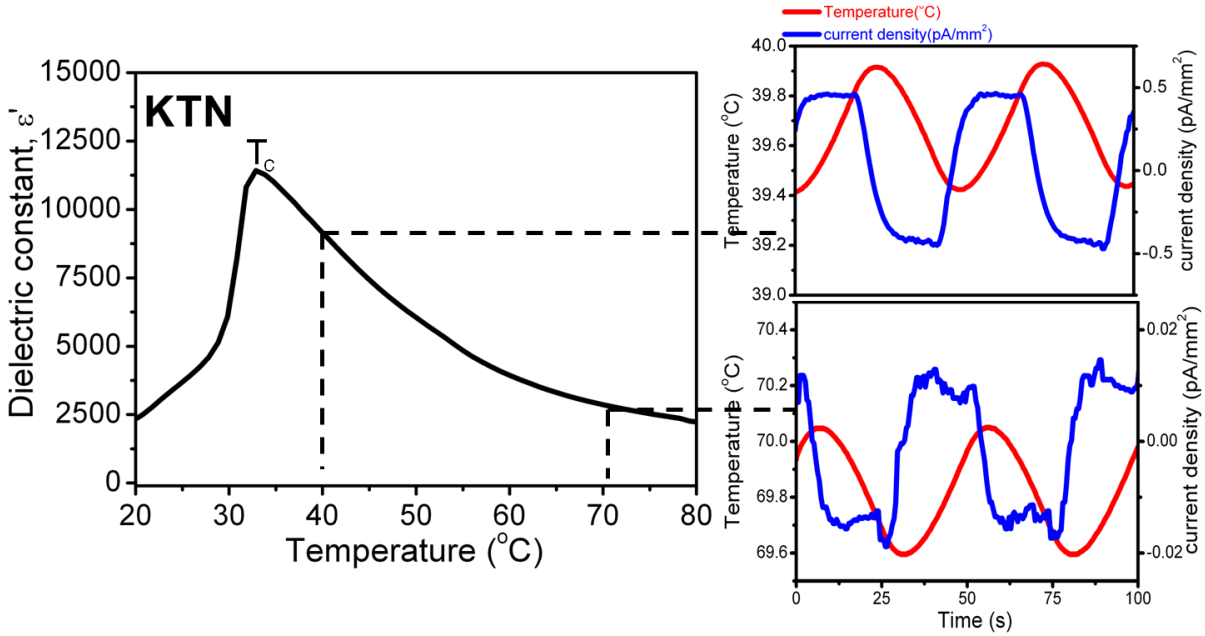

Figure 5.2-Pyroelectric response in the paraelectric phase of unpoled KTN single crystal. The pyroelectric current amplitude progressively decreases upon heating above T_c and it is still clearly visible at 70°C (almost 40 degree above the Curie point). The single crystal (dimensions 6 x 5 mm^2) was grown in FEE GmbH, Germany.

5.3 Surface contributions to the symmetry breaking

A second important aspect which needs to be clarified is the possibility that the symmetry breaking involves only the surface of the samples.

It is known that, for different reasons, the surfaces may exhibit a lower symmetry with respect to the bulk[1] For example, it was demonstrated theoretically [4] and observed experimentally [5, 6] that in paraelectric $SrTiO_3$, a ferroelectric state can be present within one or few layers from the surface while the bulk of the material remains paraelectric. Recently, Morozovska et al [7] have predicted that surface polar states and even pyroelectricity can be created by the coupling of the flexoelectric effect and stresses induced by the rotation of oxygen octahedra. Since octahedral rotation is common in a wide range of materials, the authors propose that this mechanism can be responsible for polar surfaces state and improper pyroelectricity in a wide range of otherwise non polar materials.

To study the contribution of the surface to the observed pyroelectric response, the samples of BST6040 ceramics were mechanically polished to obtain surfaces with optical grade. During the polishing process, about 200μm of thickness of the material were removed on both sides of the samples. As shown in Figure 5.3, the surface after polishing to optical quality has clearly a much lower roughness with respect to the as–sintered surface.

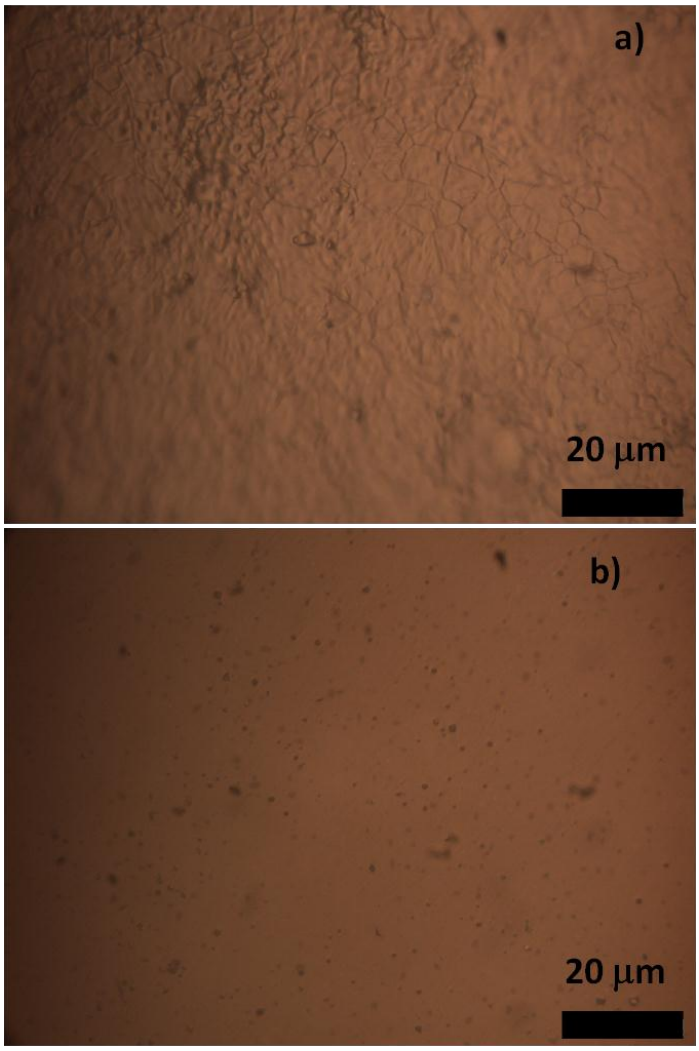

Figure 5.3-Surface of BST6040 ceramics a) as–sintered and b) after polishing down to the optical grade. The images were taken with an optical microscope aa Leica DFC 420 digital camera. The samples were polished first with foils of SiC grinding papers of different roughness (particle size from 30μm down to 5 μm) and then with diamond paste with particle size down to 1 μm.

Despite the removal of thick layer of material and a substantial change in the morphology of the surface, the pyroelectric current is still observed. The amplitude of the current in some cases is even higher than in the unpolished sample. Furthermore the correlation of the sign of the pyroelectric current with the temperature for a given side of the sample does not change before and after polishing (Figure 5.4). If a surface layer is

responsible for the polarization one would expect that orientation of the polarization is not fixed but may depend, even randomly, on how the surface is changed by the polishing procedure. This was never observed in our experiments, i.e. the polarization direction is fixed once the sample is removed from the furnace.

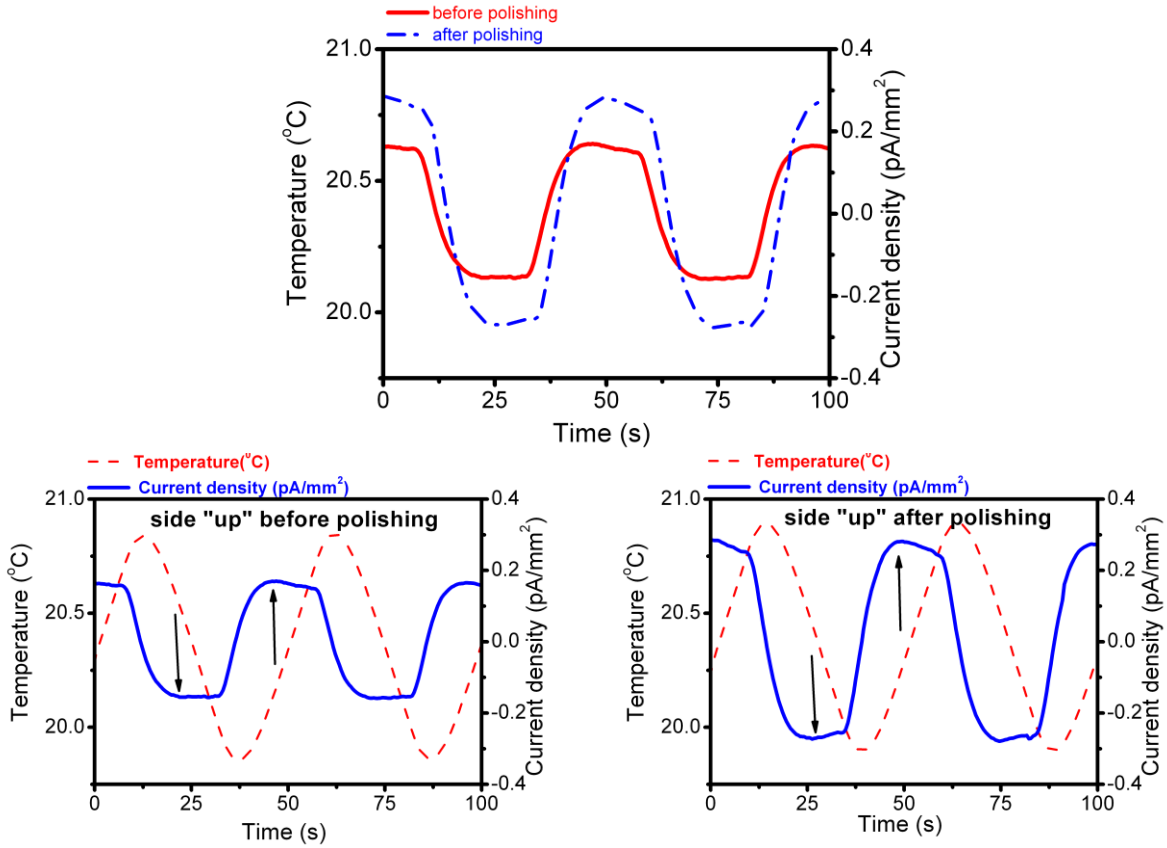

Figure 5.4-Amplitude of the pyroelectric current before and after the polishing of the surface to optical quality (top panel) in a BST6040 ceramics. On the same side of the samples (here by convention labeled as "up in the furnace" during sintering), the correlation between the pyroelectric current and the temperature is the same before and after polishing.

One may argue that each time that a layer of material is removed, a reconstruction of the surface occurs, for example associated to a surface rich in TiO_2 terminations, analogue to those reported in $SrTiO_3$ [8], inducing again the same type of symmetry breaking on the fresh surface. However, such possibility does not easily explain the presence of the pyroelectric response, since the terminations on the two surfaces of one pellet are oriented in opposite directions and should cancel out on the macroscopic scale. Furthermore any symmetry breaking involving only the surface of the ceramics does not explain the inversion of the signs of the pyroelectric current on the opposite sides of the samples (Chapter 4) and the preservation of the direction of the pyroelectric response after polishing.

The possibility that the polar response is caused from artifacts related to charges trapped at the interface between the ceramics and the electrode can be ruled out because piezoelectric measurements were done on samples where the electrodes were not deposited by sputtering or another method and sample was only in a mechanical contact with metal caps through which the charge was collected. Furthermore, the influence of the deposited electrodes was studied using different metals. For the most part, measurements were done on samples covered with gold deposited by sputtering. Some samples were sputtered with platinum and others were painted with silver. In all cases, regardless of the electrode used, the pyroelectric response is observed and its magnitude does not vary significantly (Figure 5.5). The presence of the pyroelectric response in samples covered with silver paint also excludes the possibility that the pyroelectricity is caused by some asymmetrical surface effects induced by the sputtering process.

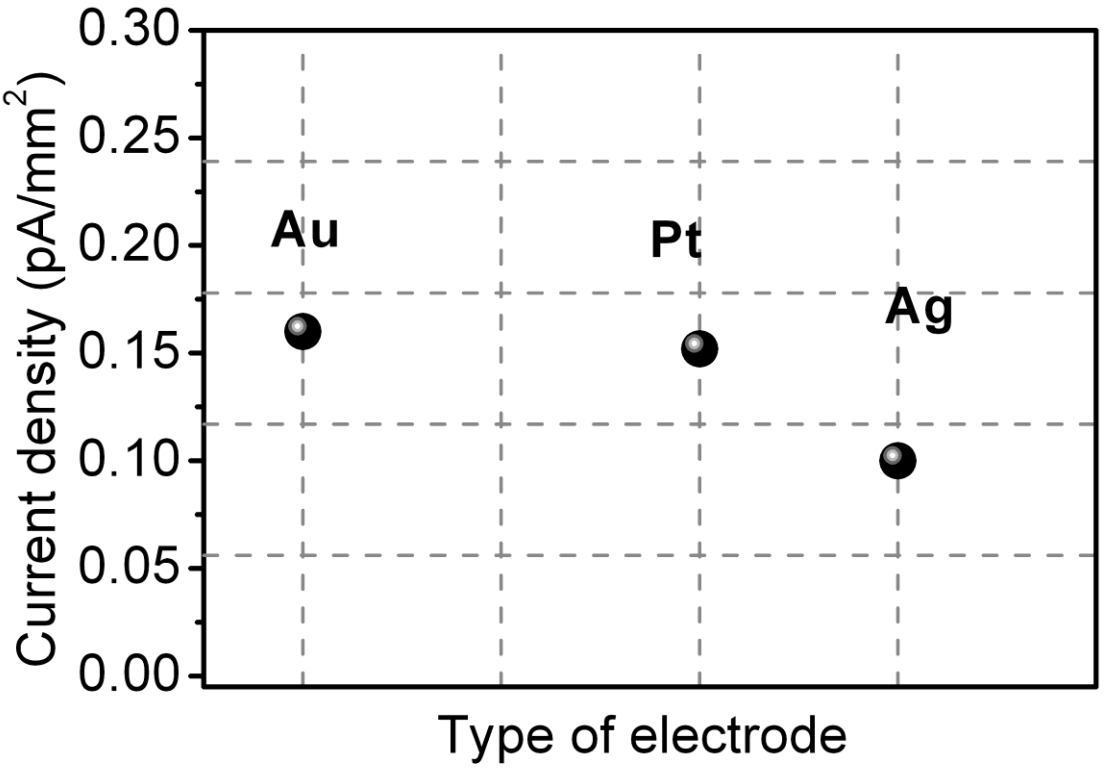

Figure 5.5-Amplitude of the pyroelectric current measured in BST6040 ceramics covered with different electrodes. Gold and platinum were deposited by sputtering while silver was painted on the samples and let dry at room temperature.

All these arguments are strongly in favor of hypothesis that the symmetry breaking has no significant surface contribution but involves the bulk of the ceramics. A bulk origin of the symmetry breaking implies necessarily the existence of a polar direction which appears in the samples at some point during their synthesis.

5.4 Role of the preparation of the ceramics on the origin of the symmetry breaking

Systematic measurements on different BST6040 ceramics reveal that the sign of the pyroelectric current depends on the orientation of the samples, with respect to the support (normally a thin platinum foil used to prevent the reaction with alumina) during sintering (Figure 5.6).

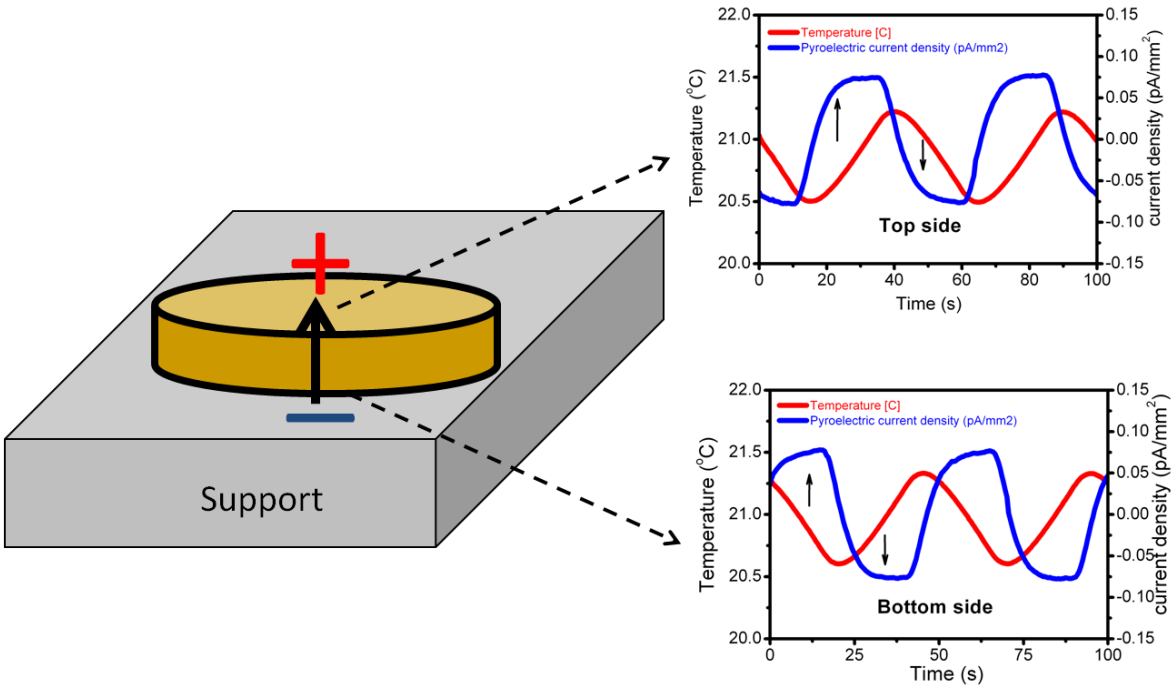

Figure 5.6-Correlation of the pyroelectric current amplitude and temperature in BST6040 ceramics after sintering. The top of the sample with respect to the substrate shows positive current amplitude when the temperature is increased and negative current amplitude when the sample is cooled (top panel on the left). The bottom side shows the exactly opposite correlation (bottom panel on the left). The positive and negative signs are assigned according to such correlation.

In particular the upper surface (with respect to the support) during sintering always shows positive amplitude of the pyroelectric current when the temperature is increased. For the sake of simplicity, this surface is labeled here as positive (this is the same direction of pyroelectric current that would be obtained in a ferroelectric sample poled by a positive field and measured on the electrode on which the field was applied). Consequently, the side in contact with the support is assigned a negative sign.

The presence of pyroelectricity in the BST6040 ceramics was found tens of degrees centigrade above the ferroelectric to paraelectric phase transition (Figure 5.7).

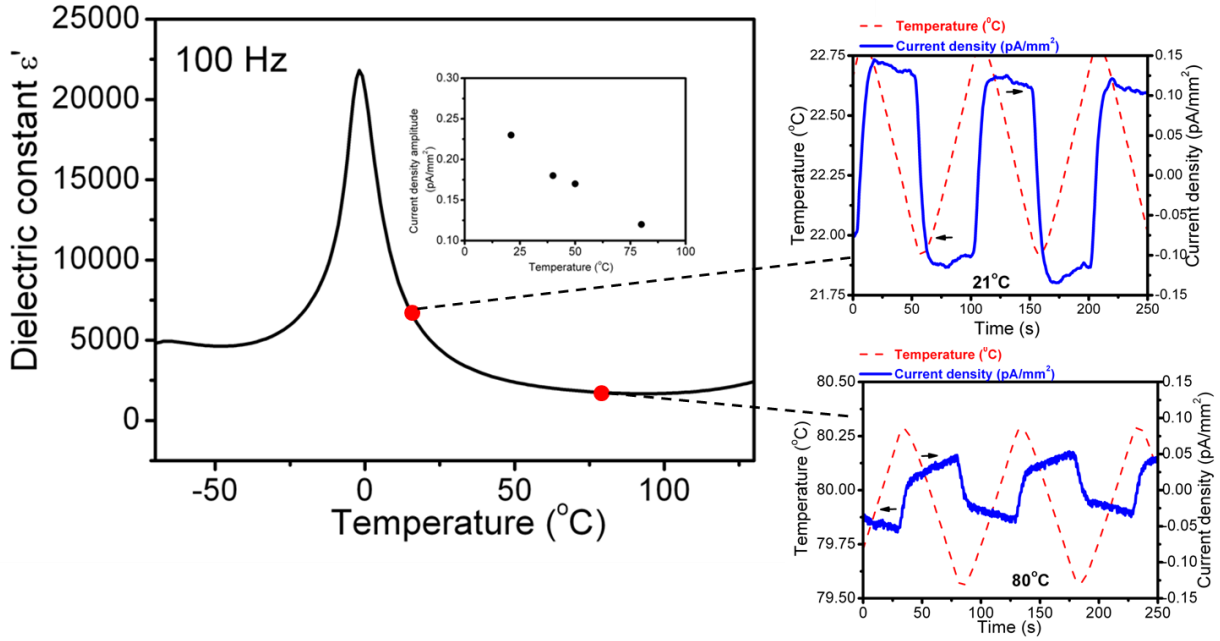

Figure 5.7-The dielectric permittivity as a function of temperature and pyroelectric response of BST6040 ceramics at 21°C and 80°C. The Curie temperature of this material is T_C = -1°C. The inset shows the amplitude of the pyroelectric current at four temperatures above T_C.

To identify the moment at which the polar direction is created, the different steps of the preparation of the ceramics were systematically investigated.

The first possibility is that the polarity appears already before sintering, during the pressing of the powders to form sample shape. A true uniaxial load, in principle cannot induce a polar orientation in the ceramics, since the stresses applied on two sides of the powders have opposite directions of ideally the same magnitude However, there is the possibility, that some asymmetry, present for example in the die used for pressing, causes a non homogeneous application of the pressure and induces preferential orientation along the axis of the compacted powders.

This possibility was verified by inverting the position of the green bodies (compacted powders) after pressing. Independently from the orientation of the sample in the press during compaction, the top of all samples shows a positive sign of the pyroelectric current after sintering (Figure 5.8). This test indicates that the preferred orientation appears in the ceramics during sintering.

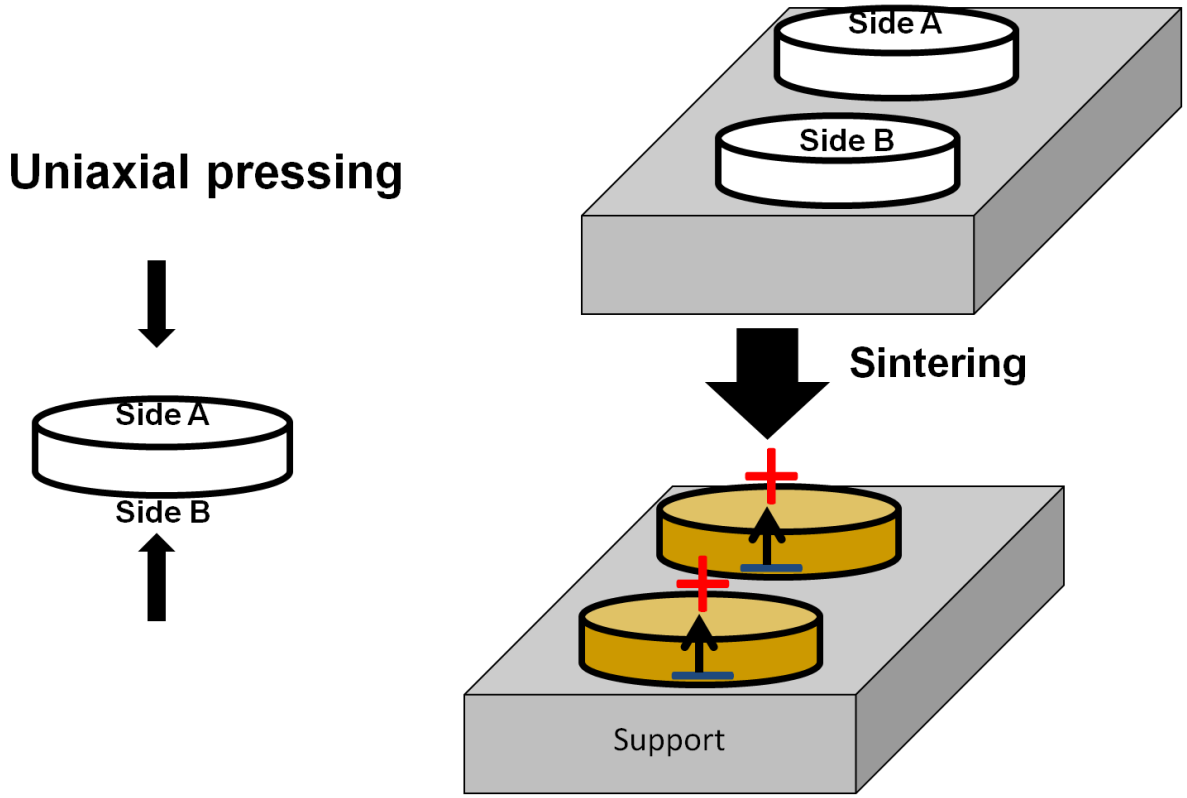

Figure 5.8-Study of the effect of the uniaxial pressing on the pyroelectric current in BST6040 ceramics. The face oriented up with respect to the substrate during sintering always shows a positive sign in the pyroelectric current, independently from its orientation during pressing.

A first, simple explanation for this observation could be that the sintering support causes the macroscopic asymmetry in the samples. An obvious mechanism for such asymmetry can be thermal gradient originating from different cooling rates between the top (in contact with air) and the bottom (in contact with the support) of the sample. It was observed, for example, that intentionally generated thermal gradient during sintering can induce self-polarization in ferroelectric $BiFeO_3$ ceramics [9]. Another explanation is that mechanical contact with the surface of the support may promote formation of defects (e.g., oxygen vacancies) on the side of the sample in contact with the support; concentration of the vacancies would then vary across the sample.

The influence of the support on the generation of the direction of the pyroelectric response in the BST6040 ceramics was investigated using different supports during sintering.

In order to reduce the asymmetry between the two sides of the pellet during sintering, some ceramics were sintered by placing them on platinum wires instead of on platinum sheets, to minimize the contact surface with the support. Other ceramics were squeezed between identical foils of platinum to have the same thermal conductivity on

both sides and see if platinum itself plays a role (for example, by promoting formation of oxygen vacancies).

In all cases, the ceramics show after sintering a pyroelectric response with amplitude comparable (within an order of magnitude) to the samples sintered with only the bottom side in contact with the platinum sheet. The fact that different sintering supports always result in the same preferred orientation of polarization in the samples suggests that if a thermal gradient is the origin of the polarization, the asymmetry introduced by the support is not the main cause for it.

In fact, when the pellets are sintered with the two large faces vertical with respect to the support (Figure 5.9), a pyroelectric response is still observed in the ceramics along the two major faces. In this case, too, the sign of the pyroelectric response is correlated with the orientation of the pellets during sintering. The asymmetry responsible for the appearance of the polar axis in the ceramics is thus present not only in the direction perpendicular to the substrate but it has components in other directions also. As we will discuss in section 5.7, the pyroelectric response is observed even in samples which are not directly in contact with the support, for example in samples that were completely buried into a powder of the same composition as the samples.

All these observations suggest that asymmetry responsible for the polarization of the samples does not have its origin in the substrate. In the chamber furnace used for sintering, the ceramics are surrounded by heating elements only on two sides. This configuration can already introduce an asymmetry in the heat flow inside the furnace and lead to a thermal gradient. A second source of asymmetry may be different aging states of the heating elements. To verify this possibility some ceramics were completely closed in a platinum box in order to screen them in all directions from the radiation of the heating elements. Such an arrangement also provides short-circuit boundary conditions. This did not affect the polarization of the samples.

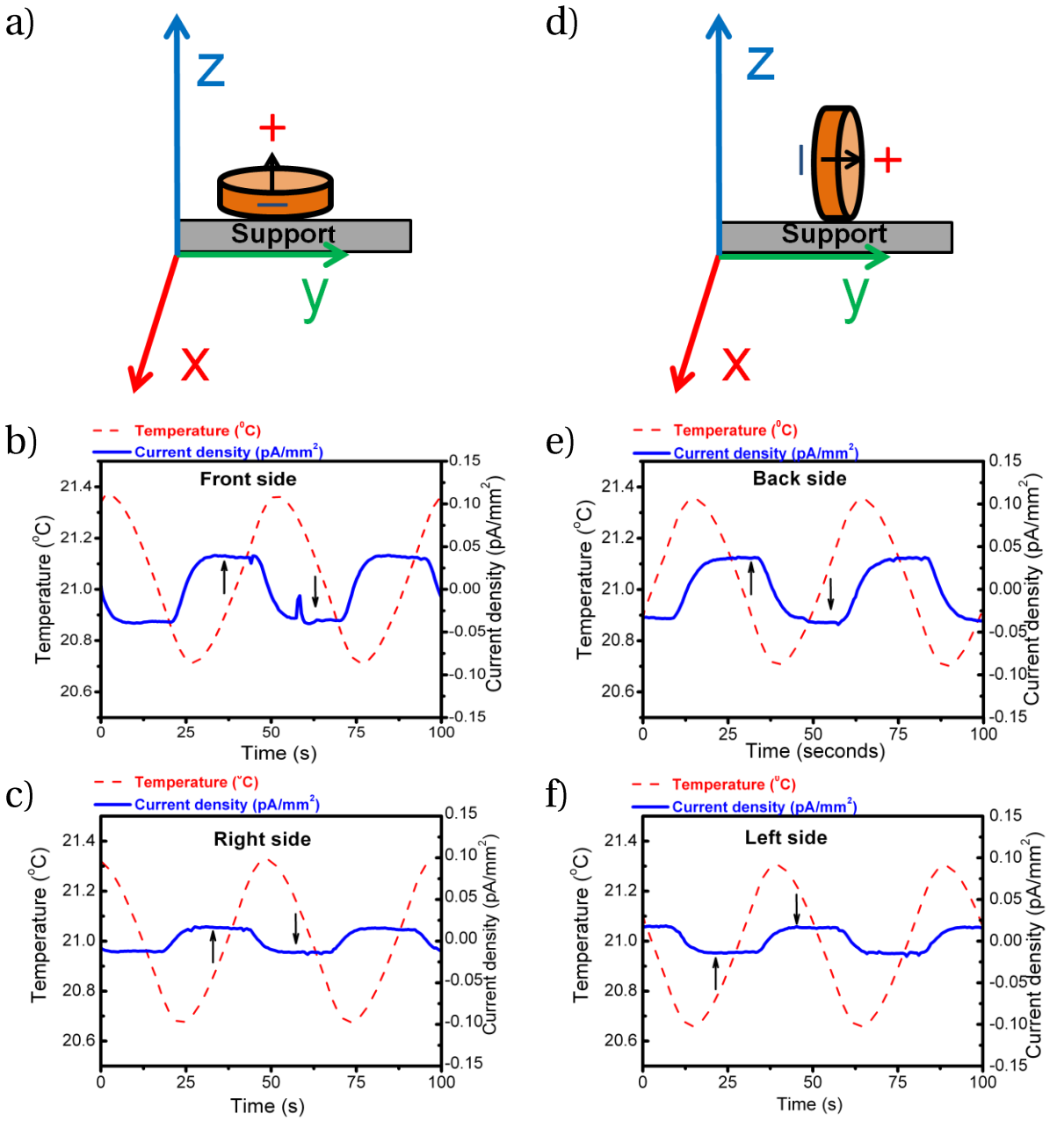

Figure 5.9-Pyroelectric response in BST6040 ceramics disk sintered with the two faces oriented parallel with respect to the support a) and perpendicular to it d). The pyroelectric current amplitude in the ceramics sintered vertically c)-f) is about five times smaller than in ceramics sintered with the face parallel to the support suggesting that the component of polarization in this direction is less pronounced. A pyroelectric response is also present when the ceramics are oriented with the faces in the direction of the x axis (b and c).). For the ceramics sintered in the vertical position, in agreement with the convention previously introduced, the positive sign is attributed to the side which shows the positive current amplitude upon heating.

To rule out the possibility that the polarity of the ceramics was caused by the specific furnace used for sintering, some samples were sintered in other furnaces.

The variation of the sintering environment did not have much effect on the final

state of the sample: similar amplitude of the pyroelectric response and the same direction of the pyroelectric response was observed in all ceramics (Figure 5.10), regardless of changes in the samples environment.

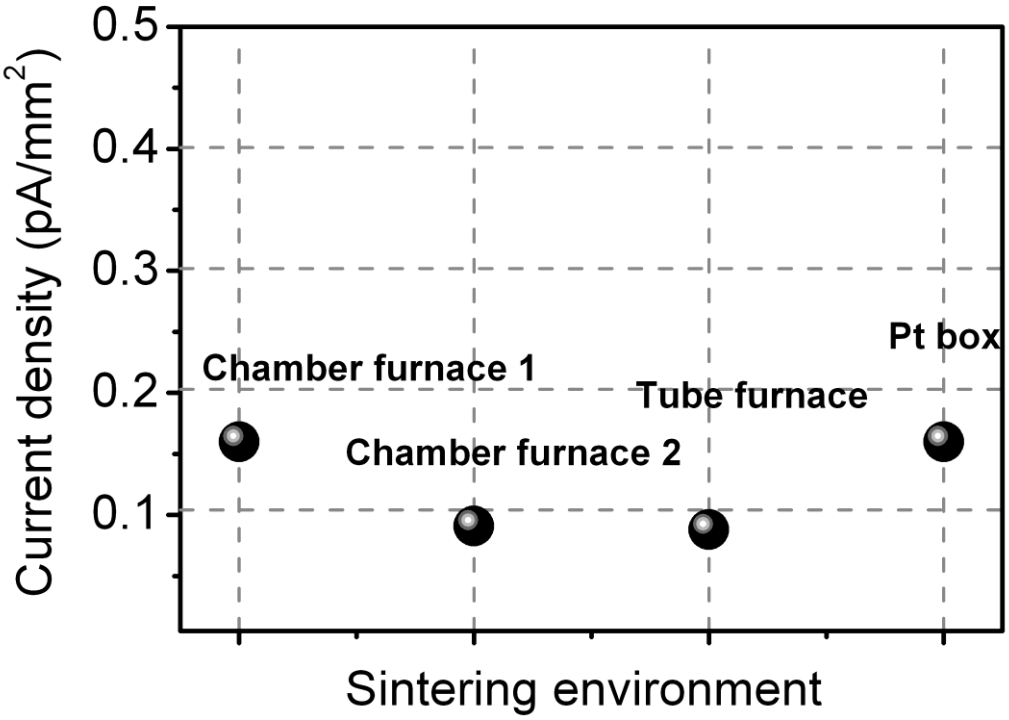

Figure 5.10-Pyroelectric current amplitude for samples prepared in different sintering environment. The chamber furnace 1, the standard furnace where most ceramics used in this study were sintered is manufactured by Lenton furnaces (UK). As control furnaces, a second chamber furnace from Nabertherm GmbH (Germany) and a tube furnace from Lenton were used. All the furnaces have a different design and configuration of the heating elements. The samples enclosed in the platinum box were sintered in the chamber furnace 1.

The experiments conducted so far show that the asymmetry is present in all samples regardless of the type of the furnace used for sintering and the type of support used to support the samples during sintering. This would suggest that the inhomogeneity is not associated to a thermal gradient. However without further studies it is not possible to complete rule out this possibility.

In principle, it should not be excluded that gravity is at the origin of the asymmetry in the ceramics. This is one constant external factor that is always present during sintering. It is known since long time that the gravity has an effect on sintering process and densification of ceramics [10]. The gravity induces material transport which results in a characteristic “elephant foot” shape of the samples after sintering. Finite-element calculations show that such distortions can occur during both liquid and solid sintering

[11] and for specimens sintered with a support on the bottom or suspended from the top [12]. In the case of the BST6040 ceramics, no macroscopic shape change is observed after sintering, although this is not surprising because of the very fine thickness of the ceramics. Measurements with a profilometer on the surface of the as prepared ceramics did not reveal any curvature in the shape of the pellets, confirming that, if present, such shape distortion is very small and may be screened by the roughness of the surface (about 6 μm).

5.5 Effect of the densification on the orientation of the built-in polarization

All the experiments discussed until this point suggest that the preferred orientation in ceramics, whatever is the physical origin of the asymmetry causing it, is created during the sintering and is related to the densification process.

This is directly confirmed by the possibility to invert the direction of the polarization by controlling the degree of densification in the ceramics. The experiment is discussed below and is summarized in Figure 5.11.

The freshly pressed green bodies (65%-70% of the theoretical density) of BST6040 ceramics were initially fired at 1300^0C instead of the usual sintering temperature (1450^oC). At this lower sintering temperature, the ceramics reach only up to 80% of their theoretical density. The pyroelectric measurement on those partially densified ceramics indicates that the polarization develops, as expected, along the orientation which gives (according to the convention introduced previously) positive sign of the pyroelectric current on the top of the pellet. After the pyroelectric measurement the sample is placed in the furnace again, the orientation of the ceramics on the support is reversed with respect to original, and the sample was re-sintered at 1450^oC. At this temperature, a further densification takes place and the density of the ceramics reaches 96% of its theoretical value.

After re-sintering, the top sides of the ceramics show always a positive sign of the pyroelectric current, indicating that the direction of the built in polarization has reversed during the re-sintering step.

If the sintering temperature is now increased even more (to 1500^oC), no additional densification occurs and the direction of the built-in polarization does not invert when the orientation of the samples is inverted. This indicates that when the mass transport that takes place during the sintering is complete, there is no more driving force for the generation of the asymmetry in the ceramics.

Being related to the densification process, during which a large mass transport takes place, the asymmetry created during densification and which lead to polar character of the sample is most likely associated with an (even slight) gradient in chemical composition, defects and/or in elastic strain across the samples.

In analogy to what is observed in ceramics, the polar character present in the paraelectric phase of single crystals (see section 5.2) can originate from asymmetries created by the mass transport and atom rearrangement (e.g., creation of dislocations) occurring during the crystal growth and subsequent cooling.

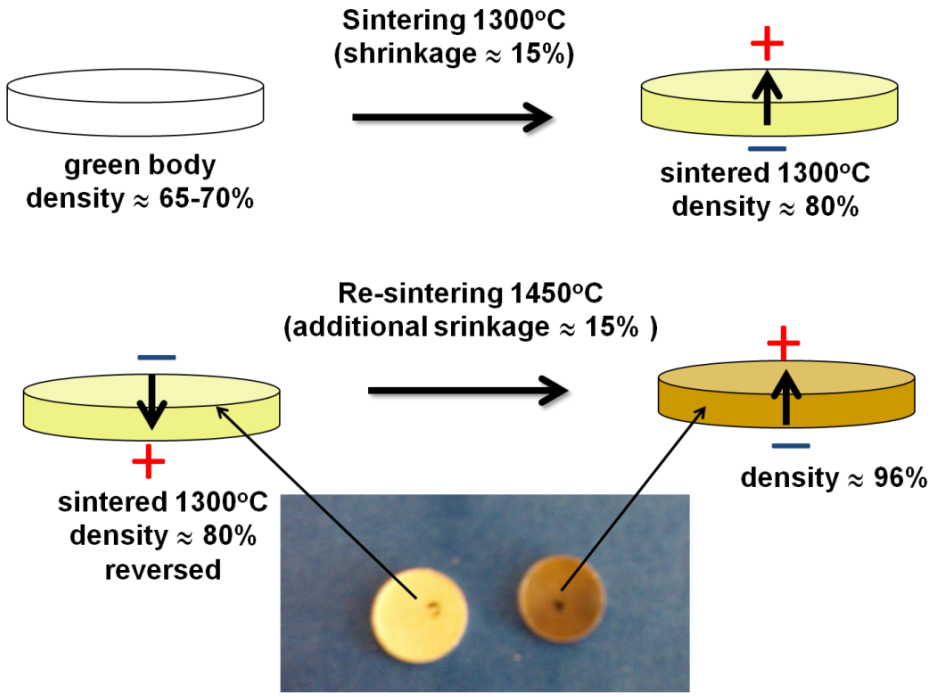

Figure 5.11-Inversion of the direction of built in polarization in BST6040 ceramics by densification control. The sintering process lead to densification of the green body (up corner on the left) through diffusion When the partially densified (up corner on the right) sample is inverted on the support and sintered at higher temperature (bottom corner on the left) additional mass transport take places inducing a redistribution of the inhomogeneities in the ceramics and reorienting the direction of the polarization (bottom corner on the right).The change of dimension due to densification is clearly seen in the of the ceramics sintered at 1300°C and 1450°C(photographs center bottom).

The evidences collected so far demonstrate that the existence of polarization in the paraelectric phase of unpoled BST6040 ceramics is the consequence of the appearance of an asymmetry in the samples during sintering.

The orientation of the polar axis is strongly associated with the densification of the ceramics and settles in the samples permanently during the mass transport. However, the simple presence of a preferred direction in the sample is not sufficient to explain the pyroelectric response observed at room temperature in the BST6040 and other BST ceramics. In fact, in $SrTiO_3$ ceramics, sintered in the same environment and with similar processing conditions as BST samples, one would expect the same preferred orientation to be present; however, the pyroelectric response is not observed.

The fact that the pyroelectric response is not observed in as–sintered $SrTiO_3$ ceramics raises the question if their low room temperature dielectric permittivity (ε_r about 260 at 21°C) with respect to BST6040 (ε_r about 6000 at 21°C) plays a role in decreasing the amplitude of the pyroelectric signal. An experiment conducted on unpoled $BaTiO_3$ ceramics provides evidence that the magnitude of the pyroelectric response in unpoled ceramics does not scale directly and exclusively with the relative permittivity of the samples.

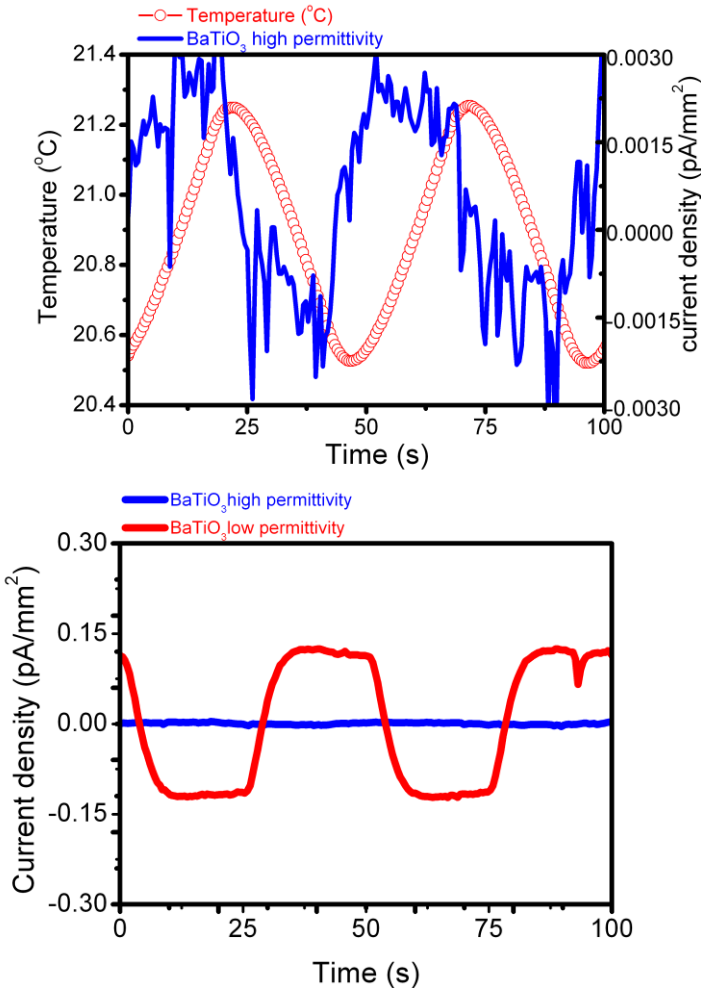

Figure 5.12-Room temperature pyroelectric response in unpoled $BaTiO_3$ ceramics with high permittivity (around 5000) before annealing at high temperature (top) and comparison of the pyroelectric current amplitude in the same ceramics before and after annealing at 1400°C for 18 minutes (bottom). The room temperature permittivity after annealing decreases to 1800. This drop is related the substantial increase in the grain size [13] caused by annealing. The grain size in samples before annealing was on the order of 1 μm and after annealing 50 μm. The $BaTiO_3$ ceramics samples were produced by Dr. Marlyse Demartine according to the processing method described in [14].

Samples of unpoled $BaTiO_3$ ceramics with the grain size of 1 μm and relative permittivity at room temperature of about 5000, show a very weak pyroelectric response (see Figure 5.12 top). After the pyroelectric measurement, the same samples were annealed

in air at 1400^{o}C (150^{o}C above their initial sintering temperature).The annealing treatment increases the size of the grains up to about 50 μm and causes permittivity at room temperature to drop down to 1800. The amplitude of the pyroelectric current in the samples with the low permittivity is found to be 50 times larger than before annealing (Figure 5.12 bottom).

Acknowledging the fact that different mechanisms can account for the huge increase of the pyroelectric current in ferroelectric $BaTiO_3$ ceramics after additional high temperature annealing, such for example different averaging of the ferroelectric domains in fine–grain and coarse–grain ceramics, this experiment gives the important insight that the magnitude of the permittivity is not by itself the most important parameter which controls the magnitude of the pyroelectric current (or in general, electromechanical coupling) in unpoled ceramics. More direct evidences for the relation with permittivity is given by the systematic study of the whole $Ba_{1-x}Sr_xTiO_3$ solid solution presented in section 5.7.

The absence of pyroelectric response in $SrTiO_3$ ceramics depends more likely from the fact that the $SrTiO_3$ ceramics develop a lower amount of inhomogeneities during sintering whit respect to the (Ba,Sr)TiO_3 ceramics. This is directly confirmed by the analysis of the microstrain with XRD which will be discussed in the next section (5.6).

5.6 XRD characterizaion of the strain in the ceramics

X-rays diffraction technique was used to map the strain across the ceramics, in order to establish if the asymmetry which develops during sintering is associated to a variation of stress across the samples. As it is shown in Figure 6.1, the pattern collected on the two opposite flat sides of a trapezoid of BST6040 ceramics shows a significant broadening of the full width at half maximum (FWHM) of the diffracted peaks between the two sides, while in the $SrTiO_3$ trapezoid the difference between the two sides is much smaller.

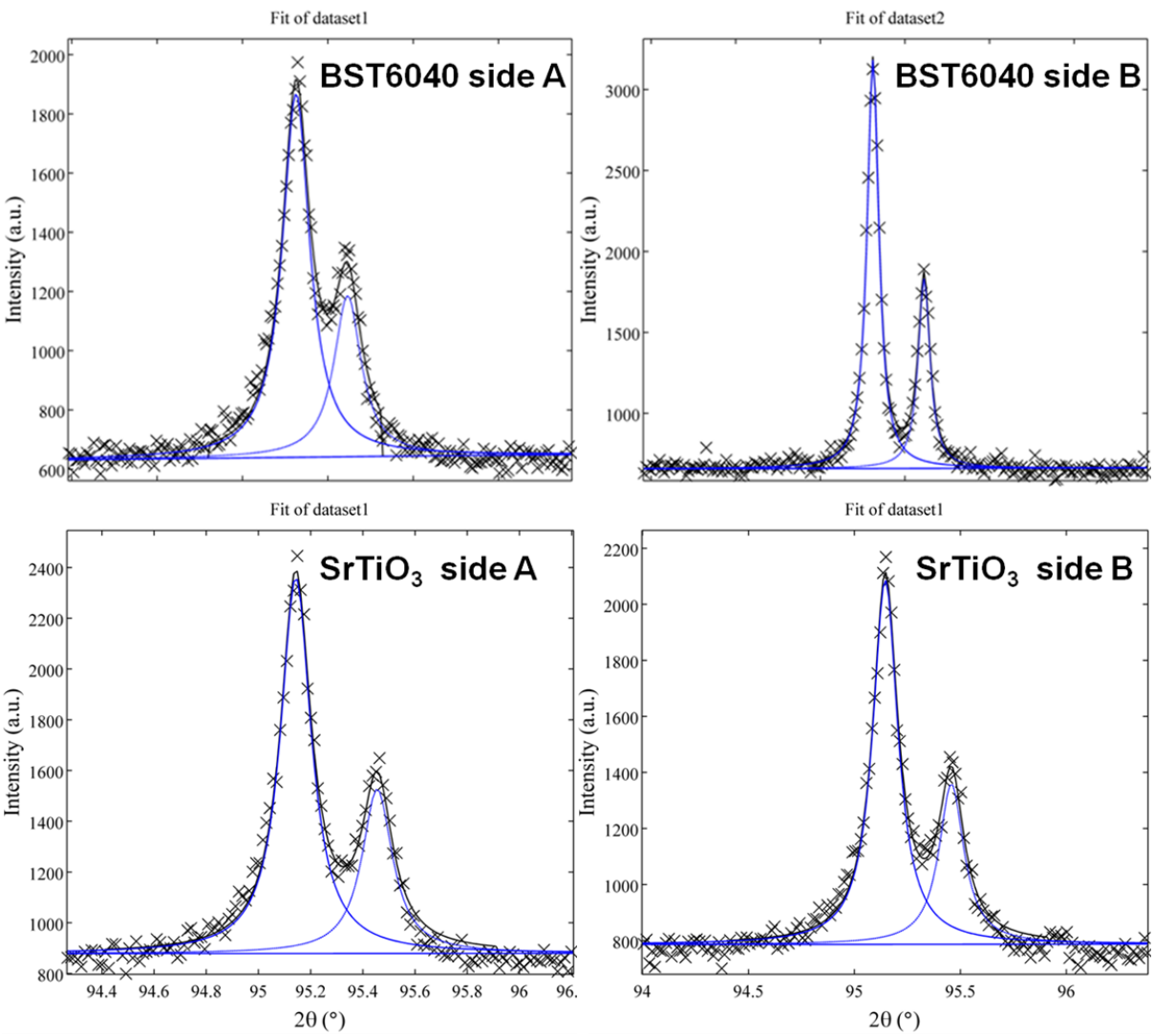

Figure 6.1- X Ray [3 2 1] reflection, collected scanning the two opposite flat sides of trapezoids of BST6040 (top) and $SrTiO_3$ (bottom), ceramics. While the two opposite sides of BST6040 shows a significant broadening in the width of the peak (top), in $SrTiO_3$ the peak broadening is much less pronounced. The XRD measurements were performed with a PANalytical Empyrean at North Carolina State University in collaboration with professor Jacob L. Jones and Dr. Chris Fancher.

The change in the FWHM of the peaks can originate either from a difference in the size of the crystallites across the samples or from the presence of microstrain, which is the non-uniform variation of the lattice parameter, in the crystallites. The two contributions to the broadening can be distinguished by means of a Williamson-Hall analysis [10]. The analysis consists in a linear fit of the breadth of the diffracted peaks plotted as a function of the diffraction angle θ. Since the broadening the peaks due to the presence of non-homogeneous strain (microstrain) is proportional to the tangent of the diffraction angle θ and broadening of the peaks related to finite crystallite is inversely proportional to $\cos\theta$, the two contributions can be separated. The contribution of the crystallites size is given by the intercept of the fit while that of strain is given by the slope of the fit. In the case of

BST6040 ceramics, an appreciable change in the slope of the Williamson-Hall plot indicates that the peaks broadening is due to the presence of microstrain. The Williamson-Hall plot referring to the two opposite sides of $SrTiO_3$ ceramics show a less pronounced change in the slope, implying a much smaller difference in microstrain between the two sides of the sample (Figure 6.2).

The difference in microstrain present in BST6040 and in pure $SrTiO_3$ ceramics suggests that the compositional inhomogeneities in the samples are related to the barium content of the samples.

As discussed in Chapter 5, in $(Ba,Sr)TiO_3$ this decreasing of the compositional inhomogeneities might be due to the reduction of the off-centering of the Ti ions and the shrinkage of oxygen octahedra with the increase of the concentration of strontium, recently reported in $Ba_{1-x}Sr_xTiO_3$, solid solution [26].

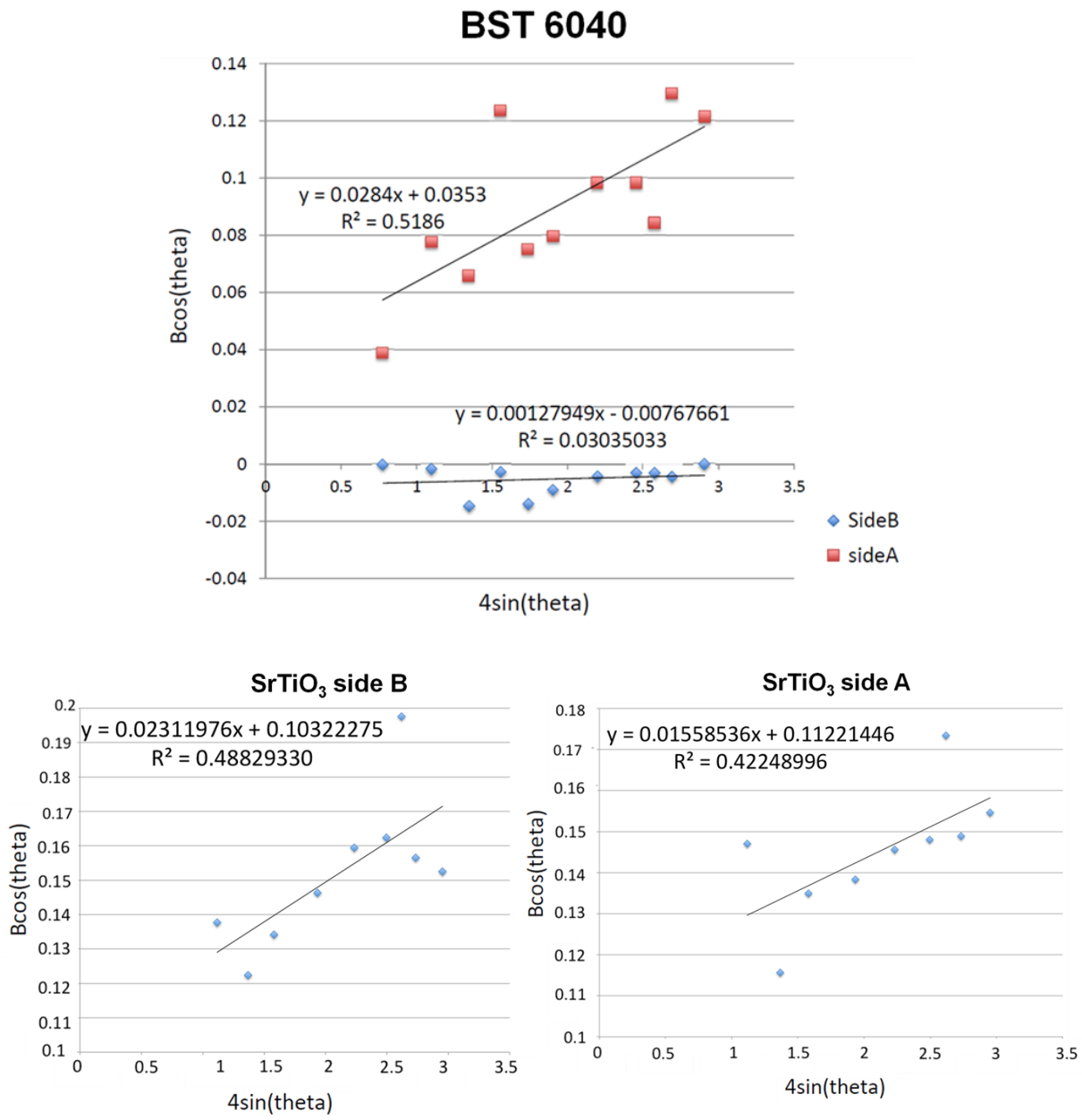

Figure 6.2-Williamson-Hall plot of the diffraction peaks on two sides of BST6040 (top) and $SrTiO_3$ ceramics trapezoids (bottom).On the vertical axis is plotted the broadening of the peaks B multiplied by cosθ. The slope of the linear fit is related to the presence of inhomogeneous strain in the ceramics crystallites. The slope change is more drastic in BST6040 than in $SrTiO_3$, indicating qualitatively that a higher microstrain variation is present in BST6040 than in pure $SrTiO_3$. The Williamson-Hall analysis was performed by professor Jacob L. Jones and Dr. Chris Fancher at the North Carolina State University.

5.7 Proposed mechanisms of symmetry breaking in $Ba_{1-x}Sr_xTiO_3$ ceramics

The difference between BST6040 and the $SrTiO_3$ ceramics, since they are sintered in the same environment, cannot be simply explained by the fact that the asymmetry present in the furnace breaks the centric symmetry only macroscopically.

This reasoning leads us to formulate a model to explain the symmetry breaking in unpoled as-sintered ceramics. One possibility, is that the breaking of the symmetry takes place on two different scales (Figure 5.13 a). A first mechanism of symmetry breaking occurs on the microscopic scale of the ceramics and breaks the symmetry of the paraelectric phase locally. We propose that this local symmetry breaking is represented by the existence of some kind of polar or charged defects. In macroscopically homogeneous samples, these defects would be randomly oriented and no macroscopic polarization would be observed. However, the asymmetry present in the sintering environment introduces a preferred orientation in the samples which aligns the polar defects and breaks also the macroscopic symmetry of the samples.

A second possibility is that the asymmetric sintering environment induces a different concentration of polar or charged defects across the ceramics inducing a macroscopic gradient between the bottom and the top of the ceramics (Figure 5.13 b).
In both cases, the difference observed between BST6040 and $SrTiO_3$ implies that the polar defects at the origin of the polarity in BST6040, in $SrTiO_3$ ceramics are not present or, at least, are much less concentrated in $SrTiO_3$ (as indicated from the investigation of the microstrain discussed in section 5.6). This model raises the fundamental question about the nature of such polar defects.

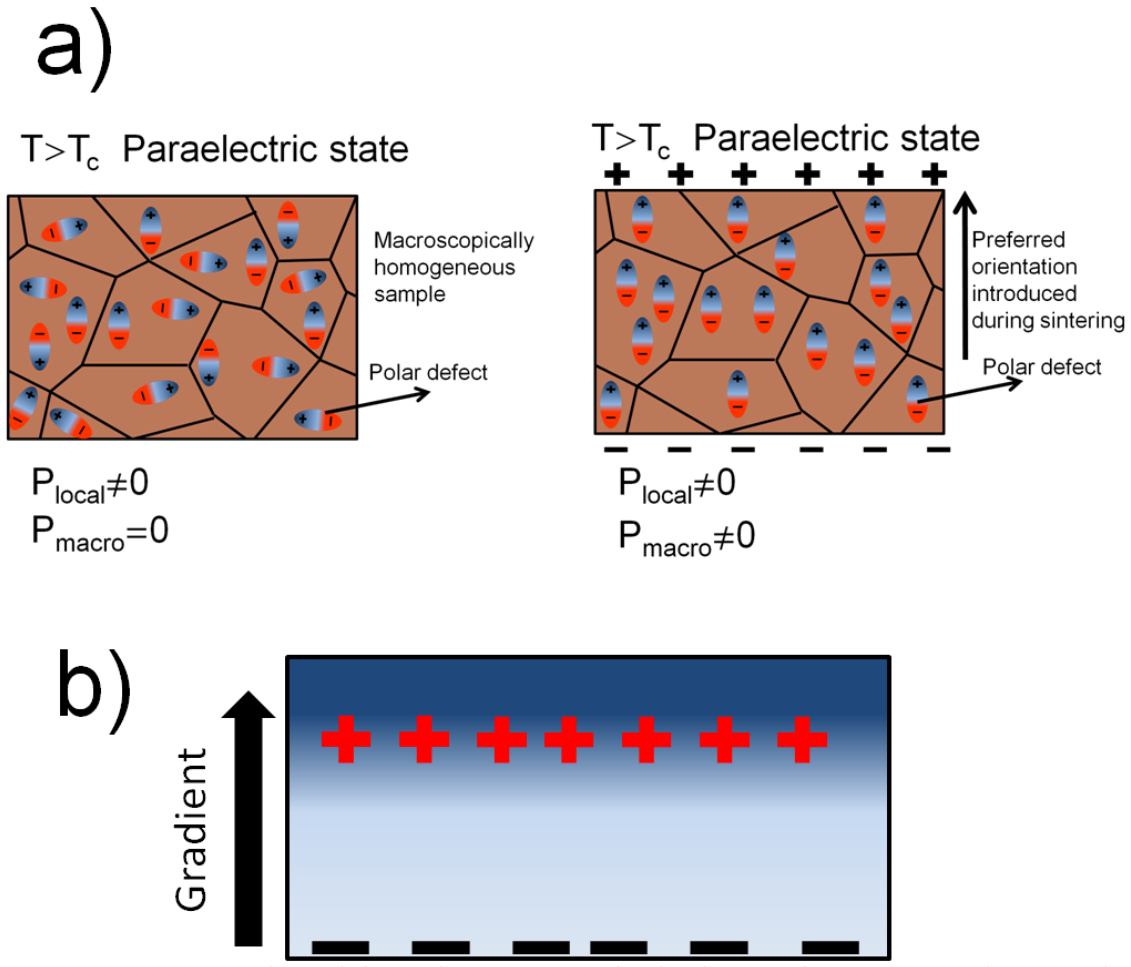

Figure 5.13-Proposed models of the origin of the built-in polarization in the paraelectric phase of BST6040 ceramics: a) The centric symmetry is broken, on the local scale by the existence of polar or charged defects, distributed in the main paraelectric matrix. In macroscopically homogeneous samples this situation would lead to the absence of macroscopic polarization. However, the asymmetric sintering environment induces the alignment of the polar defects, breaking also the macroscopic symmetry. In alternative b) the asymmetry in the sintering environment induces a gradient in the concentration of the defects across the thickness of the ceramics which results in macroscopically polar samples.

A first kind of polar defects can be represented by the ionic vacancies created during sintering. In (Ba,Sr)TiO_3 ceramics, the cationic defects are represented by V_{Ti}^{4-} or V_{Ba}^{2-} /V_{Sr}^{2-}vacancies while the anionic vacancies are oxygen vacancies (V_O^{2+}). Although the activation energy for titanium vacancies in $BaTiO_3$ is lower than for A-sites vacancies [15], the latter cannot be excluded since the sintering temperature of the ceramics (1450^oC) is not far from the melting point of $BaTiO_3$ (1625^oC). Two types of defects are possible. The first is represented by isolated cationic and anionic vacancies while the second is related to anionic cationic vacancy pairs or complex. If the polar defects at the origin of the polarization in BST6040 are barium vacancies and oxygen vacancies the absence of

pyroelectric response in $SrTiO_3$ could be explained by the fact that since the melting temperature of $SrTiO_3$ is 2080°C, more than 300°C above that one of $BaTiO_3$, at 1450°C, in BST solid solution, the concentration of cationic V_{Ba}^{2-} vacancies is higher than V_{Sr}^{2-} vacancies in Sr-rich compositions and in $SrTiO_3$ in particular. Since ionic defects usually appear as Schottky defects (i.e.,V_O-V_{Sr}/V_{Ba}), one would expect a lower concentration of both anionic and cationic defects in $SrTiO_3$. However, first principles calculations show, actually, a lower energy formation for V_{Sr}+V_O defects than for the V_{Ba}+V_O defects [16], suggesting that this interpretation is not correct.

Recently, first-principle calculations in epitaxial thin films of $CaMnO_3$ [17], have shown that oxygen vacancies formation is stabilized by the presence of in–plane tensile strain in the films and such tensile strain can cause the concentration of the oxygen vacancies. Similarly, cation vacancies would form preferentially under compressive pressure. These results are valid not only for the Pnma structure of the $CaMnO_3$ but, in principle, for any oxide with non equivalent oxygen sites. It is therefore possible that the inhomogeneous strain, developed during sintering, whose presence is shown by the XRD analysis (see section 5.6), has caused the preferential orientation of the oxygen vacancies in the $(Ba,Sr)TiO_3$ ceramics.

In order to evaluate the evaporation of metallic ions in BST during sintering the weight loss of the ceramics was measured and estimated to be less than 0.1 % (sensitivity of our analytical balance). This suggests that the formation of a very small amount of intrinsic ionic vacancies, if that is the reason for the polar response, can be enough to observe the pyroelectric current.

In the attempt to limit the evaporation in BST6040 ceramics, some pellets were sintered on the flat support or in a closed alumina crucible and completely buried in a powder of the same composition. After sintering, the ceramics covered with the powder show comparable amplitude of the pyroelectric current with respect to samples sintered at the same time but exposed to air (Figure 5.14). The absence of substantial weight loss and difference in pyroelectric current between samples prepared in two different ways suggests that defects may be formed by the barium segregation and formation a secondary phase inside the ceramics rather than evaporation of BaO (barium oxide), This is actually consistent with the presence of the small amount of a barium rich phase (most likely barium orthotitanate) detected with SEM and mapped by EDS technique (see Chapter 2).

In the attempt to limit the formation of the oxygen vacancies, the ceramics were sintered and cooled under a partial pressure of 1.2 bar of oxygen. The pyroelectric response of the ceramics sintered in oxygen was similar to that of ceramics sintered in air.

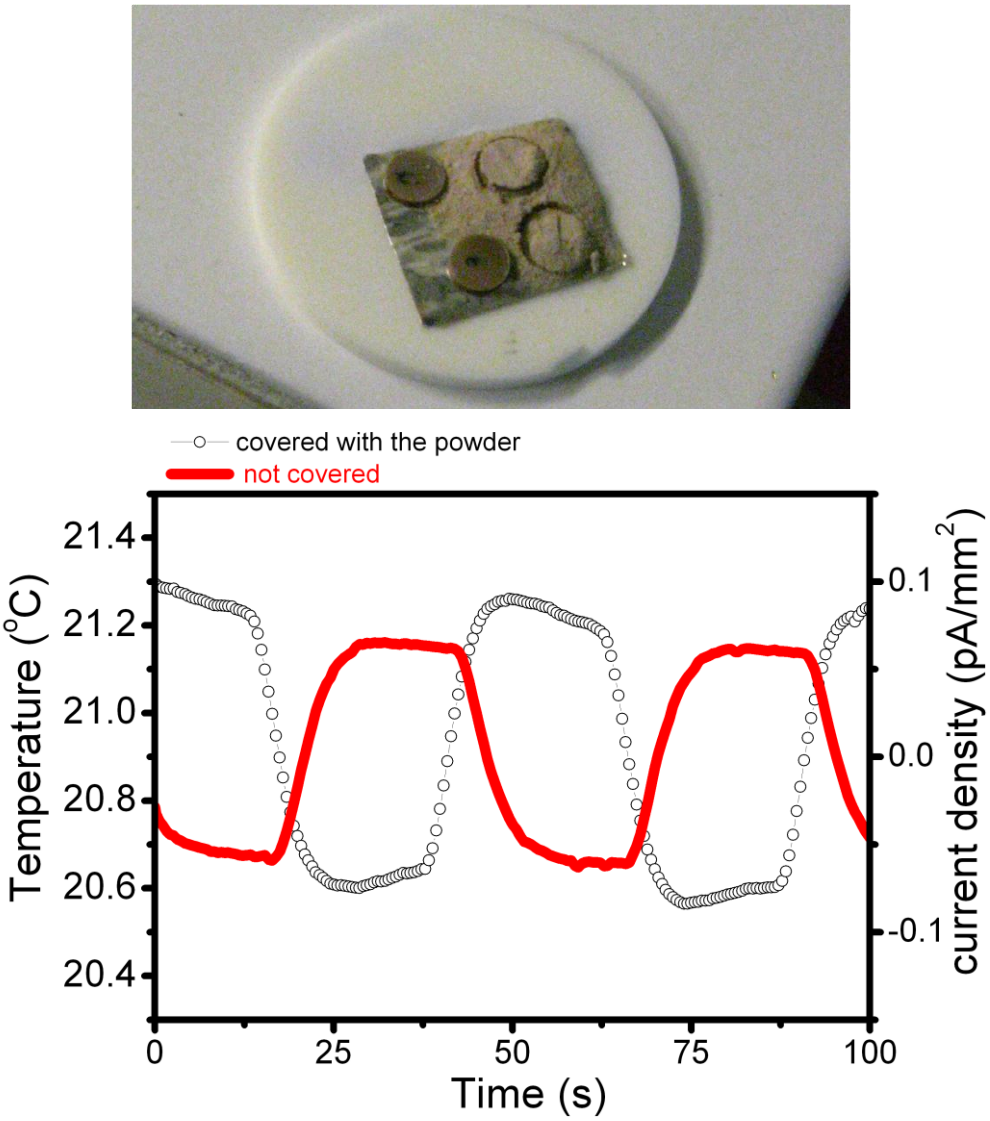

Figure 5.14-Comparison of the pyroelectric current for BST6040 ceramics completely covered with the powder of the same composition and ceramics exposed to air, sintered at the same time. The amplitude of the pyroelectric current in the ceramics covered with the powder can be even larger than in the ceramics exposed to air.

If the inhomogeneity in the ceramics originates from a gradient in the concentration of barium vacancies between the top and the bottom of the samples, such compositional variation, might be revealed by means of chemical analysis. A cross section of BST6040 ceramics of the thickness of about 270 μm was analyzed with Electron dispersive X-Ray Spectrometry (EDS) in search for difference in the barium and strontium concentration.

The EDS spectra were collected by scanning ten approximately equally spaced areas across the sample thickness; this is the same direction, along which the pyroelectric current was measured.

As can be seen in Figure 5.15, a first series of measurements, show a clear trend in the ceramics indicating a lower concentration of barium with respect to strontium close to

the top surface. However, when the measurements were repeated the second time, across the same cross–section the lower content of barium is found in the central part of the sample.

These conflicting results are probably partly due to a very small variation of barium concentration across the sample thickness. In fact the maximum difference in barium concentration determined with the first series of measurements does not exceed 1%. Such a value is in the limit of the analytical precision of the EDS technique itself, which is in the range of 1% and 2%. Thus, these results cannot be taken as conclusive.

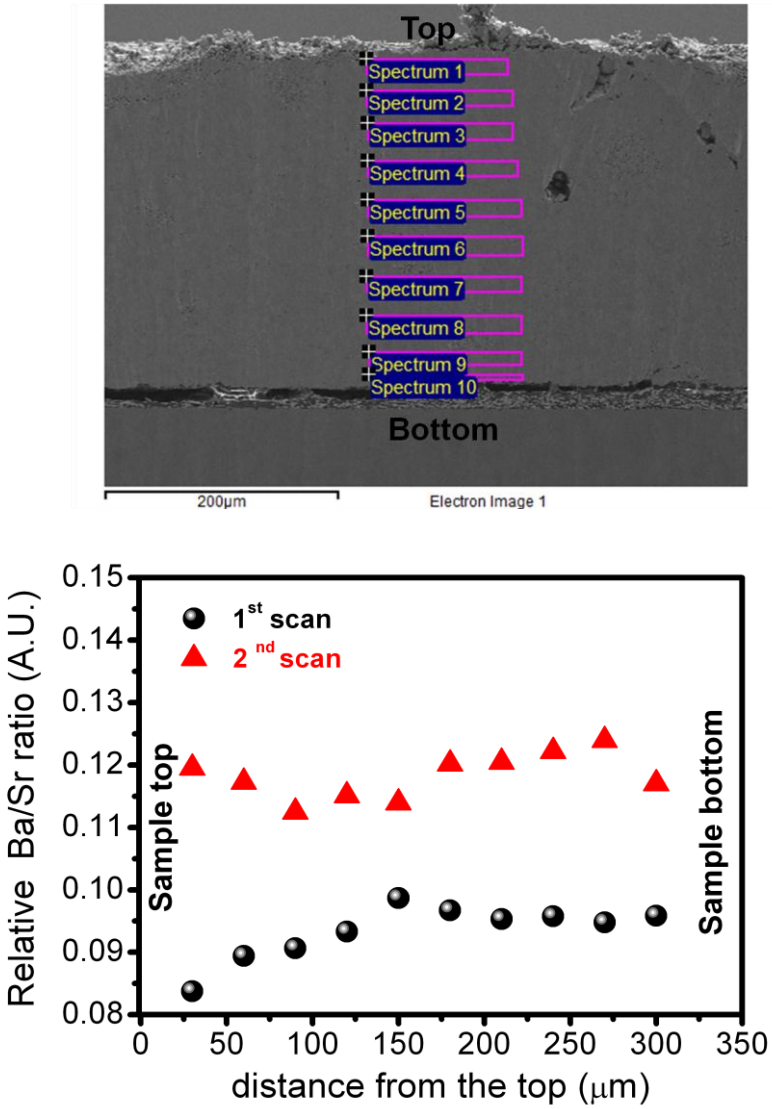

Figure 5.15-SEM image of the BS6040 ceramics cross section analyzed in search of compositional gradients (top image).Each spectrum was collected scanning a rectangle of about 120 µm x 15 µm in area. Variation of the barium concentration across the sample thickness (bottom image).The quantification was made taking the Mα line of barium and the Lα line of strontium. For each scan the strontium line was taken as reference and the barium line was normalized with respect to it.

The fact that the variation of atmosphere and in general of the sintering conditions does not affect drastically the amplitude of the pyroelectric response in BST6040 ceramics opens the possibility that the charge separation in the ceramics is not originated from the formation of vacancies in the lattice, which are expected to be sensitive to material preparation. Also, this approach probably cannot explain absence of signal in $SrTiO_3$ samples.

This would be also consistent with the observation that BST6040 ceramics sintered at different temperatures, show pyroelectric currents with very similar amplitudes (Figure 5.16).

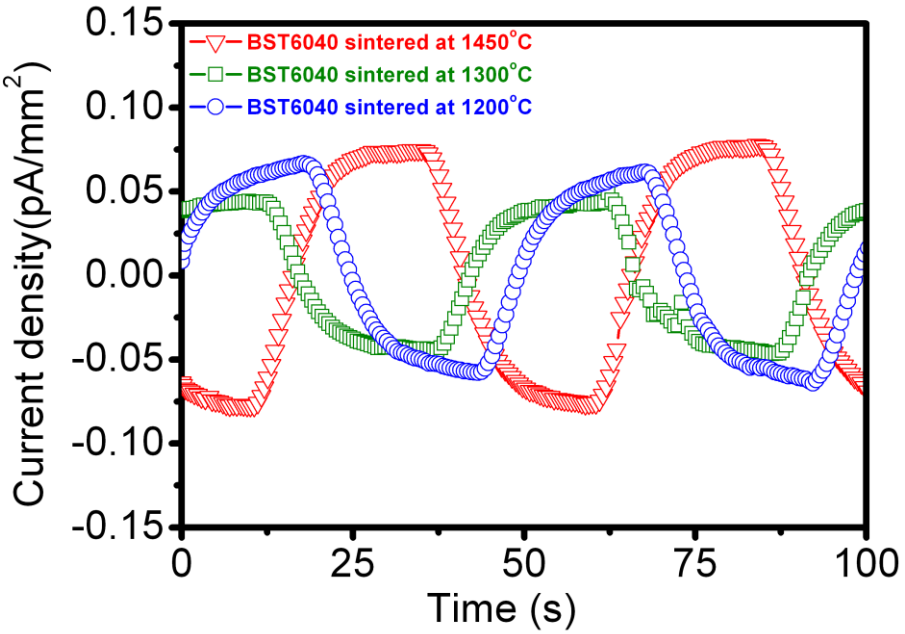

Figure 5.16-Pyroelectric current amplitude at 21°C in BST6040 ceramics sintered in air at different temperatures.

Interestingly the comparison of the BST6040 ceramics sintered at different temperatures indicates that the amplitude of the pyroelectric current is not substantially affected by the microstructure of the ceramics as can be inferred by the micrographs of the BST6040samples sintered at 1300°C and those of the samples sintered at 1450°C (Figure 5.17).

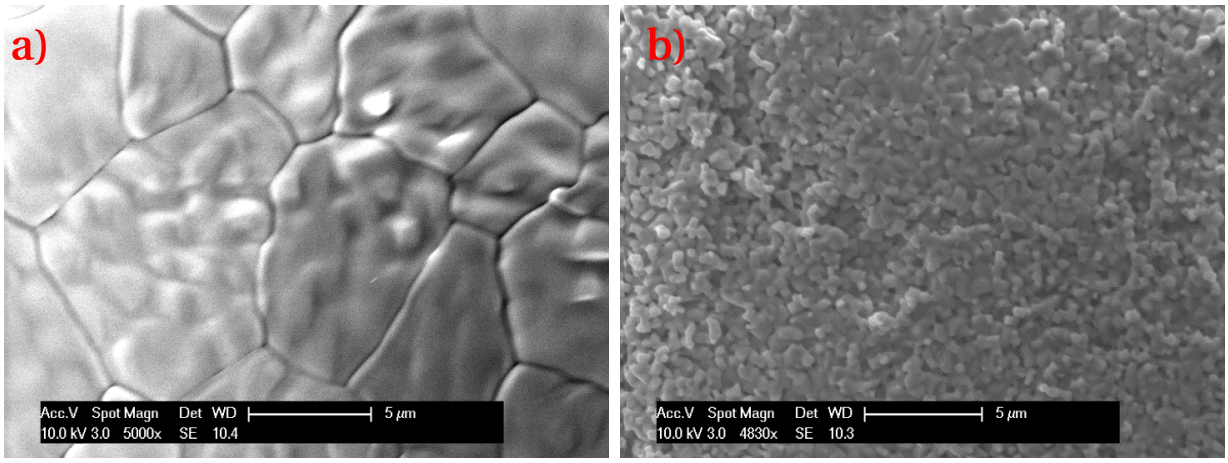

Figure 5.17-Comparison of the microstructure in BST6040 ceramics samples sintered at 1450°C (a) and at 1300°C (b).

Beyond ionic vacancies, the polar defects present in BST6040 ceramics might have a more intrinsic origin related to the ferroelectric nature of $BaTiO_3$ and $(Ba,Sr)TiO_3$ solid solution.

In the paraelectric phase of ferroelectrics perosvkites, a breaking of the symmetry on the local scale is often associated with the presence of polar precursors [18, 19], therefore a second candidate for the charge separation in BST6040 ceramics are polar entities which appear at the level of the crystal lattice, including polar clusters [20], polar nano-regions [21] and distorted interacting oxygen octahedra [22]. These polar entities, if elastically active [23], can freeze–in or be aligned by chemical or stain gradients created during the sintering process. It has been shown theoretically that in epitaxial films of related perovskite material, relaxor $BaZrO_3$, the polar nano-regions are microscopically coupled with the elastic strain, can get preferentially oriented and their average size is influenced by the magnitude of the strain [24].

Following this second hypothesis, the absence of the pyroelectric response in $SrTiO_3$ could be explained by the fact that the polar entities are not present in the incipient ferroelectric $SrTiO_3$ where a more displacive phase transition is expected with respect to $BaTiO_3$ [25].

It is also possible that the concentration of the polar entities progressively decreases with the substitution of barium with strontium. Recently, refinement of the $(Ba,Sr)TiO_3$ structure based on Reverse Monte Carlo modeling [26] demonstrate a progressive

reduction of the off centering in Ti ions and shrinking of the oxygen octahedral as the content of Sr increases.

To better understand the evolution of the polar character from BST6040 (barium rich composition) to the pure $SrTiO_3$ ceramics, the pyroelectric studies were extended to the whole (Ba,Sr)TiO_3 solid solution.

5.8 Evolution of the pyroelectric response in the (Ba,Sr)TiO_3 solid solution

The new (Ba,Sr)TiO_3 compositions were prepared, keeping constant all the processing parameters. The increase in strontium concentration in the ceramics, progressively shifts the Curie temperature of pure $BaTiO_3$ (120^oC-130^oC) toward lower temperature and produce a change in the behavior of the solid solution from normal ferroelectric to a relaxor ferroelectric in the strontium rich region (Figure 5.18).

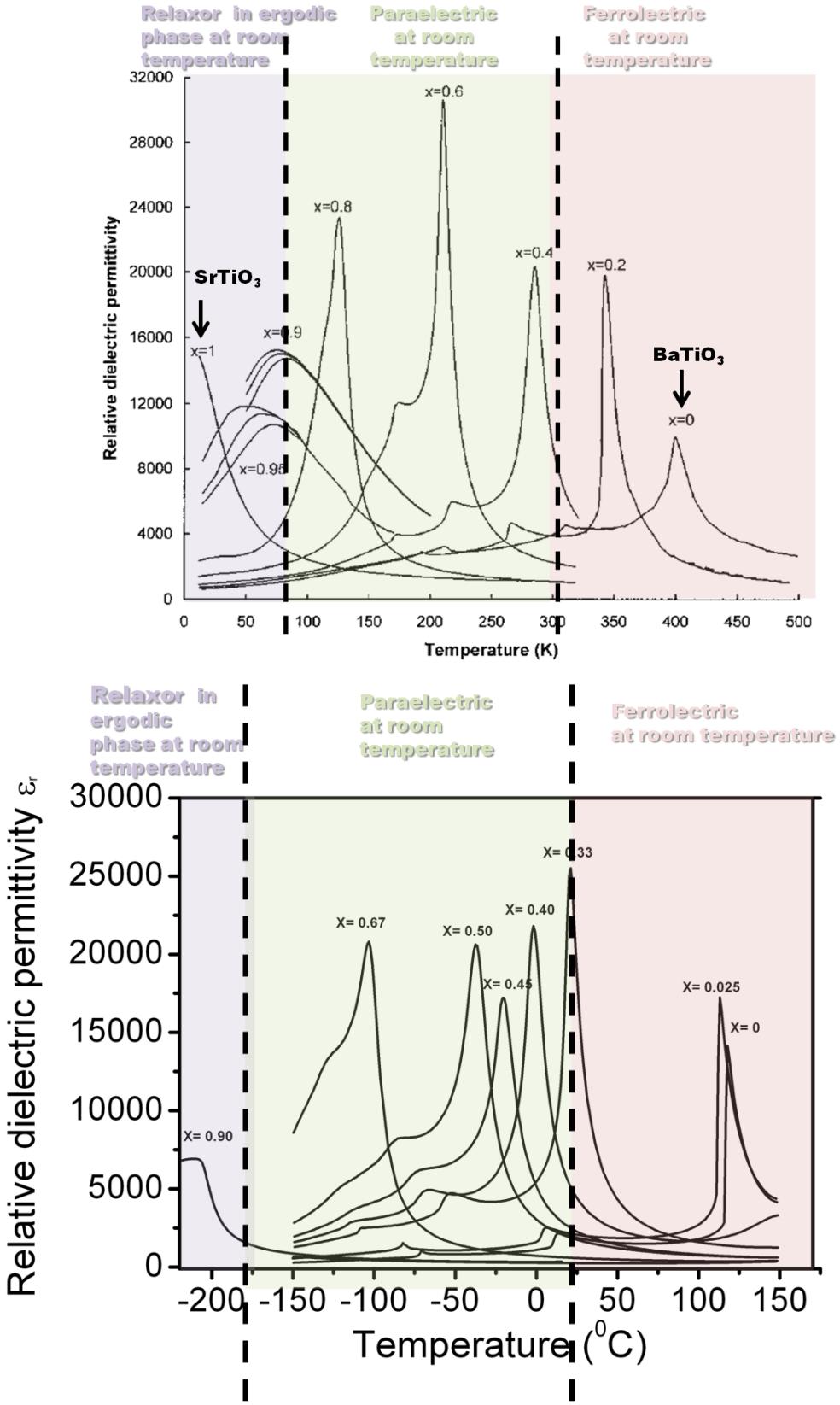

Figure 5.18-Evolution of the relative permittivity in (Ba,Sr)TiO_3 solid solution over the whole range of the solid solution as reported in [27] (top) and in the ceramics processed in this work (bottom) The x refers to the strontium content.

For our study, this system presents two main advantages. The first one is that, as a consequence of the lowering of the Curie temperature, different compositions of $(Ba,Sr)TiO_3$ have very different values of the dielectric permittivity at room temperature. The second advantage is that the pyroelectric response can be compared in the ferroelectric and paraelectric phases of a normal ferroelectric and in the ergodic phase of relaxors in materials with the same chemical background.

The pyroelectric response is observed in unpoled ceramics of $(Ba,Sr)TiO_3$ across the entire range of the solid solution up to a content 90 % in strontium and is not present only in the composition containing 2.5 % of barium (BST025975) and, as already discussed, in pure $SrTiO_3$.

As can be seen in Figure 5.19, the amplitude of the pyroelectric current is larger in barium rich compositions than strontium rich compositions; however it remains comparable within an order of magnitude in all ceramics.

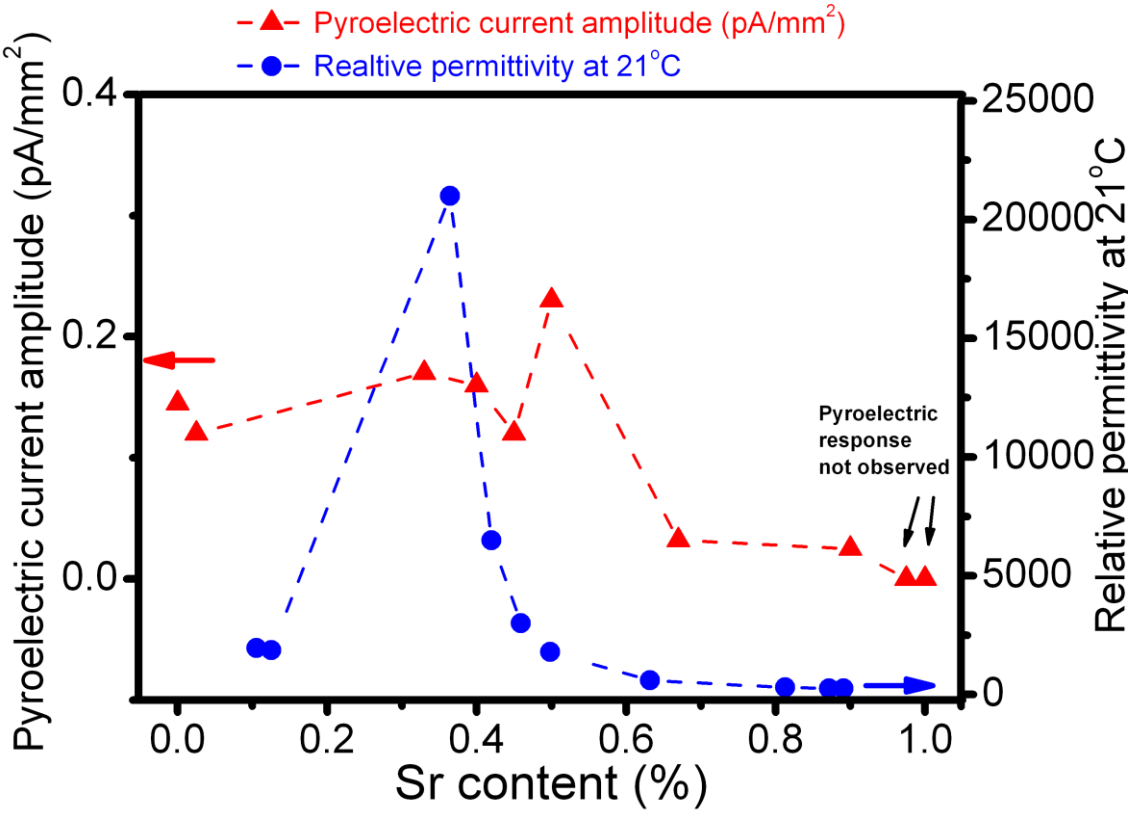

Figure 5.19-Comparison of the pyroelectric current amplitude and the relative permittivity at room temperature in the $(Ba,Sr)TiO_3$ solid solution. The values of the pyroelectric current, reported for each composition are an average on several samples.

In agreement with the results of the annealing experiment in unpoled $BaTiO_3$ discussed previously (see Figure 5.12 and related text), the comparison between the amplitude of the pyroelectric current and the relative permittivity at 21°C, chosen as reference temperature, indicates that there is no direct proportionality, between the

magnitude of the permittivity, and the amplitude of the pyroelectric current supporting the argument that the absence of pyroelectric response in pure $SrTiO_3$ (and BST025975) cannot be explained by the low values of the relative permittivity. For example, the maximum in current does not coincide with the maximum in permittivity, and permittivity changes much more than current for different compositions.

This is even more evident if one consider that BST1090, which still exhibits a pyroelectric response, at room temperature, has practically the same permittivity (ε_r about 300) as BST025975 and pure $SrTiO_3$ (ε_r about 260 in both), compositions which do not show any pyroelectric current.

In agreement to what is observed for the electromechanical response (Chapter 4), the study of $(Ba,Sr)TiO_3$ solution also reveals that the pyroelectric responses in the paraelectric and in the ferroelectric phases have the same magnitude reinforcing the evidence of a common origin of the symmetry breaking in polycrystalline samples for both phases; that is, the macroscopic symmetry breaking in random oriented unpoled ferroelectric samples is not a simple consequence of some domains not being perfectly compensated by domains of opposite polarization. If this happens, this asymmetry in domain orientation has a driving force in alignment of polar entities developed already in the paraelectric phase.

The fact that in strontium rich compositions, the pyroelectric current amplitude remains within the same order of magnitude as in barium rich compositions points against the V_{Ba}^{2-} vacancies as origin of the charge separation in the ceramics, since one would expect, if barium vacancies are the cause of the pyroelectric current, that the amplitude would decrease more substantially with the decreasing of the barium concentration. This is also in agreement with the predicted lower formation energy for V_{Sr}+V_O with respect to the V_{Ba}+V_O defect d already mentioned above [16].

To follow up this idea, we explored the possibility to cause a drastic increase in the concentration of the defects in $SrTiO_3$, to possibly induce an observable pyroelectric response at room temperature. For this purpose, some $SrTiO_3$ ceramics were sintered with a block of graphite placed on the top of samples at 1500^oC for 4 hours (Figure 5.20 top left); this is a similar approach to the one used in the preparation of the lead zirconate titanate–based Rainbow ceramics, exploited in actuation applications [28]. In such kind of material, the reaction between the graphite (the reducing agent) and ceramic oxide induces the reduction of a layer in the ceramics at the interface with the graphite. The reaction is associated with the formation and diffusion of oxygen vacancies [29].

The black coloration (Figure 5.20 top right) of the side of the pellet in contact with graphite after sintering, is an indication that the reduction has effectively taken place [30]

However, the $SrTiO_3$ ceramics sintered in such reducing conditions do not exhibit any pyroelectric response (Figure 5.20 bottom).

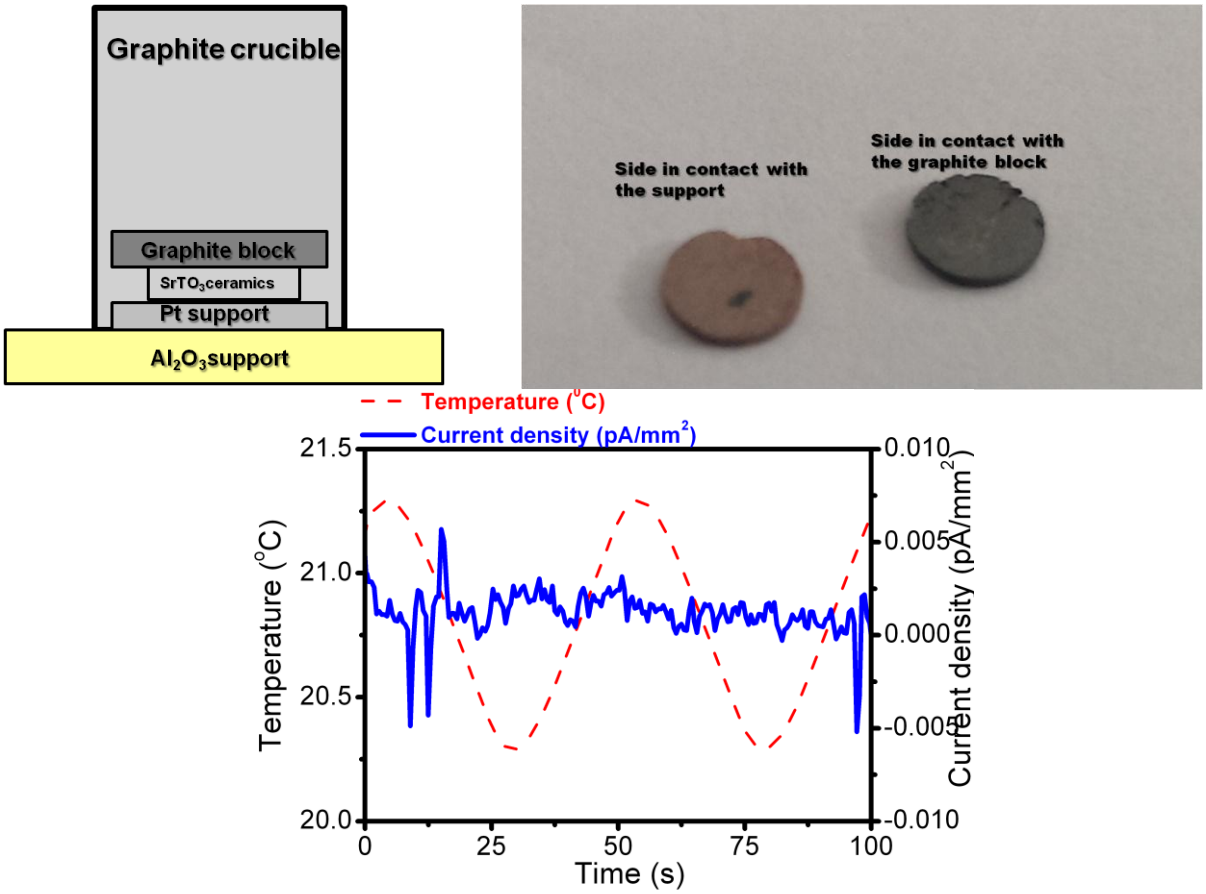

Figure 5.20-Scheme of the geometry adopted for the reduction experiment of $SrTiO_3$ ceramics (top left). The reduction is indicated by the black color of the side which was in contact with the graphite with respect to the side in contact with the support or exposed to air(photo top right). After reduction with graphite, no pyroelectric response is observed in the $SrTiO_3$ ceramics (bottom).

The absence of pyroelectric current can indicate that the concentration of vacancies formed during sintering, is still not sufficient to produce a detectable pyroelectric current in $SrTiO_3$.

The result of this experiment is however useful as it shows that, the creation of defects does not produce necessarily polar response in ceramics, and points in favor of the hypothesis that the polar defects causing the charge separation in $(Ba,Sr)TiO_3$ ceramics could be more related to polar entities associated to its ferroelectric nature.

5.9 Depolarization mechanism in the ceramics

Independently from which polar defects in $(Ba,Sr)TiO_3$ ceramics are responsible for symmetry breaking (intrinsic ionic vacancies or polar entities (precursors, polar nano-regions...)), those defects must be able to respond to temperature variation applied during pyroelectric measurements which is as small as 0.5K. Those defects thus cannot be

completely frozen at room temperature. Experiments suggest that their orientation is strongly imprinted during the densification process of the ceramics, and that they do not relax and de-orient even after annealing at high temperatures. It should also be considered that the defects may randomize at some critical temperature and then realign when the samples are cooled again below such critical temperature. It is possible that, upon heating between room temperature and sintering temperature, a fraction of polar defects acquire enough energy to partially relax and become randomly oriented. The increase of the thermal energy can reorient the defect dipoles originated from vacancies [31]. In the case of polar nano-regions in relaxors, for example, it is possible that their dipole moment varies the orientation due to thermal motion [32]. In this direction, we focused our studies to identify the temperature, or rather, the range of temperatures at which the partial depolarization may occur. Another possibility is that these polar entities trap space charges in the material reinforcing the polarization built-in during the sintering. Our frequency dependent measurements (section 4.4) suggest that such space charges indeed participate in the electromechanical response of the samples. During the high temperature annealing a fraction of these trapped charges could be released affecting macroscopic polarization and current.

A first evidence of a partial depolarization process is revealed when the ceramics were progressively annealed at different temperatures up to the sintering temperature (1450^{o}C).

The amplitude of the pyroelectric current measured at room temperature after annealing (Figure 5.21), shows a sharp decrease for annealing temperatures between 200^{o}C-500^{o}C, annealing above 500°C temperature no longer affects the amplitude of the pyroelectric current which remains practically constant.

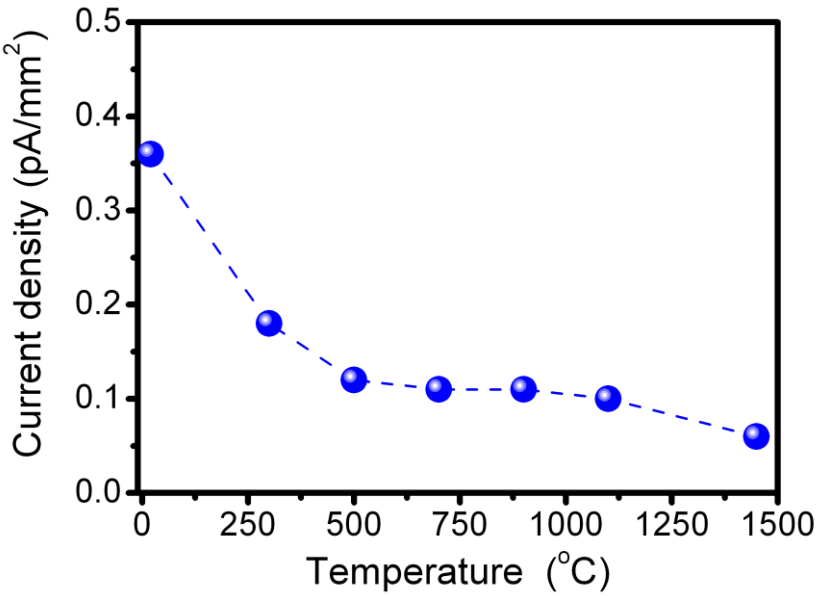

Figure 5.21-Variation of the amplitude of the pyroelectric current at ambient temperature after annealing at different temperatures in air for 1 hour in BST6040 ceramics. The reduction in the amplitude of the pyroelectric current shows a clear saturation after annealing at 500^{o}C. The samples were heated and cooled under open circuit conditions.

This trend in the variation of the pyroelectric response after annealing seems to suggest a partial relaxation of the polar defects located in the temperature range between 200^{o}C-500^{o}C. The saturation of the response above a certain temperature (roughly 500°C) is consistent with the expectation that the relaxation is not complete; only part of the total charge is relaxed. However, the conclusion that the reduction in the pyroelectric current amplitude is due to a relaxation of the polar defects or to a de-alignment of polar entities is not straightforward since the study of the depolarization mechanism is affected by the aging of the pyroelectric response in the ceramics. It is observed that over the time, the amplitude of the pyroelectric current, which is reduced immediately after the annealing, raises back to the initial value or larger (Figure 5.22).

The increase of the pyroelectric current can be explained by the fact that over time, free space charges become aligned in the direction of the built-in polarization and add their contribution to the measured pyroelectric response.

A second possibility, if the polar defects are represented by polar entities, is that this kind of defects disappear when the samples are heated above a certain temperature and then reappear when the samples are cooled again below such temperature and realign progressively under the inhomogeneous field imprinted during the sintering (most likely strain).

It was considered whether these charges might come from the absorption of molecules of water from the air. However this origin of charges probably cannot be

dominant since the aging process is observed in samples kept, in a dry atmosphere, inside a glass dessicator for a month.

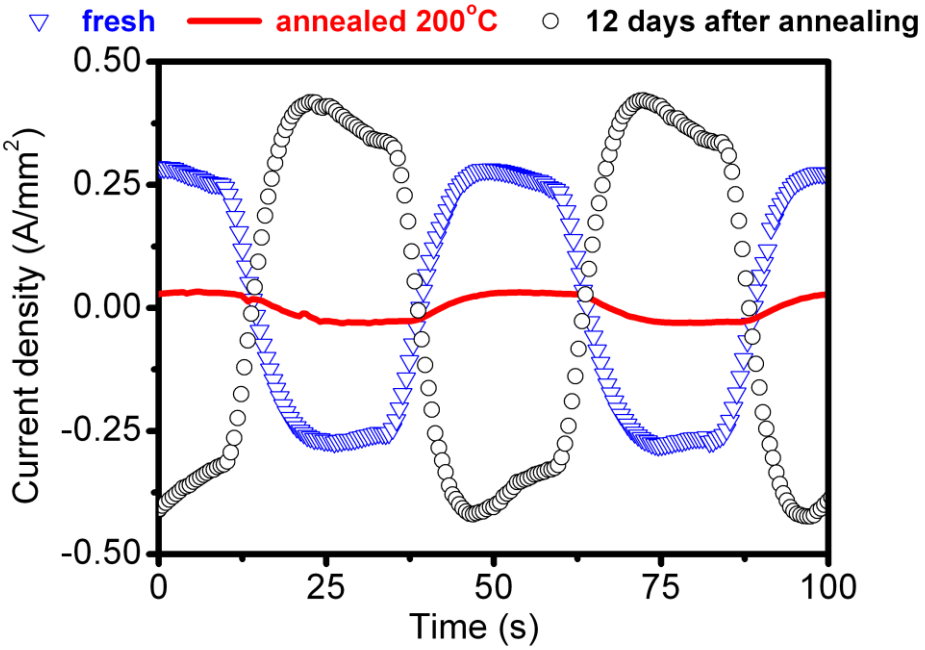

Figure 5.22-Aging effect of the amplitude of the pyroelectric current in the paraelectric phase of BST6040 ceramics. The annealing in air at 200°C, for 2 hours, leads to a reduction (about 8 times in this case) in the amplitude of the pyroelectric current. However after several days, the pyroelectric response increases again reaching an amplitude even larger than the initial one.

The aging effect is thus most probably due to the alignment of free charges that are present in the bulk of the ceramics. The existence of such mobile charges is demonstrated by the possibility to “pole” (polarize) the BST6040 ceramics to form an electret [1].

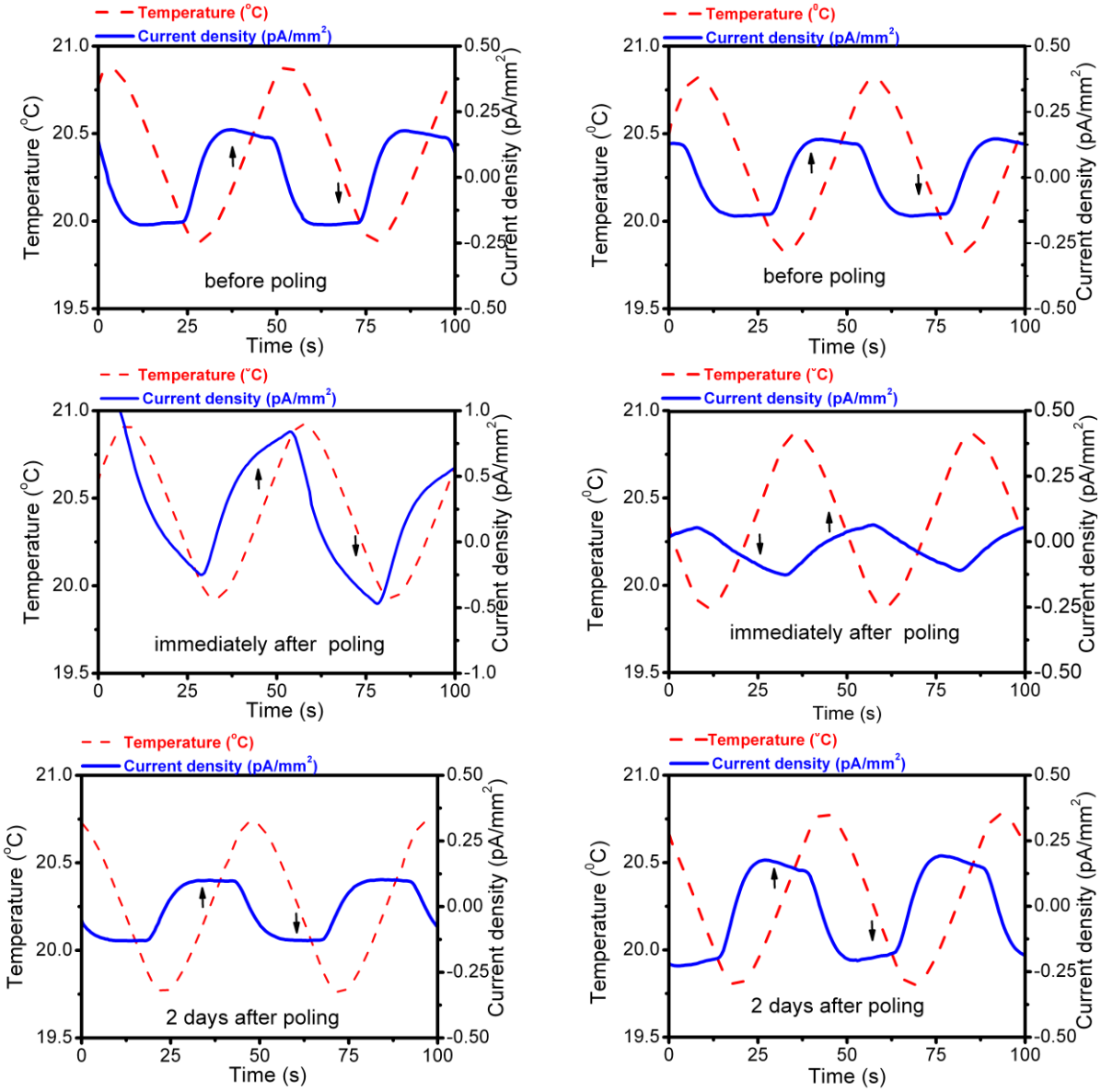

Figure 5.23-Formation of electret in BST6040. The pyroelectric response (solid line) and the driving temperature (dashed line) at ambient temperature for: a sample poled in the direction of built in polarization (left) and a sample poled opposite to the direction of the built-in polarization (right) before poling (top) immediately after poling (middle) and two days after poling and decay of the space charges ((bottom). Note that the poling against the built-in polarization (right, middle) leads to a phase change of the pyroelectric signal. The ceramics were poled with a field of 2500 V/mm for 10 minutes at 23°C.

The results of such an experiment are shown in Figure 5.23. When an external field is applied to the BST6040 ceramics, the free charges move or the polar entities reorient, temporarily, stabilizing in new positions and enhancing or reducing the amplitude of the pyroelectric current, according to the direction of the application of the electric field with respect to the polarization direction set in during the sintering process.

In particular, when the field is applied in the direction opposite to that of the built-in polarization (Figure 5.23 right, middle) the phase of the pyroelectric current

immediately after poling, is shifted by 180° with respect to its phase before poling, indicating that the polarization induced by the field dominates over the built-in polarization.

After the decay of the free spaces charges over time, the built-in polarization dominates again and the phase of the pyroelectric current reverts to the initial direction (Figure 5.23 right bottom).

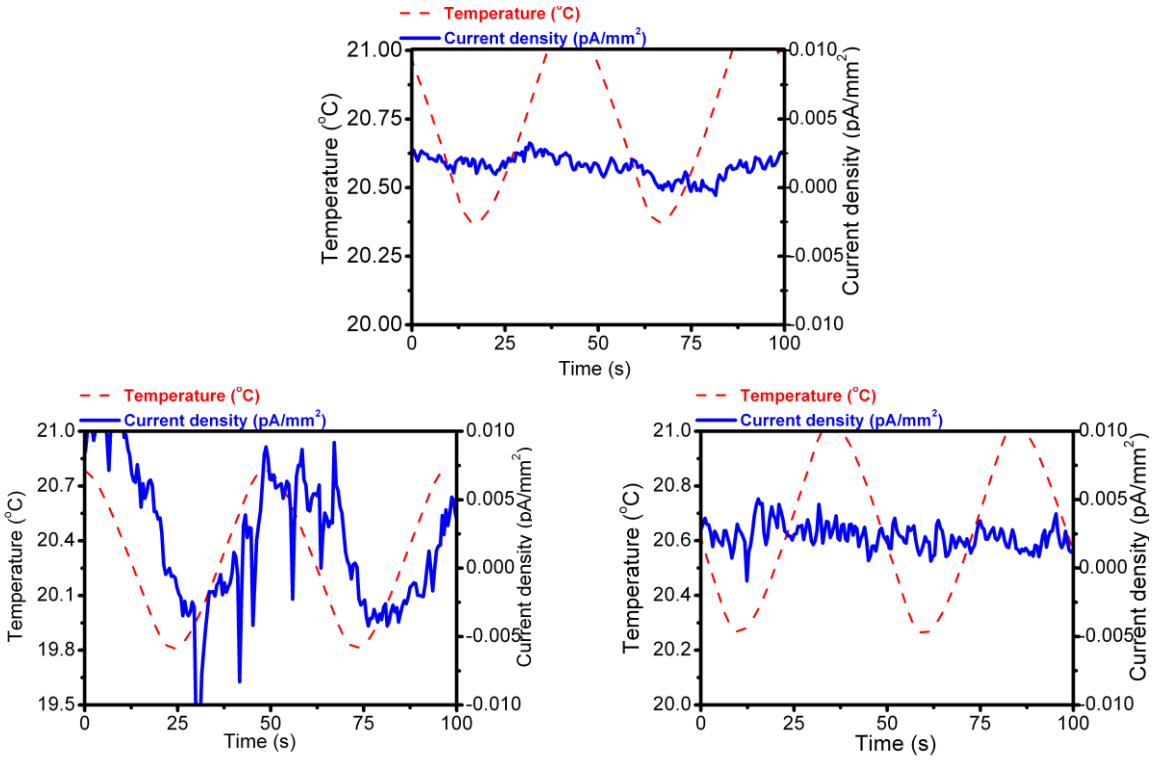

Figure 5.24-Formation of electret in $SrTiO_3$ ceramics. Before poling (top) no pyroelectric response is observed in the samples. The application of an external electric field (bottom left) induces a small pyroelectric current in the samples, indicating the presence of inhomogeneous space charges aligned under the action of the electric field. After 72 hours from the application of the field the space charge decay and the pyroelectric response disappears (bottom). The samples were poled for 10 minutes at 2500V/mm at 23°C.

The presence of free space charges is shown in $SrTiO_3$ ceramics as well. Immediately after the application of the field, a very week pyroelectric response (about 20 times smaller than in BST6040 ceramics) is observed. The decay of the free space charges over time leads to the disappearance of the pyroelectric current within few days after poling (Figure 5.24) in samples kept at ambient temperature. The pyroelectric response can also be totally erased immediately after the application of the field if the ceramics are heated up to 50°C.

This demonstrate that, despite the fact that a pyroelectric current is not observed in $SrTiO_3$, a certain number of mobile space charges (associated with defects) are present and can be stable enough to produce a temporary polarization in the ceramics.

The aging effect, poling experiments and frequency dependent permittivity and piezoelectric response show that the pyroelectric response in (Ba,Sr)TiO_3 ceramics consists more likely of two components, one associated to the built-in polarization, which is more persistent and a second one, more volatile, associated to the mobile, free space charges.

In the experiments discussed so far, the investigations of the depolarization behavior in the BST ceramics has been studied analyzing the pyroelectric response at room temperature and after high temperature annealing. This type of measurements provides an indirect probing of the charge release and mobility in BST ceramics. In order to study the depolarization of the ceramics deep in the paraelectric phase and at higher thermal energies (related to higher temperature), we turn to the Thermally Stimulated Current (TSC) technique. The results of the TSC measurements will be discussed in the next chapter.

5.10 Summary

In this chapter, the pyroelectric technique is used to investigated the origin of the symmetry breaking which gives non–zero piezoelectric and pyroelectric responses in the paraelectric phase of unpoled (Ba,Sr)TiO_3 ceramics. The measurements demonstrate that the polarity is not related to the granular nature of the ceramics since it can be, in general, observed also in the paraelectric phase of unpoled single crystals. In addition, pure $SrTiO_3$ ceramics do not give detectable pyroelectric current at room temperature, also suggesting that the granular nature of ceramics is not the origin of the symmetry breaking. Comparison between measurements made on samples with as–sintered and polished surfaces also shows that the main contribution to the pyroelectric current comes from the bulk of the ceramics and that symmetry breaking is not caused by the surface effects.

The polarity is not only limited to the BST6040 composition (taken as reference for this study) but is observed in several compositions covering the whole range of the $Ba_{1-x}Sr_xTiO_3$ solid solution (x=0, 0.025, 0.33, 0.45, 0.50, 0.67, 0.90); it is not detected by pyroelectric measurements only in BST025975 (containing 2.5% of barium) and in pure $SrTiO_3$.

It is proposed that the symmetry breaking in the ceramics is based on two different mechanisms: the presence of a macroscopic preferred orientation in the samples and the existence of microscopic polar defects which provide charge separation.

It is demonstrated that the macroscopic preferential orientation in the ceramics (macroscopic symmetry breaking) is introduced during sintering and it is produced by some inhomogeneities (compositional gradient, strain gradient, density gradient,...) which form or settle–in during the densification process itself, when the mass transport in the ceramics is maximal.

Two kinds of polar defects can be proposed as possible origin of the charge separation in (Ba,Sr)TiO_3 ceramics: intrinsic ionic vacancies created during samples preparation or intrinsic polar entities (polar cluster, polar nano-regions....) related to the specific chemical (or ferroelectric) nature of $BaTiO_3$ and (Ba,Sr)TiO_3 solid solution. The effect of extrinsic defects is probably small or can be entirely eliminated because the Curie point is at the expected temperatures. Any contamination during sintering and the amount of impurities present in the starting powders must be very low (see Chapter 2).

An incomplete relaxation (de-alignment) of the polar defects/entities at high temperatures, is indicated by the partial depoling of the ceramics when samples are annealed in the temperature range between 250^{o}C 500^{o}C. The observed reduction of the current amplitude is most likely associated to the release of free space charges which align, over time, along the direction of the built-in polarization of the ceramics. The built-in polarization appears to be unaffected by the annealing even at temperatures higher than the sintering temperature. In the case that the polar defects are polar entities akin polar nanoregions, it is possible that they disappear at some critical temperature and then, when the samples are cooled again below the critical temperature, they reappear and align along the preferential direction introduced in the ceramics during sintering. The presence of free charges in both (Ba,Sr)TiO_3 ceramics and $SrTiO_3$ is indicated by the possibility to temporarily pole the samples to form an electret.

5.11 Bibliography

[1] M. E. Lines and A. M. Glass, *Principles and applications of ferroelectrics and related materials*: Clarendon Press, 1977.

[2] J. F. Daniels, K. H. Härdtl, and R. Wernicke, "The PTC effect of barium titanate " *Philips Technical Review,* vol. 38, pp. 73-82, 1978.

[3] J. Petzelt, T. Ostapchuk, I. Gregora, I. Rychetsky, S. Hoffmann-Eifert, A. V. Pronin*, et al.*, "Dielectric, infrared, and Raman response of undoped $SrTiO_3$ ceramics: Evidence of polar grain boundaries," *Physical Review B,* vol. 64, Nov 2001.

[4] V. Ravikumar, D. Wolf, and V. P. Dravid, "Ferroelectric monolayer reconstruction of the $SrTiO_3$ (100) surface," *Physical Review Letters,* vol. 74, pp. 960-963, Feb 1995.

[5] N. Bickel, G. Schmidt, K. Heinz, and K. Müller, "Ferroelectric realxation of the $SrTiO_3$ (100) surface," *Physical Review Letters,* vol. 62, pp. 2009-2011, Apr 1989.

[6] R. Herger, P. R. Willmott, O. Bunk, C. M. Schlepuetz, B. D. Patterson, and B. Delley, "Surface of strontium titanate," *Physical Review Letters,* vol. 98, Feb 2007.

[7] A. N. Morozovska, E. A. Eliseev, S. V. Kalinin, L. Q. Chen, and V. Gopalan, "Surface polar states and pyroelectricity in ferroelastics induced by flexo-roto field," *Applied Physics Letters,* vol. 100, Apr 2012.

[8] R. Herger, P. R. Willmott, O. Bunk, C. M. Schleputz, B. D. Patterson, B. Delley, *et al.*, "Surface structure of $SrTiO_3$ (001)," *Physical Review B,* vol. 76, Nov 2007.

[9] X. Chen, Y. Zou, G. Yuan, M. Zeng, J. M. Liu, J. Yin, *et al.*, "Temperature Gradient Introduced Ferroelectric Self-Poling in $BiFeO_3$ Ceramics," *Journal of the American Ceramic Society,* vol. 96, pp. 3788-3792, Dec 2013.

[10] F. V. Lenel, H. H. Hausner, G. S. Ansell, and O. V. Roman, "Influence of gravity in sintering," *Transactions of the Metallurgical Society of Aime,* vol. 227, pp. 640-&, 1963.

[11] J. X. Liu, Y. Liu, A. Lal, and R. M. German, "Shape distortion induced by gravity in the initial stage of solid phase sintering," *Scripta Materialia,* vol. 40, pp. 1221-1227, May 1999.

[12] E. A. Olevsky and R. M. German, "Effect of gravity on dimensional change during sintering I. Shrinkage anisotropy," *Acta Materialia,* vol. 48, pp. 1153-1166, Mar 2000.

[13] W. R. Buessem, L. E. Cross, and A. K. Goswami, "Phenomenological Theory of High Permittivity in Fine-Grained Barium Titanate," *Journal of the American Ceramic Society,* vol. 75, pp. 2923-2926, 1992.

[14] M. Demartin, "Influence de l'élaboration et de la microstructure sur le déplacement des parois de domaine et les propriétés électro-mécaniques de céramiques de Pb(Zr, Ti)O_3 et $BaTiO_3$",*Thesis*, EPFL, 1997.

[15] P. Erhart and K. Albe, "Thermodynamics of mono- and di-vacancies in barium titanate," *Journal of Applied Physics,* vol. 102, Oct 2007.

[16] H. Lee, T. Mizoguchi, T. Yamamoto, S. L. Kang, and Y. Ikuhara, "First-principles calculation of defect energetic in $BaTiO_3$ and $SrTiO_3$: a possible relationship to grain growth behaviour," *AMTC Letters,* vol. 1, 2008.

[17] U. Aschauer, R. Pfenninger, S. M. Selbach, T. Grande, and N. A. Spaldin, "Strain-controlled oxygen vacancy formation and ordering in $CaMnO_3$," *Physical Review B,* vol. 88, Aug 2013.

[18] A. Bussmann-Holder, H. Beige, and G. Volkel, "Precursor effects, broken local symmetry, and coexistence of order-disorder and displacive dynamics in perovskite ferroelectrics," *Physical Review B,* vol. 79, May 2009.

[19] O. Aktas, E. K. H. Salje, S. Crossley, G. I. Lampronti, R. W. Whatmore, N. D. Mathur, *et al.*, "Ferroelectric precursor behavior in $PbSc_{0.5}Ta_{0.5}O_3$ detected by field-induced resonant piezoelectric spectroscopy," *Physical Review B,* vol. 88, Nov 2013.

[20] W. Kleemann, F. J. Schäfer, and M. D. Fontana, "Crystal optical studies of spontaneous and precursor polarization in $KNBO_3$," *Physical Review B,* vol. 30, pp. 1148-1154, 1984.

[21] G. Burns and F. H. Dacol, "Crystalline ferrolectrics with glassy polarization behavior," *Physical Review B,* vol. 28, pp. 2527-2530, 1983.

[22] A. I. Frenkel, D. Ehre, V. Lyahovitskaya, L. Kanner, E. Wachtel, and I. Lubomirsky, "Origin of polarity in amorphous $SrTiO_3$," *Physical Review Letters,* vol. 99, Nov 2007.

[23] A. S. Nowick and W. R. Heller, "Dielectric and anaelastic relaxation of crystal containing point defects," *Advances in Physics,* vol. 14, pp. 101-&, 1965.
[24] S. Prosandeev, D. W. Wang, and L. Bellaiche, "Properties of Epitaxial Films Made of Relaxor Ferroelectrics," *Physical Review Letters,* vol. 111, Dec 2013.
[25] K. A. Müller and W. Berlinger, "Microscopic probing of order-disorder versus displacive behaviour in $BaTiO_3$ BY Fe^{3+} electron-paramagnetic RES," *Physical Review B,* vol. 34, pp. 6130-6136, Nov 1986.
[26] I. Levin, V. Krayzman, and J. C. Woicik, "Local structure in perovskite (Ba,Sr)TiO_3: Reverse Monte Carlo refinements from multiple measurement techniques," *Physical Review B,* vol. 89, pp. 4106-4106, Jan 2014.
[27] L. Q. Zhou, P. M. Vilarinho, and J. L. Baptista, "Dependence of the structural and dielectric properties of $Ba_{1-x}Sr_xTiO_3$ ceramic solid solutions on raw material processing," *Journal of the European Ceramic Society,* vol. 19, pp. 2015-2020, 1999.
[28] G. H. Haertling, "Rainbow Ceramics - a new-type of ultra-high-displacement actuator," *American Ceramic Society Bulletin,* vol. 73, pp. 93-96, Jan 1994.
[29] Q. M. Wang and L. E. Cross, "Analysis of high temperature reduction processing of RAINBOW actuator," *Materials Chemistry and Physics,* vol. 58, pp. 20-25, Feb 1999.
[30] A. Polotai, K. Breece, E. Dickey, C. Randall, and A. Ragulya, "A novel approach to sintering nanocrystalline barium titanate ceramics," *Journal of the American Ceramic Society,* vol. 88, pp. 3008-3012, Nov 2005.
[31] P. Erhart, P. Traskelin, and K. Albe, "Formation and switching of defect dipoles in acceptor-doped lead titanate: A kinetic model based on first-principles calculations," *Physical Review B,* vol. 88, Jul 2013.
[32] A. A. Bokov, B. J. Rodriguez, X. H. Zhao, J. H. Ko, S. Jesse, X. F. Long, *et al.*, "Compositional disorder, polar nanoregions and dipole dynamics in $Pb(Mg_{1/3}Nb_{2/3})O_3$-based relaxor ferroelectrics," *Zeitschrift Fur Kristallographie,* vol. 226, pp. 99-107, 2011.

Chapter 6 :Thermally stimulated currents in unpoled ceramics and single crystals

6.1 Introduction

The decrease of the amplitude of the pyroelectric current measured at room temperature after annealing of (Ba,Sr)TiO_3 ceramics above 500^{o}C, (Chapter 5) indicates a partial depolarization of the samples. In this chapter, the paraelectric phase of the (Ba,Sr)TiO_3 ceramics is investigated with the thermally stimulated current (TSC) technique in the same temperature region where the partial depolarization occurs in order to better understand the depolarization process. The TSC of (Ba,Sr)TiO_3 ceramics are compared with those of ceramics and single crystals of $SrTiO_3$ which do not exhibit any pyroelectric response at room temperature. The comparison reveals that the TSC technique is a complementary tool with respect to the pyroelectric measurement to identify the presence of polarity in single crystals and ceramics. This technique also helps us to establish presence of two types of polarization in samples, one which is built in the sample, and the other which is unstable, associated with mobile charges and dependent on high temperature treatment.

6.2 Thermally stimulated peaks in the paraelectric phase of (Ba,Sr)TiO_3 ceramics

The background of the thermally stimulated current technique is discussed in Chapter 3. It is however worth mentioning here that our use of the TSC technique differs substantially from the traditional approach which usually requires that the materials are exposed to an external excitation such as an electric field (poling to form an electret) before the measurements. This is standard approach in the study of the dipole relaxation in polymers [1], and defects dipoles in ionic solids [2]. Excitation may also be electromagnetic radiation (e.g., visible light) in the case of the characterization of the trap levels in semiconductors [3]. In our case none of the characterized samples were exposed to an even smallest electric field. The theory of TSC in materials which were not previously exposed to any excitation has not been developed, despite the observation of thermally stimulated peaks in non polarized materials, such as Teflon reported in the same work where the theoretical basis of the technique was established [2].

The setup used for the measurement is described in Chapter 3. The thermally stimulated currents were first measured upon heating and cooling under open circuit conditions (without sample) in the temperature range of interest (26°C-540°C) to test the presence of possible artifacts in the measuring system and to estimate the magnitude of the background current in the setup.

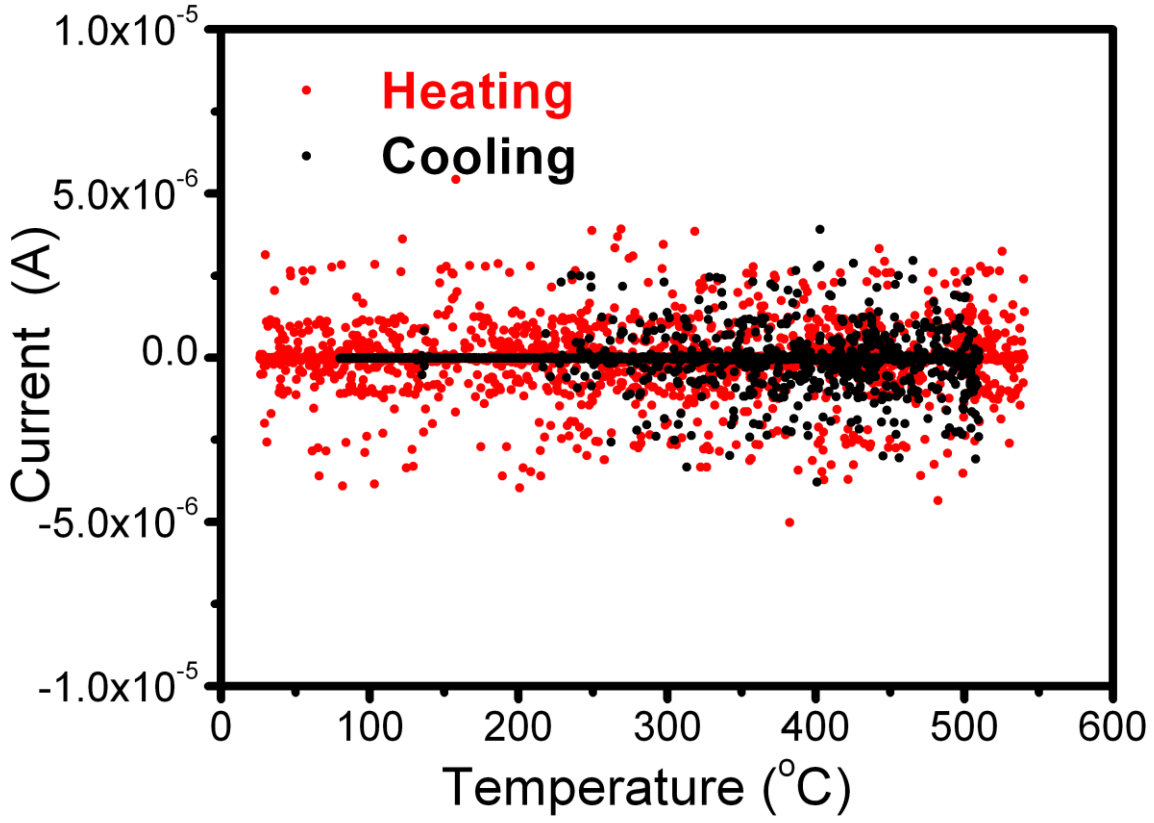

Figure 6.3-Thermally stimulated current measured upon heating and cooling in our setup under open circuit conditions. The temperature range of the measurement is 26°C to 540°C, the heating rate was 2.5°C/minute and the cooling rate was 2.0°C/minute.

As it is shown in Figure 6.3, no anomalies are present, between room temperature and 540°C under open circuit conditions and the current has a flat profile with only small noise superimposed on the current signal. The noise is mostly caused by the electrical interference from the furnace heating system. It is absent during cooling, below about 200°C, when the power regulator is always in the off-position.

In general, origins of TSC include the field-induced polarization, built-in or spontaneous polarization, small voltage bias on the picoammeter, and the thermoelectric effect. Only the first two mechanisms are sensitive to the orientation of the sample [4]. For example, the release of electrons trapped at the interface between the ceramics and the two electrodes would produce peaks whose sign does not change with the samples orientation, if the two electrodes are identical. The sign of the current coming from the

small voltage burden on picoammeter (in our case about 200μV) would not be sensitive to orientation of the samples. The current originating from the thermoelectric effect due to temperature gradient in the sample would also not be sensitive to the sample orientation.

Before measuring the TSC of the $Ba_{1-x}Sr_xTiO_3$, the effective correlation between the sign of the thermally stimulated peak and the direction of the polarization present in the ceramics was tested in poled ferroelectric ceramics of the $0.5(Ba_{0.7}Ca_{0.3})TiO_3$-$0.5Ba(Zr_{0.2}Ti_{0.8})O_3$ (BCZT50) composition. In BCZT50, the two structural phase transitions present between 26°C and 100°C result in two sharp peaks in the thermally stimulated current. When the orientation of the poled ceramics is inverted with respect to the top electrode contact, the thermally stimulated peaks corresponding to the phase transitions have opposite sign (Figure 6.4).

The experiment on poled BCZT50 ceramics indicates clearly that the sign of the thermally stimulated peaks which originate from the polarization is dependent on the orientation of the polar axis of the samples.

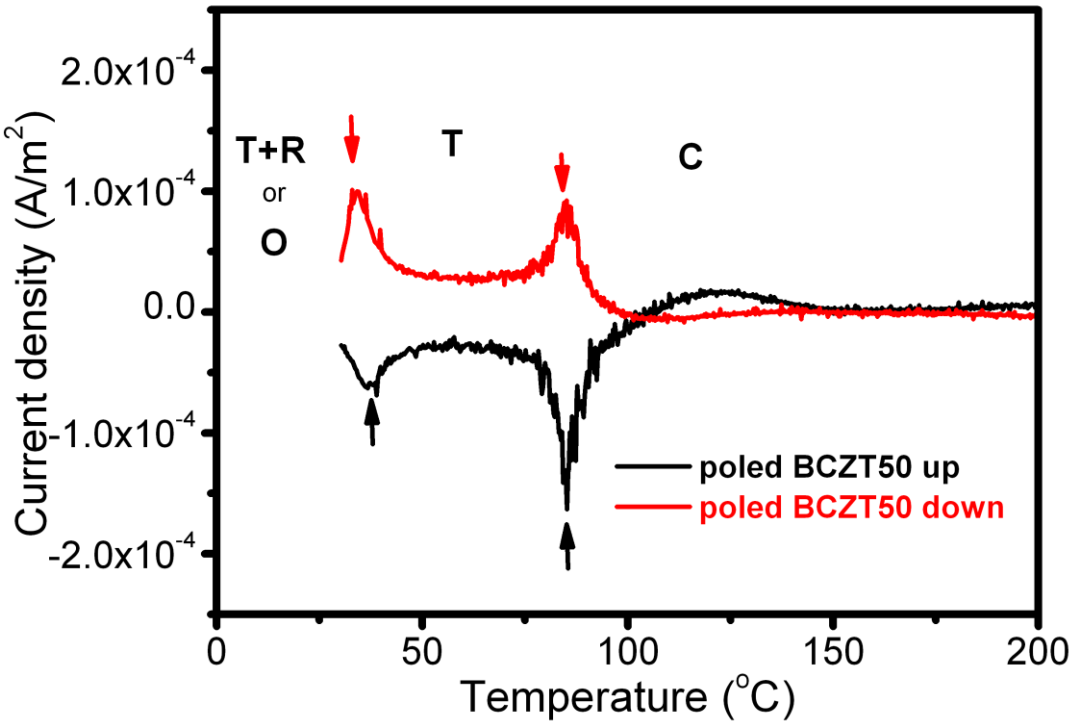

Figure 6.4-Profile of the thermally stimulated current in poled BCZT50 ceramics. The first peak (around 35°C) is related to the polarization change at the structural phase transition from the tetragonal (T) to a mixed tetragonal and rhombohedral (T+R) phase [5] or from the tetragonal to an orthorhombic phase (O) [6]. The second peak at around 84°C corresponds to the vanishing of the polarization at the transition from the ferroelectric tetragonal to the cubic (C) paraelectric phase [7]. The sign of the current inverts when the orientation of the samples is reversed in the setup. The ceramics were poled with a field of 3000 V/mm applied for 10 minutes at 23°C. The up and down direction are assigned arbitrarily.

In analogy to what is observed for poled BCZT50 ceramics, the thermally stimulated peaks in (Ba,Sr)TiO_3 ceramics therefore must be sensitive to the orientation of the ceramics if there is built-in polarization present. The current should therefore invert sign when the samples are reversed.

An example of thermally stimulated currents in BST6040 ceramics are shown in Figure 6.5.

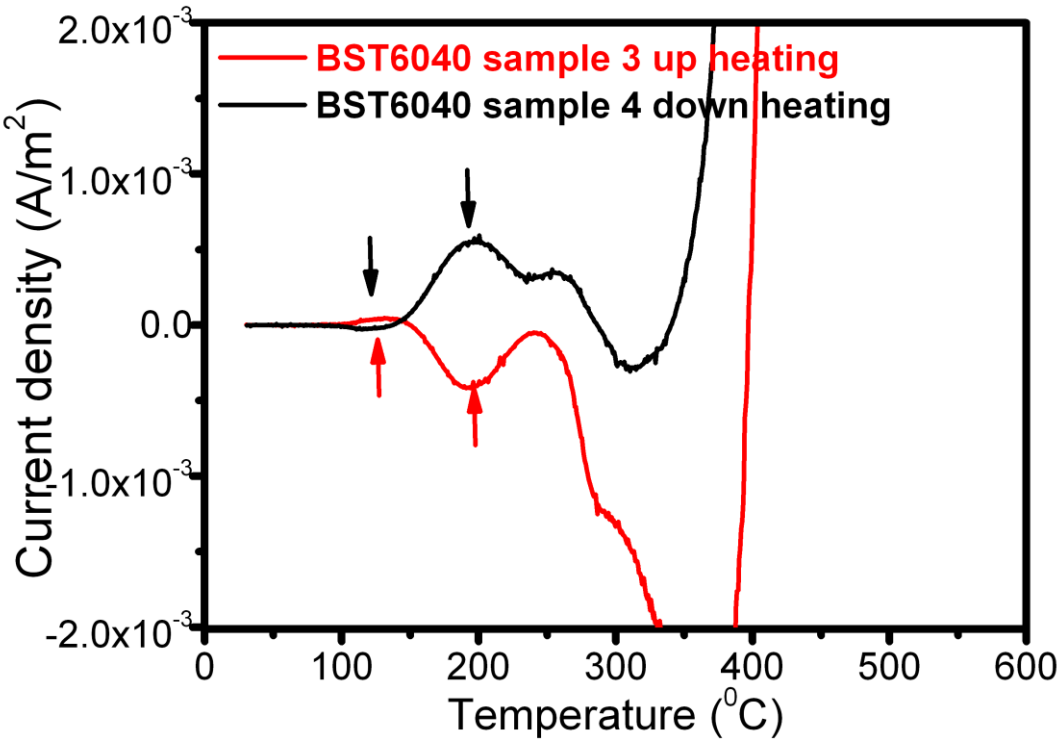

Figure 6.5-Thermally stimulated current profile in two BST6040 ceramic samples with opposite orientation measured upon heating between 26^{o}C and 550^{o}C with a rate of 2.5^{o}C/minute. The peaks whose sign is sensitive to the sample orientation are marked with the arrows The up and down labels are assigned according to the orientation of the ceramics in the furnace during sintering.

The TSC profile reveals a group of peaks in the temperature range between 100^{0}C and 300^{0}C. The sign of the peaks below 200°C is clearly sensitive to the sample orientation and it is therefore associated to the built-in polarization.

Above 400^{0}C, a large increase in the current whose sign does not depend on the sample orientation is observed. This increase could be due to thermo-electric currents (temperature gradient across sample thickness) [8] or current due to low resistance of the sample and burden voltage across picoammeter [4]. The large minima present above 300^{o}C are typical results of competing currents of different sign [9].

The peaks sensitive to the samples orientation are observed in other $Ba_{1-x}Sr_xTiO_3$ compositions and in pure $BaTiO_3$, approximately in the same temperature region (Figure 6.6).

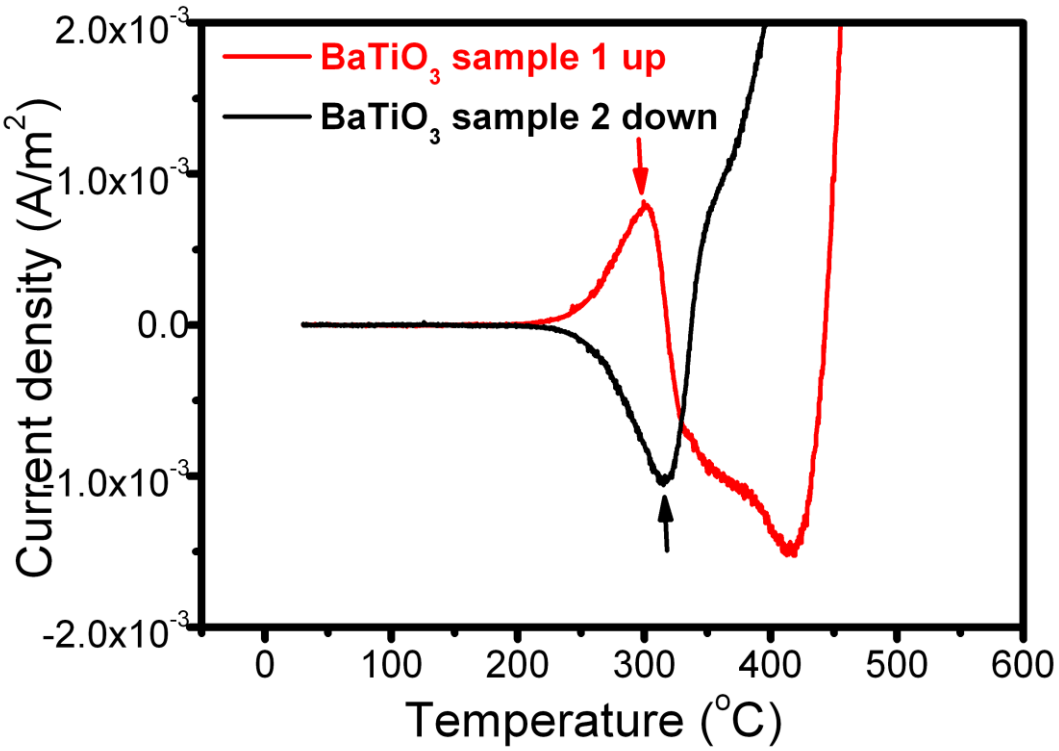

Figure 6.6-Thermally stimulated current profile in two $BaTiO_3$ unpoled ceramic samples measured upon heating between 26°C and 550°C with a rate of 2.5°C/minute. The peaks whose sign is sensitive to the sample orientation are marked with the arrows. The up and down label are assigned according to the orientation of the ceramics in the furnace, during sintering.

The peaks between 100°C and 200°C are not observed in the cooling curve (Figure 6.7). If the peaks were due to permanent built-in polarization, peaks would be seen on cooling, too, only their sign would be inverted. Therefore the peaks have a different origin. A pyroelectric response is still present at room temperature in the samples measured immediately after the TSC experiment. This means that the peaks observed in the ceramics during heating are not due to the disappearance of the built–in polarization itself (as would happen in a ferroelectric material passing through T_c) but to the detrapping of trapped space charges. However, the direction of the current originating from trapped charges is determined by the direction of the built in polarization. The fact that the sign of the current during cooling is the same for both orientations of the samples indicates that the space charge is released during heating and only a background current, which is independent from the sample orientation, is observed during cooling. The peaks proper to the built-in polarization are not seen because, as high temperature annealing experiments showed, the built-in polarization is stable as temperatures as high as 1500°C in BST6040.

The temperature range of the thermally stimulated peaks caused by the release of the space charge and the fact that they are not observed on cooling correlates well with the

partial depolarization process observed after the annealing of the ceramics under open circuit conditions mentioned in Chapter 5 (see Figure 5.21).

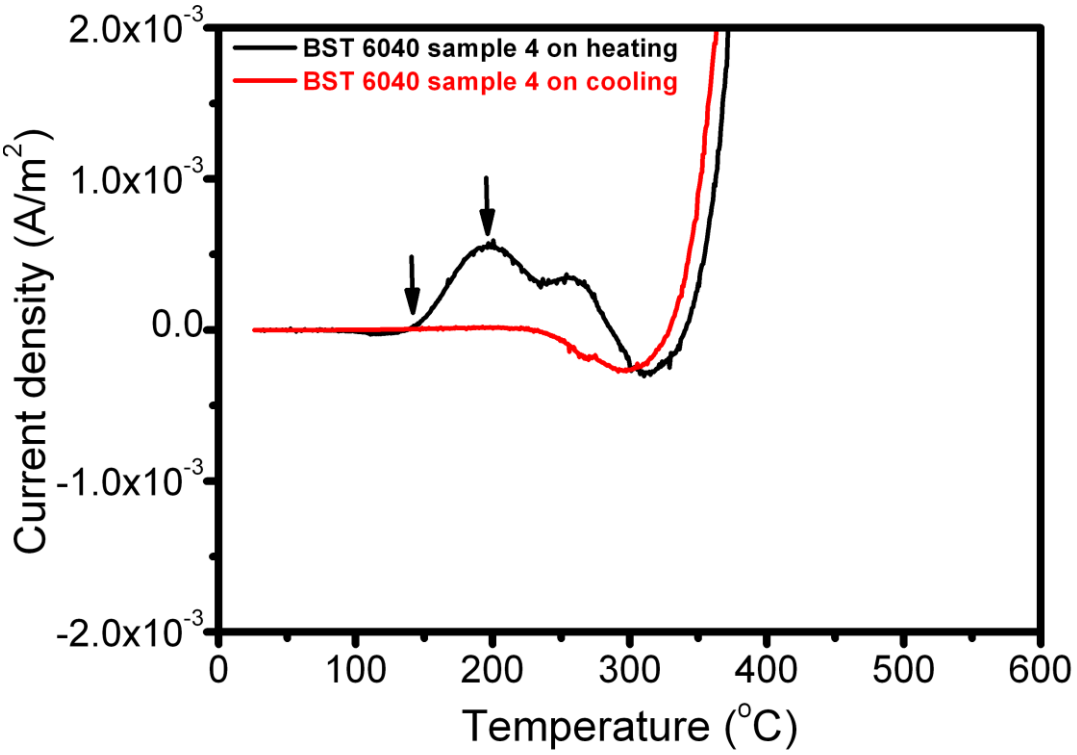

Figure 6.7- Thermally stimulated current on heating (from 30^{o}C to 550^{o}C) and on cooling (from 550^{o}Cto 26^{o}C) for BST6040 ceramics. In the cooling curve the peaks observed during heating are not present indicating that the charge associated to them has been released during the heating step. The peaks whose sign is sensitive to the sample orientation are marked with the arrows. These peaks do not belongs to the built in polarization but their direction, however is sensitivity to it.

The partial depolarization of the BST6040 ceramics is observed also in the pyroelectric measurements at room temperature taken before and immediately after the thermally stimulated current cycle, which show a clear reduction of the amplitude of the pyroelectric current (Figure 6.8).

Furthermore, following a significant reduction after the first heating cycle, the amplitude of the pyroelectric current remains substantially unaffected by the following thermally stimulated current measurements. The annealing experiments under open circuit condition, described in Chapter 5, and the thermally stimulated current measurements support the conclusion that the pyroelectric response has two different components: one coming from charges which become mobile at relatively low temperatures (below 300^{o}C) and are completely released during heating, and the second which is caused by charged defects which are firmly built-in in the ceramics and cannot be released even at very high temperature. Interestingly, when the samples are left for some time at room temperature,

after the TSC experiment, the pyroelectric current starts to increase (see Chapter 5, Figure 5.22). This observation also supports our hypothesis of two components of polarization: we interpret the increase in pyroelectric current as settling of de-trapped mobile charges, which reinforce built-in polarization.

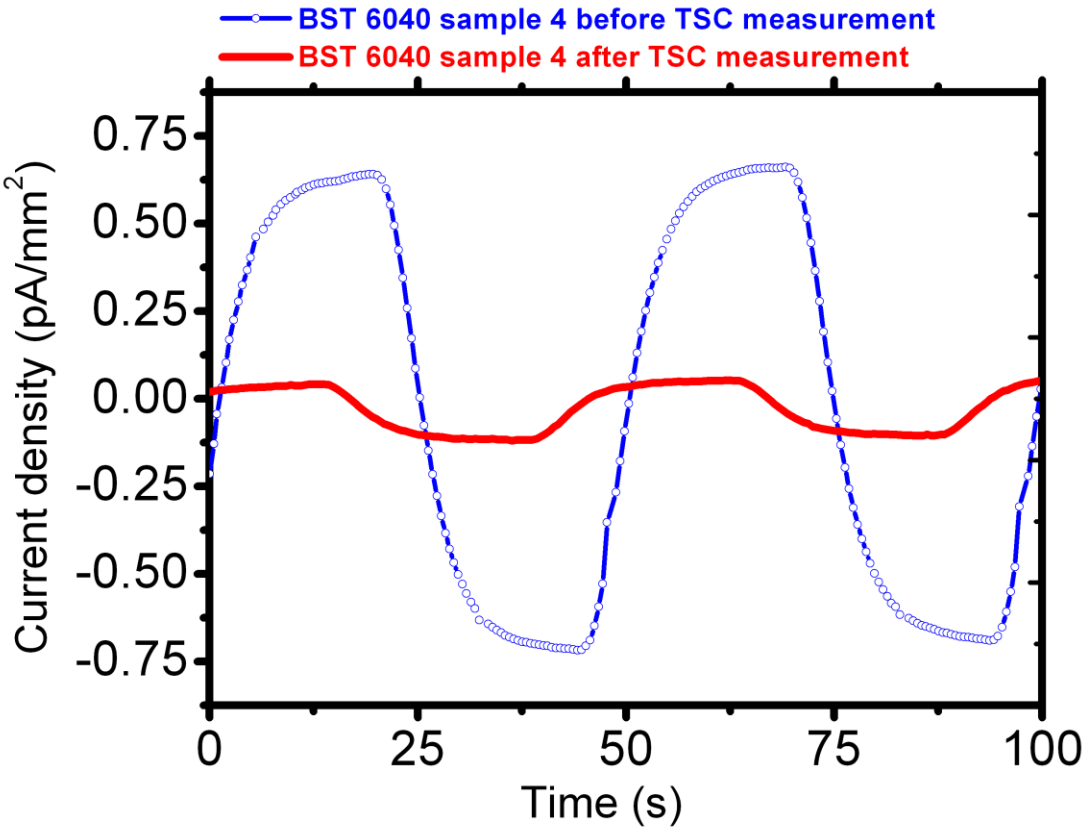

Figure 6.8-Variation of the amplitude of the pyroelectric current at room temperature in BST6040 ceramics before and immediately after the thermally stimulated current measurement (from 26°C to 550°C). The reduction of the amplitude the pyroelectric response indicates that during heating, some space charges are released, and do not contribute any more to the pyroelectric response measured at room temperature. The pyroelectric measurement was done at 21°C.

Interestingly, in the temperature range where the TSC peaks are observed, several anomalies are present in the dielectric permittivity and in the loss tangent of BST6040 ceramics and others (Ba, Sr)TiO_3 compositions. The observed anomalies are in agreement with a dielectric relaxation process due to the release of the space charges which, at low temperature, are aligned in the direction of the built in polarization and are thermally activated upon heating.

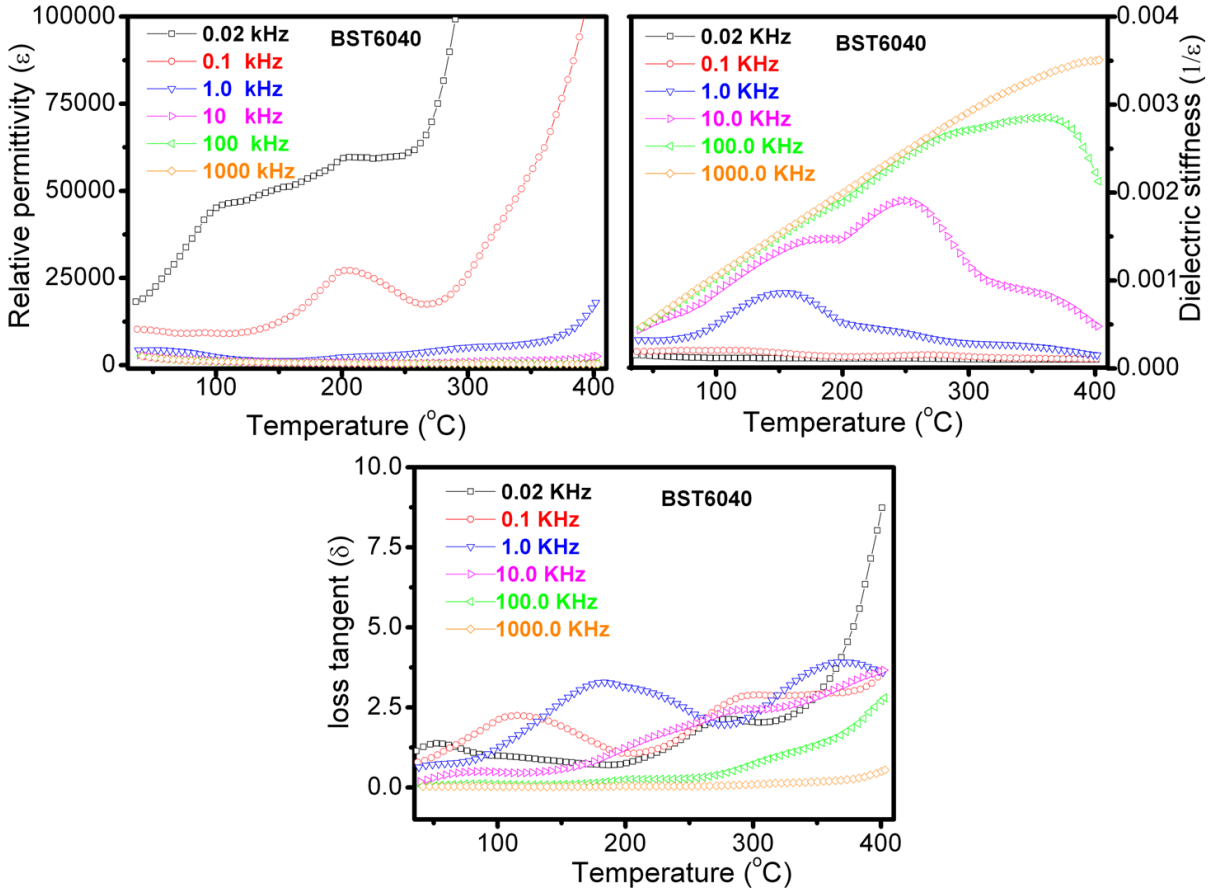

Figure 6.9-Anomalies measured in the real part of the dielectric constant (ε), dielectric stiffness (1/ε), and the loss tangent of BST6040 ceramics between room temperature and 400°C. A total of 19 frequencies between 0.02 kHz and1MHz were measured. Here only 5 frequencies are shown for clarity. The maximum of the peaks shift to higher temperature with the increase of the frequency. The anomalies are less pronounced at very low frequencies (0.02KHz) and at high frequencies (above 100) KHz. The measurements were performed with a HP 4284A LCR meter in the same furnace used for the TSC measurement. The amplitude of the probing field was 1 V.

On the basis of the results obtained on $(Ba,Sr)TiO_3$, we first postulated that $SrTiO_3$ ceramics, which do not show any pyroelectric response at room temperature, are not polar and should, therefore, not show any thermally stimulated peak whose direction depends on the sample orientation.

To verify this conjecture, we performed TSC measurements on $SrTiO_3$ samples. From the TSC results reported in Figure 6.10, it is clear that peaks, which are sensitive to the sample orientation, are present in $SrTiO_3$ ceramics as well. This demonstrates that as–sintered ceramics of pure $SrTiO_3$ possess a built-in polarization. The existence of a polarity in $SrTiO_3$ ceramics is actually not surprising since, the preferred orientation in $(Ba,Sr)TiO_3$ ceramics is related to the inhomogeneities induced during the sintering of the samples. It is therefore logical that, since the ceramics of $(Ba,Sr)TiO_3$ and $SrTiO_3$ are produced in the same environment, with similar processing conditions, they are exposed to the same kind

of asymmetry. The fact that, at room temperature, no pyroelectric current is detected in $SrTiO_3$ ceramics can be due to several reasons. One possibility, mentioned already in Chapter 5, is that the polar defects have a lower concentration. The assumption that $SrTiO_3$ ceramics develop lowest degree of inhomogeneities with respect to the BST6040 during sintering is in agreement with the mapping of the microstrain performed with X-Rays diffraction, which will be discussed in section 5.6.

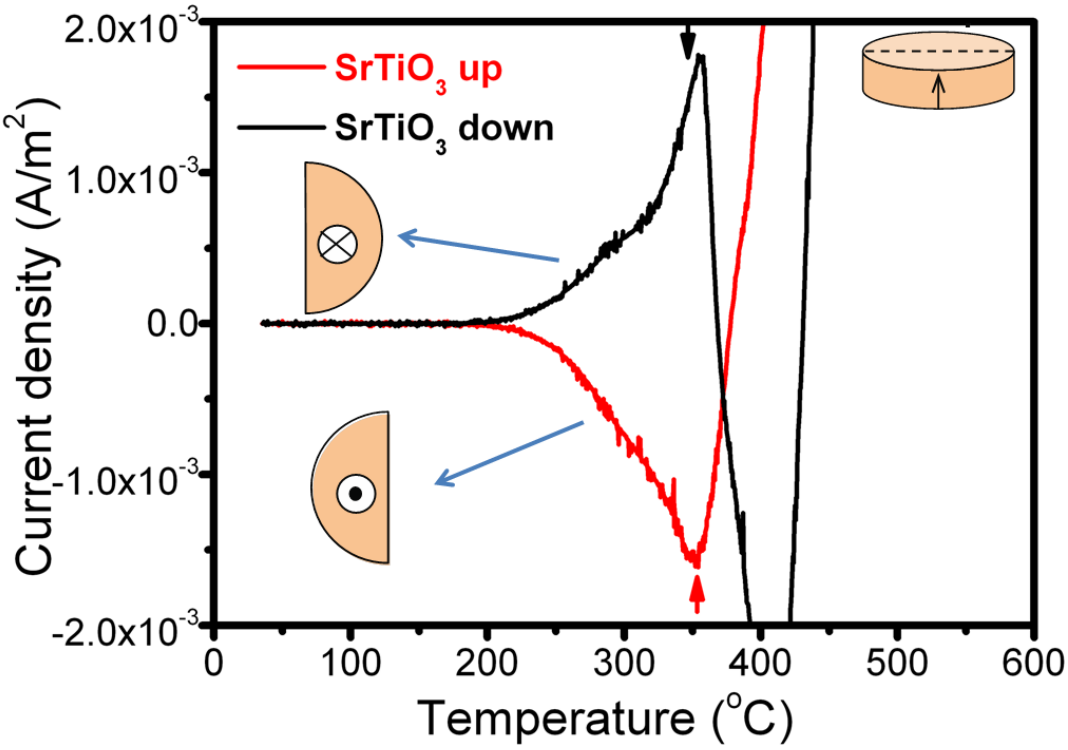

Figure 6.10-Thermally stimulated current between 26°C and 550°C on heating with a rate of 2.5°C/minute of two halves cut from the same $SrTiO_3$ ceramics disk measured with opposite orientation. The sign of the peak at around 350°C depends on the direction of the samples during the measurement and indicates that in $SrTiO_3$ ceramics the center of symmetry is absent. The up and down label refers to the ceramics orientation in the furnace during sintering.

6.3 Presence of polarity in $SrTiO_3$ single crystals

Another explanation for the absence of the pyroelectric response is that the polar defects in $SrTiO_3$ ceramics at room temperature, are completely frozen and they do not respond to the small variation of temperature of the pyroelectric measurement. The temperature of the thermally stimulated peak in $SrTiO_3$ ceramics is, in fact, about 100°C

higher than in BST6040 ceramics, suggesting higher activation energy of the charged defects in $SrTiO_3$.

The hypothesis that in $SrTiO_3$ ceramics the pyroelectric response is not observed because of the high activation energy of the defects associated to the polarization is supported by the results of the thermally stimulated current measurement on Al_2O_3 ceramics slightly doped with MgO (Chapter 4), which also do not show any pyroelectric response at room temperature. TSC peaks which change the sign when the orientation of the samples is inverted are present in the TSC curves of MgO-doped Al_2O_3 ceramics (Figure 6.11) and therefore indicate that the ceramics are macroscopically polar. In Al_2O_3 the polar defects responsible for the charge separation are most likely defects which form to charge compensation of the substitution of Al^{3+} atoms by lower valance Mg^{2+} atoms. The charge compensation can be achieved by formation of $V_O{}^{2+}$ vacancies [10, 11]. In Mg doped Al_2O_3 ceramics the TSC peaks are observed at around 400^o C, suggesting even higher activation energy than for the polar defects in $SrTiO_3$ ceramics.

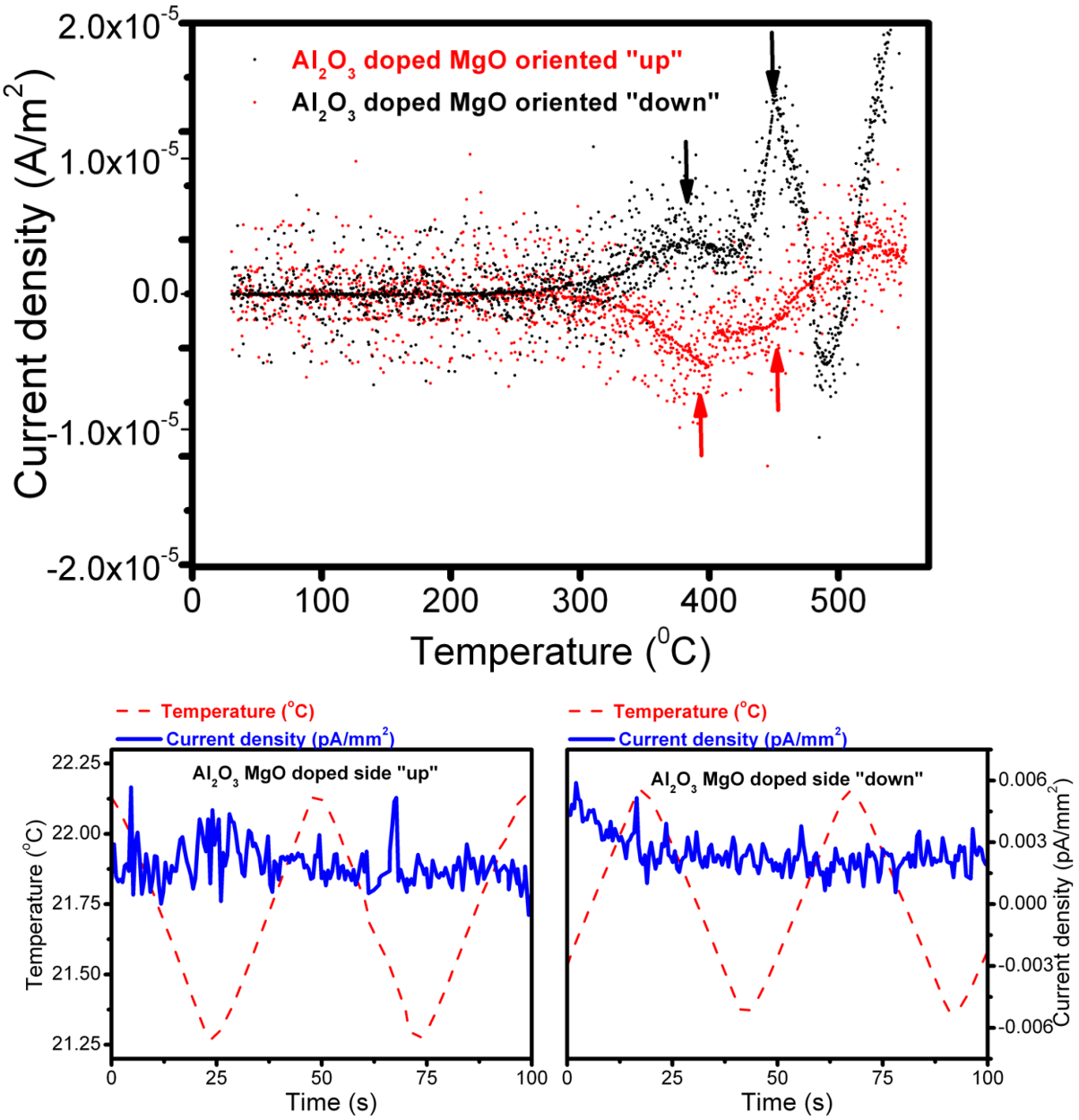

Figure 6.11-Thermally stimulated current on heating of a sample of Al_2O_3 ceramics doped with MgO (sample area 10.32 mm^2) measured in the range between 26°C and 550°C with a heating rate of 2.5°C /minute (top). Above 400°C, several peaks whose direction is dependent on the orientation of the samples are observed. The pyroelectric measurement does not reveal any response on either side of the ceramics (bottom).The pyroelectric response is not observed probably because, as suggested by the high temperature of the peaks, the defects related to the polarization are completely frozen at room temperature. The "up" and "down" side are chosen arbitrarily. The samples were a courtesy of Mr. Jacques Castano.

To verify that TSC signal in $SrTiO_3$ ceramics and Al_2O_3 doped ceramics is indeed property of the material and not an artifact, the TSC was measured in a high quality

sapphire single crystal (α-Al_2O_3) which represents an ideal material for comparison because it is expected to have much lower concentration of defects. In the sapphire crystals, no pyroelectric response is detected at room temperature and no peak is present in the thermally stimulated current between 26^{o}C and 550^{o}C (Figure 6.12).

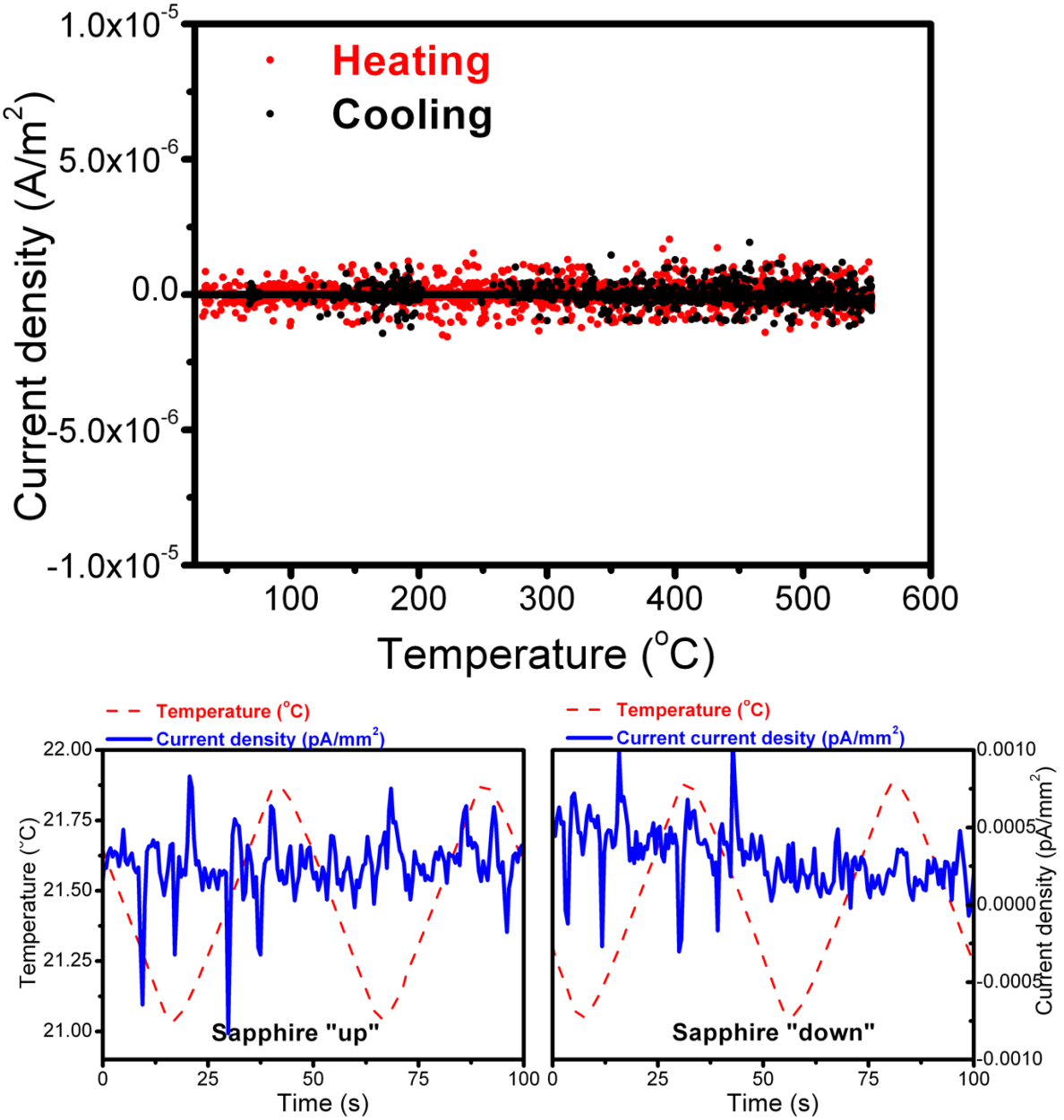

Figure 6.12-Thermally stimulated current on heating and cooling (top) sapphire single crystal (diameter 15.01 mm, thickness 0.49 mm). The heating and cooling rate was 2.5°C/minute and the temperature range was 26°C-550°C. In sapphire, no pyroelectric response is observed at room temperature (bottom).

The results of the measurements of TSC collected so far are important because they clearly demonstrate that the absence of pyroelectric response cannot be taken as unique criterion to rule out the presence of macroscopic polarity in the samples.

Considering these new observations, the MaTeck $SrTiO_3$ single crystals which did not show any pyroelectric response at room temperature (see Chapter 4 and Chapter 5) were tested by measuring thermally stimulated current.

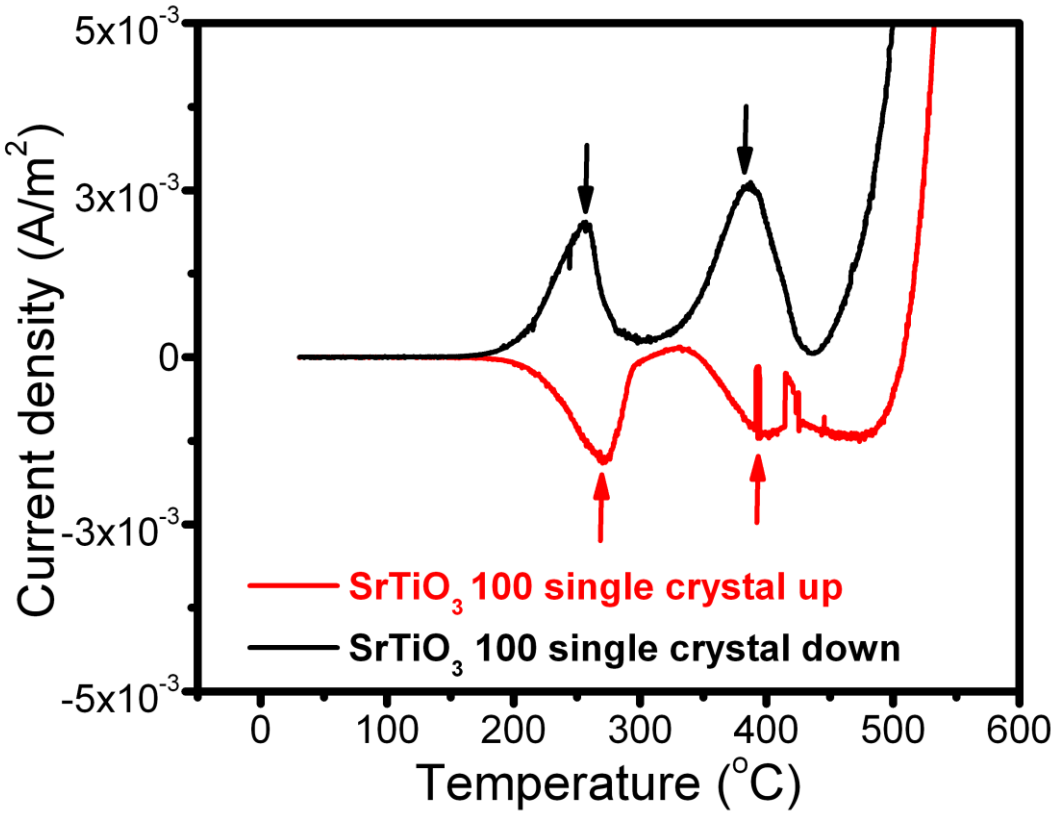

Figure 6.13-Thermally stimulated current on heating between 26°C and 550°C measured on two plates of [100] oriented single crystals of $SrTiO_3$. The plates with dimensions 4.99 x 4.50 mm ^{2} and 4.53 x 4.59 mm^2 and 0.49 mm of thickness, were cut from a bigger plate which is used as substrate for thin films growth and was produced by MaTeck GmbH in Germany. The peaks which change their sign when the sample is inverted, marked with the arrows, are observed around 260°C and at around 390°C. The "up" and "down" label are assigned arbitrarily.

The measurements reveal the presence of peaks dependent on the orientation of the single crystals (Figure 6.13).The peak's maximum is in the range around 260°C and thus at a lower temperature than in $SrTiO_3$ ceramics. This fact suggests that the type of trapped charged defects may be dependent not only on the chemistry of the specific system but also on the preparation method of the samples.

This latter possibility was investigated by measuring two single crystals of $SrTiO_3$ grown under different conditions. Both types of single crystals were produced with the top-seeded solution growth (TSSG) method at FEE, Idar-Oberstein, Germany. One, labeled Y143-1/1, was grown at 1600°C from a solution with TiO_2 flux while the second one, labeled Y157-1, was grown at 1150°C with a flux containing SrO, Li_2O and B_2O_3. The Y143 crystal has much higher strain and dislocations density (between 10^2 to the 10^4

dislocations/cm^2) than the Y157 single crystal.

Before the measurements, the two single crystals were cut into two halves of approximately the same area. The results of pyroelectric measurement and the thermally stimulated currents for the two halves of Y143 sample are shown in Figure 6.14. The TSC were measured on each half of the crystal, whit one side being flipped over with respect to the other (see Figure 6.14).The sign of the TSC peaks were opposite for the two halves, indicating presence of asymmetry in the samples, i.e. presence of built-in polarization. Both halves show a current response which inverts when the samples are turned upside down and change the sign of the thermally stimulated current peaks when the sample is flipped over. Interestingly, Y143 exhibits pyroelectric response in as-received state, in contrast to $SrTiO_3$ ceramics and MaTech and Y157-1 crystal. However, it should be noted that the profile of the pyroelectric current is highly distorted with respect to the square shape expected for a pyroelectric response for triangular temperature waveform; in other words, the current variation with the temperature does not follow the ($d\Delta T/dt$) dependency but looks more as directly proportional to the temperature change ΔT. This distortion of the current profile is not understood at present and might be related to a different response between the surface region and the bulk of the crystal. Distortions of the pyroelectric current induced by a difference between the bulk and the surface region has been previously observed in the case of single c domain single crystal of $BaTiO_3$ [12] and were ascribed to a rapid thermal relaxation of the surface region.

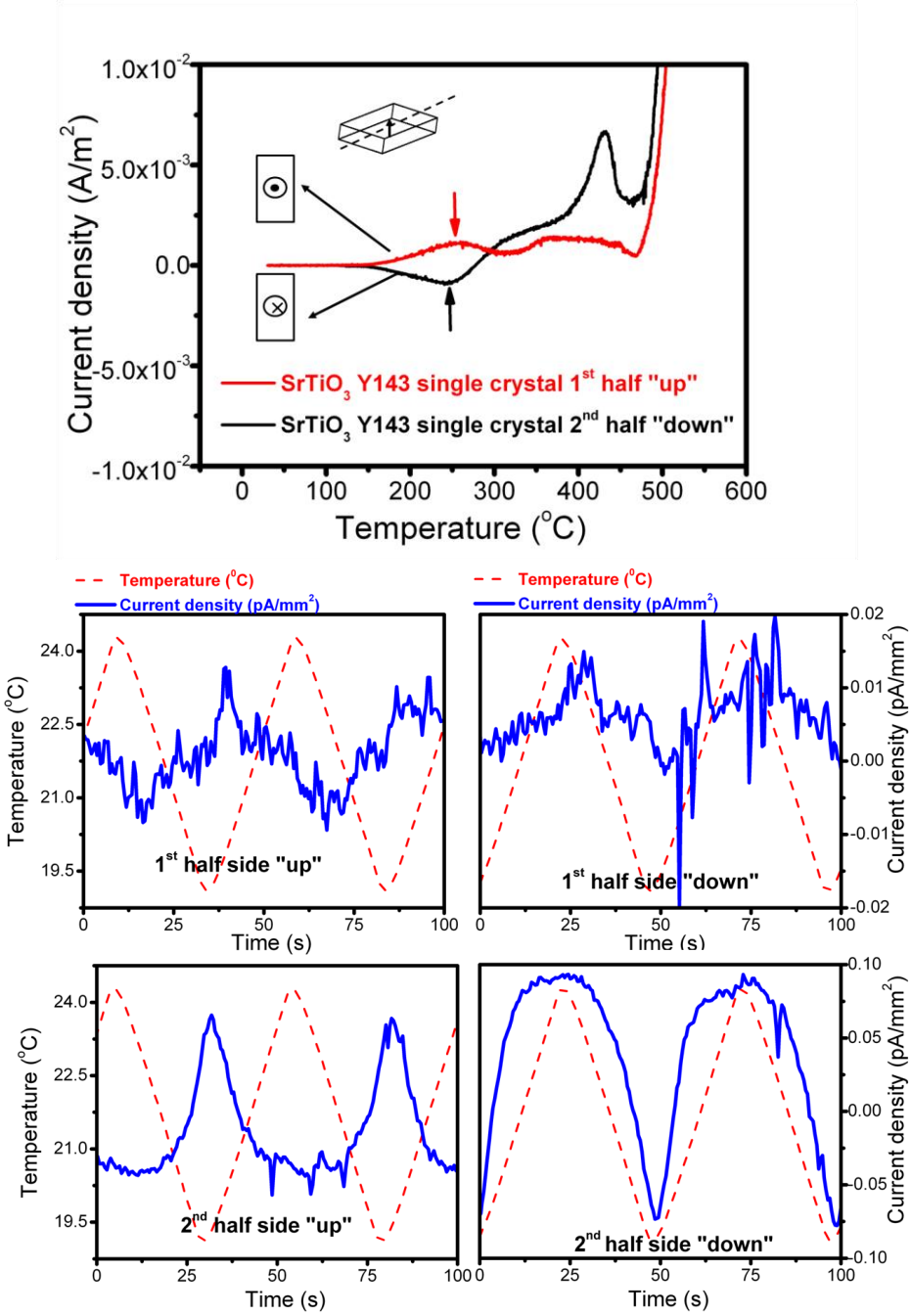

Figure 6.14-Thermally stimulated current measured on heating between 26°C and 550°C, on the two halves of the Y 143 $SrTiO_3$ single crystal with opposite orientation (top) and pyroelectric current at room temperature (bottom) before the TSC measurement. The peaks whose sign is sensitive to the sample orientation are marked with the arrows. The two halves (dimensions 2.48 x 3.83 mm^2 and 2.0 x 3.82 mm^2 and about 0.20 mm of thickness) were cut from a [001] oriented plate produced at the FEE in Germany. The single crystal was grown at 1600°C by the TSSG with a flux of TiO_2. The sample was a courtesy of Dr. Daniel Rytz. The up and down sides are assigned arbitrarily.

The measurement of the thermally stimulated current in the $SrTiO_3$ Y157 reveals the presence of a peak at about 250°C in both halves. The intensity of the thermally stimulated

peak in the two half also differs significantly. In one half only a small anomaly is observed (Figure 6.15 bottom) with a much smaller intensity than in the peak observed in the other half.

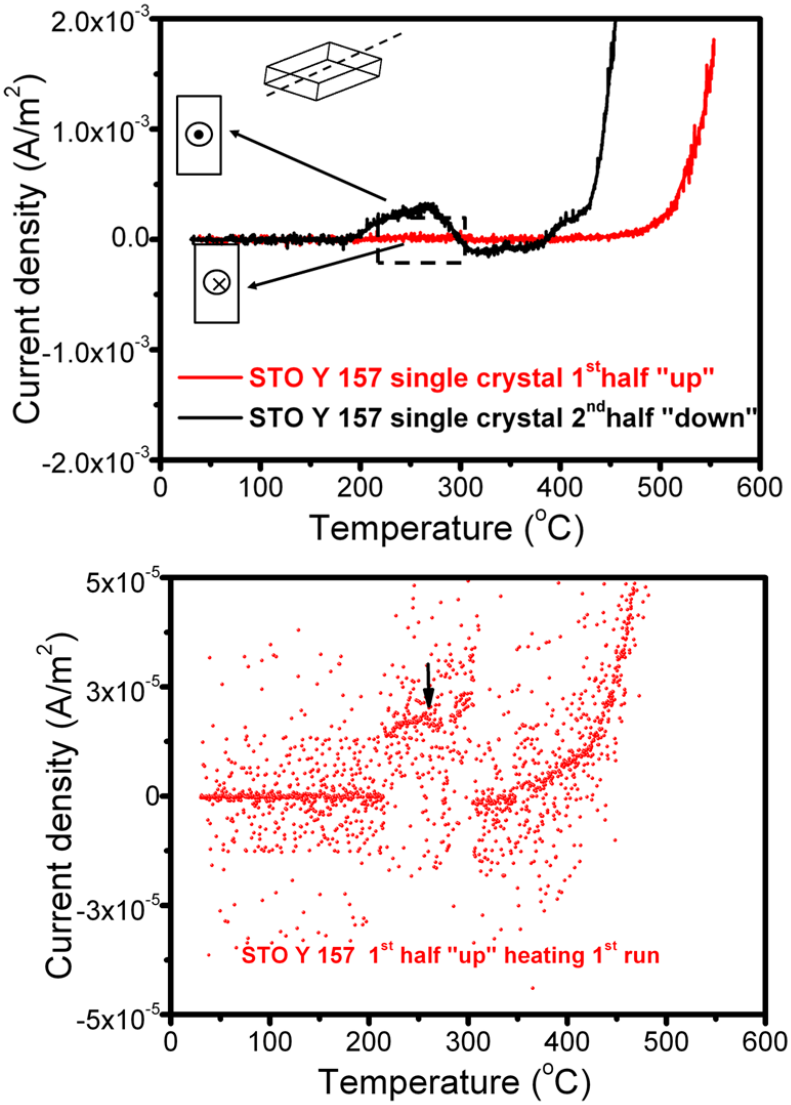

Figure 6.15-Thermally stimulated current (top) of two halves (dimensions 1.86 x 2.52mm^2 and 2.41 x 1.54 mm^2 and about 0.20 mm of thickness) cut from a plate of Y157 $SrTiO_3$ single crystal and magnification of the current profile of the first half (bottom). Peaks of different intensities are present in both halves at around 250^{o}C. Note that in the half which shows the less intense peak (bottom picture), the sudden increase of the current with respect to the background between 200^{o}C and 300^{o}C is caused by a problem; with the contact, the small peak to which we are referring is marked with the arrow. The sign of the peaks is the same for both orientations of the sample. The single crystal was grown at 1150^{o}C with the TSSG with a flux of SrO, Li_2O and B_2O_3 at FEE in Germany. The sample was a courtesy of Dr. Daniel Rytz. The "up" and "down" sides are assigned arbitrarily.

The pyroelectric measurement does not show any current at room temperature in either half of this crystal (Figure 6.16).

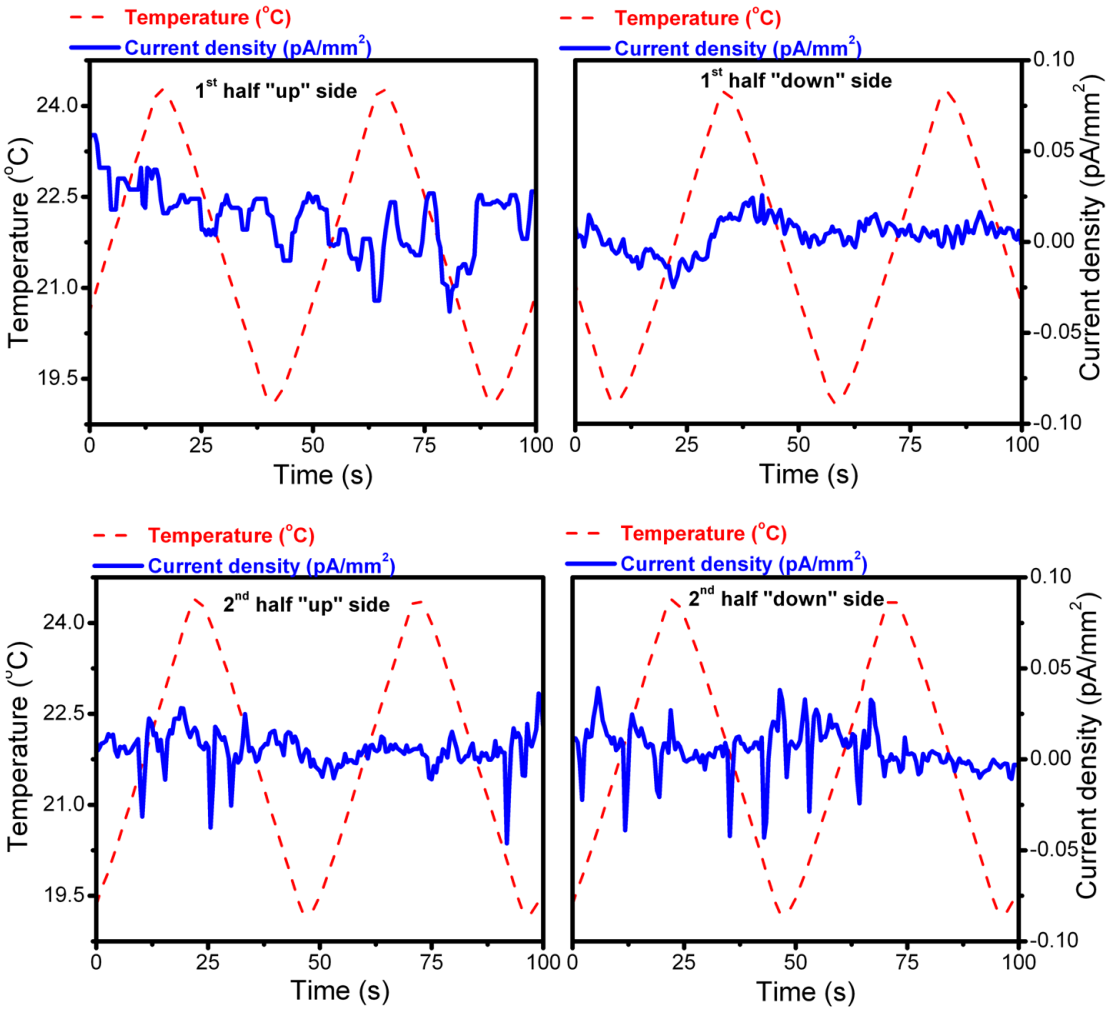

Figure 6.16-Pyroelectric current density of two halves cut from a plate of Y157 $SrTiO_3$ single crystal. The up and down sides are assigned arbitrarily.

Importantly, the peaks observed in the $SrTiO_3$ Y157 single crystals do not change sign with the orientation of the sample. This strongly suggests that these single crystals are centrosymmetric and that the small peaks in the thermally stimulated current are associated with trapped charges which are not equally distributed across the plate from where the samples were originally cut. This argument is further supported by a second measurement of the thermally stimulated current on the same two halves of the $SrTiO_3$ Y157 single crystal. During the second measurement, each half was placed with the opposite orientation with respect to the first measurement. In the half which showed the less intense peak, a peak was again observed approximately at the same temperature as during the first measurement (Figure 6.17 top). The sign of the peak however did not change despite the sample being turned upside down with respect to the first measurement.

In the second half of the single crystal Y157 which exhibited the more intense peak during the first measurement, no peak was observed during the second measurement but only a monotone increase of the current (Figure 6.17 bottom). The starting temperature of the continuous current increase during the second heating coincides with the temperature range where the peak is observed during the first heating, therefore it is possible that a weak peak is present also during the second heating but its presence is shaded by the rise of the current.

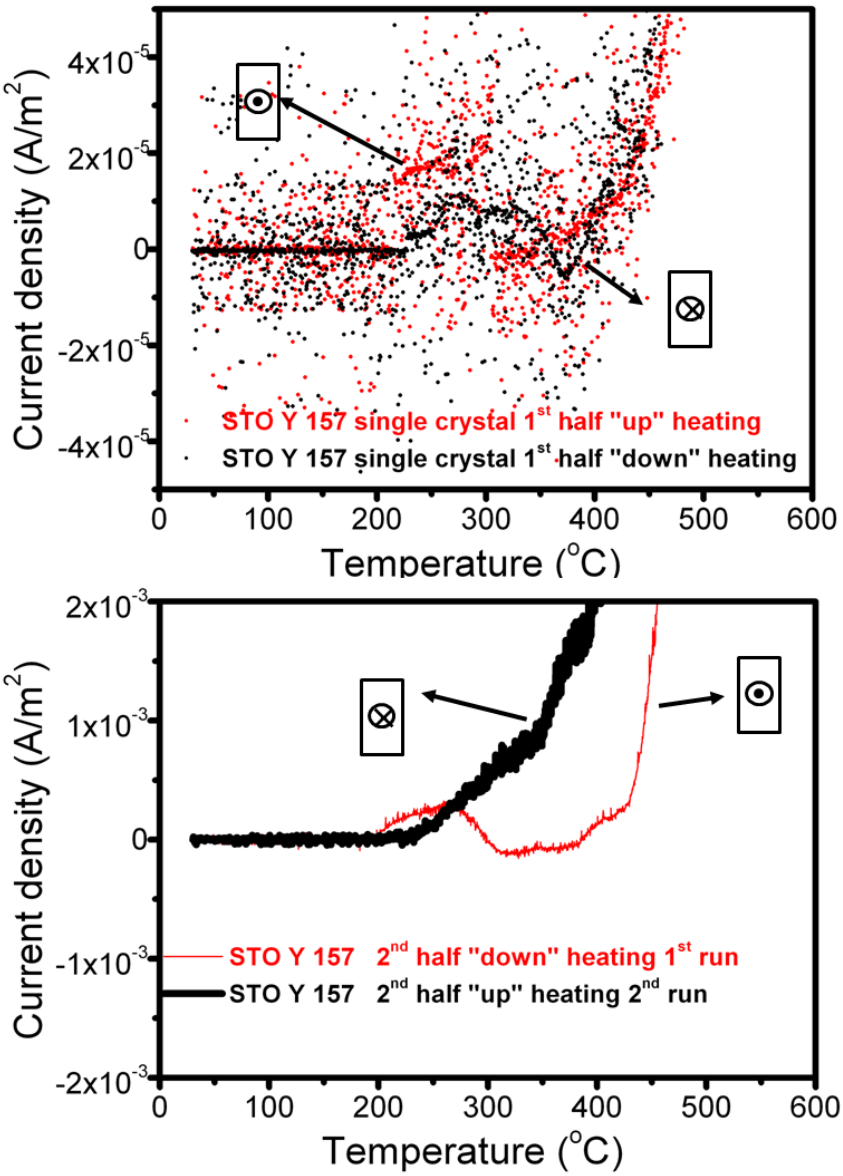

Figure 6.17-Thermally stimulated current on heating, measured between 26^{o}C and 550^{o}C for the two opposite orientation of the first (top) and the second half (bottom) of the $SrTiO_3$ Y157 single crystal. In the first half a small peak is observed around 250^{o}C. However the sign of the peak is the same for both orientation of the sample. In the second half, when the orientation of the sample is inverted the thermally stimulated peak observed in the first measurement is not detected anymore and the current shows only the constant increase usually observed at high temperature.

The different behavior in the thermally stimulated current profiles of the two halves of the Y157 single crystals suggests a different distribution of the space charges trapped in the samples. The driving signal for these currents could be the small voltage (bias) of the picoammeter or the thermal gradient. Note the current peaks in Y157 are about one to two orders of magnitude smaller (10^{-4} compared to 10^{-3}) than in Y143.

The results of the pyroelectric response and thermally stimulated current measurements of the two types of $SrTiO_3$ single crystals are consistent with the hypothesis

proposed in Chapter 5 for ceramics that the formation of the inhomogeneities leading to the symmetry breaking in single crystals occurs during the growth process. In fact, the Y 143 single crystals, which exhibits a “pyroelectric response” and a thermally stimulated peak sensitive to the orientation of the samples, was grown at a considerably higher temperature (1600^{o}C) than the Y157 single crystal (1150^{o}C). In the Y143 the preferred direction causing the symmetry breaking is likely related to the strain and charge trapping associated to the higher number of inhomogeneously distributed dislocations present in this single crystal with respect to the Y157 single crystal.

This experiment on single crystals supports the idea that the disappearance of the center of symmetry most likely takes place when the material is processed at high temperature conditions, where thermal gradients are more important and difficult to avoid, and transport of material is high. This is the same conclusion as drawn for ceramics samples in Chapter 5. Importantly, in both ceramics and single crystals the symmetry breaking appears to be related to inhomogeneous strain distribution. The evidence for strain is the difference in concentration of dislocations in crystals and inhomogeneous microstrain in ceramics.

6.4 Summary

In this chapter, the thermally stimulated current technique was used to verify the polar character in the paraelectric phase of unpoled ceramics and single crystals. The presence of a built-in polarization in the paraelectric phase was associated with the observation of current peaks whose sign depends on the orientation of the sample with respect to the measuring electrode. The peaks are observed in different compositions of (Ba,Sr)TiO_3 and in pure $BaTiO_3$ ceramics. Importantly the thermally stimulated current reveals peaks sensitive to the sample orientation even in materials which do not exhibit pyroelectric response at room temperature (i.e. $SrTiO_3$ ceramics and single crystals). This demonstrates that the absence of a pyroelectric response cannot be assumed as an exclusive proof of the centro-symmetric character of a material; observation of pyroelectric current may be simply a question of instrumental resolution or thermal stability of apparent polarization. The TSC measurements on $SrTiO_3$ single crystals with different concentration of dislocations suggests that the inhomogeneities responsible for the disappearance of the center of the symmetry are formed during the crystal growth and are intimately associated with the high temperature process. These observations are consistent with the sintering experiments on BST6040 ceramics discussed in Chapter 5. In both cases it seems that the symmetry breaking is related to inhomogeneous strain associated with high temperature processing.

6.5 Bibliography

[1] J. v. Turnhout, "Thermally Stimulated Discharge of Polymer Electrets," *Polym J,* vol. 2, pp. 173-191, 03//print 1971.

[2] C. Bucci, R. Fieschi, and G. Guidi, "Ionic thermocurrents in dielectrics," *Physical Review,* vol. 148, pp. 816-&, 1966.

[3] U. V. Desnica and B. Santic, "Optically enhanced photoconductivity in Semi-insulating gallium-arsenide," *Applied Physics Letters,* vol. 54, pp. 810-812, Feb 1989.

[4] W. S. Lau, T. C. Chong, L. S. Tan, C. H. Goo, and K. S. Goh, "The characterization of traps in seimiinsulating gallium-arsenide buffer layers grown at low-temperature by molecular-beam epitaxy with an improved zero-bias theramlly stimulated current technique," *Japanese Journal of Applied Physics Part 2-Letters,* vol. 30, pp. L1843-L1846, Nov 1991.

[5] A. B. Haugen, J. S. Forrester, D. Damjanovic, B. Z. Li, K. J. Bowman, and J. L. Jones, "Structure and phase transitions in 0.5($Ba_{0.7}Ca_{0.3}TiO_3$)-0.5($BaZr_{0.2}Ti_{0.8}O_3$) from -100 degrees C to 150 degrees C," *Journal of Applied Physics,* vol. 113, Jan 2013.

[6] D. S. Keeble, F. Benabdallah, P. A. Thomas, M. Maglione, and J. Kreisel, "Revised structural phase diagram of ($Ba_{0.7}Ca_{0.3}TiO_3$)-($BaZr_{0.2}Ti_{0.8}O_3$)," *Applied Physics Letters,* vol. 102, Mar 2013.

[7] W. F. Liu and X. B. Ren, "Large Piezoelectric Effect in Pb-Free Ceramics," *Physical Review Letters,* vol. 103, Dec 2009.

[8] W. S. Lau, K. F. Wong, T. Han, and N. P. Sandler, "Application of zero-temperature-gradient zero-bias thermally stimulated current spectroscopy to ultrathin high-dielectric-constant insulator film characterization," *Applied Physics Letters,* vol. 88, Apr 2006.

[9] J. v. Turnhout, *Thermally stimulated discharge of polymer electrets: a study on nonisothermal dielectric relaxation phenomena*: Elsevier, 1975.

[10] H. Haneda and C. Monty, "Oxygen self diffusion in magnesium doped or titanium-doped alumina single crystals," *Journal of the American Ceramic Society,* vol. 72, pp. 1153-1157, Jul 1989.

[11] S. K. Mohapatra and F. A. Kroger, "Defect structure of alpha-Al_2O_3 doped with magnesium," *Journal of the American Ceramic Society,* vol. 60, pp. 141-148, 1977.

[12] M. E. Lines and A. M. Glass, *Principles and applications of ferroelectrics and related materials*: Clarendon Press, 1977.

Chapter 7 : Conclusions and perspectives

The initial motivation of this work was to improve the understanding of the flexoelectric polarization in bulk ceramics. The fundamental aspect to clarify was the origin of the unexpected high flexoelectric polarization measured in the paraelectric phase of different ferroelectric and relaxor systems, in particular in the lead-free $Ba_{0.67}Sr_{0.33}TiO_3$ composition. Our early tests of the direct flexoelectric response in the paraelectric phase of the unpoled ceramics of $Ba_{1-x}Sr_xTiO_3$ lead to the uncovering of an electro-mechanical coupling whose origin could not be ascribed to the flexoelectric effect generated by a pure geometrical strain gradient. The subsequent investigations conducted on the ferroelectric and paraelectric phases of unpoled ceramics demonstrated that the dominant electromechanical coupling is the manifestation of a built-in polarization that causes as–sintered samples to exhibit non-zero pyroelectric and piezoelectric responses. The existence of polar and non centrosymmetric properties such as pyroelectricity and piezoelectricity in the paraelectric phase of as–sintered ceramics implies a mechanism of breaking of the centric symmetry of the samples. The investigations were than focused to understand the origin of the symmetry breaking and to identify the mechanism causing the charge separation in the ceramics.

The studies were carried out mainly by means of dynamic pyroelectric measurements and of the thermally stimulated current (TSC) measurements. Piezoelectric measurements were performed as well. The combined use of these techniques allowed clarifying some aspects about the origin of the polarity:

- The observation of pyroelectric response in the paraelectric phase of single crystals of ferroelectric (i.e. $BaTiO_3$ and $KTaNbO_3$) and non ferroelectric materials ($SrTiO_3$ grown at high temperature) and of peaks in the thermally stimulated currents of single crystals of non ferroelectric material ($SrTiO_3$) that are dependent on sample orientation indicate that the origin of the symmetry breaking cannot be simply ascribed to the presence of the grain boundaries in ceramics.

- The comparison of the pyroelectric response of unpoled as-sintered ceramics of $(Ba,Sr)TiO_3$ before and after polishing shows that the polarization is present in the bulk of the samples and it is not due to a surface contribution.

- The analysis of the electrical response during different processing steps demonstrates that the direction of the polarization is determined (and polarization itself probably formed) during the densification of the ceramics, when the material transport is the highest. The hypothesis is that the driving force for the symmetry breaking in the material during sintering arises from asymmetric surrounding of the sample, which is characteristic for all high temperature processes commonly used in fabrication of the ceramics and single crystals; this environmental asymmetry cannot be avoided with simple precautions i.e. imbedding the samples into a powder of the same composition as the sample, to limit interaction between the samples and the support or with atmosphere. The environmental asymmetry (or inhomogeneity) is intimately related to the high temperature processing rather than specific equipment used for sample preparation: samples prepared in other laboratories with different techniques were tested and all showed the symmetry breaking. At present, the exact nature of environmental asymmetry remains unknown; a very small thermal gradient or gravity could be possible sources for it. The same arguments based on high temperature preparation conditions can be used to interpret symmetry breaking in single crystals, although the precise mechanism of symmetry breaking in ceramics and crystals could be different.

- The systematic study of several compositions of (Ba,Sr)TiO_3 and pure $BaTiO_3$ and $SrTiO_3$ ceramics shows a disappearance of the pyroelectric response for low barium concentration (2.5 %) and pure $SrTiO_3$ although the thermally stimulated current measurements prove that as-sintered $SrTO_3$ ceramics are polar as well. This fact implies that, while the densification process is at the origin of the appearance of the polar direction in the ceramics, the permanent charge separation is caused by the presence of polar defects/entities, which depends on the chemical composition of the ceramics. We argue that the two most plausible kind of polar defects are intrinsic ionic vacancies (oxygen vacancies and Schottky defects) or polar entities akin to polar regions (PR) or polar clusters often encountered in ferroelectrics and relaxors. The breaking of the macroscopic symmetry in the samples is the consequence of interaction of these intrinsic charged defects/entities with structural inhomogeneities formed during the high temperature processing.

- The pyroelectric and the thermally stimulated current experiments consistently indicate that the polar response in the ceramics of (Ba,Sr)TiO_3 is composed of two contributions: one, coming from the polar defects (vacancies or polar entities) permanently oriented during the densification of the samples, which cannot be erased during heating (even at temperatures higher than the temperature of the practically full densification, once densification process is completed) and the second, associated to mobile space charges, which is unstable and can be erased when the samples are heated to relatively low temperatures (up to 500^{o}C). Once lost, this component can be recovered under the driving force of the built-in polarization owing to the high mobility of space charges.

- It was shown that the absence of pyroelectric response in some unpoled ceramics and single crystals, in general, is not a reliable criterion to exclude the presence of polarity and absence of centric symmetry. The thermally stimulated current technique can be used to detect polarization and symmetry breaking even when a room-temperature pyroelectric response is not observed. This is possible when space charges are sufficiently mobile and move asymmetrically in presence of built-in polarization.

- The built-in polarization is responsible for the electro-mechanical coupling which is of the same order of magnitude as the unexpectedly high flexoelectric effect reported in recent studies in the same materials. This electromechanical effect competes with the flexoelectricity making interpretation of the results of flexoelectric studies difficult.

- Space-charge component of the total polarization is responsible for the low-frequency dependence of the permittivity and electromechanical response.

The knowledge acquired during our work allows us to make some conclusions about the mechanism of the symmetry breaking in the specific case of the (Ba,Sr)TiO_3 ceramics and some general considerations about the ceramics and single crystals.

In the $Ba_{1-x}Sr_xTiO_3$ ceramics, one can state that the symmetry breaking originates from the preferential alignment of polar defects (vacancy complexes or polar entities (nano-regions, clusters)) during sintering. These charged defects, whatever they are, depend on the chemistry of sample, that is, they are related to the barium/strontium concentration in the samples. At present, we could not make direct observation of these

defects. The driving force for alignment of the defects is probably inhomogeneous distribution of the strain in the samples. While the X-rays analysis revealed a variation of the local microstrain across the ceramics thickness, giving information about the strain gradient in one dimension, it did not give us the exact direction of the strain gradient.

The two possible scenarios proposed to explain the symmetry breaking in (Ba,Sr)TiO_3 ceramics, intrinsic vacancies or polar entities, open interesting perspectives for theoretical studies. On one side, it has been shown from Extended X-rays Absorption Fine Structure (EXAFS) combined with Reverse Monte Carlo refinements [1] that ,in the $Ba_{1-x}SrxTiO_3$ solid solution, an off–centering of Ti ions decreases progressively with the increase of the content of strontium. The local off–centering of the Ti atoms may be a good candidate for the polar entities at the origin of the polarization in the (Ba,Sr)TiO_3 ceramics. However a fundamental aspect that needs to be explored theoretically is if the displacement of the titanium atoms can be stabilized by the presence of strain, whether resulting polar entities can interact with the strain and cause polarization on the macroscopic scale in the ceramics.

Evidences that polar nano regions (PNRs) may be coupled with strain were obtained by calculations based on effective Hamiltonian approach [2] in relaxor $BaZrO_3$ epitaxial thin films. However, the coupling between the dipoles and the strain in $BaZrO_3$ is predicted to occur only on the local scale and no macroscopic polarization is expected in the system. It would be interesting to study theoretically other systems, especially ferroelectrics with respect to the coupling of the polar nano regions with strain to establish if the strain can align the polar regions and lead to a macroscopic polarization. Recent experimental studies in the laboratory showed that the polar nano regions in prototypical relaxor $Pb(Mg_{1/3}Nb_{2/3})O_3$, are sensitive to mechanical excitations and exhibit the same relaxor characteristics as when excited by electric field [3].

Although in different materials the breaking of the centric symmetry can arise from different type of inhomogeneities than the ones in $Ba_{1-x}Sr_xTiO_3$ solid solution, our study shows that, in general, the statement that unpoled single crystals and ceramics in the ferroelectrics and paraelectric phases are centro-symmetric and therefore do not exhibit any polar properties cannot be taken as valid without being verified experimentally. This does not mean that the crystal structure of a paraelectric phase of a ferroelectric is non centrosymmetric. What this statement implies is that the macroscopic sample exhibits non centro-symmetric, or even polar character.

The measurements show that the breaking of the expected centric symmetry in unpoled ferroelectric ceramics and paraelectric phase of ceramics and single crystals is a phenomenon encountered in many systems because the conditions leading to the symmetry breaking are intimately associated with the high temperature techniques commonly used for the growth of the single crystals and for the preparation of the ceramics. We have verified symmetry breaking in (Ba,Ca)(Zr,Ti)O_3, $BaTiO_3$, $Ba_{1-x}Sr_xTiO_3$,

$SrTiO_3$, $Pb(Zr_{1-x}Ti_xO_3)$, $BiFeO_3$, $Pb(Mg_{1/3}Nb_{2/3})O_3$, $KTaNbO_3$, modified $KNbO_3$ and even in doped–Al_2O3.

It has been shown with fist principle calculations that oxygen vacancies in epitaxial $CaMnO_3$ thin films can be stabilized and ordered by strain [4]. Conversely, presence of oxygen vacancies is responsible for strain in the material, through mechanism of chemical expansivity [5]. Since oxygen vacancies are the most mobile type of ionic defects in ceramic oxides, in particular perovskites, their ordering by inhomogeneous strain induced by the high temperature processing can be the most common mechanism for the breaking of the centric symmetry in oxides. It would be important to further explore this aspect with calculations to have an estimate of the order of magnitude of the strain needed to order the oxygen vacancies, especially in bulk ceramics.

The obtained results are important for studies of the flexoelectric effect, where quantification of the magnitude of the response is based on the assumption that in the paraelectric phase the piezoelectric coupling is zero and thus does not contribute at all to the measured charge. The presence of the polarity implies the existence of inhomogeneous built-in field (electric, elastic or a combination of both) in the samples. This raises the question if the structural bending model developed for homogeneous materials used to calculate flexoelectric coefficients is applicable to samples with inhomogeneous polar structure. The results of this thesis may solve the controversy of the large flexoelectric coefficients reported in the literature. The discrepancy (up to three-four orders of magnitude) between the theoretical and experimental values of flexoelectric coefficients has not been fully explained and at least part, if not all, of the apparent flexoelectric response may be accounted for by the built-in polarization revealed in this work.

The uncovering of the built in polarization in ceramics shows that not only thin films (< 1 μm scale) but also materials with macroscopic scale (hundreds of μm to several mm) can be self-polarized. Although at present the magnitude of the self-polarization is very small for practical uses it is possible to conceive, providing that the mechanism which causes it is identified and can be controlled, to enhance this effect and produce self-polarized samples with a polarization large enough to be exploited in applications.

Presence of self-polarization in single crystals is important when crystals are used as substrates for thin film growth. As shown here, this is the case of $SrTiO_3$, typical crystal used for growth of epitaxial thin films. Our results suggest that crystals with a large density of dislocations may release charge during heating and this charge may contribute to often-observed self-polarization of the films.

The fact that, in $Ba_{1-x}Sr_xTiO_3$ ceramics at least, the polarization is strongly imprinted in the samples once they are fully densified and it is not erased, even at very high temperatures, could potentially solve the problem of depoling which limits the use of ferroelectrics in high temperature applications. However, this great potential can be exploited providing that the built-in polarization is high enough and can be stabilized with

respect to its volatile component that limits the temperature stability and causes a change of the response over time which is undesired in applications.

The results may also contribute to the interpretation of the second harmonic generation [6], and piezoelectric effect [7, 8] often observed in paraelectric phase of ferroelectric materials.

[1] I. Levin, V. Krayzman, and J. C. Woicik, "Local structure in perovskite (Ba,Sr)TiO_3: Reverse Monte Carlo refinements from multiple measurement techniques," *Physical Review B,* vol. 89, pp. 4106-4106, Jan 2014.

[2] S. Prosandeev, D. W. Wang, and L. Bellaiche, "Properties of Epitaxial Films Made of Relaxor Ferroelectrics," *Physical Review Letters,* vol. 111, Dec 2013.

[3] H. Ursic and D. Damjanovic, "Anelastic relaxor behavior of $Pb(Mg_{1/3}Nb_{2/3})O_3$," *Applied Physics Letters,* vol. 103, Aug 2013.

[4] U. Aschauer, R. Pfenninger, S. M. Selbach, T. Grande, and N. A. Spaldin, "Strain-controlled oxygen vacancy formation and ordering in $CaMnO_3$," *Physical Review B,* vol. 88, Aug 2013.

[5] S. B. Adler, "Chemical expansivity of electrochemical ceramics," *Journal of the American Ceramic Society,* vol. 84, pp. 2117-2119, Sep 2001.

[6] A. M. Pugachev, V. I. Kovalevskii, N. V. Surovtsev, S. Kojima, S. A. Prosandeev, I. P. Raevski*, et al.*, "Broken Local Symmetry in Paraelectric $BaTiO_3$ Proved by Second Harmonic Generation," *Physical Review Letters,* vol. 108, Jun 2012.

[7] E. M. Anton, W. Jo, D. Damjanovic, and J. Rödel, "Determination of depolarization temperature of $(Bi_{1/2}Na_{1/2})TiO_3$-based lead-free piezoceramics," *Journal of Applied Physics,* vol. 110, Nov 2011.

[8] K. Wieczorek, A. Ziebinska, Z. Ujma, K. Szot, M. Gorny, I. Franke*, et al.*, "Electrostrictive and piezoelectric effect in $BaTiO_3$ and $PbZrO_3$," *Ferroelectrics,* vol. 336, pp. 61-67, 2006.

Curriculum vitae

Alberto Biancoli

Adress: Chemin de la Prairie 62
1007 LAUSANNE (VD), SWITZERLAND

email: alberto.biancoli@hotmail.it

PERSONAL INFORMATION

Date of birth: April 4th 1983
Place of Birth: Moncalieri (Torino), ITALY
Nationality: Italian

EDUCATION

March 2010- Sep 2014 PhD
Thesis title "*Breaking of the macroscopic centric symmetry in $Ba_{1-x}Sr_xTiO_3$ ceramics and single crystals*".

Ceramics Laboratory,EPFL, Lausanne Switzerland

Sept 2005- Dec 2007 Master degree in Material Science

Thesis Title: "*Synthesis and characterization of an Nd_2NiO_{4+d} single crystal as oxygen conductor in State Solid Fuel Cell.*"

University of Torino, Turin ,Italy

Sep 2002- Sep 2005 Bachelor degree in Material Science

Thesis Title: "Coating di nanofibre per polimerizzazione in situ"

University of Torino, Turin ,Italy

Working experience

Apr 2008- Apr 2009 Laboratory Technician
Apprenticeship as winner of the "Master dei Talenti Neolaureati" funded by Fondazione CRT of Turin

OCV (OWENS CORNING), Chambéry, France

Languages Skills

English: Fluent
French : Fluent
Italian: Native

Computer skills

Microsoft Office programs (MS Word, Excell, Power Point), good knowledge of Matchad, Origin, Wolfram Mathematica , basics on Comsol Multiphysics.

Contributed Publications

D. Damjanovic, A. Biancoli, L. Batooli, A. Vahabzadeh, and J. Trodahl, "Elastic, dielectric, and piezoelectric anomalies and Raman spectroscopy of 0.5Ba(Ti0.8Zr0.2)O-3 0.5(Ba0.7Ca0.3)TiO3," *Applied Physics Letters,* vol. 100, May 2012.

M. G. Sahini, T. Grande, B. Fraygola, A. Biancoli, D. Damjanovic, and N. Setter, "Solid Solution of Lead Metaniobate-Stabilization of the Ferroelectric Polymorph and the Effect on the Lattice Parameters, Dielectric, Ferroelectric, and Piezoelectric Properties," *Journal of the American Ceramic Society,* vol. 97, pp. 220-227, Jan 2014.

Conferences presentations

"Elastic, Dielectric and Piezoelectric Anomalies In (Ba,Ca)(Zr,Ti)O_3 ceramics",
oral contribution, 21st International Symposium on the Applications of Ferroelectrics and 11thEuropean Conference on Applications of Polar Dielectrics and Piezoresponse Force Microscopy Workshop (ISAF-ECAPD-PFM), Aveiro, Portugal

"Breaking of the centric symmetry in ferroelectric and paraelectric phases of unpoled ceramics",
oral contribution 22nd International Symposium on the Applications of Ferroelectrics-Piezoresponse Force Microscopy Workshop (ISAF–PFM), Prague, Czech Republic